# A Higher Order Closure Turbulence Model of the Planetary Boundary Layer

by

JOSEPH STEPHEN SCIRE

B.S., Massachusetts Institute of Technology
(May, 1977)

Submitted in Partial Fulfillment
of the Requirements of the
Degree of

Master of Science

at the

Massachusetts Institute of Technology
(October, 1978)

Signature of Author...................................................
Department of Meteorology, October, 1978

Certified by...................................................
Thesis Supervisor

Accepted by...................................................
Chairman, Department Committee
on Graduate Students

A Higher Order Closure
Turbulence Model of the
Planetary Boundary Layer

by

JOSEPH STEPHEN SCIRE

Submitted to the Department of Meteorology
on October 10, 1978 in partial fulfillment of
the requirements for the Degree of Master of Science

ABSTRACT

A higher order closure turbulence model, using the full level 3 equations (Mellor and Yamada, 1974; Yamada and Mellor, 1975) is described in detail. A new formulation for the length scale, $\ell$, which appears in each of the modeled terms, is employed. Equilibrium boundary conditions for the second moments are applied at the lower boundary.

Day 33-34 of the Wangara experiment is simulated. Surface temperature and mixing ratio are predicted with a ground thermodynamics model. The effect of the inclusion of the Coriolis terms of the second moment equations on the results is evaluated and is found to be small.

The similarity functions A, B, C, and D are evaluated. Vertically averaged variables are used in

the deficit relations (Arya, 1977, 1978). With this formulation, the similarity functions C and D are found to be equal in the unstable boundary layer. In the stable boundary layer D appears to be smaller than C.

Name and Title of Thesis Supervisor:

Professor David Randall

Assistant Professor of Meteorology

## ACKNOWLEDGEMENTS

I would like to express my sincere gratitude to Professor David Randall for his valuable guidance and active interest throughout the course of this project.

I wish to thank Isabelle Kole for skillfully drafting the figures and Joanne Klotz for expertly typing the difficult material.

I would like to extend special thanks to my fiancee, Debby, for her constant encouragement and moral support, and to my family and friends for their encouragement throughout the preparation of this thesis.

# TABLE OF CONTENTS

# LIST OF FIGURES

# LIST OF TABLES

# 1. INTRODUCTION

The random nature of turbulence makes the study of turbulent flows difficult. For this reason, it is convenient to use a statistical approach to turbulence problems, based on the concept of ensemble averaging. An ensemble average refers to an average taken over a collection of an infinite number of observations for which the mean conditions are identical. Due to the randomness and irregularity of turbulence, the details of each realization are different even though the mean conditions are the same. It is impossible to obtain an ensemble average from real atmospheric data because mean conditions are never identical. Certainly it is not possible to obtain an infinite number of instantaneous measurements over which to average. One must adopt an ergodic hypothesis, that is, an assumption regarding the equivalence of different types of averages, to establish the equality of an ensemble average over an infinite number of observations with a time average over an infinitely long averaging period under conditions of stationary flow (Lumley and Panofsky, 1964; Busch, 1973). A finite averaging time will yield an estimate with an accuracy which increases as the order of the moment being averaged decreases (Wyngaard, 1973). For the time scales involved in atmospheric turbulence, it is possible to relate ensemble averages to measurable time averages.

The statistical approach, however, results in a situation in which the number of unknowns exceeds the number of equations. It is necessary, therefore, to make simplifying modeling assumptions in order to obtain closure.

Mellor and Yamada (1974) describe a hierarchy of turbulence closure models. Based on a systematic simplification of the appropriate equations, four model levels are produced. The most complex (level 4) model requires the solution of prognostic simultaneous partial differential equations for all of the components of the Reynolds stress tensor, the heat flux vector, and the temperature variance, as well as for the components of the mean flow and the mean potential temperature. If water vapor is to be included in the model, additional equations for moisture variables need to be solved. The most simplified (level 1) model is a set of diagnostic algebraic equations corresponding to a mixing length model. The level 3 model, to be used in this study, represents an intermediate degree of complexity. As shown by Mellor and Yamada, the choice of the level 3 model represents a compromise between the small increase in relative accuracy obtained with a level 4 model and the resulting large increase in computation time.

The level 3 model is a subset of a group of models called Mean Turbulent Field (MTF) closure models (Mellor and Herring, 1973). MTF closure models consist of two subsets, Mean Turbulent Energy (MTE) and Mean Reynolds Stress (MRS) closure models. Because the turbulence energy in level 3 is calculated prognostically while the individual components of the Reynolds stress tensor are calculated diagnostically, the level 3 model falls into the category of MTE closure.

Yamada and Mellor (1975) use the level 3 model to simulate the Wangard boundary layer data. The present model differs from Yamada's and Mellor's model in several important respects:

i) A ground thermodynamics model predicts the surface temperature and mixing ratio.

ii) The full level 3 moisture equations are employed.

iii) Equilibrium boundary conditions for the prognostic turbulence variables are applied at the lower boundary.

iv) A new formulation for the length scale, $\ell$, is used.

v) The Coriolis terms are included.

vi) A 5 second time step and a staggered grid system are used.

The model is used to simulate Day 33-34 of the Wangara experiment, and the results compared to those of Yamada and Mellor (1975). The effect of the Coriolis terms on turbulent fluxes in the PBL is evaluated by turning these terms on and off in the model and examining the results. Finally, the functions A, B, C, and D of similarity theory are evaluated.

# 2. DEVELOPMENT OF THE BASIC EQUATIONS

## 2.1 Equations for the Mean Variables

The variables of interest are the velocity components $u_i$ ($i = 1,2,3$), potential temperature $\Theta$, pressure $P$, and water vapor mixing ratio $R$. The basic equations governing these variables are:

Continuity equation

$$\frac{\partial u_k}{\partial x_k} = 0 \tag{1}$$

Momentum equations

$$\frac{\partial u_j}{\partial t} + u_k \frac{\partial u_i}{\partial x_k} = -\frac{1}{\rho_o} \frac{\partial P}{\partial x_j} + \beta g \Theta \delta_{3j} - \varepsilon_{jk\ell} f_k u_\ell + \nu \frac{\partial}{\partial x_k} \left(\frac{\partial u_j}{\partial x_k}\right) \tag{2}$$

Thermodynamic energy equation

$$\frac{\partial \Theta}{\partial t} + u_k \frac{\partial \Theta}{\partial x_k} = k_T \frac{\partial}{\partial x_k} \left(\frac{\partial \Theta}{\partial x_k}\right) + \sigma \tag{3}$$

Water vapor equation

$$\frac{\partial R}{\partial t} + u_k \frac{\partial R}{\partial x_k} = \eta \frac{\partial}{\partial x_k} \left(\frac{\partial R}{\partial x_k}\right) \tag{4}$$

where $\beta$ is the coefficient of thermal expansion, $f_k = (0, f_y, f_z)$ is the Coriolis parameter, $\nu$ is the kinematic viscosity, $k_t$ is the thermal diffusivity, $\rho$ is the density, $\eta$ is the kinematic diffusivity for water vapor, and $\sigma$ is the longwave flux divergence. The Einstein summation convention is employed so that whenever an index is repeated in a term, summation is implied. $\varepsilon_{jk\ell}$ is the alternating unit tensor and $\delta_{ij}$ is the Kronecker delta.

$$\varepsilon_{jk} = \begin{cases} 1 \text{ if } j,k,\ell = (1,2,3),\ (2,3,1),\ \text{or } (3,1,2) \\ 0 \text{ if any index is repeated} \\ -1 \text{ if } j,k,\ell = (3,2,1),\ (2,1,3),\ \text{or } (1,3,2) \end{cases}$$

$$\delta_{ij} = \begin{cases} 0 \text{ if } i \neq j \\ 1 \text{ if } i = j \end{cases}$$

The effects of evaporation and condensation of water are not included. The Boussinesq approximation, in which density is treated as constant except when it is multiplied by g (in which case it is allowed to be temperature dependent), has been used (Busch, 1973; Mellor, 1973).

Each variable can be represented as a sum of a mean part and a fluctuating part.

$$u_i = \overline{u}_i = u_i' \qquad (4a)$$

$$\Theta = \overline{\Theta} + \theta' \qquad (4b)$$

$$P = \overline{P} + p' \tag{4c}$$

$$R = \overline{R} + r' \tag{4d}$$

The overbar signifies an ensemble average.

To obtain equations for the mean variables, average equations (1-4).

$$\frac{\partial \overline{u}_k}{\partial x_k} = 0 \tag{6}$$

$$\frac{\partial \overline{u}_j}{\partial t} + \frac{\partial}{\partial x_k} [\overline{u}_j \overline{u}_k + \overline{u_j' u'_k}] = -\frac{1}{\rho_o} \frac{\partial \overline{P}}{\partial x_j} + \beta g \overline{\Theta} \delta_{3_j} - \varepsilon_{jk\ell} f_k \overline{u}_\ell$$

$$+ \nu \frac{\partial}{\partial x_k} (\frac{\partial \overline{u}_j}{\partial x_k}) \tag{7}$$

$$\frac{\partial \overline{\Theta}}{\partial t} + \frac{\partial}{\partial x_k} [\overline{u}_k \overline{\Theta} + \overline{u_k' \theta'}] = k_T \frac{\partial}{\partial x_k} (\frac{\partial \overline{\Theta}}{\partial x_k}) + \sigma \tag{8}$$

$$\frac{\partial \overline{R}}{\partial t} + \frac{\partial}{\partial x_k} [\overline{R}\ \overline{u}_k + \overline{r' u_k'}] = \eta \frac{\partial}{\partial x_k} (\frac{\partial \overline{R}}{\partial x_k}) \tag{9}$$

2.2 Equations for the Second Moments

Equations (1-4) contain second order correlations of perturbation quantities of the form $\overline{u_j' u_k'}$. In order to evaluate these second moments, first obtain equations for the fluctuating components by subtracting equations (6-9) from equations (1-4). Using equations (4a-4d) yields:

$$\frac{\partial u'_k}{\partial x_k} = 0 \tag{10}$$

$$\frac{\partial u'_j}{\partial t} + \frac{\partial}{\partial x_k} [\bar{u}_j u'_k + u'_j \bar{u}_k + u'_j u'_k - \overline{u'_j u'_k}] =$$

$$- \frac{1}{\rho_o} \frac{\partial p'}{\partial x_j} + \beta g \theta' \delta_{3_j} - \varepsilon_{jk\ell} f_k u'_\ell + \nu \frac{\partial}{\partial x_k} (\frac{\partial u'_j}{\partial x_k}) \tag{11}$$

$$\frac{\partial \theta'}{\partial t} + \frac{\partial}{\partial x_k} [\bar{u}_k \theta' + u'_k \bar{\Theta} + u'_k \theta' - \overline{u'_k \theta'}] = k_T \frac{\partial}{\partial x_k} (\frac{\partial \theta'}{\partial x_k}) \tag{12}$$

$$\frac{\partial r'}{\partial t} + \frac{\partial}{\partial x_k} [\bar{u}_k r' + u'_k \bar{R} + u'_k r' - \overline{u'_k r'}] = \eta \frac{\partial}{\partial x_k} (\frac{\partial r'}{\partial x_k}) \tag{13}$$

To obtain an equation for $\overline{u'_i u'_j}$, multiply equation (11) by $u'_i$ and use the continuity equations (6) and (11):

$$u'_i \frac{\partial u'_j}{\partial t} + u'_i \frac{\partial}{\partial x_k} [\bar{u}_j u'_k + u'_j \bar{u}_k + u'_j u'_k - \overline{u'_j u'_k}]$$

$$= -u'_i \frac{\partial}{\partial x_j} (\frac{p'}{\rho_o}) + \beta g u'_i \theta' \delta_{3_j} - \varepsilon_{jk\ell} f_k u'_i u'_\ell$$

$$+ u'_i \frac{\partial}{\partial x_k} (\frac{\partial u'_j}{\partial x_k}) \quad . \tag{14}$$

A second equation is then obtained by switching the indexes i and j in equation (14). Adding this equation to equation (14), and using continuity and averaging, yields the prognostic second moment Reynolds stress equations:

$$\frac{\partial}{\partial t}(\overline{u_i'u_j'}) + \overline{u_i'u_k'}\frac{\partial \overline{u}_j}{\partial x_k} + \overline{u_j'u_k'}\frac{\partial \overline{u}_i}{\partial x_k} + \overline{u}_k\frac{\partial}{\partial x_k}(\overline{u_i'u_j'})$$

$$+ \frac{\partial}{\partial x_k}(\overline{u_i'u_j'u_k'}) = \beta g[\overline{u_i'\theta'}\delta_{3_j} + \overline{u_j'\theta'}\delta_{3_i}]$$

$$- \varepsilon_{jk\ell}f_k\overline{u_i'u_\ell'} - \varepsilon_{ik\ell}f_k\overline{u_j'u_\ell'} - \frac{\partial}{\partial x_j}\left(\frac{\overline{u_i'p'}}{\rho_o}\right) - \frac{\partial}{\partial x_i}\left(\frac{\overline{u_j'p'}}{\rho_o}\right)$$

$$+ \overline{\frac{p'}{\rho_o}\left(\frac{\partial u_i'}{\partial x_j} + \frac{\partial u_j'}{\partial x_i}\right)} + \nu\frac{\partial}{\partial x_k}\left(\frac{\partial \overline{u_i'u_j'}}{\partial x_k}\right) - 2\nu\overline{\frac{\partial u_i'}{\partial x_k}\frac{\partial u_j'}{\partial x_k}} \;. \tag{15}$$

Equation (7) requires that the second moment $\overline{u_i'u_j'}$ be known in order to find $\overline{u}_j$. Equation (15), an equation for $\overline{u_i'u_j'}$, contains the third moment $\overline{u_i'u_j'u_k'}$. An equation for the $n^{th}$ moment will contain a term with the (n+1)th moment. In other words, the number of equations is less than the number of unknowns and the problem is not closed. In order to obtain closure, the unknown moments are parameterized in terms of known quantities. This parameterization is, however, an approximation. The approximations are not necessarily more physically valid than parameterizations of second moments in terms of mean quantities, as in less complex models. However, the fact that the approximations are made at a higher order allows one to hope that the results will be less sensitive to the parameterization. The results of models using this higher order closure technique support this notion.

In the case $i \neq j$, $\rho_o \overline{u_i' u_j'}$ represents a flux of $\hat{j}$ momentum by the $\hat{i}$ turbulent component. The interpretation of the terms of equation (15) is as follows:

$$\frac{\partial}{\partial t} (\overline{u_i' u_j'})$$

represents the local time rate of change of the ensemble averaged turbulent momentum flux $\overline{u_i' u_j'}$ (normalized by density)

$$\overline{u_i' u_k'} \frac{\partial \bar{u}_j}{\partial x_k} + \overline{u_j' u_k'} \frac{\partial \bar{u}_i}{\partial x_k}$$

represents the mechanical production of Reynolds stress due to an interaction of the mean velocity gradient with the Reynolds stress

$$\bar{u}_k \frac{\partial}{\partial x_k} (\overline{u_i' u_j'})$$

represents advection of Reynolds stress by the mean wind

$$\frac{\partial}{\partial x_k}\,(\overline{u_i'u_j'u_k'})$$

is the triple correlation term which represents the turbulent flux of $u_i'u_j'$ by the fluctuating component $u_k'$ (i.e., turbulent diffusion)

$$\beta g[\overline{u_i'\theta'}\delta_{3_j} + \overline{u_j'\theta'}\delta_{3_i}]$$

represents the bouyant production (or destruction) of Reynolds stress

$$\varepsilon_{jk\ell}f_k\overline{u_i'u_\ell'} + \varepsilon_{ik\ell}f_k\overline{u_j'u_\ell'}$$

represents the effect of Coriolis forces on the Reynolds stress

$$\frac{1}{\rho_o}\,[\frac{\partial}{\partial x_j}\,(\overline{u_i'p'}) + \frac{\partial}{\partial x_i}\,(\overline{u_j'p'})]$$

represents the effect of the pressure perturbation-velocity perturbation correlation on Reynolds stress destruction

$$\overline{\frac{p'}{\rho_o}\,(\frac{\partial u_i'}{\partial x_j} + \frac{\partial u_j'}{\partial x_i})}$$

is the "energy redistribution" or "return to isotrcpy" term representing the way the pressure-velocity gradient correlation distributes energy among the three energy components

$$\nu \frac{\partial}{\partial x_k} \left(\frac{\partial \overline{u_i' u_j'}}{\partial x_k}\right) - 2\nu \overline{\frac{\partial u_i'}{\partial x_k} \frac{\partial u_j'}{\partial x_k}}$$

represents the viscous diffusion and viscous dissipation of Reynolds stress

In the case i = j, equation (15) is an equation for the i component of the turbulence energy. Summing the individual components, with $q^2 \equiv \overline{u_i'^2}$, gives the turbulence kinetic energy equation.

$$\frac{\partial}{\partial t} (q^2/2) + \overline{u_i' u_k'} \frac{\partial \bar{u}_i}{\partial x_k} + \bar{u}_k \frac{\partial}{\partial x_k} \left(\frac{q^2}{2}\right) + \frac{\partial}{\partial x_k} \overline{\left(u_k' \frac{u_i'^2}{2}\right)}$$

$$= \beta g \overline{u_i' \theta'} \delta_{3i} - \overline{\frac{u_i'}{\rho_o} \frac{\partial p'}{\partial x_i}} + \nu \frac{\partial}{\partial x_k} \left[\frac{\partial}{\partial x_k} \left(\frac{q^2}{2}\right)\right]$$

$$- \nu \overline{\frac{\partial u_i'}{\partial x_k} \frac{\partial u_i'}{\partial x_k}} \qquad (16)$$

The Coriolis terms do not appear in equation (16) because the Coriolis force cannot contribute to the total turbulent kinetic energy. Likewise, the energy redistribution term of the Reynolds stress equation is not present in the total kinetic energy budget because its role is to redistribute energy without contributing to the total. The interpretation of the terms of equation (16) is analogous to that of the Reynolds stress equation.

To obtain an equation for the heat flux vector $\overline{u_i'\theta'}$, first multiply equation (12) by $u_j'$ and equation (11) by $\theta'$ and average to obtain

$$\frac{\partial}{\partial t}(\overline{u_j'\theta'}) - \overline{\theta' \frac{\partial u_j'}{\partial t}} + \frac{\partial}{\partial x_k}[\bar{u}_k\overline{u_j'\theta'} + \overline{u_j'u_k'}\,\bar{\Theta} + \overline{u_j'u_k'\theta'}]$$

$$- \bar{u}_k \overline{\theta' \frac{\partial u_j'}{\partial x_k}} - \bar{\Theta}\,\overline{u_k' \frac{\partial u_j'}{\partial x_k}} - \overline{u_k'\theta' \frac{\partial u_j'}{\partial x_k}} = k_T \frac{\partial}{\partial x_k}(\overline{u_j' \frac{\partial \theta'}{\partial x_k}})$$

$$- k_T \overline{\frac{\partial \theta'}{\partial x_k} \frac{\partial u_j'}{\partial x_k}}\ , \tag{17}$$

and,

$$\overline{\theta' \frac{\partial u_j'}{\partial t}} = - \frac{\partial}{\partial x_k}[\bar{u}_j\overline{u_k'\theta'} + \overline{u_j'\theta'}\ \bar{u}_k + \overline{u_j'u_k'\theta'}] + \bar{u}_j\ \overline{u_k' \frac{\partial \theta'}{\partial x_k}}$$

$$+ \bar{u}_k\ \overline{u_j' \frac{\partial \theta'}{\partial x_k}} + \overline{u_j'u_k' \frac{\partial \theta'}{\partial x_k}} - \frac{1}{\rho_o}\overline{\theta' \frac{\partial p'}{\partial x_j}} + \beta g \overline{\theta'^2}\delta_{3_j}$$

$$- \varepsilon_{jk\ell}f_k\overline{u_\ell'\theta'} + \nu \frac{\partial}{\partial x_k}(\overline{\theta' \frac{\partial u_j'}{\partial x_k}}) - \nu \overline{\frac{\partial u_j'}{\partial x_k} \frac{\partial \theta'}{\partial x_k}}\ . \tag{18}$$

Adding equations (17) and (18), and using continuity, yields the desired heat flux equation:

$$\frac{\partial}{\partial t}(\overline{u_j'\theta'}) + \frac{\partial}{\partial x_k}[\bar{u}_k\ \overline{u_j'\theta'} + \overline{u_j'u_k'\theta'} - k_T\ \overline{u_j' \frac{\partial \theta'}{\partial x_k}} - \nu\ \overline{\theta' \frac{\partial u_j'}{\partial x_k}}\ ]$$

$$+ \frac{1}{\rho_o} \frac{\partial}{\partial x_j} (\overline{p'\theta'}) + \varepsilon_{jk\ell} f_k \overline{u'_\ell \theta'} = \beta g \overline{\theta'^2} \delta_{3_j} + \overline{\frac{p'}{\rho_o} \frac{\partial \theta'}{\partial x_j}}$$

$$- (k_T + \nu) \overline{\frac{\partial u'_j}{\partial x_k} \frac{\partial \theta'}{\partial x_k}} - \overline{u'_j u'_k} \frac{\partial \overline{\Theta}}{\partial x_k} - \overline{u'_k \theta'} \frac{\partial \overline{u}_j}{\partial x_k} \quad . \tag{19}$$

An equation for the potential temperature variance $\overline{\theta'^2}$ is obtained by multiplying equation (12) by $\theta'$, using continuity, and averaging.

$$\frac{\partial \overline{\theta'^2}}{\partial t} + \frac{\partial}{\partial x_k} [\overline{u}_k \overline{\theta'^2} + \overline{u'_k \theta'^2}] = - 2 \overline{u'_k \theta'} \frac{\partial \overline{\Theta}}{\partial x_k}$$

$$+ k_T \frac{\partial}{\partial x_k} (\frac{\partial \overline{\theta'^2}}{\partial x_k}) - 2 k_T \overline{\frac{\partial \theta'}{\partial x_k} \frac{\partial \theta'}{\partial x_k}} \tag{20}$$

The terms of equations (19) and (20) are of the same form as those of equation (15). Their interpretation is analogous.

Equation (9) requires the turbulent moisture flux $\overline{u'_j r'}$. An equation for $\overline{u'_j r'}$ is obtained by multiplying equation (11) by r' and multiplying equation (13) by $u'_j$. Averaging these equations and adding them yields:

$$\frac{\partial}{\partial t} (\overline{u'_j r'}) + \frac{\partial}{\partial x_k} [\overline{u}_k \overline{u'_j r'} + \overline{u'_j u'_k r'} - \eta \overline{u'_j \frac{\partial r'}{\partial x_k}} - \nu \overline{r' \frac{\partial u'_j}{\partial x_k}} ]$$

$$+ \frac{1}{\rho_o} \frac{\partial}{\partial x_j} (\overline{p'r'}) + \varepsilon_{jk\ell} f_k \overline{u'_\ell r'} = \beta g \overline{r'\theta'} \delta_{3_j} + \overline{\frac{p'}{\rho_o} \frac{\partial r'}{\partial x_j}}$$

$$- (\eta+\nu) \overline{\frac{\partial u'_i}{\partial x_k} \frac{\partial r'}{\partial x_k}} - \overline{u'_j u'_k} \frac{\partial \overline{R}}{\partial x_k} - \overline{u'_k r'} \frac{\partial \overline{u}_j}{\partial x_k} \tag{21}$$

An equation for the potential temperature-mixing ratio covariance $\overline{\theta'r'}$ is also necessary because it appears in equation (21). Multiplying equation (12) by $r'$ and equation (13) by $\theta'$, averaging, and adding yields:

$$\frac{\partial}{\partial t} (\overline{\theta'r'}) + \frac{\partial}{\partial x_k} [\overline{u}_k \overline{\theta'r'} + \overline{u'_k \theta' r'} - \eta \overline{\theta' \frac{\partial r'}{\partial x_k}} - k_T \overline{r' \frac{\partial \theta'}{\partial x_k}} ]$$

$$= - (\eta+k_T) \overline{\frac{\partial \theta'}{\partial x_k} \frac{\partial r'}{\partial x_k}} - \overline{u'_k \theta'} \frac{\partial \overline{R}}{\partial x_k} - \overline{u'_k r'} \frac{\partial \overline{\Theta}}{\partial x_k} \tag{22}$$

An equation for the mixing ratio variance, $\overline{r'^2}$, is obtained by multiplying equation (13) by $r'$. After using continuity and averaging:

$$\frac{\partial}{\partial t} (\overline{r'^2}) + \frac{\partial}{\partial x_k} [\overline{u}_k \overline{r'^2} + \overline{u'_k r'^2}] = -2\overline{u'_k r'} \frac{\partial \overline{R}}{\partial x_k} + \eta \frac{\partial^2 \overline{r'^2}}{\partial x_k^2}$$

$$- 2\eta \overline{\frac{\partial r'}{\partial x_k} \frac{\partial r'}{\partial x_k}} \; . \tag{23}$$

# 3. MODELING OF THE EQUATIONS

## 3.1 The Modeling Assumptions

It is necessary to parameterize the unknown variables of the equations in order to obtain closure. It is also desirable to neglect small terms that do not affect the results so that unnecessary complexity is avoided and computation time is minimized. The system of equations consists of equations (7-9), (15), and (19-23). These equations are summarized in Table I. The terms to be modeled have been doubly underlined. The numbers associated with each line correspond to the numbered modeling assumptions which are collected into Table II.

The modeling assumptions in Table II are of two types. The first type concerns terms containing unknown variables, i.e., variables for which there are no equations in Table I expressing the variable in terms of only other known variables. The parameterization of these terms is required by closure considerations. The triple correlation terms are of this type. The other type of assumption concerns terms which are known (in terms of other variables) but are small in the planetary boundary layer (PBL), or are difficult (although possible given the set of equations in Table I) to evaluate and are assumed small in the PBL. The Coriolis terms are of the second type. They have been neglected in the models of Mellor and Yamada, 1974, 1975,

Table I

Unmodeled Equations for the Mean Variables and the Second Moments

Equation No.

Equations for the mean flow

(7) $$\frac{\partial \bar{u}_j}{\partial t} + \frac{\partial}{\partial x_k}\left[\bar{u}_j \bar{u}_k + \overline{u_j' u_k'}\right] = -\frac{1}{\rho_0}\frac{\partial \bar{p}}{\partial x_j} + \beta g \bar{\Theta} \delta_{3j} - \epsilon_{jkl} f_k \bar{u}_l + \nu \frac{\partial}{\partial x_k}\left(\frac{\partial \bar{u}_j}{\partial x_k}\right)$$

(8) $$\frac{\partial \bar{\Theta}}{\partial t} + \frac{\partial}{\partial x_k}\left[\bar{u}_k \bar{\Theta} + \overline{u_k' \theta'}\right] = k_T \frac{\partial}{\partial x_k}\left(\frac{\partial \bar{\Theta}}{\partial x_k}\right) + \sigma$$

(9) $$\frac{\partial \bar{R}}{\partial t} + \frac{\partial}{\partial x_k}\left[\bar{R} \bar{u}_k + \overline{r' u_k'}\right] = \eta \frac{\partial}{\partial x_k}\left(\frac{\partial \bar{R}}{\partial x_k}\right)$$

Second moment equations

(15) $$\frac{\partial}{\partial t}\left(\overline{u_i' u_j'}\right) + \overline{u_i' u_k'}\frac{\partial \bar{u}_j}{\partial x_k} + \overline{u_j' u_k'}\frac{\partial \bar{u}_i}{\partial x_k} + \bar{u}_k \frac{\partial}{\partial x_k}\left(\overline{u_i' u_j'}\right)$$

$$+ \underbrace{\frac{\partial}{\partial x_k}\left(\overline{u_i' u_j' u_k'}\right)}_{(1)} = \beta g\left[\overline{u_i' \theta'}\delta_{3j} + \overline{u_j' \theta'}\delta_{3i}\right]$$

$$\underbrace{- \epsilon_{jkl} f_k \overline{u_i' u_l'} - \epsilon_{ikl} f_k \overline{u_j' u_l'}}_{(2)}$$

$$\underbrace{- \frac{\partial}{\partial x_j}\left(\frac{\overline{u_i' p'}}{\rho_0}\right) - \frac{\partial}{\partial x_i}\left(\frac{\overline{u_j' p'}}{\rho_0}\right)}_{(3)} + \underbrace{\overline{\frac{p'}{\rho_0}\left(\frac{\partial u_i'}{\partial x_j} + \frac{\partial u_j'}{\partial x_i}\right)}}_{(4)}$$

$$+ \underbrace{\nu \frac{\partial}{\partial x_k}\left(\frac{\partial \overline{u_i' u_j'}}{\partial x_k}\right)}_{(5)} \underbrace{- 2\nu \overline{\frac{\partial u_i'}{\partial x_k}\frac{\partial u_j'}{\partial x_k}}}_{(6)}$$

Equation No.

Table I (continued)

(19)
$$\frac{\partial}{\partial t}\left(\overline{u_j'\theta'}\right) + \overline{u_j'u_k'}\,\frac{\partial\bar{\Theta}}{\partial x_k} + \overline{u_k'\theta'}\,\frac{\partial\bar{u}_j}{\partial x_k} + \bar{u}_k\,\frac{\partial}{\partial x_k}\left(\overline{u_j'\theta'}\right)$$

$$+\underbrace{\frac{\partial}{\partial x_k}\left(\overline{u_j'u_k'\theta'}\right)}_{(7)} = \underbrace{\frac{\partial}{\partial x_k}\left[k_T\,\overline{u_j'\frac{\partial\theta'}{\partial x_k}} + \nu\,\overline{\theta'\frac{\partial u_j'}{\partial x_k}}\right]}_{(8)}$$

$$\underbrace{-\frac{1}{\rho_0}\frac{\partial}{\partial x_j}\left(\overline{p'\theta'}\right)}_{(9)} \underbrace{-\,\epsilon_{jkl}\,f_k\,\overline{u_l'\theta'}}_{(10)} + \beta g\,\overline{\theta'^2}\,\delta_{3j}$$

$$\underbrace{+\,\overline{\frac{p'}{\rho_0}\frac{\partial\theta'}{\partial x_j}}}_{(11)} \underbrace{-\,(k_T+\nu)\,\overline{\frac{\partial u_j'}{\partial x_k}\frac{\partial\theta'}{\partial x_k}}}_{(12)}$$

(20)
$$\frac{\partial}{\partial t}\left(\overline{\theta'^2}\right) + \bar{u}_k\,\frac{\partial\overline{\theta'^2}}{\partial x_k} + \underbrace{\frac{\partial}{\partial x_k}\left(\overline{u_k'\theta'^2}\right)}_{(13)} + 2\,\overline{u_k'\theta'}\,\frac{\partial\bar{\Theta}}{\partial x_k} =$$

$$\underbrace{k_T\frac{\partial}{\partial x_k}\left(\frac{\partial\overline{\theta'^2}}{\partial x_k}\right)}_{(14)} \underbrace{-\,2k_T\,\overline{\left(\frac{\partial\theta'}{\partial x_k}\right)\left(\frac{\partial\theta'}{\partial x_k}\right)}}_{(15)}$$

(21)
$$\frac{\partial}{\partial t}\left(\overline{u_j'r'}\right) + \overline{u_j'u_k'}\,\frac{\partial\bar{R}}{\partial x_k} + \overline{u_k'r'}\,\frac{\partial\bar{u}_j}{\partial x_k} + \bar{u}_k\,\frac{\partial}{\partial x_k}\left(\overline{u_j'r'}\right)$$

$$+\underbrace{\frac{\partial}{\partial x_k}\left(\overline{u_j'u_k'r'}\right)}_{(16)} = \underbrace{\frac{\partial}{\partial x_k}\left[\eta\,\overline{u_j'\frac{\partial r'}{\partial x_k}} + \nu\,\overline{r'\frac{\partial u_j'}{\partial x_k}}\right]}_{(17)}$$

$$\underbrace{-\frac{1}{\rho_0}\frac{\partial}{\partial x_j}\left(\overline{p'r'}\right)}_{(18)} \underbrace{-\,\epsilon_{jkl}\,f_k\,\overline{u_l'r'}}_{(19)} + \beta g\,\overline{r'\theta'}\,\delta_{3j}$$

$$\underbrace{+\,\overline{\frac{p'}{\rho_0}\frac{\partial r'}{\partial x_j}}}_{(20)} \underbrace{-\,(\eta+\nu)\,\overline{\frac{\partial u_j'}{\partial x_k}\frac{\partial r'}{\partial x_k}}}_{(21)}$$

Equation No.

Table I (continued)

(22) $$\frac{\partial}{\partial \tau}\left(\overline{r'\theta'}\right) + \overline{\mu_k' \theta'}\,\frac{\partial \bar{R}}{\partial x_k} + \overline{\mu_k' r'}\,\frac{\partial \bar{\Theta}}{\partial x_k} + \bar{\mu}_k \frac{\partial}{\partial x_k}\left(\overline{r'\theta'}\right)$$

$$+ \underset{(22)}{\underline{\underline{\frac{\partial}{\partial x_k}\left(\overline{\mu_k' r'\theta'}\right)}}} = \underset{(23)}{\underline{\underline{\frac{\partial}{\partial x_k}\left[\eta\,\overline{\theta' \frac{\partial r'}{\partial x_k}} + \kappa_T\,\overline{r' \frac{\partial \theta'}{\partial x_k}}\right]}}}$$

$$\underset{(24)}{\underline{\underline{-\left(\eta + \kappa_T\right)\overline{\frac{\partial \theta'}{\partial x_k}\,\frac{\partial r'}{\partial x_k}}}}}$$

(23) $$\frac{\partial}{\partial \tau}\left(\overline{r'^2}\right) + 2\,\overline{\mu_k' r'}\,\frac{\partial \bar{R}}{\partial x_k} + \bar{\mu}_k \frac{\partial \overline{r'^2}}{\partial x_k} + \underset{(25)}{\underline{\underline{\frac{\partial}{\partial x_k}\left(\overline{\mu_k' r'^2}\right)}}} =$$

$$\underset{(26)}{\underline{\underline{\eta\,\frac{\partial^2 \overline{r'^2}}{\partial x_k^2}}}} - \underset{(27)}{\underline{\underline{2\eta\,\overline{\frac{\partial r'}{\partial x_k}\,\frac{\partial r'}{\partial x_k}}}}}$$

Underlined terms have been modeled. The numbers correspond to the order in which tne modeling assumptions are listed in Table II.

Table II

Modeling Assumptions

(1) $$\frac{\partial}{\partial x_k}\left(\overline{u_i' u_j' u_k'}\right) = \frac{\partial}{\partial x_k}\left[-q\lambda_1\left(\frac{\partial \overline{u_i' u_j'}}{\partial x_k} + \frac{\partial \overline{u_i' u_k'}}{\partial x_j} + \frac{\partial \overline{u_j' u_k'}}{\partial x_i}\right)\right]$$

(2) $$\epsilon_{jkl} f_k \overline{u_i' u_l'} + \epsilon_{ikl} f_k \overline{u_j' u_l'} = \begin{cases} 0 \\ \epsilon_{jkl} f_k \overline{u_i' u_l'} + \epsilon_{ikl} f_k \overline{u_j' u_l'} \end{cases}$$

(3) $$\frac{\partial}{\partial x_j}\left(\overline{u_i' p'}\right) = 0$$

(4) $$\overline{\frac{p'}{\rho_0}\left(\frac{\partial u_i'}{\partial x_j} + \frac{\partial u_j'}{\partial x_i}\right)} = \frac{-q}{3\ell_1}\left(\overline{u_i' u_j'} - \frac{\delta_{ij}}{3} q^2\right) + Cq^2\left(\frac{\partial \bar{u}_i}{\partial x_j} + \frac{\partial \bar{u}_j}{\partial x_i}\right)$$

(5) $$\nu \frac{\partial}{\partial x_k}\left(\frac{\partial \overline{u_i' u_j'}}{\partial x_k}\right) = 0$$

(6) $$2\nu \overline{\frac{\partial u_i'}{\partial x_k}\frac{\partial u_j'}{\partial x_k}} = \frac{2}{3}\frac{q^3}{\Lambda_1}\delta_{ij}$$

(7) $$\frac{\partial}{\partial x_k}\left(\overline{u_j' u_k' \theta'}\right) = \frac{\partial}{\partial x_k}\left[-q\lambda_2\left(\frac{\partial \overline{u_k' \theta'}}{\partial x_j} + \frac{\partial \overline{u_j' \theta'}}{\partial x_k}\right)\right]$$

(8) $$\frac{\partial}{\partial x_k}\left[k_T \overline{u_j' \frac{\partial \theta'}{\partial x_k}} + \nu \overline{\theta' \frac{\partial u_j'}{\partial x_k}}\right] = 0$$

(9) $$\frac{\partial}{\partial x_j}\left(\overline{p'\theta'}\right) = 0$$

Table II (continued)

(10) $$\epsilon_{jkl} f_k \overline{u_l'\theta'} = \begin{cases} 0 \\ \epsilon_{jkl} f_k \overline{u_l'\theta'} \end{cases}$$

(11) $$\overline{\frac{p'}{\rho_0}\frac{\partial\theta'}{\partial x_j}} = -\frac{g}{3l_2}\overline{u_j'\theta'}$$

(12) $$(\kappa_T + \nu)\overline{\frac{\partial u_j'}{\partial x_k}\frac{\partial\theta'}{\partial x_k}} = 0$$

(13) $$\frac{\partial}{\partial x_k}\left(\overline{u_k'\theta'^2}\right) = \frac{\partial}{\partial x_k}\left(-q\,\lambda_3\frac{\partial\overline{\theta'^2}}{\partial x_k}\right)$$

(14) $$\kappa_T\frac{\partial}{\partial x_k}\left(\frac{\partial\overline{\theta'^2}}{\partial x_k}\right) = 0$$

(15) $$2\kappa_T\overline{\frac{\partial\theta'}{\partial x_k}\frac{\partial\theta'}{\partial x_k}} = 2\frac{q}{\Lambda_2}\overline{\theta'^2}$$

(16) $$\frac{\partial}{\partial x_k}\left(\overline{u_j'u_k'r'}\right) = \frac{\partial}{\partial x_k}\left[-q\,\lambda_2\left(\frac{\partial\overline{u_k'r'}}{\partial x_j} + \frac{\partial\overline{u_j'r'}}{\partial x_k}\right)\right]$$

(17) $$\frac{\partial}{\partial x_k}\left[\eta\overline{u_j'\frac{\partial r'}{\partial x_k}} + \nu\overline{r'\frac{\partial u_j'}{\partial x_k}}\right] = 0$$

(18) $$\frac{\partial}{\partial x_j}\left(\overline{p'r'}\right) = 0$$

Table II (continued)

(19) $$\epsilon_{jkl}\, f_k\, \overline{u_l' r'} = \begin{cases} 0 \\ \epsilon_{jkl}\, f_k\, \overline{u_l' r'} \end{cases}$$

(20) $$\overline{\frac{p'}{\rho_0}\frac{\partial r'}{\partial x_j}} = -\frac{g}{3 l_2}\overline{u_j' r'}$$

(21) $$(\eta + \nu)\,\overline{\frac{\partial u_i'}{\partial x_k}\frac{\partial r'}{\partial x_k}} = 0$$

(22) $$\frac{\partial}{\partial x_k}\left(\overline{u_k' \theta' r'}\right) = \frac{\partial}{\partial x_k}\left(-g\,\lambda_2\,\frac{\partial \overline{r'\theta'}}{\partial x_k}\right)$$

(23) $$\frac{\partial}{\partial x_k}\left[\eta\,\overline{\theta'\frac{\partial r'}{\partial x_k}} + K_T\,\overline{r'\frac{\partial \theta'}{\partial x_k}}\right] = 0$$

(24) $$(\eta + K_T)\,\overline{\frac{\partial \theta'}{\partial x_k}\frac{\partial r'}{\partial x_k}} = \frac{2g}{\lambda_2}\overline{r'\theta'}$$

(25) $$\frac{\partial}{\partial x_k}\left(\overline{u_k' r'^2}\right) = \frac{\partial}{\partial x_k}\left(-g\,\lambda_3\,\frac{\partial \overline{r'^2}}{\partial x_k}\right)$$

(26) $$\frac{\partial}{\partial x_k}\left(\eta\,\frac{\partial \overline{r'^2}}{\partial x_k}\right) = 0$$

(27) $$2\eta\,\overline{\frac{\partial r'}{\partial x_k}\frac{\partial r'}{\partial x_k}} = \frac{2g}{\lambda_2}\overline{r'^2}$$

and Donaldson, 1973. Wyngaard et al., 1974, however, discuss the importance of the Coriolis terms in the Reynolds stress budget. In this study an option has been included in the model to turn the Coriolis terms on or off to allow their importance to be evaluated. Both modeling options appear in Table II.

One of the basic modeling assumptions contained in the model is the energy redistribution assumption of Rotta (1951). The total turbulence kinetic energy (per unit mass) is the sum of three components:

$$\frac{1}{2} q^2 \equiv \frac{1}{2} (\overline{u_1'^2} + \overline{u_2'^2} + \overline{u_3'^2})$$

The term $\overline{p'(\partial u_i'/\partial x_j + \partial u_j'/\partial x_i)}$ appears in the equations for the individual components of the turbulence energy, but not in the equation for the total turbulence kinetic energy (equation 16). As has already been noted, the role of this term is to redistribute the energy among the three components of energy without contributing to the total. The redistribution term is therefore modeled as:

$$\overline{p'(\frac{\partial u_i'}{\partial x_j} + \frac{\partial u_j'}{\partial x_i})} = \frac{-q}{3\ell_1} (\overline{u_i'u_j'} - \frac{\delta_{ij}}{3} q^2) + Cq^2 (\frac{\partial \overline{u}_i}{\partial x_j} + \frac{\partial \overline{u}_j}{\partial x_i}) \quad ,$$

where C is a constant and $\ell_1$ is a length scale which will be prescribed. Characteristic of this formulation is that a departure from isotropy of the Reynolds stress tensor will result in a tendency back toward isotropy.

"Return to isotropy" terms also appear in equations (19) and (21) as $\overline{\frac{p'}{\rho_o}\frac{\partial\theta'}{\partial x_j}}$ and $\overline{\frac{p'}{\rho_o}\frac{\partial r'}{\partial x_j}}$, respectively. An analogous formulation is adopted for these terms:

$$\overline{\frac{p'}{\rho_o}\frac{\partial\theta'}{\partial x_j}} = -\frac{q}{3\ell_2}\overline{u_j'\theta'} \quad , \quad \overline{\frac{p'}{\rho_o}\frac{\partial r'}{\partial x_j}} = -\frac{q}{3\ell_2}\overline{u_j'r'} \quad .$$

A second length scale $\ell_2$ is introduced.

It is necessary to model the triple correlation term $\frac{\partial}{\partial x_k}(\overline{u_i'u_j'u_k'})$, representing a diffusion of Reynolds stress, in terms of known second moments. A symmetric construction in i, j, and k, using second moments, is:

$$\frac{\partial}{\partial x_k}(\overline{u_i'u_j'u_k'}) = \frac{\partial}{\partial x_k}\left[-q\lambda_1\left\{\left(\frac{\partial\overline{u_i'u_j'}}{\partial x_k}\right) + \left(\frac{\partial\overline{u_i'u_k'}}{\partial x_j}\right) + \left(\frac{\partial\overline{u_j'u_k'}}{\partial x_i}\right)\right\}\right]$$

This formulation represents a down gradient diffusion of Reynolds stress.

The triple correlation terms $\frac{\partial}{\partial x_k}(\overline{u_j'u_k'\theta'})$ and $\frac{\partial}{\partial x_k}(\overline{u_j'u_k'r'})$ are modeled as down gradient turbulent diffusion of potential temperature-velocity covariance and mixing ratio-velocity covariance, respectively.

$$\frac{\partial}{\partial x_k}(\overline{u_j'u_k'\theta'}) = \frac{\partial}{\partial x_k}[-q\lambda_2(\frac{\partial\overline{u_k'\theta'}}{\partial x_j} + \frac{\partial\overline{u_j'\theta'}}{\partial x_k})]$$

$$\frac{\partial}{\partial x_k}(\overline{u_j'u_k'r'}) = \frac{\partial}{\partial x_k}[-q\lambda_2(\frac{\partial\overline{u_k'r'}}{\partial x_j} + \frac{\partial\overline{u_j'r'}}{\partial x_k})]$$

Analogously, the third moments involving potential temperature variance-velocity correlation, potential temperature-mixing ratio-velocity correlation and mixing ratio variance are also modeled as down gradient turbulent diffusion.

$$\frac{\partial}{\partial x_k}(\overline{u_k'\theta'^2}) = \frac{\partial}{\partial x_k}[-q\lambda_3\frac{\partial\overline{\theta'^2}}{\partial x_k}]$$

$$\frac{\partial}{\partial x_k}(\overline{u_k'\theta'r'}) = \frac{\partial}{\partial x_k}[-q\lambda_2\frac{\partial\overline{\theta'r'}}{\partial x_k}]$$

$$\frac{\partial}{\partial x_k}(\overline{u_k'r'^2}) = \frac{\partial}{\partial x_k}[-q\lambda_3\frac{\partial\overline{r'^2}}{\partial x_k}]$$

The variables $\lambda_1$, $\lambda_2$ and $\lambda_3$ are diffusion length scales which are prescribed.

Kolmogoroff (1941) hypothesized the isotropy of small-scale turbulence. In accordance with this widely accepted hypothesis, the viscous dissipation term $2\nu\overline{(\partial u_i'/\partial x_k)(\partial u_j'/\partial x_k)}$ is modeled as proportional to $q^3$

for i=j, and is neglected for the nonisotropic components $i \neq j$.

$$2\nu \overline{\frac{\partial u_i'}{\partial x_k} \frac{\partial u_j'}{\partial x_k}} = \frac{2}{3} \frac{q^3}{\Lambda_1} \delta_{ij}$$

The dissipation term $k_T\overline{(\partial\theta'/\partial x_k)(\partial\theta'/\partial x_k)}$ is similarly taken to be proportional to the potential temperature variance.

$$2k_T \overline{\frac{\partial\theta'}{\partial x_k} \frac{\partial\theta'}{\partial x_k}} = 2 \frac{q}{\Lambda_2} \overline{\theta'^2}$$

Analogously, the dissipation terms for $\overline{r'\theta_v'}$ and $\overline{r'^2}$ are modeled as:

$$(\eta+k_T) \overline{\frac{\partial\theta'}{\partial x_k} \frac{\partial r'}{\partial x_k}} = 2 \frac{q}{\Lambda_2} \overline{r'\theta'}$$

$$2\eta \overline{\frac{\partial r'}{\partial x_k} \frac{\partial r'}{\partial x_k}} = 2 \frac{q}{\Lambda_2} \overline{r'^2}$$

$\Lambda_1$ and $\Lambda_2$ are dissipation length scales which are prescribed.

The remaining modeling assumptions in Table II concern diffusion terms of the form $\frac{\partial}{\partial x_k} [k_T\overline{u_j' \frac{\partial\theta'}{\partial x_k}} + \nu\overline{\theta' \frac{\partial u_j'}{\partial x_k}}]$. In the PBL these terms are relatively small, and we neglect them.

$$\frac{\partial}{\partial x_k}\left[k_T \overline{u_j' \frac{\partial \theta'}{\partial x_k}} + \nu \overline{\theta' \frac{\partial u_j'}{\partial x_k}}\right] = 0$$

$$\frac{\partial}{\partial x_k}\left[\eta \overline{u_j' \frac{\partial r'}{\partial x_k}} + \nu \overline{r' \frac{\partial u_j'}{\partial x_k}}\right] = 0$$

$$\frac{\partial}{\partial x_k}\left[\eta \overline{\theta' \frac{\partial r'}{\partial x_k}} + k_T \overline{r' \frac{\partial \theta'}{\partial x_k}}\right] = 0$$

$$\frac{\partial}{\partial x_k}\left[2\eta \frac{\partial \overline{r'^2}}{\partial x_k}\right] = 0$$

Inserting the modeling assumptions (1-27) from Table II into the appropriate equations in Table I will yield the modeled level 4 equations. The complete level 4 model consists of equations (7-9), and (24-29).

$$\frac{\partial}{\partial t}(\overline{u_i' u_j'}) + \overline{u_i' u_k'}\frac{\partial \bar{u}_j}{\partial x_k} + \overline{u_j' u_k'}\frac{\partial \bar{u}_i}{\partial x_k} + \bar{u}_k \frac{\partial}{\partial x_k}(\overline{u_i' u_j'})$$

$$+ \frac{\partial}{\partial x_k}\left[-q\lambda_1\left(\frac{\partial \overline{u_i' u_j'}}{\partial x_k} + \frac{\partial \overline{u_i' u_k'}}{\partial x_j} + \frac{\partial \overline{u_j' u_k'}}{\partial x_i}\right)\right] =$$

$$\beta g\left[\overline{u_i'\theta'}\delta_{3j} + \overline{u_j\theta'}\delta_{3i}\right] - \frac{q}{3\Lambda_1}\left(\overline{u_i' u_j'} - \frac{\delta_{ij}}{3}q^2\right)$$

$$+ C q^2\left(\frac{\partial \bar{u}_i}{\partial x_j} + \frac{\partial \bar{u}_j}{\partial x_i}\right) - \frac{2}{3}\frac{q^3}{\Lambda_1}\delta_{ij} - \epsilon_{jk\ell} f_k \overline{u_i' u_\ell'} - \epsilon_{ik\ell} f_k \overline{u_j' u_\ell'} \qquad (24)$$

$$\frac{\partial}{\partial \tau}(\overline{u_j'\theta'}) + \frac{\partial}{\partial x_k}\left[\bar{u}_k \overline{u_j'\theta'} - q\,\lambda_2\left(\frac{\partial \overline{u_k'\theta'}}{\partial x_j} + \frac{\partial \overline{u_j'\theta'}}{\partial x_k}\right)\right] =$$

$$\beta g\,\overline{\theta'^2}\,\delta_{3j} - \frac{q}{3\ell_2}\overline{u_j'\theta'} - \overline{u_j'u_k'}\frac{\partial \bar{\Theta}}{\partial x_k} - \overline{u_k'\theta'}\frac{\partial \bar{u}_j}{\partial x_k}$$

$$- \epsilon_{jk\ell}\, f_k\, \overline{u_\ell'\theta'} \tag{25}$$

$$\frac{\partial \overline{\theta'^2}}{\partial \tau} + \frac{\partial}{\partial x_k}\left[\bar{u}_k \overline{\theta'^2} - q\,\lambda_3 \frac{\partial \overline{\theta'^2}}{\partial x_k}\right] = -2\,\overline{u_k'\theta'}\frac{\partial \bar{\Theta}}{\partial x_k} - \frac{2q}{\Lambda_2}\overline{\theta'^2} \tag{26}$$

$$\frac{\partial}{\partial \tau}(\overline{u_j'r'}) + \frac{\partial}{\partial x_k}\left[\bar{u}_k \overline{u_j'r'} - q\,\lambda_2\left(\frac{\partial \overline{u_k'r'}}{\partial x_j} + \frac{\partial \overline{u_j'r'}}{\partial x_k}\right)\right] =$$

$$\beta g\,\overline{r'\theta'}\,\delta_{3j} - \frac{q}{3\ell_2}\overline{u_j'r'} - \overline{u_j'u_k'}\frac{\partial \bar{R}}{\partial x_k} - \overline{u_k'r'}\frac{\partial \bar{u}_j}{\partial x_k}$$

$$- \epsilon_{jk\ell}\, f_k\, \overline{u_\ell'r'} \tag{27}$$

$$\frac{\partial}{\partial \tau}(\overline{r'\theta'}) + \frac{\partial}{\partial x_k}\left[\bar{u}_k \overline{r'\theta'} - q\,\lambda_2 \frac{\partial}{\partial x_k}(\overline{r'\theta'})\right] = -\frac{2q}{\Lambda_2}\overline{r'\theta'}$$

$$- \overline{u_k'\theta'}\frac{\partial \bar{R}}{\partial x_k} - \overline{u_k'r'}\frac{\partial \bar{\Theta}}{\partial x_k} \tag{28}$$

$$\frac{\partial}{\partial \tau}(\overline{r'^2}) + \frac{\partial}{\partial x_k}\left[\bar{u}_k \overline{r'^2} - q\,\lambda_3 \frac{\partial \overline{r'^2}}{\partial x_k}\right] = -\frac{2q}{\Lambda_2}\overline{r'^2} - 2\,\overline{u_k'r'}\frac{\partial \bar{R}}{\partial x_k} \tag{29}$$

## 3.2 The Level 3 Model Equations

Mellor and Yamada (1974) make use of the fact that the departure from isotropy of atmospheric turbulence is small, to simplify equations (24-29) even further. Defining non-dimensional departures from isotropy, $a_{ij}$ and $b_i$:

$$\overline{u_i'u_j'} \equiv \left(\frac{\delta_{ij}}{3} + a_{ij}\right)q^2 \quad , \quad a_{ii} = 0$$

$$\overline{u_i'\theta'} \equiv b_i q(\overline{\theta'^2})^{1/2}$$

The level 3 and level 2 models neglect terms of order $a^2$ and $b^2$. The two levels are distinguished by the fact that the tendency, advection, and diffusion terms are assumed to be of order a or b in level 3 and order $a^2$ or $b^2$ in level 2. The result for the level 3 model of interest here is that equations (24-29), representing 15 prognostic equations for second moments, are reduced to 4 prognostic equations with 11 diagnostic equations. The prognostic equations are for $q^2$, $\overline{\theta'^2}$, $\overline{\theta'r'}$ and $\overline{r'^2}$. The mean variables require the solution of an additional five prognostic equations. The level 3 model, therefore, consists of a total of 9 prognostic differential equations and 11 diagnostic equations. The level 3 equations are collected into Table III. Equations (26), (28), and (29) are unchanged.

Table III

Level 3 Model Equations

$$\frac{\partial}{\partial t}(q^2) + \bar{u}_k \frac{\partial}{\partial x_k}(q^2) - \frac{\partial}{\partial x_k}\left[\frac{5}{3} q \lambda_1 \frac{\partial q^2}{\partial x_k}\right] = -2\,\overline{u_k' u_i'}\,\frac{\partial \bar{u}_i}{\partial x_k}$$
$$+ 2\beta g\,\overline{u_i'\theta'}\,\delta_{3i} - \frac{2q^3}{\Lambda_1} \tag{30}$$

$$\overline{u_i' u_j'} = \frac{q^2}{3}\delta_{ij} - \frac{3\ell_1}{q}\left[\left(\overline{u_k' u_i'} - C q^2 \delta_{ki}\right)\frac{\partial \bar{u}_j}{\partial x_k} + \left(\overline{u_k' u_j'} - C q^2 \delta_{kj}\right)\frac{\partial \bar{u}_i}{\partial x_k}\right.$$
$$\left. - \frac{2}{3}\delta_{ij}\,\overline{u_k' u_\ell'}\,\frac{\partial \bar{u}_\ell}{\partial x_k}\right] + \frac{3\ell_1}{q}\beta g\left[\overline{u_i'\theta'}\,\delta_{3j} + \overline{u_j'\theta'}\,\delta_{3i} - \frac{2}{3}\delta_{ij}\delta_{3\ell}\,\overline{u_\ell'\theta'}\right]$$
$$+ \frac{3\ell_1}{q}\left[-\epsilon_{jk\ell} f_k \overline{u_i' u_\ell'} - \epsilon_{ik\ell} f_k \overline{u_j' u_\ell'}\right] \tag{31}$$

$$\frac{\partial}{\partial t}(\overline{\theta'^2}) + \bar{u}_k \frac{\partial \overline{\theta'^2}}{\partial x_k} - \frac{\partial}{\partial x_k}\left[q \lambda_3 \frac{\partial \overline{\theta'^2}}{\partial x_k}\right] = -2\,\overline{u_k'\theta'}\,\frac{\partial \bar{\Theta}}{\partial x_k} - \frac{2q}{\Lambda_2}\overline{\theta'^2} \tag{26}$$

$$\overline{u_j'\theta'} = \frac{3\ell_2}{q}\left[\beta g\,\overline{\theta'^2}\delta_{3j} - \overline{u_j' u_k'}\,\frac{\partial \bar{\Theta}}{\partial x_k} - \overline{u_k'\theta'}\,\frac{\partial \bar{u}_j}{\partial x_k} - \epsilon_{jk\ell} f_k \overline{u_\ell'\theta'}\right] \tag{32}$$

$$\frac{\partial}{\partial t}(\overline{r'\theta'}) + \bar{u}_k \frac{\partial}{\partial x_k}(\overline{r'\theta'}) = \frac{\partial}{\partial x_k}\left[q \lambda_2 \frac{\partial \overline{r'\theta'}}{\partial x_k}\right] - \overline{u_k'\theta'}\,\frac{\partial \bar{R}}{\partial x_k}$$
$$- \overline{u_k' r'}\,\frac{\partial \bar{\Theta}}{\partial x_k} - \frac{2q}{\Lambda_2}\overline{r'\theta'} \tag{28}$$

$$\overline{u_i' r'} = \frac{3\ell_2}{q}\left[\beta g\,\overline{r'\theta'}\,\delta_{3i} - \overline{u_i' u_k'}\,\frac{\partial \bar{R}}{\partial x_k} - \overline{u_k' r'}\,\frac{\partial \bar{u}_i}{\partial x_k} - \epsilon_{ik\ell} f_k \overline{u_\ell' r'}\right] \tag{33}$$

$$\frac{\partial}{\partial t}(\overline{r'^2}) + \bar{u}_k \frac{\partial}{\partial x_k}(\overline{r'^2}) = \frac{\partial}{\partial x_k}\left[q \lambda_3 \frac{\partial \overline{r'^2}}{\partial x_k}\right] - 2\,\overline{u_k' r'}\,\frac{\partial \bar{R}}{\partial x_k} - \frac{2q}{\Lambda_2}\overline{r'^2} \tag{29}$$

In the PBL, the horizontal length scale is much greater than the vertical scale height. The final equations, therefore, contain only z derivatives of perturbation quantities. Neglecting advection of mean velocity and mean mixing ratio by the mean wind while retaining temperature advection (because it may be estimated by the thermal wind relationship) will yield equations (34-37) for the mean variables. In this model, the vertical velocity, $\overline{w}$, has been set equal to zero at all levels. Also, virtual potential temperature, $\overline{\Theta}_v$, is used to take into account the presence of water vapor and its effect on density. The term of equation (9) containing the kinematic diffusivity of water vapor is neglected.

$$\frac{\partial \overline{u}}{\partial t} - f\overline{v} = - \frac{\partial}{\partial z} (\overline{u'w'}) - \frac{1}{\rho_o} \frac{\partial \overline{P}}{\partial x} \tag{34}$$

$$\frac{\partial \overline{v}}{\partial t} + f\overline{u} = - \frac{\partial}{\partial z} (\overline{v'w'}) - \frac{1}{\rho_o} \frac{\partial \overline{P}}{\partial y} \tag{35}$$

$$\frac{\partial \overline{\Theta}_v}{\partial t} + \overline{u} \frac{\partial \overline{\Theta}_v}{\partial x} + \overline{v} \frac{\partial \overline{\Theta}_v}{\partial y} = - \frac{\partial}{\partial z} (\overline{w'\theta'_v}) + \sigma \tag{36}$$

$$\frac{\partial \overline{R}}{\partial t} = - \frac{\partial}{\partial z} (\overline{w'r'}) \tag{37}$$

An estimation of the horizontal virtual potential temperature gradient can be obtained as follows (Hess, 1959). Geostrophically,

$$u_g = - \frac{1}{f\rho_o} \frac{\partial \overline{P}}{\partial y} \tag{38}$$

$$v_g = \frac{1}{f\rho_o} \frac{\partial \overline{P}}{\partial x} \tag{39}$$

therefore, $fv_g = R\overline{T} \dfrac{\partial \ln \overline{P}}{\partial x}$

Taking a $\hat{z}$ derivative of this expression and using the hydrostatic approximation,

$$\frac{\partial \ln \overline{P}}{\partial x} = - \frac{g}{T}$$

$$R \frac{\partial}{\partial x} \left(- \frac{g}{T}\right) = f \frac{\partial}{\partial x} \left(\frac{v_g}{\overline{T}}\right)$$

$$\frac{\partial v_g}{\partial z} = \frac{g}{f\overline{T}} \frac{\partial \overline{T}}{\partial x} + \overset{\approx 0}{\cancel{\frac{v_g}{\overline{T}} \frac{\partial \overline{T}}{\partial x}}}$$

Therefore, $\dfrac{\partial \overline{T}}{\partial x} \simeq \dfrac{f\overline{T}}{g} \dfrac{\partial v_g}{\partial z}$

with $\overline{\Theta}_v = \overline{T}_v + (1 + 0.61\overline{R})\nu_d z$

$$\frac{\partial \overline{\Theta}_v}{\partial x} \simeq \frac{\partial \overline{T}_v}{\partial x} \simeq \frac{f\overline{T}_v}{g} \frac{\partial v_g}{\partial z} \tag{40}$$

similarly, $$\frac{\partial\overline{\Theta}_v}{\partial y} \simeq - \frac{f\overline{T}_v}{g} \frac{\partial u_g}{\partial z} \qquad (41)$$

The approximations (38-41) in equations (34-37) will yield the final equations (42-45) for the mean variables. All the final equations appear in Table IV.

The final equations for the second moments are obtained from the equations of Table III by neglecting advection by the mean wind and retaining only vertical derivatives of perturbation variables in an analogous fashion with the procedure for the mean variable equations. The results are equations (46-61) in Table IV. Equations (46, 50, 51, and 52) represent only three independent equations because $q^2 \equiv \overline{u_k'^2}$. The Coriolis terms appear in all the appropriate equations in Table IV.

Table IV

The Final Level 3 Model Equations

Equations for the Mean Variables

$$\frac{\partial \bar{u}}{\partial t} - f(\bar{v} - v_g) = -\frac{\partial}{\partial z}(\overline{u'w'}) \tag{42}$$

$$\frac{\partial \bar{v}}{\partial t} + f(\bar{u} - u_g) = -\frac{\partial}{\partial z}(\overline{v'w'}) \tag{43}$$

$$\frac{\partial \bar{\Theta}_v}{\partial t} + \bar{u}\frac{f\bar{T}_v}{g}\frac{\partial v_g}{\partial z} - \bar{v}\frac{f\bar{T}_v}{g}\frac{\partial u_g}{\partial z} = -\frac{\partial}{\partial z}(\overline{w'\theta_v'}) \tag{44}$$

$$\frac{\partial \bar{R}}{\partial t} = -\frac{\partial}{\partial z}(\overline{w'r'}) \tag{45}$$

Equations for the Second Moments

$$\frac{\partial}{\partial t}(q^2) = \frac{\partial}{\partial z}\left[q\lambda_1 \frac{5}{3}\frac{\partial q^2}{\partial z}\right] - 2\overline{u'w'}\frac{\partial \bar{u}}{\partial z} - 2\overline{v'w'}\frac{\partial \bar{v}}{\partial z}$$

$$+ 2\beta g\overline{w'\theta_v'} - 2q^3/\Lambda_1 \tag{46}$$

$$\frac{\partial}{\partial t}(\overline{\theta_v'^2}) = \frac{\partial}{\partial z}\left[q\lambda_3 \frac{\partial \overline{\theta_v'^2}}{\partial z}\right] - 2\overline{w'\theta_v'}\frac{\partial \bar{\Theta}_v}{\partial z} - 2q\,\overline{\theta_v'^2}/\Lambda_2 \tag{47}$$

$$\frac{\partial}{\partial t}(\overline{r'\theta_v'}) = \frac{\partial}{\partial z}\left[q\lambda_2 \frac{\partial \overline{r'\theta_v'}}{\partial z}\right] - \overline{w'\theta_v'}\frac{\partial \bar{R}}{\partial z} - \overline{w'r'}\frac{\partial \bar{\Theta}_v}{\partial z} - \frac{2q}{\Lambda_2}\overline{r'\theta_v'} \tag{48}$$

$$\frac{\partial}{\partial t}(\overline{r'^2}) = \frac{\partial}{\partial z}\left[q\lambda_3 \frac{\partial \overline{r'^2}}{\partial z}\right] - 2\overline{w'r'}\frac{\partial \bar{R}}{\partial z} - 2q\frac{\overline{r'^2}}{\Lambda_2} \tag{49}$$

$$\overline{u'^2} = \frac{q^2}{3} - \frac{\ell_1}{q}\left[4\overline{u'w'}\frac{\partial\bar{u}}{\partial z} - 2\overline{v'w'}\frac{\partial\bar{v}}{\partial z} + 2\beta g\,\overline{w'\theta_v'}\right] + 6\frac{\ell_1}{q}\left[f_z\overline{u'v'} - f_y\overline{u'w'}\right] \tag{50}$$

$$\overline{v'^2} = \frac{q^2}{3} - \frac{\ell_1}{q}\left[4\overline{v'w'}\frac{\partial\bar{v}}{\partial z} - 2\overline{u'w'}\frac{\partial\bar{u}}{\partial z} + 2\beta g\,\overline{w'\theta_v'}\right] - \frac{6\ell_1}{q}f_z\overline{u'v'} \tag{51}$$

$$\overline{w'^2} = \frac{q^2}{3} - \frac{\ell_1}{q}\left[-2\overline{u'w'}\frac{\partial\bar{u}}{\partial z} - 2\overline{v'w'}\frac{\partial\bar{v}}{\partial z} - 4\beta g\,\overline{w'\theta_v'}\right] + \frac{6\ell_1}{q}f_y\overline{u'w'} \tag{52}$$

$$\overline{u'v'} = \frac{-3\ell_1}{q}\left[\overline{u'w'}\frac{\partial\bar{v}}{\partial z} + \overline{v'w'}\frac{\partial\bar{u}}{\partial z}\right] + \frac{3\ell_1}{q}\left[-f_z\overline{u'^2} - f_y\overline{v'w'} + f_z\overline{v'^2}\right] \tag{53}$$

$$\overline{u'w'} = -\frac{3\ell_1}{q}\left[(\overline{w'^2} - Cq^2)\frac{\partial\bar{u}}{\partial z} - \beta g\,\overline{u'\theta_v'}\right] + \frac{3\ell_1}{q}\left[f_y\overline{u'^2} - f_y\overline{w'^2} + f_z\overline{v'w'}\right] \tag{54}$$

$$\overline{v'w'} = -\frac{3\ell_1}{q}\left[(\overline{w'^2} - Cq^2)\frac{\partial\bar{v}}{\partial z} - \beta g\,\overline{v'\theta_v'}\right] + \frac{3\ell_1}{q}\left[f_y\overline{u'v'} - f_z\overline{u'w'}\right] \tag{55}$$

$$\overline{u'\theta_v'} = \frac{3\ell_2}{q}\left[-\overline{u'w'}\frac{\partial\bar{\Theta}_v}{\partial z} - \overline{w'\theta_v'}\frac{\partial\bar{u}}{\partial z} - f_y\overline{w'\theta_v'} + f_z\overline{v'\theta_v'}\right] \tag{56}$$

$$\overline{v'\theta_v'} = \frac{3\ell_2}{q}\left[-\overline{v'w'}\frac{\partial\bar{\Theta}_v}{\partial z} - \overline{w'\theta_v'}\frac{\partial\bar{v}}{\partial z} - f_z\overline{u'\theta_v'}\right] \tag{57}$$

$$\overline{w'\theta_v'} = \frac{3\ell_2}{q}\left[\beta g\,\overline{\theta_v'^2} - \overline{w'^2}\frac{\partial\bar{\Theta}_v}{\partial z} + f_y\overline{u'\theta_v'}\right] \tag{58}$$

$$\overline{u'r'} = \frac{3\ell_2}{q}\left[-\overline{u'w'}\frac{\partial\bar{R}}{\partial z} - \overline{w'r'}\frac{\partial\bar{u}}{\partial z} - f_y\overline{w'r'} + f_z\overline{v'r'}\right] \tag{59}$$

$$\overline{v'r'} = \frac{3\ell_2}{q}\left[-\overline{v'w'}\frac{\partial\bar{R}}{\partial z} - \overline{w'r'}\frac{\partial\bar{v}}{\partial z} - f_z\overline{u'r'}\right] \tag{60}$$

$$\overline{w'r'} = \frac{3\ell_2}{q}\left[\beta g\,\overline{r'\theta_v'} - \overline{w'^2}\frac{\partial\bar{R}}{\partial z} + f_y\overline{u'r'}\right] \tag{61}$$

## 3.3 The Length Scale Formulation

The level 3 equations contain three types of length scales. The $\Lambda$'s are dissipation length scales. The $\lambda$'s and $\ell$'s are diffusion and return-to-isotropy length scales, respectively. Every modeled term (see Table II) contains one of these length scales. Mellor and Yamada (1974) assume all the length scales are proportional and are given by:

$$(\ell_1, \ell_2, \Lambda_1, \Lambda_2, \lambda_1, \lambda_2, \lambda_3) =$$

$$(0.78,\ 0.79,\ 15.0,\ 8.0,\ 0.23,\ 0.23,\ 0.23)\,\ell \tag{62}$$

They evaluate $\ell$ using Blackadar's interpolation formula (Blackadar, 1962).

$$\ell = \frac{kz}{1 + \dfrac{kz}{\ell_o}} \tag{63}$$

Therefore,

$$\ell \to kz \quad \text{as} \quad z \to 0$$

$$\ell \to \ell_o \quad \text{as} \quad z \to \infty$$

Mellor and Yamada proposed equation (64) as a formulation for $\ell_o$ based on the turbulence energy profile.

$$\ell_o = \alpha \frac{\int_0^\infty zqdz}{\int_0^\infty qdz}, \quad \alpha \text{ constant} \tag{64}$$

In the analysis of Yamada and Mellor (1975), $\alpha$ was assumed to be 0.10. A sensitivity test, however, showed that the mean variables were fairly insensitive to a 50% reduction in $\alpha$. The turbulence quantities, unfortunately, are not insensitive to the value of $\alpha$.

Using a typical early afternoon distribution of $q^2$, $\ell(z)$ is evaluated for values for $\alpha$ of 0.05 and 0.10 (Figure 1). The PBL top (h) is indicated. The length scale is within 10% of $\ell_o$ at about $z/h = 0.5$ for $\alpha = 0.05$ and at $z/h = 0.7$ for $\alpha = 0.10$. Above this, $\ell$ changes very little.

A new determination of $\ell_o$ (equations 65) is proposed which yields a $\ell(z)$ profile similar in shape in the PBL to Deardorff's (1973, 1974) profile of the turbulence energy dissipation length scale. Figure 2 shows $\ell(z)$ for the same $q^2$ distribution as Figure 1.

$$\ell_o = \alpha(z) \frac{\int_0^h zqdz}{\int_0^h qdz} \tag{65a}$$

where,

$$\alpha(z) = \begin{cases} \alpha_1 & z < \frac{h}{2} \\ \alpha_1 - \left(\frac{h/2 - z}{h/2 - h}\right)(\alpha_1 - \alpha_2) & \frac{h}{2} \leq z < h \\ \alpha_2 & h \leq z \end{cases} \tag{65b}$$

$$(\alpha_1, \alpha_2) = (0.10,\ 0.05) \tag{65c}$$

As one moves from h/2 down to the ground, the length scale decreases toward zero. As the ground is approached, the characteristic size of the turbulent eddies is limited by z, the distance to the solid boundary. The length scale approaches kz. For large z, the influence of the ground in limiting the characteristic eddy size diminishes quickly. As z increases beyond h/2, however, there is another factor influencing the turbulence structure, and that is the temperature inversion base at h. The larger turbulent eddies are probably found in the middle of the PBL, where the distance away from any damping influence on their size is maximized.

Above h, Deardorff (1974) points out that $\ell$ increases with height because the perturbation energy is contained in gravity waves exhibting little diffusion or dissipation of energy. The perturbation energy contained

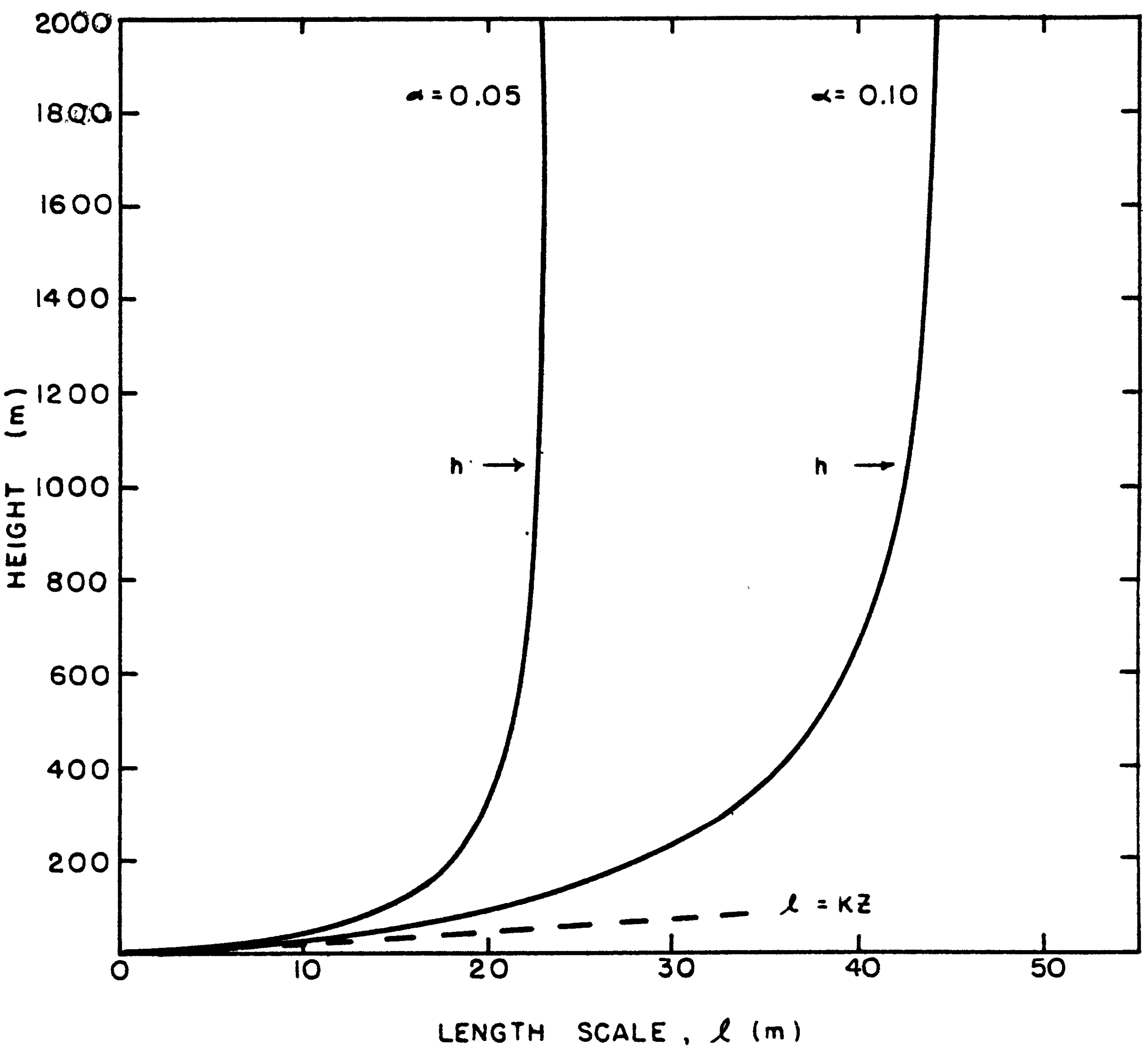


Fig. 1. Vertical profiles of the length scale, ℓ, for two values of α, based on the formulation of Yamada and Mellor (1975).

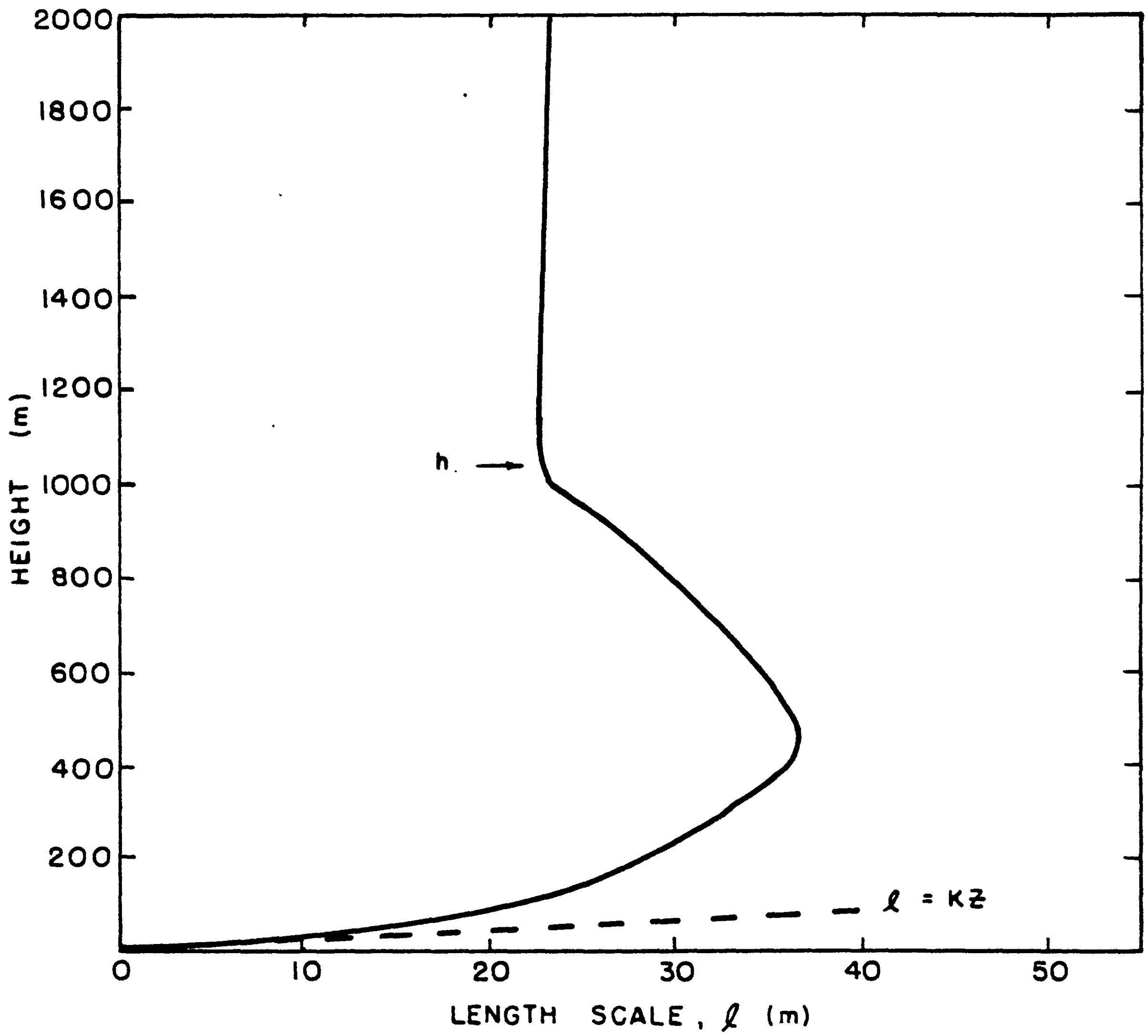


Fig. 2. Vertical profile of the length scale, $\ell$, based on the new formulation defined by equations (65).

in this region is negligible compared to $q^2$ in the PBL, and the length scale formulation above h has little effect on the turbulence structure in the PBL.

The length scale formulation represented by equation (64) (Figure 1) does not allow the stably stratified layer above the PBL to have any influence on reducing the characteristic eddy size (and therefore the length scale). Equations (65), however, force $\ell$ to approach, in the region $z > h/2$, a smaller, constant value. For these reasons, we have adopted this formulation for $\ell$.

# 4. BOUNDARY CONDITIONS

## 4.1 Mean Variables

It is necessary to provide an upper and a lower boundary condition for each prognostic variable in order to find solutions of the level 3 equations. A staggered grid is used in which the mean variables are defined at the integer grid point levels. Turbulence variables and z derivatives of mean quantities are defined at the half integer grid points. The lowest integer grid point is at the roughness height, $z_o$ (0.01 m). The top of the grid (grid point 43.5) is at 2022 m. Appendix B contains a more complete description of the grid system.

The definition of the roughness height provides the lower boundary conditions for $\overline{u}$ and $\overline{v}$:

$$\overline{u}\ (z_o) = 0.0 \tag{66}$$

$$\overline{v}\ (z_o) = 0.0 \tag{67}$$

A simplified, single layer ground thermodynacmis model ($H_a$ forcing, Deardorff, 1978) was used to predict the values of $\overline{\Theta}_v$ and $\overline{R}$ at $z_o$. The ground temperature, Tg, is predicted by the model based on net radiative heating (or cooling), phase changes of the ground water (or frost), and the heat flux at grid point 1/2 (0.07 m). The value of $\overline{\Theta}_v\ (z_o)$ is assumed to be equal to the virtual potential ground temperature $\overline{\Theta}_v$ (0). $\overline{\Theta}_v(z_o)$, therefore, is probably somewhat too high during unstable conditions and slightly underestimated during stable conditions.

The mixing ratio at $z_o$ is determined utilizing soil wetness parameters and the turbulent moisture flux at 0.07 m.

The upper boundary conditions are applied at the 2022 m level. The vertical virtual potential temperature gradient is assumed to approach a constant (stable) value. The vertical derivatives of $\overline{u}$, $\overline{v}$, and $\overline{R}$ are assumed to be zero (Yamada and Mellor, 1975; Deardorff, 1973). Therefore, at 2022 m,

$$\frac{\partial \overline{\Theta}_v}{\partial z} = 0.001 \quad {}^\circ\text{k/m} \tag{68}$$

$$\frac{\partial \overline{u}}{\partial z} = 0 \qquad \frac{\partial \overline{v}}{\partial z} = 0 \qquad \frac{\partial \overline{R}}{\partial z} = 0 \tag{69a,b,c}$$

## 4.2 Second Moments

The second moments requiring boundary conditions are: $q^2, \overline{\theta_v'^2}$, $\overline{r'^2}$, and $\overline{r'\theta_v'}$. The lower boundary conditions are obtained by assuming each of the preceding variables is in equilibrium at the lowest half integer grid point (0.07 m). The time derivatives of equations (46-49), therefore, vanish, yielding:

$$q^2(0.07\text{ m}) = \frac{\Lambda_1}{2q}\{\frac{\partial}{\partial z}[q\lambda_1 \frac{5}{3} \frac{\partial q^2}{\partial z}] - 2\overline{u'w'}\frac{\partial\overline{u}}{\partial z}$$

$$- 2\overline{v'w'}\frac{\partial\overline{v}}{\partial z} + 2\beta g\overline{w'\theta_v'}\} \tag{70}$$

$$\overline{\theta_v'^2}\ (0.07\text{ m}) = \frac{\Lambda_2}{2q}\{\frac{\partial}{\partial z}[q\lambda_3 \frac{\partial\overline{\theta_v'^2}}{\partial z}] - 2\overline{w'\theta_v'}\frac{\partial\overline{\Theta}_v}{\partial z}\} \tag{71}$$

$$\overline{r'^2}\ (0.07\text{ m}) = \frac{\Lambda_2}{2q}\{\frac{\partial}{\partial z}[q\lambda_3 \frac{\partial\overline{r'^2}}{\partial z}] - 2\overline{w'r'}\frac{\partial\overline{R}}{\partial z}\} \tag{72}$$

$$\overline{r'\theta_v'}\ (0.07\text{ m}) = \frac{\Lambda_2}{2q}\{\frac{\partial}{\partial z}[q\lambda_2 \frac{\partial\overline{r'\theta_v'}}{\partial z}] - \overline{w'\theta_v'}\frac{\partial\overline{R}}{\partial z} - \overline{w'r'}\frac{\partial\overline{\Theta}_v}{\partial z}\} \tag{73}$$

The calculated value of the ratio $|\overline{r'\theta_v'}|/(\overline{r'^2}\cdot\overline{\theta_v'^2})^{1/2}$, at z = 0.07 m, was sometimes in excess of 1. Whenever this occurred, equation (73) was replaced by:

$$|\overline{r'\theta_v'}| = (\overline{r'^2}\cdot\overline{\theta_v'^2})^{1/2}, \quad z = 0.07\text{ m}. \tag{74}$$

This restriction of $\overline{r'\theta_v'}$ was applied only at the lowest grid point. Wyngaard et al. (1978) reported observed $r'$-$\theta_v'$ correlation coefficients, above a warm evaporating surface, very close to unity.

Yamada and Mellor (1975) utilize boundary conditions for $q^2$ and $\overline{\theta_v'^2}$ of the form:

$$q^2\ (0) = C_1 u_*^2 \tag{75}$$

$$\overline{\theta_v'^2}\ (0) = C_2\ \frac{H^2}{u_*^2} \tag{76}$$

where $(C_1, C_2) = (0.61,\ 2.4)$,

$$u_*^2 = [(-\overline{u'w'}(0))^2 + (-\overline{v'w'}\ (0))^2]^{1/2} \quad ,$$

and

$$H = -\overline{w'\theta_v'}\ (0)$$

The model with equations (70-71) as boundary conditions yields ratios $q^2/u_*^2$ and $\theta_v'^2 u_*^2/H^2$ within a few percent of $C_1$ and $C_2$, respectively. The equilibrium boundary conditions, therefore, are consistent with observed surface turbulence structure, yet do not require the use of empirical constants.

The upper boundary conditions for the second moments consist of the requirements that $q^2$, $\overline{\theta_v'^2}$, $\overline{r'^2}$, and $\overline{r'\theta_v'}$ vanish at the upper boundary (2022 m).

$$q^2 = 0 \quad , \quad \overline{\theta_v'^2} = 0 \tag{76a,b}$$

$$\overline{r'^2} = 0 \quad , \quad \overline{r'\theta_v'} = 0 \tag{76c,d}$$

The 2022 m level is sufficiently high to ensure the PBL is contained within the grid, and the turbulence moments can be expected to quickly approach zero outside of the PBL.

# 5. SOLUTION OF THE EQUATIONS

## 5.1 Reducing the Prognostic Equations into a Single Form

When the mean velocity components are expressed in complex form, $\bar{u} + i\bar{v}$, equations (42-49) can be reduced to a single form:

$$\frac{\partial \phi}{\partial t} = \frac{\partial}{\partial z} (P_1 \frac{\partial \phi}{\partial z}) - P_2 \phi + P_3 \tag{77}$$

where $\phi$ is the variable to be incremented in time. Table V summarizes the discussion to follow and contains the P's for each $\phi$.

The Reynolds stress and heat flux equations (50-58) are 9 simultaneous equations. Yamada and Mellor (1974) provide a solution of the equations with the Coriolis terms omitted. The Coriolis terms, however, complicate these equations considerably. Appendix A contains the details of a solution of the 9 equations with the Coriolis terms, utilizing a back-substitution method. The solution for $\overline{u'w'}$ and $\overline{v'w'}$ is shown to reduce to Yamada's and Mellor's solution in the special case of no Coriolis terms. Also contained in Appendix A is the solution of the 3 moisture flux equations.

Due to the complexity of the expressions for $\overline{u'w'}$, $\overline{v'w'}$, and $\overline{w'\theta_v'}$, the flux divergence terms of equations (42-44) are identified with $P_3$ in Table V. The moisture flux

Table V

Representation of the Prognostic Equations in a Standard Form

| Equation No. | $\phi$ | $P_1$ | $P_2$ | $P_3$ |
|---|---|---|---|---|
| 42, 43 | $v_c$ | 0 | $if$ | $ifv_{cg} - \frac{\partial}{\partial z}(\overline{v_c'w'})$ |
| 44 | $\overline{\Theta}_v$ | 0 | 0 | $\frac{f\overline{T}_v}{g}(\overline{v}\frac{\partial u_g}{\partial z} - \overline{u}\frac{\partial v_g}{\partial z}) - \frac{\partial}{\partial z}(\overline{w'\theta_v'})$ |
| 45 | $\overline{R}$ | $K_w$ | 0 | $-\frac{\partial \gamma_R}{\partial z}$ |
| 46 | $q^2$ | $\frac{5}{3}q\lambda_1$ | $\frac{2q}{\Lambda_1}$ | $-2\overline{u'w'}\frac{\partial \overline{u}}{\partial z} - 2\overline{v'w'}\frac{\partial \overline{v}}{\partial z} + 2\beta g\overline{w'\theta_v'}$ |
| 47 | $\overline{\theta_v'^2}$ | $q\lambda_3$ | $\frac{2q}{\Lambda_2}$ | $-2\overline{w'\theta_v'}\frac{\partial \overline{\Theta}_v}{\partial z}$ |
| 48 | $\overline{r'\theta_v'}$ | $q\lambda_2$ | $\frac{2q}{\Lambda_2} + A\frac{\partial \overline{\Theta}_v}{\partial z}$ | $-\overline{w'\theta_v'}\frac{\partial \overline{R}}{\partial z} + B\frac{\partial \overline{\Theta}_v}{\partial z}$ |
| 49 | $\overline{r'^2}$ | $q\lambda_3$ | $\frac{2q}{\Lambda_2}$ | $-2\overline{w'r'}\frac{\partial \overline{R}}{\partial z}$ |

$v_c = \overline{u} + i\overline{v}$ , $v_{cg} = u_g + iv_g$ , $v_c' = u' + iv'$

divergence term of equation (45), however, is written as:

$$\frac{\partial}{\partial z}(-\overline{w'r'}) = \frac{\partial}{\partial z}\left(K_w \frac{\partial \overline{R}}{\partial z} - \gamma_R\right) \tag{78}$$

where $K_w$ and $\gamma_R$ are evaluated in Appendix A.

The identification of the terms of the second moment equations (46-49) with the P's is straightforward. It was necessary, however, to write the $\overline{w'r'}\ \frac{\partial \overline{\Theta}_v}{\partial z}$ term of equation (48) as:

$$\overline{w'r'}\ \frac{\partial \overline{\Theta}_v}{\partial z} = [A\overline{r'\theta_v'} - B]\ \frac{\partial \overline{\Theta}_v}{\partial z} \tag{79}$$

where A and B are evaluated in Appendix A. Equation (79) allows the $\overline{r'\theta_v'}$ dependence of $\overline{w'r'}$ to be evaluated implicitly, thereby eliminating some numerical stability problems which were encountered with the $\overline{r'\theta_v'}$ equation.

5.2 Finite-Difference Approximation

A transformed coordinate system is used in the model. Vertical derivatives of any quantity, $\phi$, are evaluated by:

$$\left.\frac{\partial \phi}{\partial z}\right|_j = a_j\{\phi_{j+1/2} - \phi_{j-1/2}\} \tag{80}$$

Equation (80) is the finite-difference form of equation (B-3) (see Appendix B). Equation (77) is approximated with the following finite-difference equation:

$$\frac{\phi_j^{k+1} - \phi_j^k}{\delta t} = \frac{a_j}{2} \{ [(P_1 a)_{j+1}^k + (P_1 a)_j^k] \phi_{j+1}^{k+1} - [(P_1 a)_{j+1}^k$$

$$+ 2(P_1 a)_j^k + (P_1 a)_{j-1}^k] \phi_j^{k+1} + [(P_1 a)_j^k + (P_1 a)_{j-1}^k] \phi_{j-1}^{k+1} \}$$

$$- (P_2)_j^k \phi_j^{k+1} + (P_3)_j^k \tag{81}$$

(Yamada and Mellor, 1975).

This finite difference scheme is an implicit scheme with truncation errors of order $\delta t$ and $(\delta x)^2$ (Richtmyer and Morton, 1967).

The $P_1$ for equation (45), i.e., $K_w$, is not defined at the integer grid points, but only at half integer grid levels. The terms of equation (81) involving $[(P_1 a)_{j+1}^k + (P_1 a)_j^k]/2$ are therefore replaced by $(P_1 a)_{j+1/2}^k$.

The Gaussian elimination method is used to solve the implicit finite difference equation (from Richtmyer and Morton, 1967). Expressing equation (81) in the following form:

$$-A_j^k \phi_{j+1}^{k+1} + B_j^k \phi_j^{k+1} - C_j^k \phi_{j-1}^{k+1} = D_j^k \tag{82}$$

where the coefficients $A_j$, $B_j$, $C_j$, and $D_j$ are all known at time step k. Solutions are assumed to be of the form:

$$\phi_j^{k+1} = E_j \phi_{j+1}^{k+1} + F_j \quad . \tag{83}$$

with j = j-1, equation (83) becomes:

$$\phi_j^{k+1} = E_{j-1} \phi_j^{k+1} + F_{j-1} \tag{84}$$

Inserting equation (84) into equation (82),

$$\phi_j^{k+1} = \frac{A_j}{B_j - C_j E_{j-1}} \phi_{j+1}^{k+1} + \frac{D_j + C_j F_{j-1}}{B_j - C_j E_{j-1}} \tag{85}$$

and comparing equation (83) with (85), gives expressions for $E_j$ and $F_j$.

$$E_j = \frac{A_j}{B_j - C_j E_{j-1}} \tag{86}$$

$$F_j = \frac{D_j + C_j F_{j-1}}{B_j - C_j E_{j-1}} \tag{87}$$

Applying the appropriate bottom boundary conditions will yield $E_1$ and $F_1$. Knowing $E_1$ and $F_1$, as well as the coefficients A, B, C, and D, $E_2$ and $F_2$ can be determined with equations (86-87). Applying this procedure for each level, all the E's and F's can be determined.

The upper boundary conditions and equation (83) can be used to determine $\phi$ at the top level. Because all the E's and F's are now known, equation (83) can be used to determine all the $\phi$'s, at time step k+1, from the top level down to the bottom.

# 6. SIMULATION OF DAY 33 OF THE WANGARA EXPERIMENT

## 6.1 Initial Conditions

Initial values for the mean variables, $\overline{u}$, $\overline{v}$, $\overline{\Theta}_v$, and $\overline{R}$ are the observed values at 0900 hours of Day 33 of the Wangara Experiment (Figures 3-5). Clarke et al. (1971) tabulate values for these variables at 50 m intervals below 1000 m and at 100 m intervals between 1000 m and 2000 m. Values at the grid levels are interpolated from the observed values. The $\overline{T}_v$ profile has been smoothed in the region 400-800 m to remove a slightly unstable lapse rate in that area. Initial values for the turbulence variables are generated by running the model for 1 hour starting with guessed values for the second moments (Yamada and Mellor, 1975). The initial and subsequent values of the geostrophic wind components, $u_g$ and $v_g$, were also calculated in the same way as Yamada and Mellor, using their data.

## 6.2 Results

The time-height variation of the velocity components $\overline{u}$ and $\overline{v}$ are presented in Figures 6 and 7. Agreement with the results of Yamada and Mellor and with observations is good. The nearly constant velocity profiles in the mixed layer during the day and the development of a low-level nocturnal jet are features of the velocity profiles noted by Yamada and Mellor which are also apparent in Figures 6 and 7.

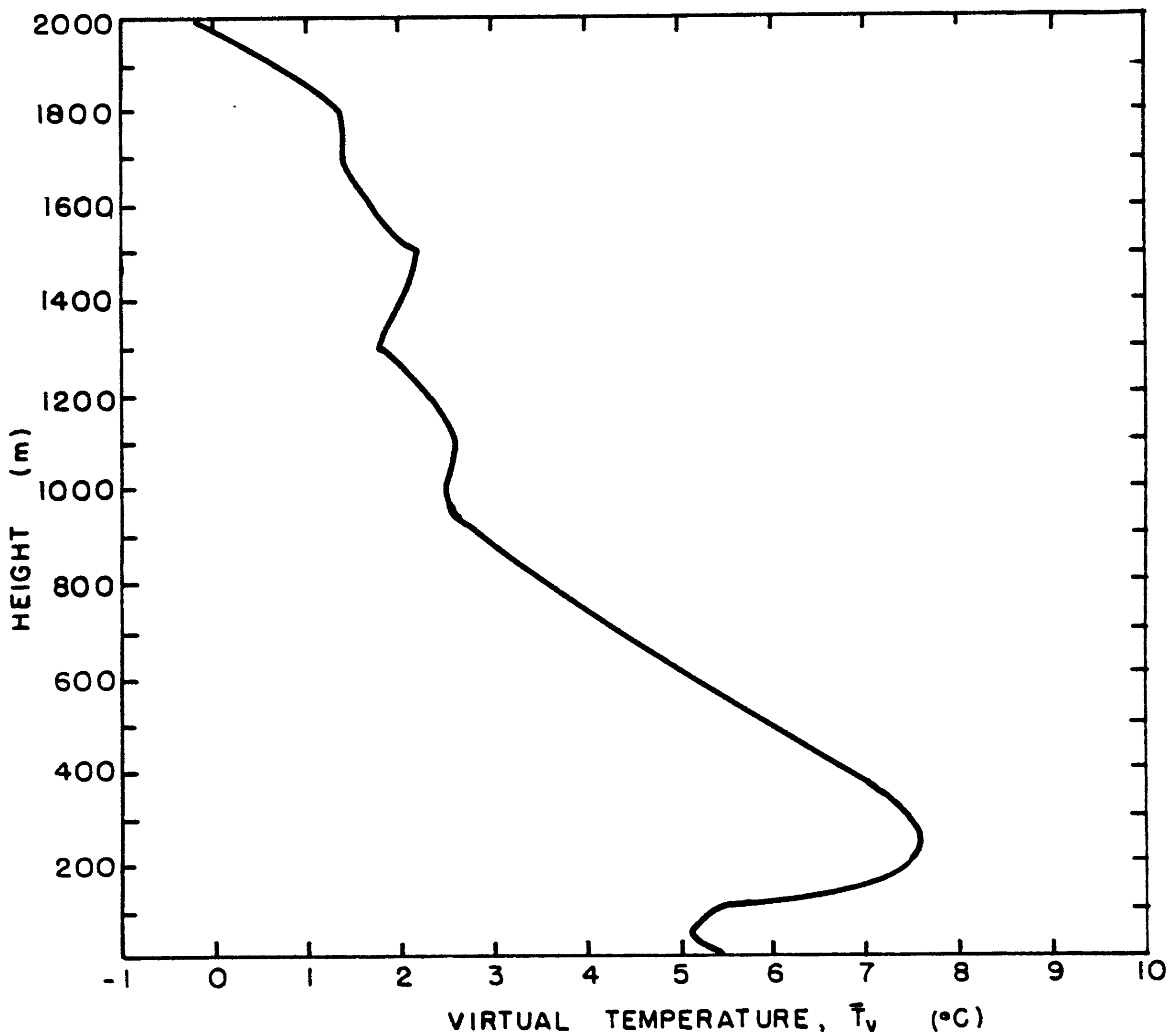


Fig. 3. Initial profile for virtual temperature, $\overline{T}_v$.

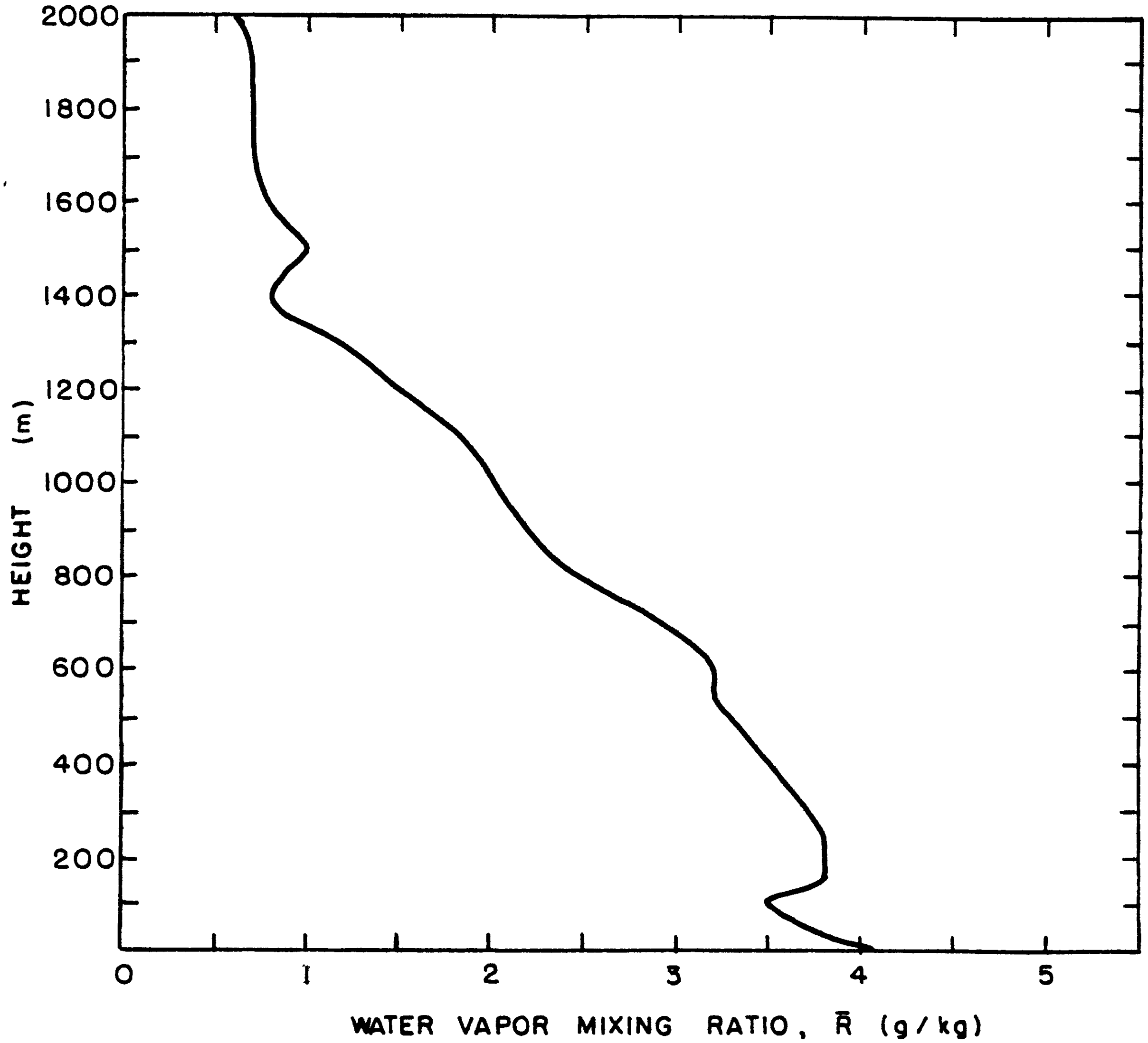


Fig. 4. Initial profile for water vapor mixing ratio, $\overline{R}$.

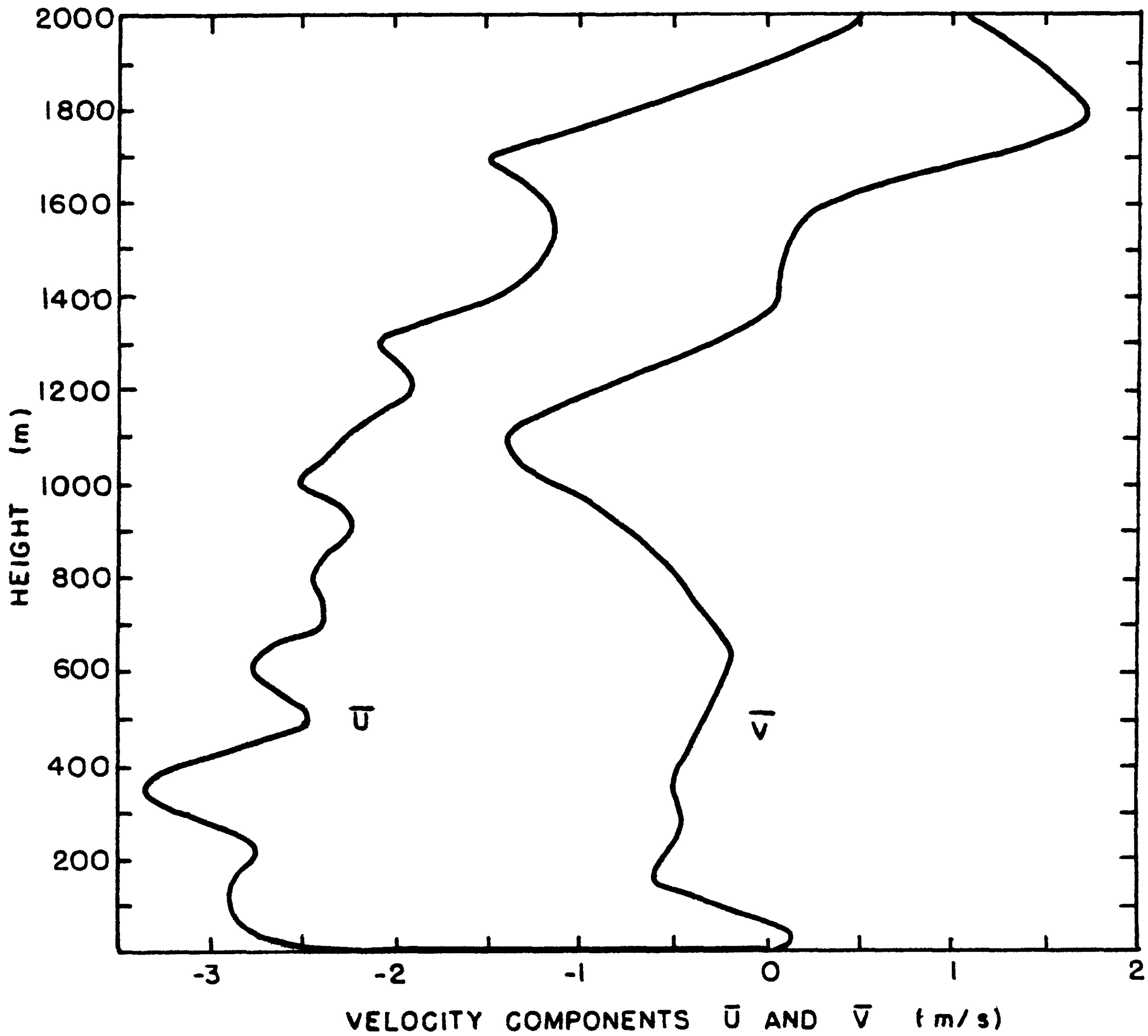


Fig. 5. Initial profiles for the eastward velocity component, $\bar{u}$, and the northward velocity component, $\bar{v}$.

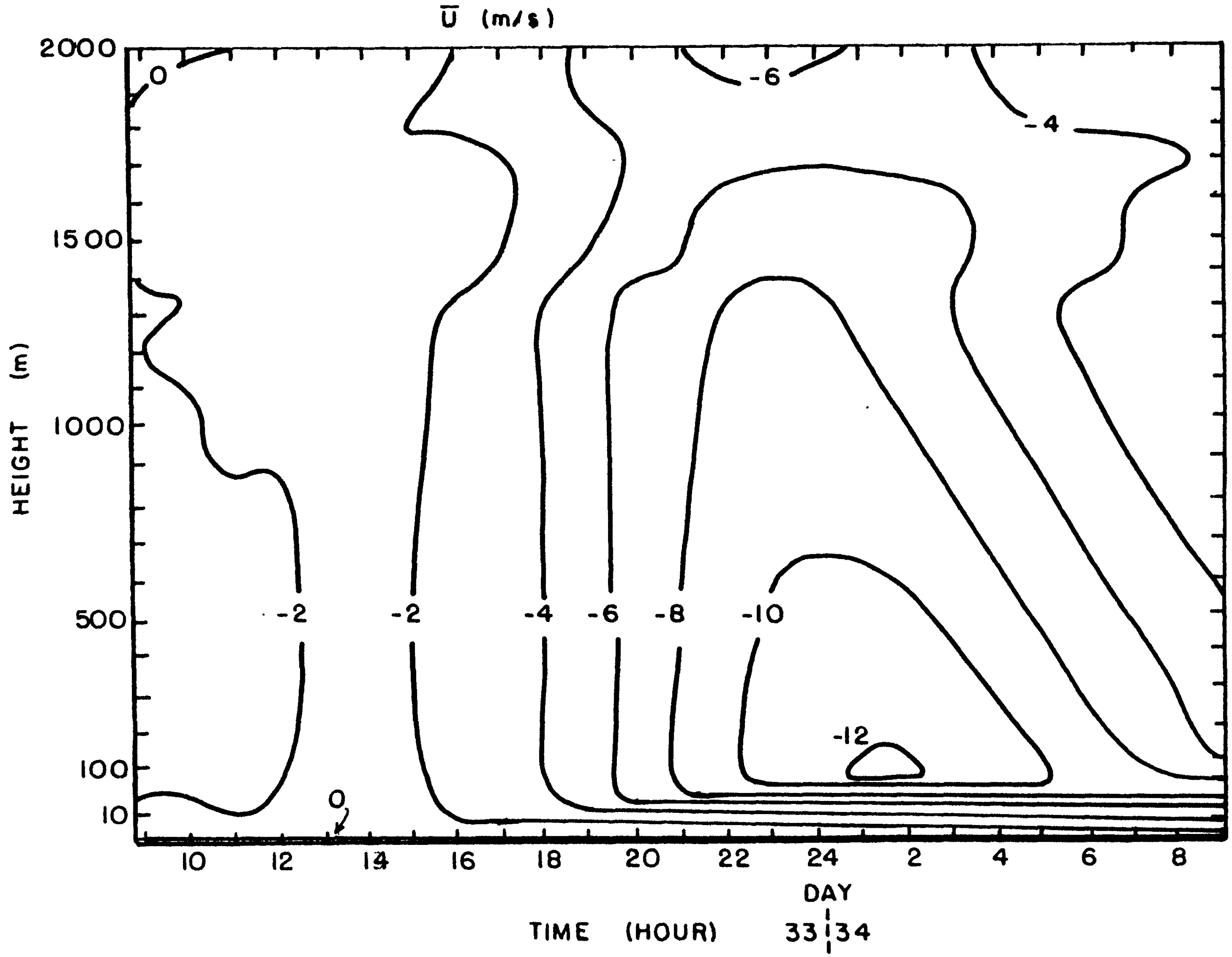


Fig. 6. Variation of the calculated mean velocity component, $\overline{u}$, as a function of time and height.

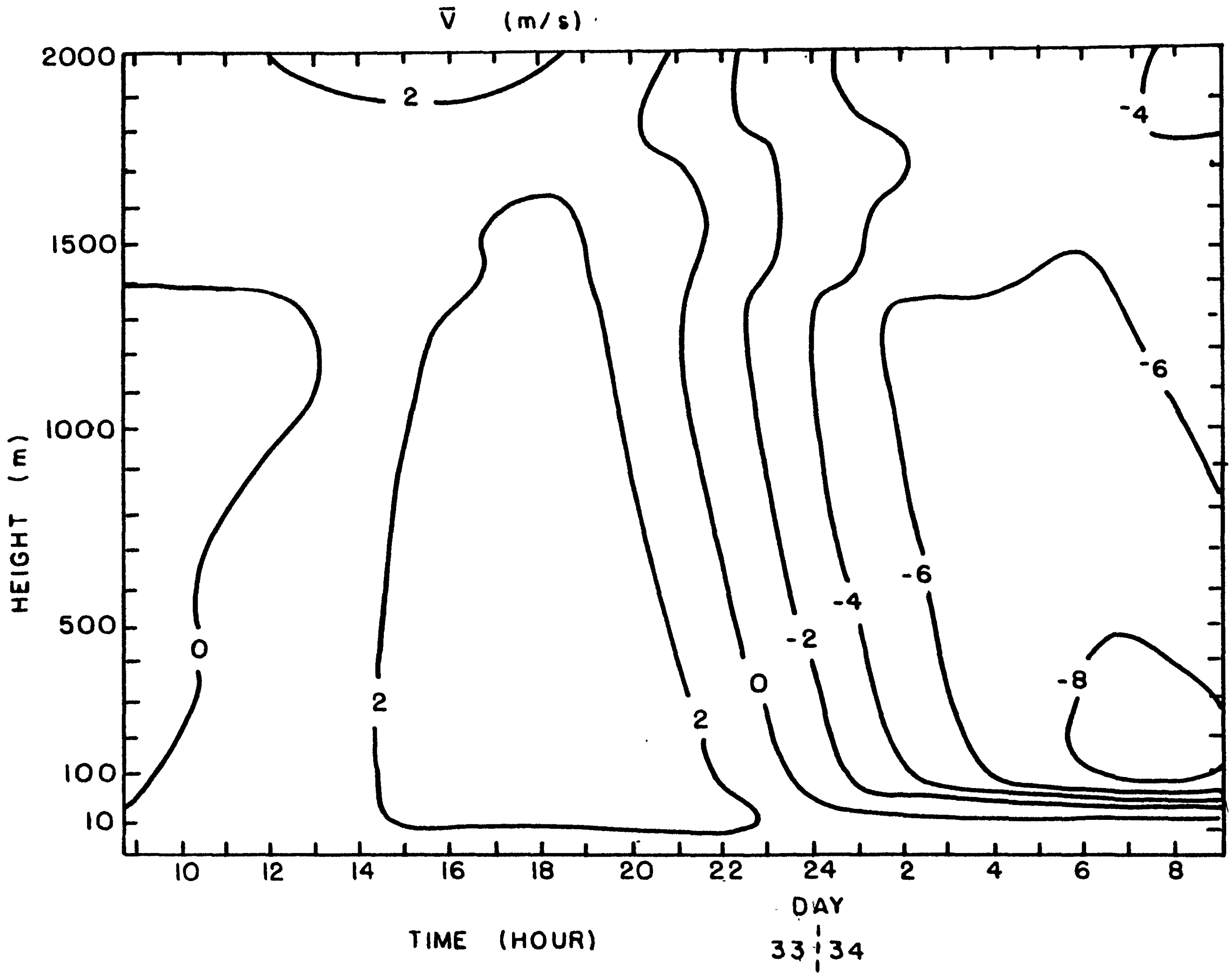


Fig. 7. Variation of the calculated mean velocity component, $\overline{v}$, as a function of time and height.

Figure 8 contains the mean virtual potential temperature variation. The rapid growth of the mixed layer with nearly constant $\overline{\Theta}_v$ can be seen. The surface layer is super-adiabatic during the late morning and afternoon hours as solar radiation heats the ground. A strong surface inversion develops after sunset. The time variation of the ground $\overline{\Theta}_v$, predicted by the ground thermodynamics model is shown in Figure 9. Agreement with Deardorff's (1974) values is good. The fall of the ground temperature after sunset is halted by the freezing of ground water, which releases latent heat. The ice is slow to melt during the morning of Day 34. This is a deficiency of the single layer ground model which keeps the ground temperature at 0°C until the ground ice in the entire layer has melted.

Examination of the observed $\overline{\Theta}_v$ variation (Yamada and Mellor, 1975) indicates that the daytime temperatures in Figure 8 are slightly too high. This can be attributed to the assumption that $\overline{\Theta}_v$ (ground) = $\overline{\Theta}_v$ $(z_o)$. The air temperature and heat flux at $z_o$ are somewhat overestimated during the day, yielding a warmer mixed layer. As a test, an additional simulation was run with $\overline{\Theta}_v$ $(z_o)$ reduced by about 8% (by increasing the ground albedo from 0.2 to 0.3). The resulting $\overline{\Theta}_v$ variation matched the observations very closely (also see Figure 28).

Yamada and Mellor reported that the longwave flux divergence term of the $\overline{\Theta}_v$ equation influenced the predicted

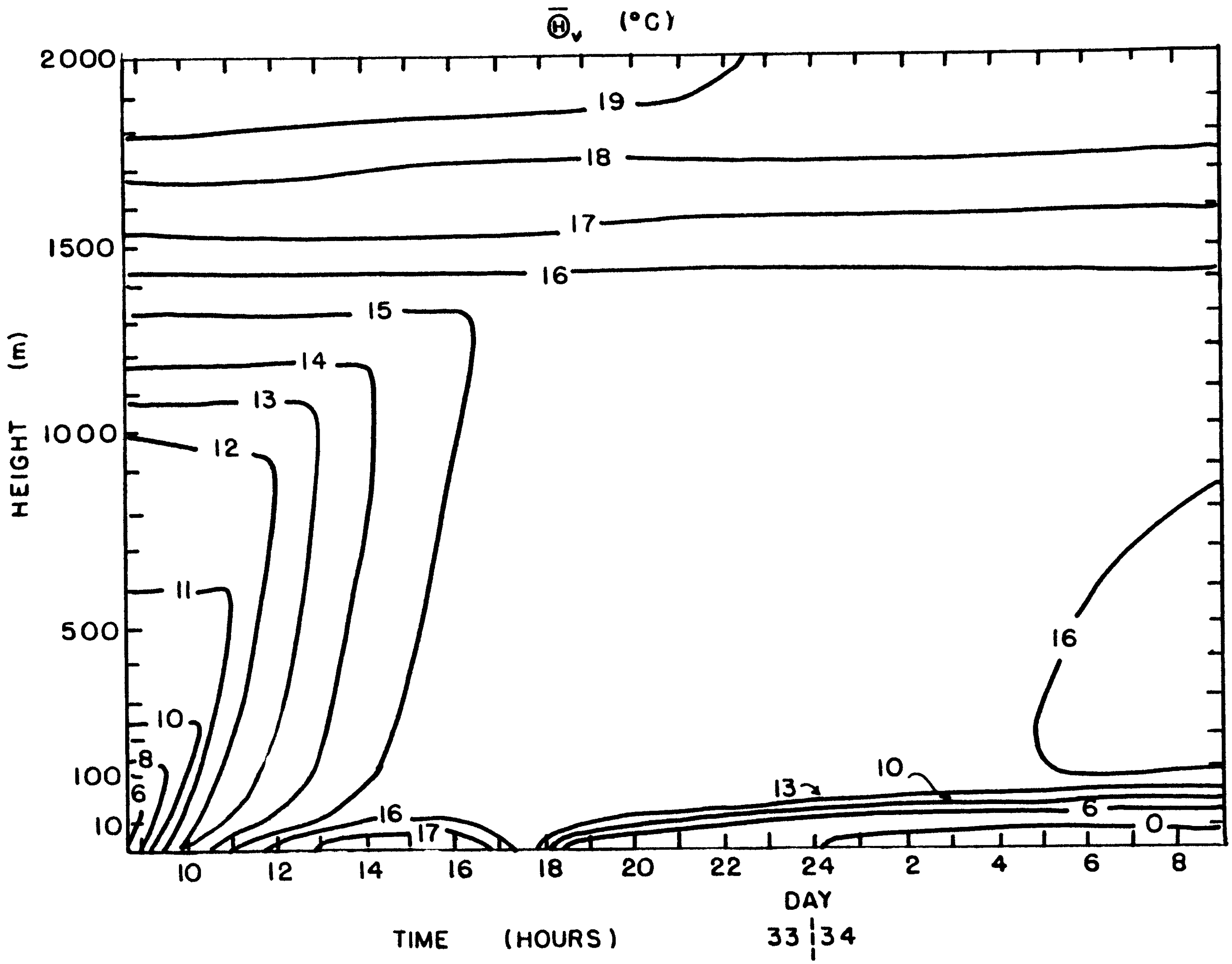


Fig. 8. Variation of the calculated mean virtual potential temperature, $\overline{\Theta}_v$, as a function of time and height.

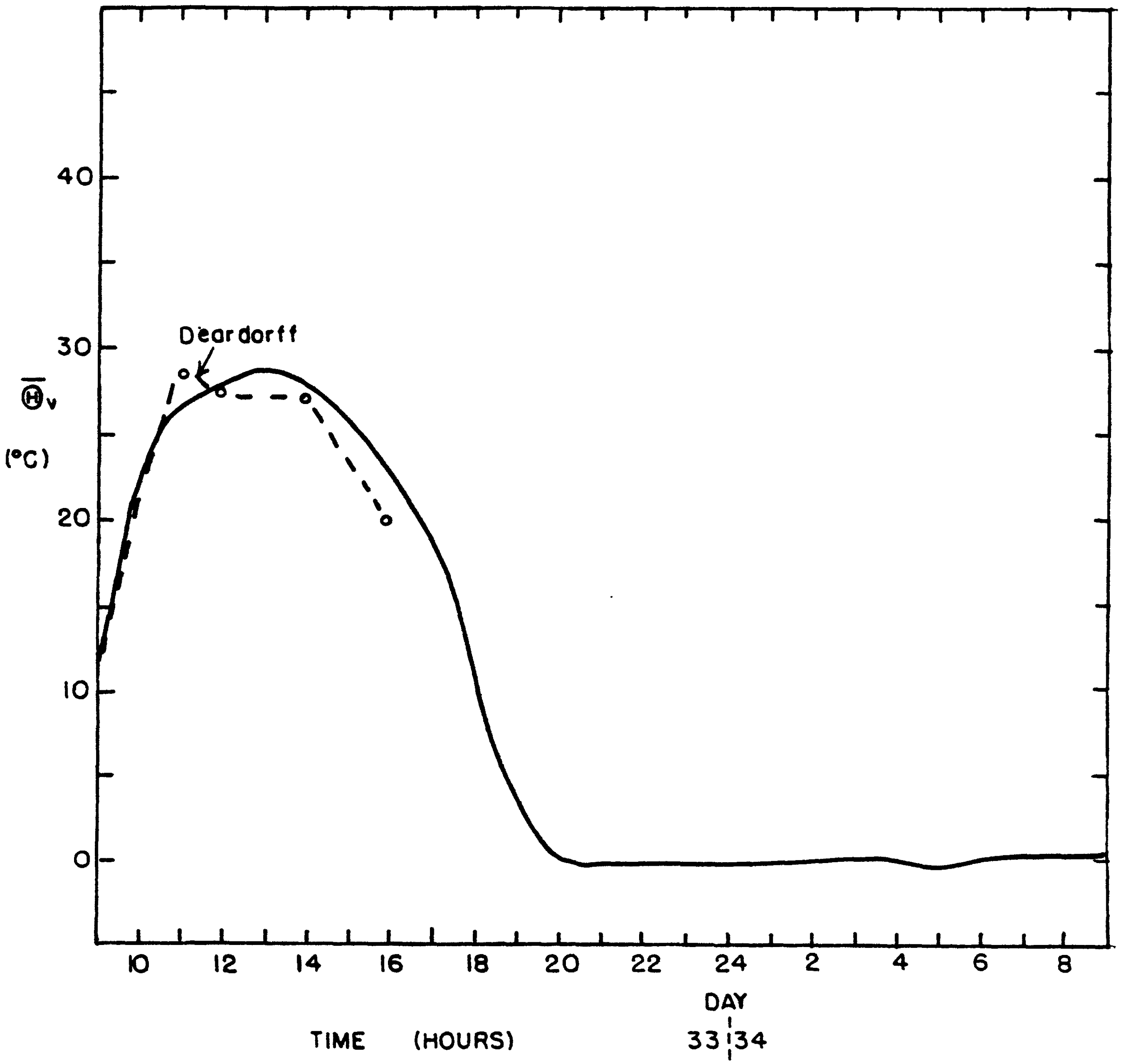


Fig. 9. Calculated surface $\overline{\Theta}_v$ as a function of time.

nighttime $\overline{\Theta}_v$ values measurably. Our neglect of the radiation term explains the warmer nighttime $\overline{\Theta}_v$ values indicated in Figure 8.

The mean water vapor mixing ratio, $\overline{R}$, is shown in Figure 10. $\overline{R}$ $(z_o)$ is shown in Figure 11. Moisture in the surface layer increases in the morning as the ground water evaporates. As the mixed layer develops from 1000-1200 hours, the surface moisture is carried upward (resulting in the bulge of the 3.5 and 4.0 contour lines at this time). The afternoon boundary layer dries out because the moisture flux at the boundary layer top exceeds the surface moisture flux as all the soil moisture evaporates.

The time-height variation of twice the turbulence kinetic energy is shown in Figure 12. The development of the strong daytime turbulence is due to bouyant generation (see Figure 13). Stress production and diffusion are negligible except close to the ground. At the end of the day bouyant generation becomes small or negative. The dissipation of turbulence energy, proportional to $q^3$ is now unopposed and quickly eliminates most of the turbulence. A second effect is the variation of the length scale (Figure 14). As the level of turbulence in the boundary layer decreases, the length scale also decreases. Dissipation, being proportional to $1/\ell$, increases for a given value of $q^3$. Figure 14 compares closely with the variation of $\ell$ calculated by Yamada and Mellor (1975) in the region $z < 500$ m.

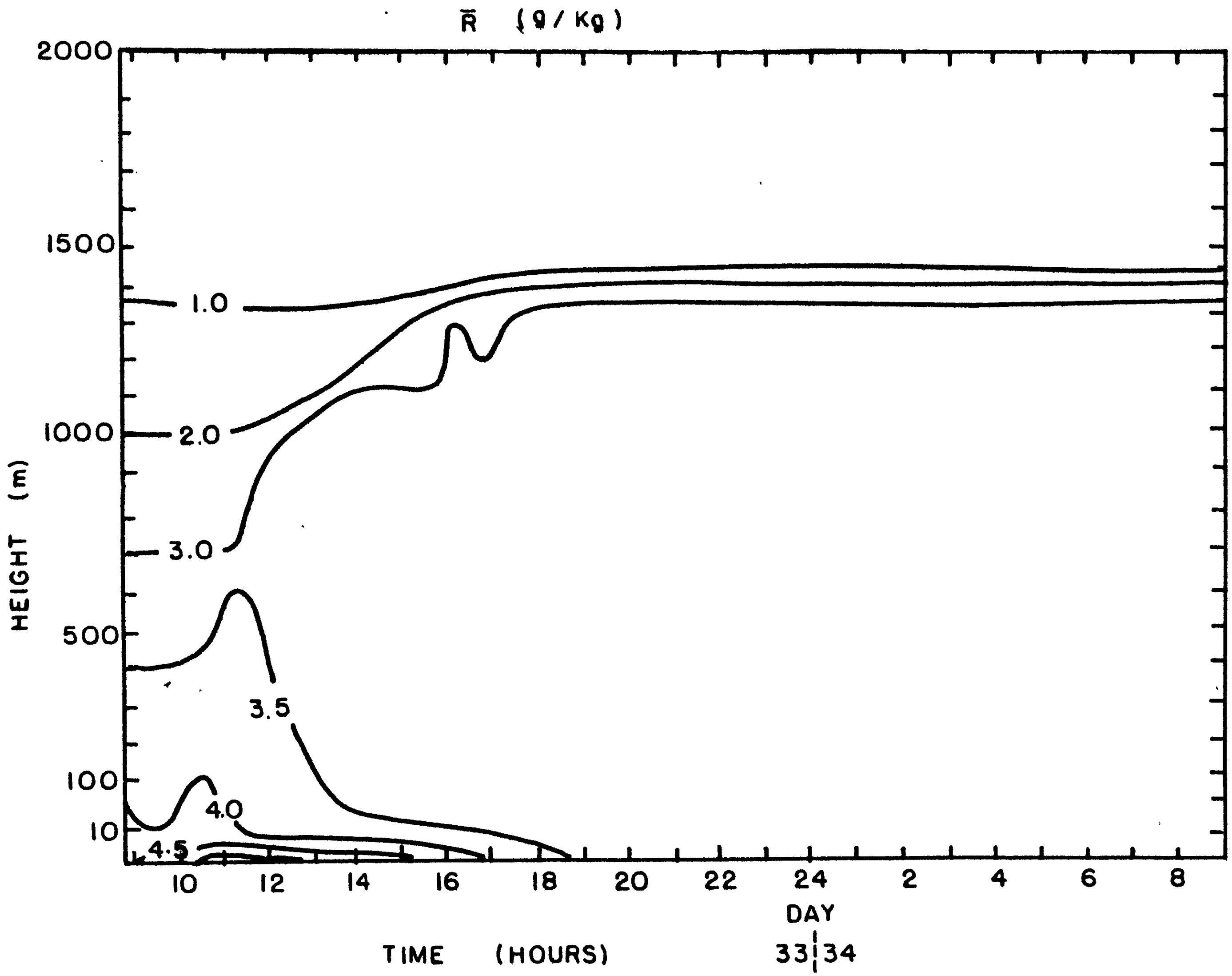


Fig. 10. Variation of the calculated mean water vapor mixing ratio, $\overline{R}$, as a function of time and height.

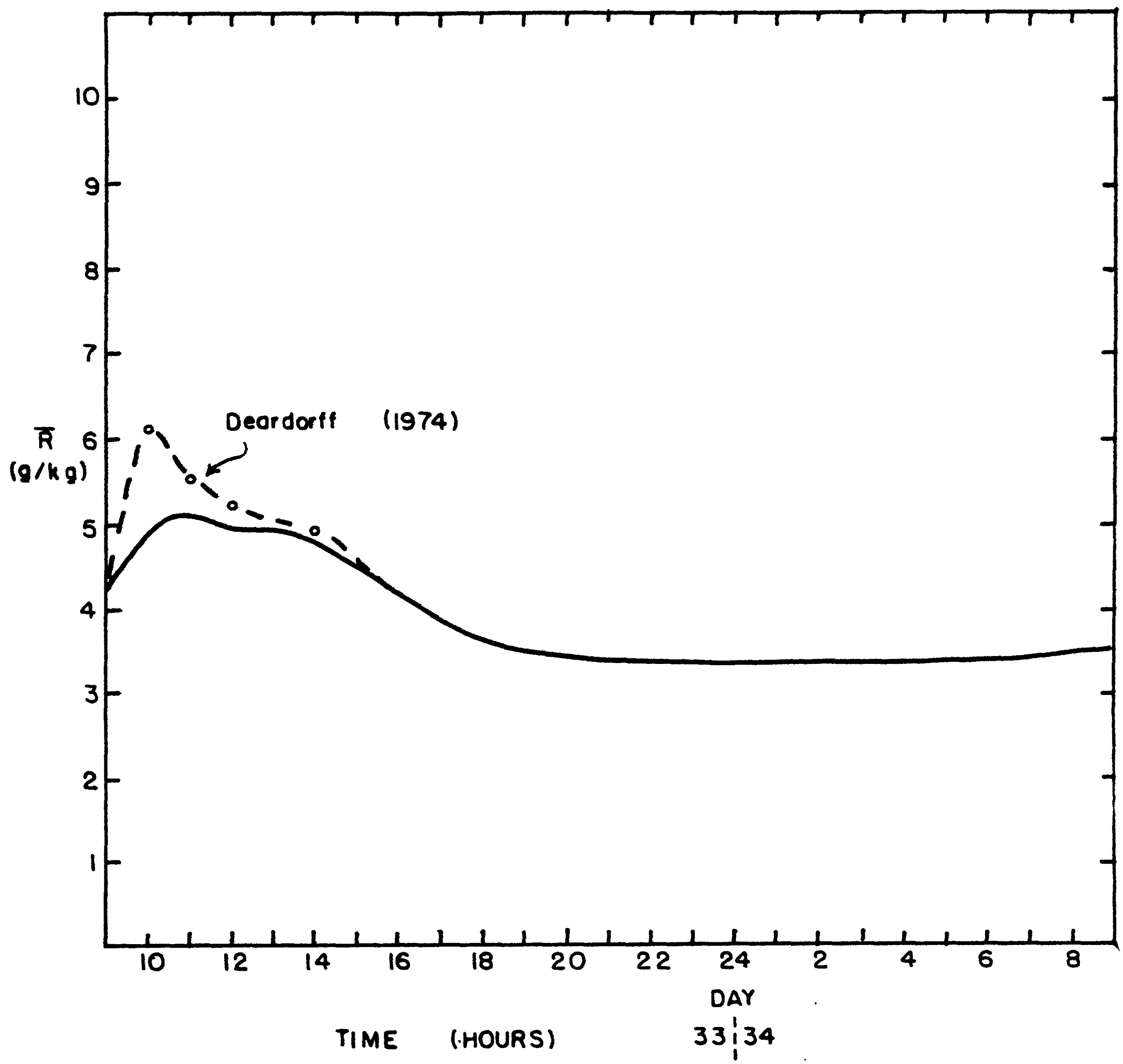


Fig. 11. Calculated surface $\overline{R}$ as a function of time.

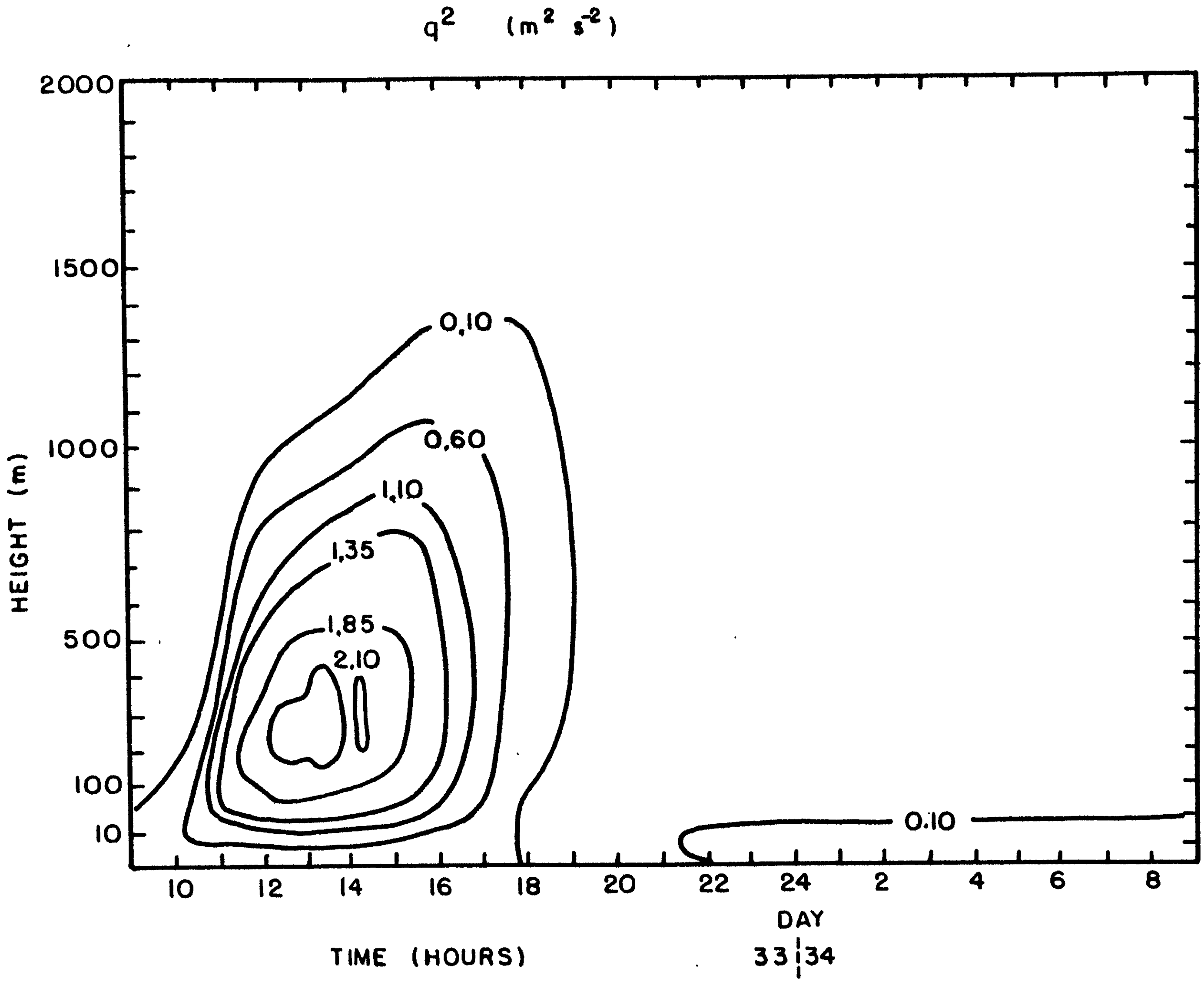


Fig. 12. Variation of the calculated values of twice the turbulence kinetic energy, $q^2$, as a function of time and height.

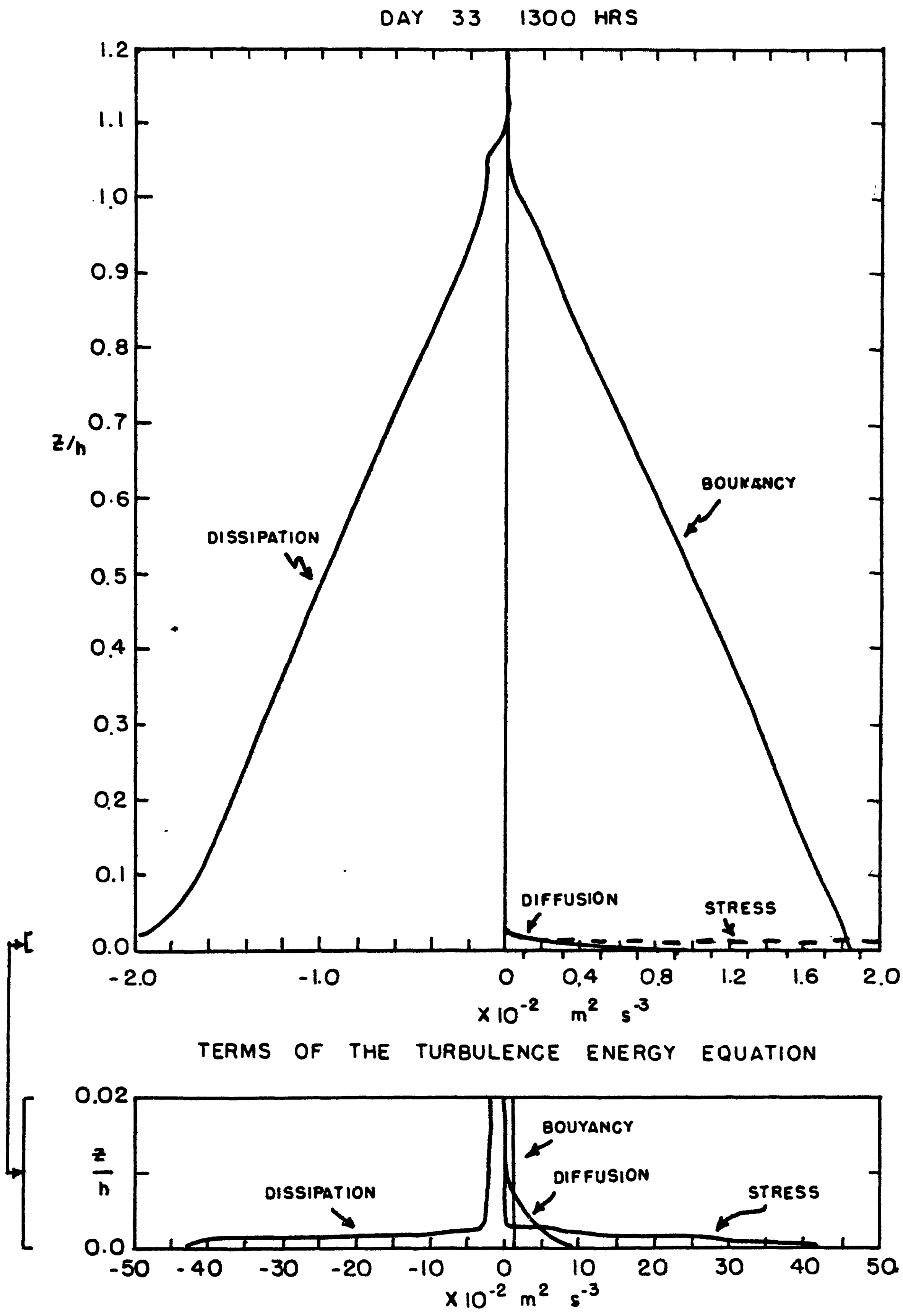


Fig. 13. Terms of the turbulence kinetic energy equation at 1300 hours, Day 33.

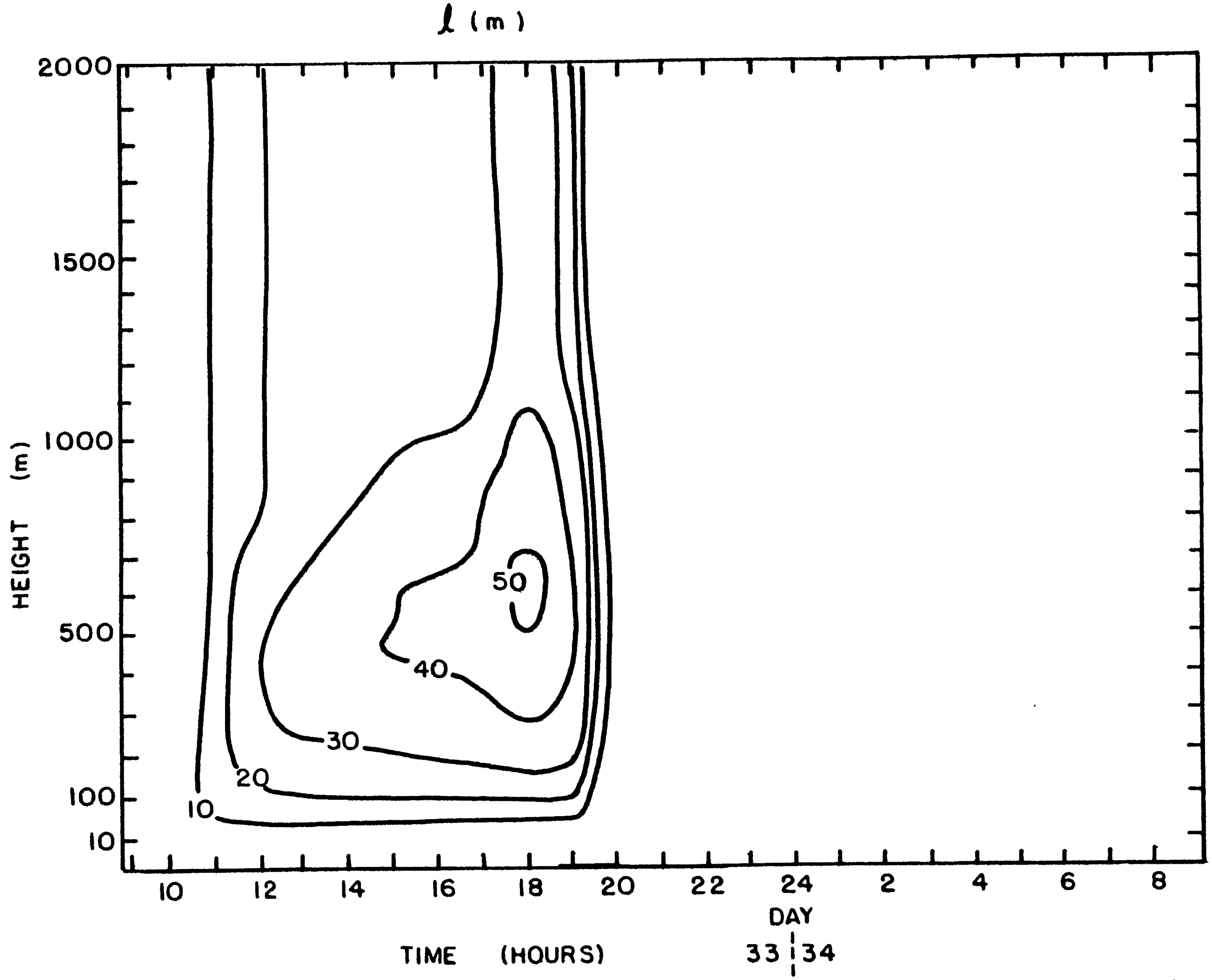


Fig. 14. Variation of the length scale, $\ell$, as a function of time and height.

Their formulation, however, continues to increase $\ell$ with height, approaching a constant limiting value. Equations (65) force $\ell$ to decrease in the upper portion of the boundary layer to a smaller, constant value in the stable region above the boundary layer.

The boundary layer height, h, used in the calculation of $\ell$, is of interest itself. It is defined here as the layer of the atmosphere containing essentially all the dissipation of turbulence kinetic energy. The model calculates h by integrating the dissipation of $q^2$ up from the ground until adding the dissipation in the next grid layer to the integration adds less than 1% of total integrated amount below this level. At this point, the integration stops, and h is determined. This definition of h yields boundary layer heights at, or within, 1 grid point of the base of the temperature inversion during the day, yet also gives a reasonable estimate for the boundary layer height at night, when identification of h from $\overline{\Theta}_v$ or $\overline{R}$ profiles is difficult. Figure 15 shows h and the $\overline{\Theta}_v$ profiles for 1100 and 1200 hours. The turbulence kinetic energy profiles for these times is shown in Figure 16. The evolution of the boundary layer height (Figure 17) is interesting. h grows rapidly in the morning hours, then more slowly in the afternoon. About an hour after sunset the boundary layer height crashes to a small, more or less constant value (108 m) through most of the night.

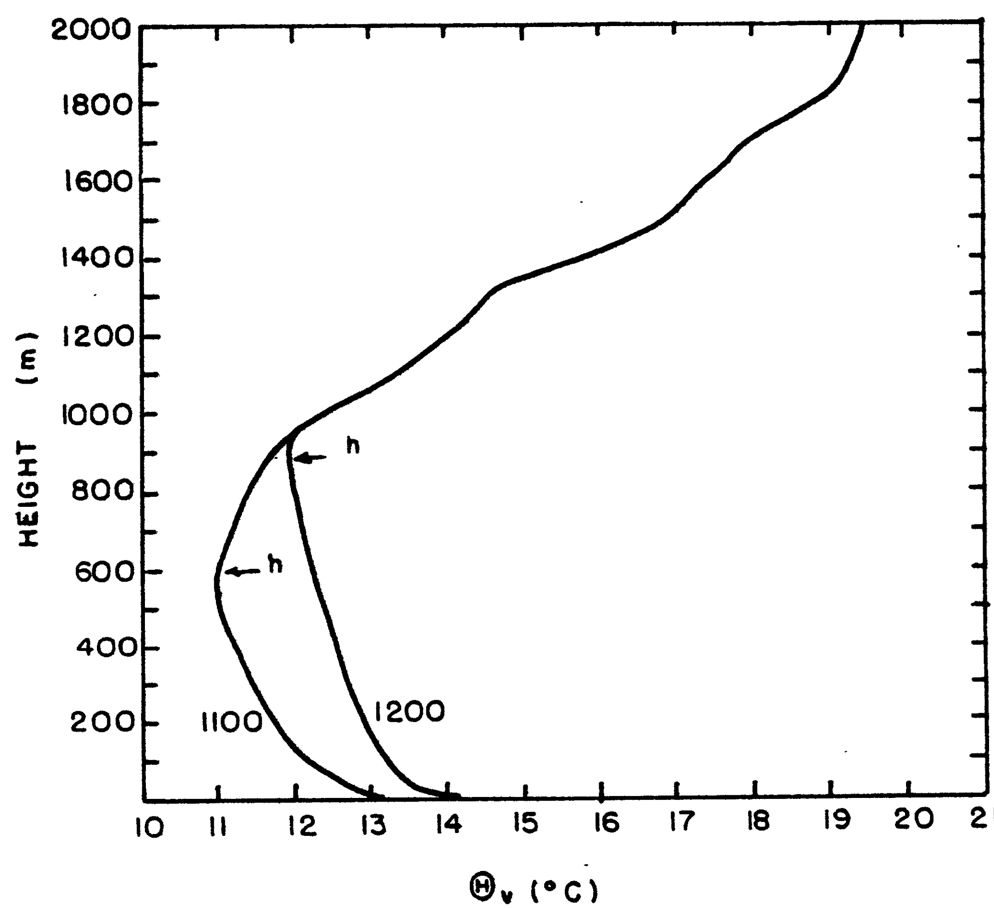


Fig. 15. Virtual potential temperature profiles for 1100 hours and 1200 hours, Day 33. The calculated PBL top for each time is indicated by h.

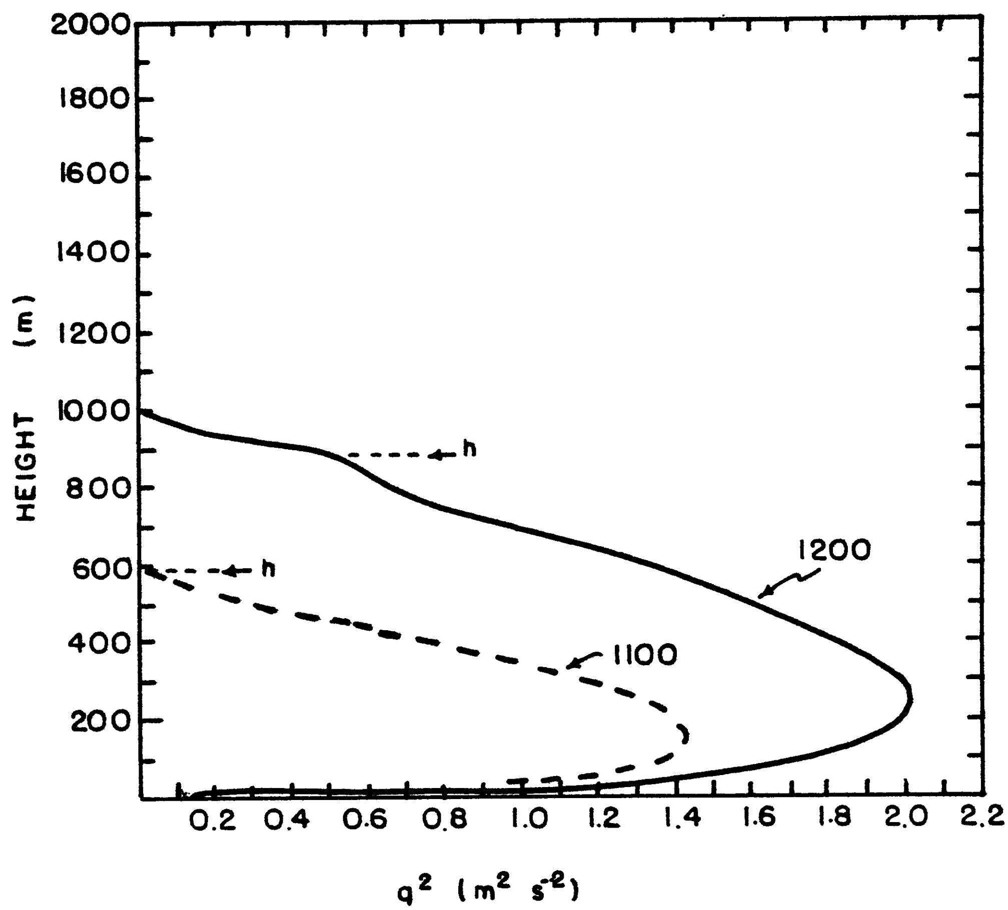


Fig. 16. Vertical profiles of $q^2$ (twice the turbulence energy) for 1100 hours and 1200 hours, Day 33. The calculated PBL top for each time is indicated by h.

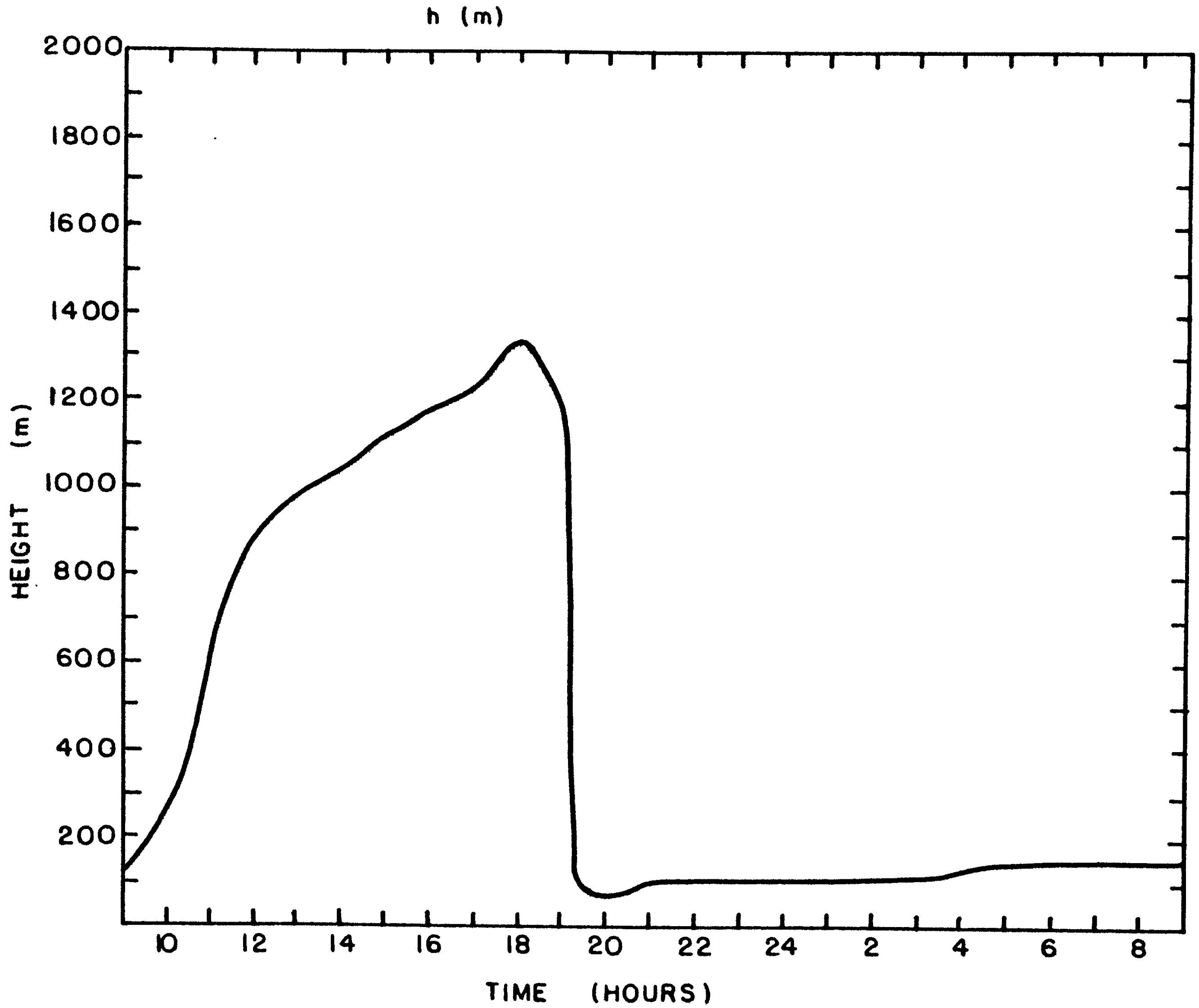


Fig. 17. The calculated boundary layer height, h, as a function of time.

The time-height variation or the virtual potential temperature variance, $\overline{\theta_v'^2}$, is shown in Figure 18. The maximum values of $\overline{\theta_v'^2}$ are found at the $z_o$ grid level during the day, and approximately 20-50 m above the ground at night. The $\overline{\theta_v'^2}$ budget, Figure 19, shows a balance between gradient production and dissipation of $\overline{\theta_v'^2}$ throughout the entire boundary layer.

The $\overline{r'^2}$ time-height variation, Figure 20, shows two areas of high mixing ratio variance, at the ground and at the boundary layer top. The gradient production of $\overline{r'^2}$, Figure 21, is strongest near the PBL top where the $\overline{R}$ profile decreases rapidly with height. Diffusion is important only around h, tending to decrease $\overline{r'^2}$ just above h and increase $\overline{r'^2}$ at h. The production of $\overline{r'^2}$ is negligible throughout the mixed layer, except in a shallow layer near the ground.

Figure 22 contains the mixing ratio-virtual potential temperature correlation, $\overline{r'\theta_v'}$, as a function of time and height. The model yields positive values for $\overline{r'\theta_v'}$ throughout the boundary layer during the day. In the stable region above the boundary layer, where $\overline{\Theta}_v$ rapidly increases and $\overline{R}$ rapidly decreases with height, negative values of $\overline{r'\theta_v'}$ occur. Throughout the shallow nighttime boundary layer (about 100 m), $\overline{r'\theta_v'}$ is negative. Figure 23 reveals that the dissipation term and the production term are in balance

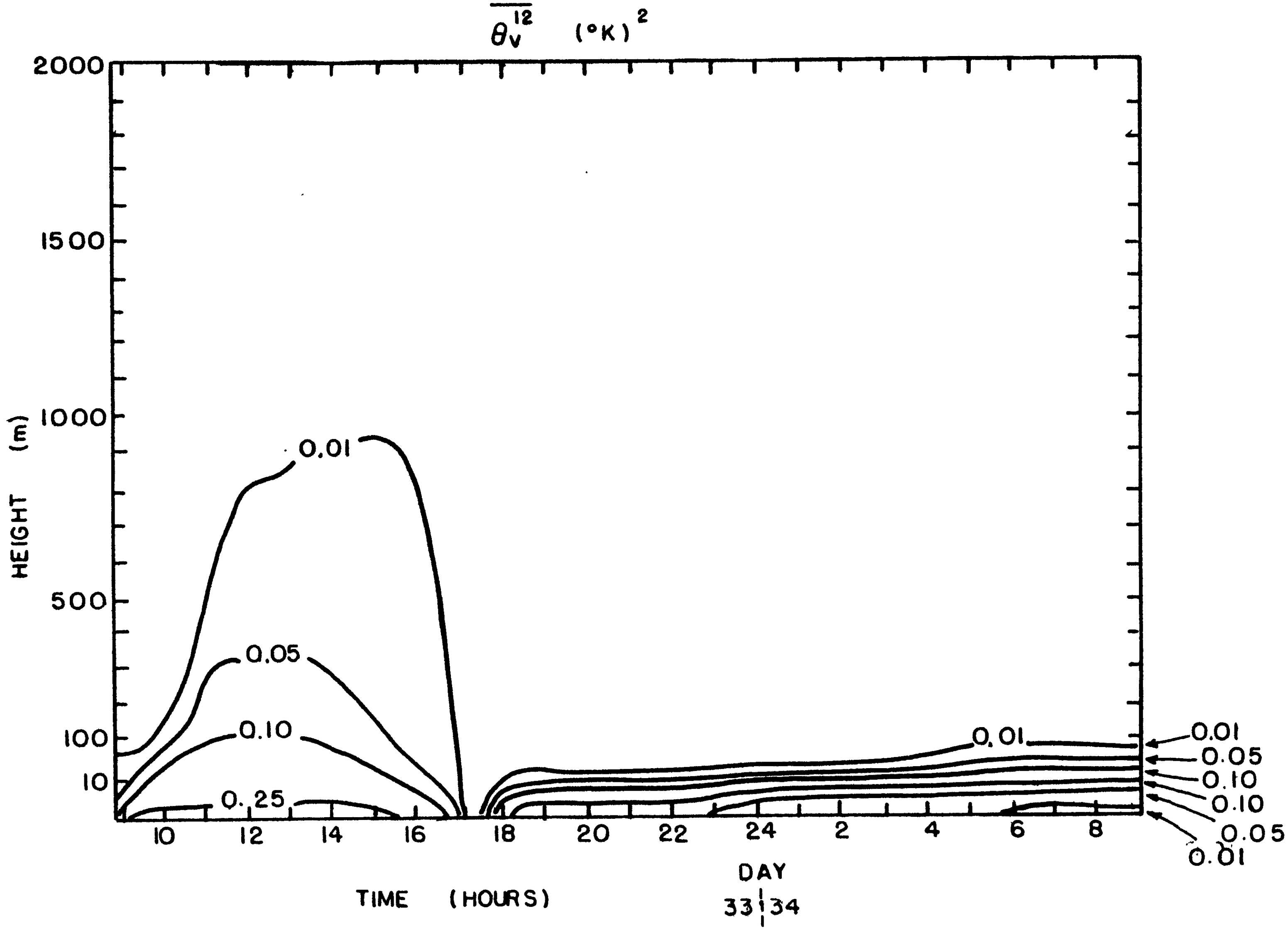


Fig. 18. Variation of the calculated virtual potential temperature variance, $\overline{\theta_v'^2}$ as a function of time and height.

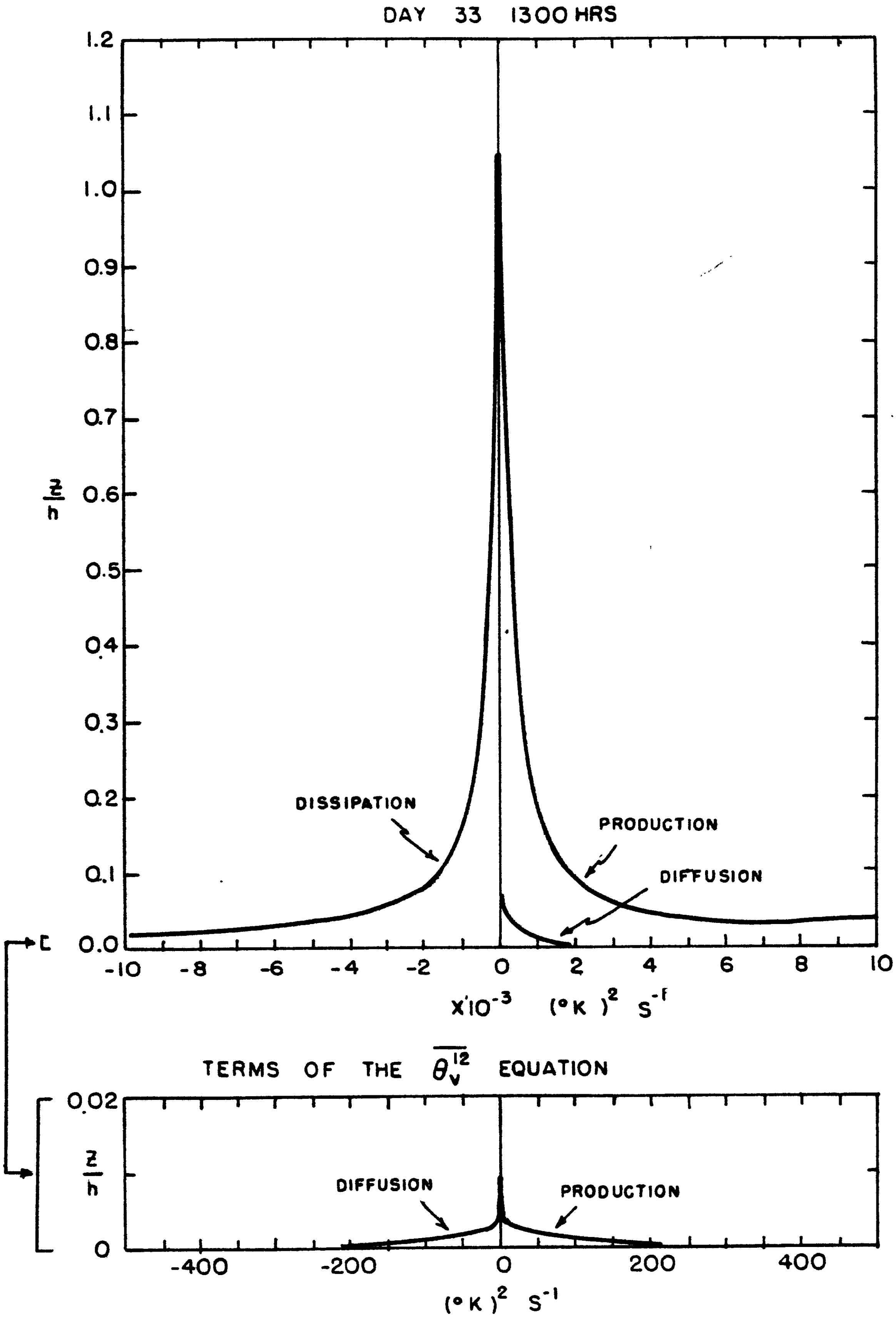


Fig. 19. Terms of the virtual potential temperature variance equation at 1300 hours, Day 33.

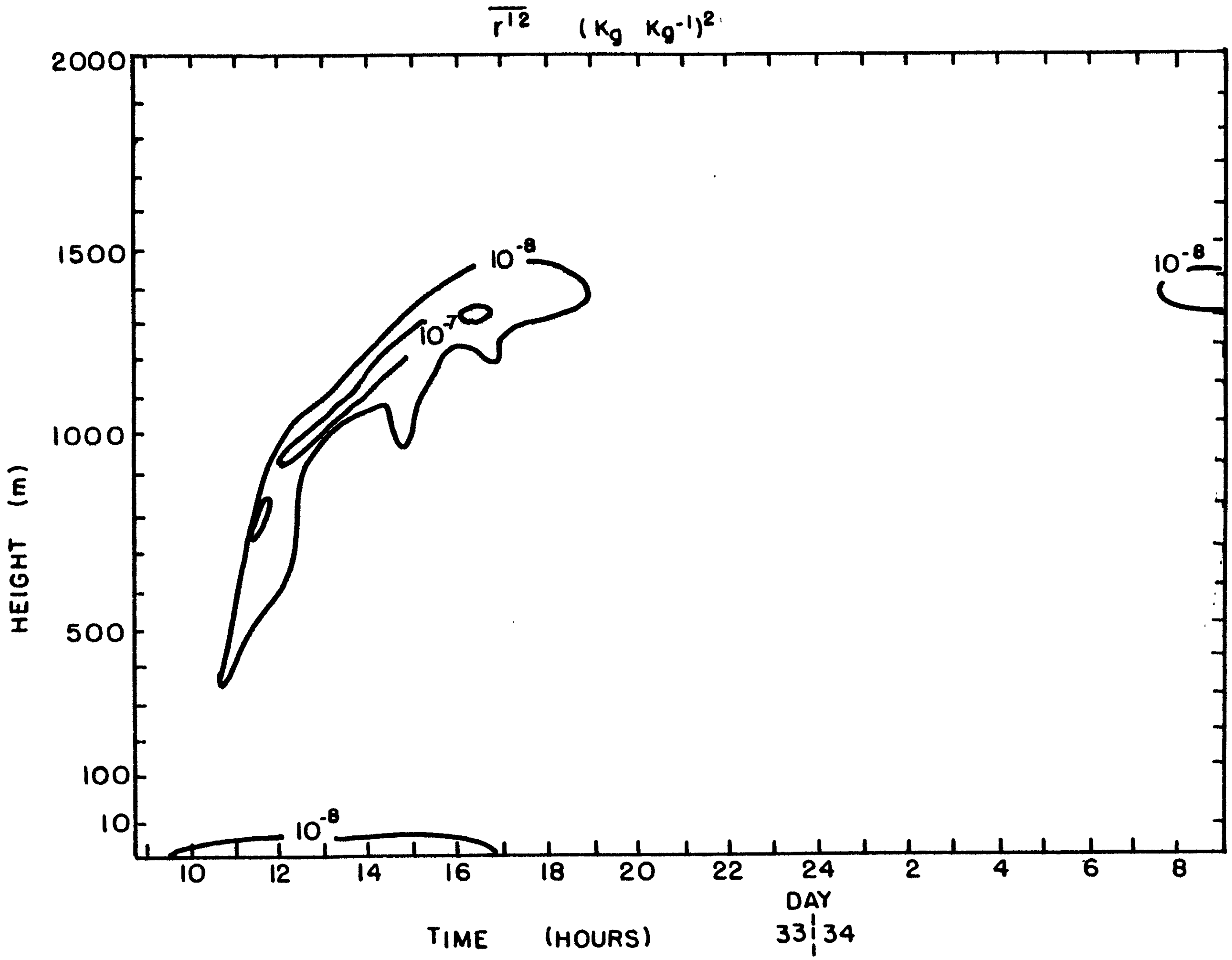


Fig. 20. Variation of the calculated water vapor mixing ratio variance, $\overline{r'^2}$, as a function of time and height.

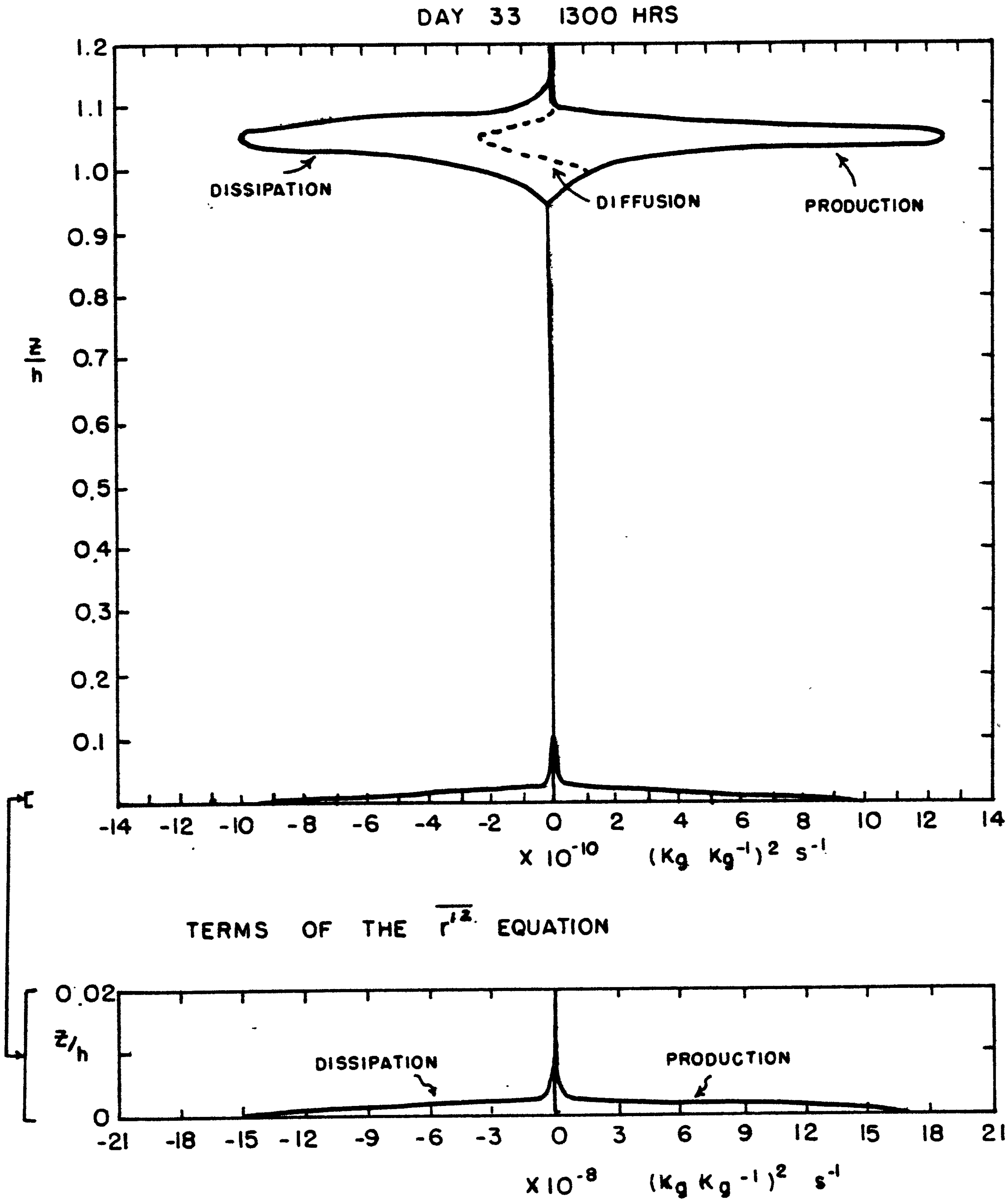


Fig. 21. Terms of the water vapor mixing ratio variance equation at 1300 hours, Day 33.

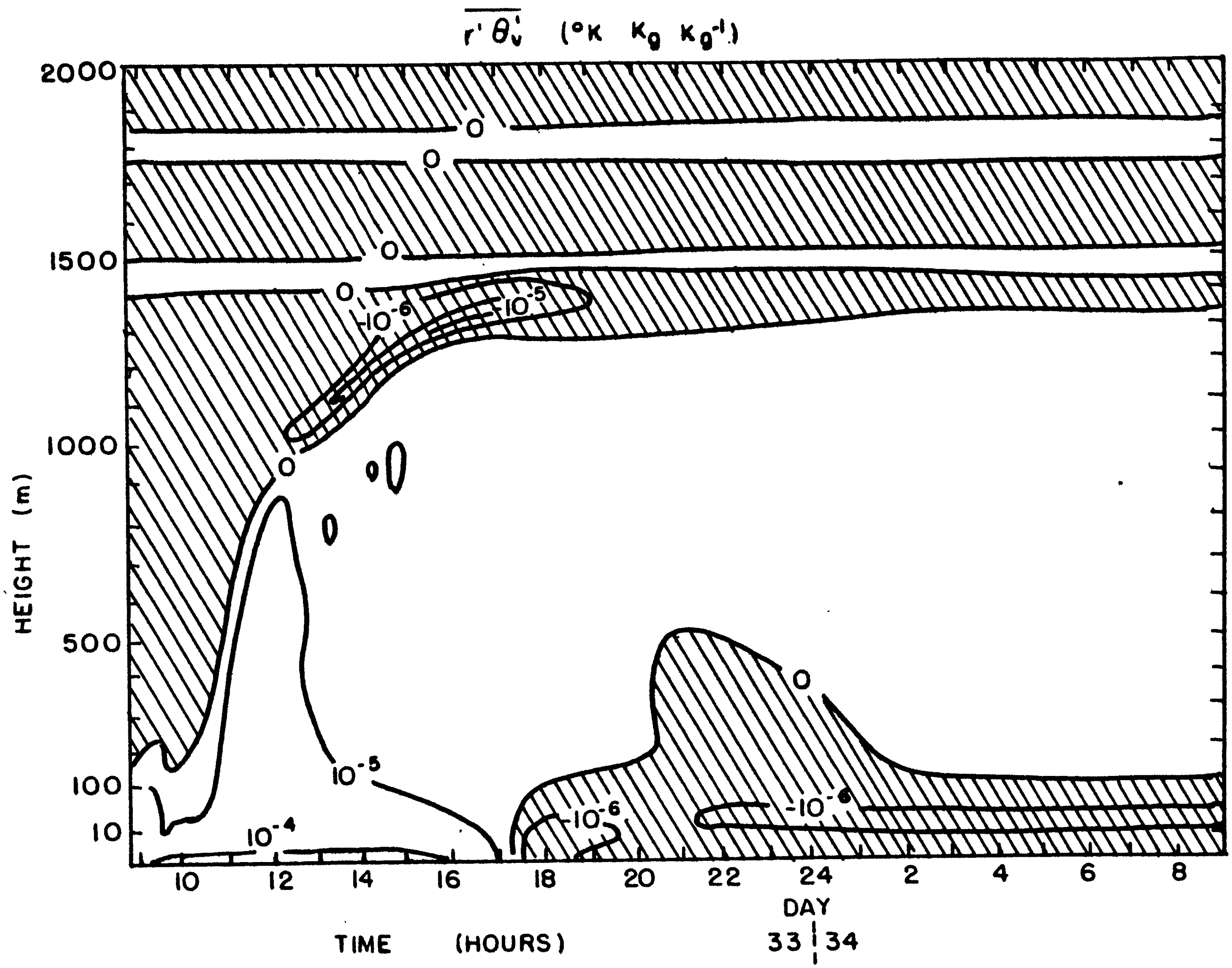


Fig. 22. Variation of the calculated water vapor mixing ratio-virtual potential temperature covariance, $\overline{r'\theta_v'}$, as a function of time and height. Areas of negative $\overline{r'\theta_v'}$ are signified by hatching.

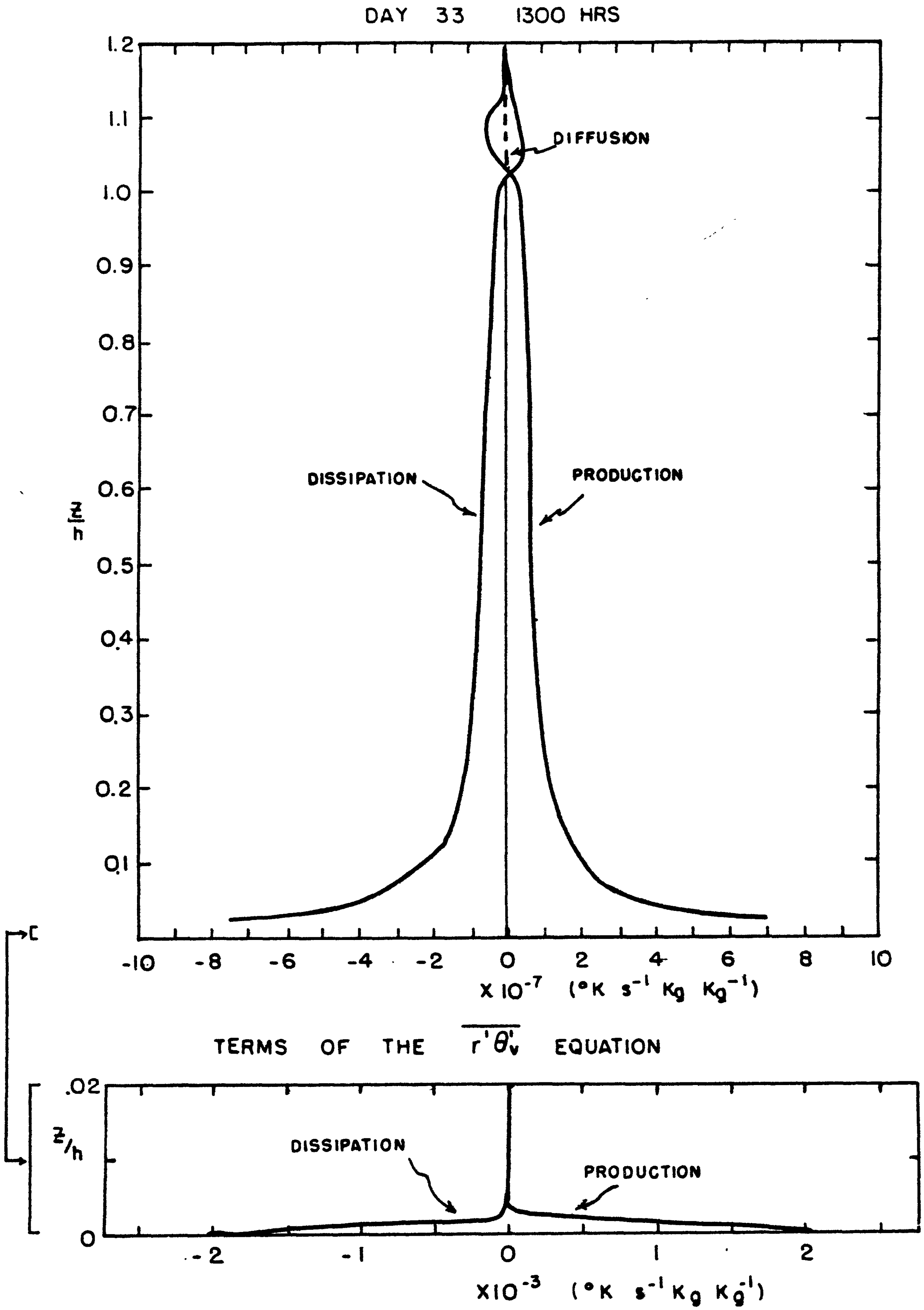


Fig. 23. Terms of the $\overline{r'\theta'_V}$ equation at 1300 hours, Day 33.

everywhere. Dissipation and production change signs above h where $\overline{r'\theta_v'}$ is negative.

The variation of the diagnostically determined Reynolds stresses ($\overline{u'w'}$, $\overline{v'w'}$), vertical heat flux ($\overline{w'\theta_v'}$) and vertical moisture flux ($\overline{w'r'}$) as a function of height and time are presented in Figures 24-27. Small negative values of the heat flux (2-8% of the surface heat flux) were calculated just above the afternoon boundary layer top. Yamada and Mellor (1975) reported downward heat fluxes above the PBL top of a maximum of 2% of the surface values. Deardorff's (1974) model calculates an average negative heat flux of 13% of the surface value.

The surface ($z_o$ level) values of $\overline{w'\theta_v'}$, $\overline{w'r'}$, and the friction velocity, $u_*$, are shown in Figures 28-30. The results of Deardorff (1974) and Yamada and Mellor (1975) are also shown, when available, on these figures for comparison. The surface moisture flux compares well with Deardorff's. The calculated high values of $\overline{w'\theta_v'}$ have already been attributed to the assumption $\overline{\theta}_v$ $(z_o)$ = $\overline{\theta}_v$ (ground).

Values of the individual turbulence energy components in the unstable boundary layer show an anisotropic distribution. The components $\overline{u'^2}$ and $\overline{v'^2}$ are approximately equal. The vertical energy component, $\overline{w'^2}$, however, is usually more than twice the other two components. This is due to the direct transfer of bouyant energy to the $\overline{w'^2}$

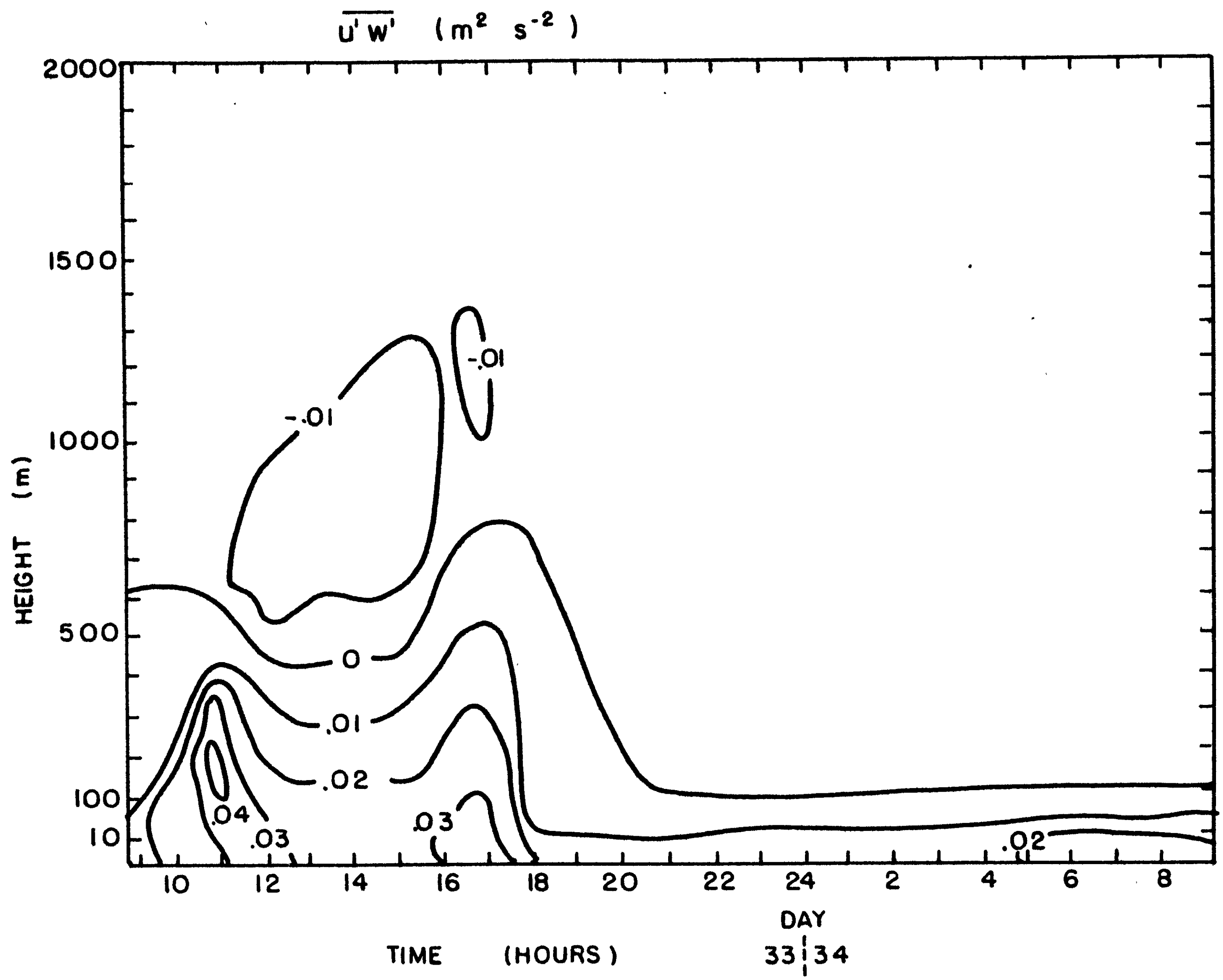


Fig. 24. Variation of the calculated Reynolds stress component, $\overline{u'w'}$, as a function of time and height.

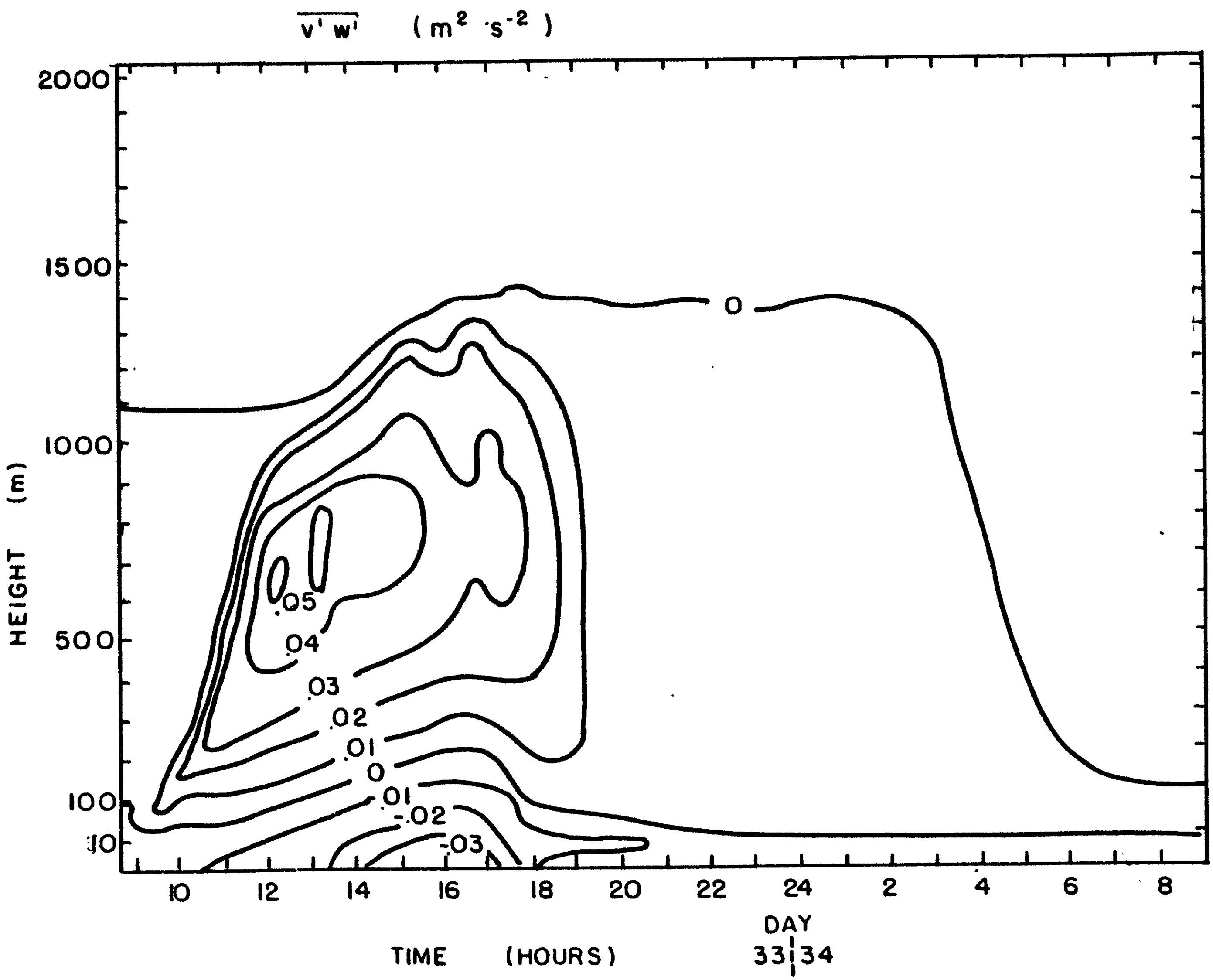


Fig. 25. Variation of the calculated Reynolds stress component, $\overline{v'w'}$, as a function of time and height.

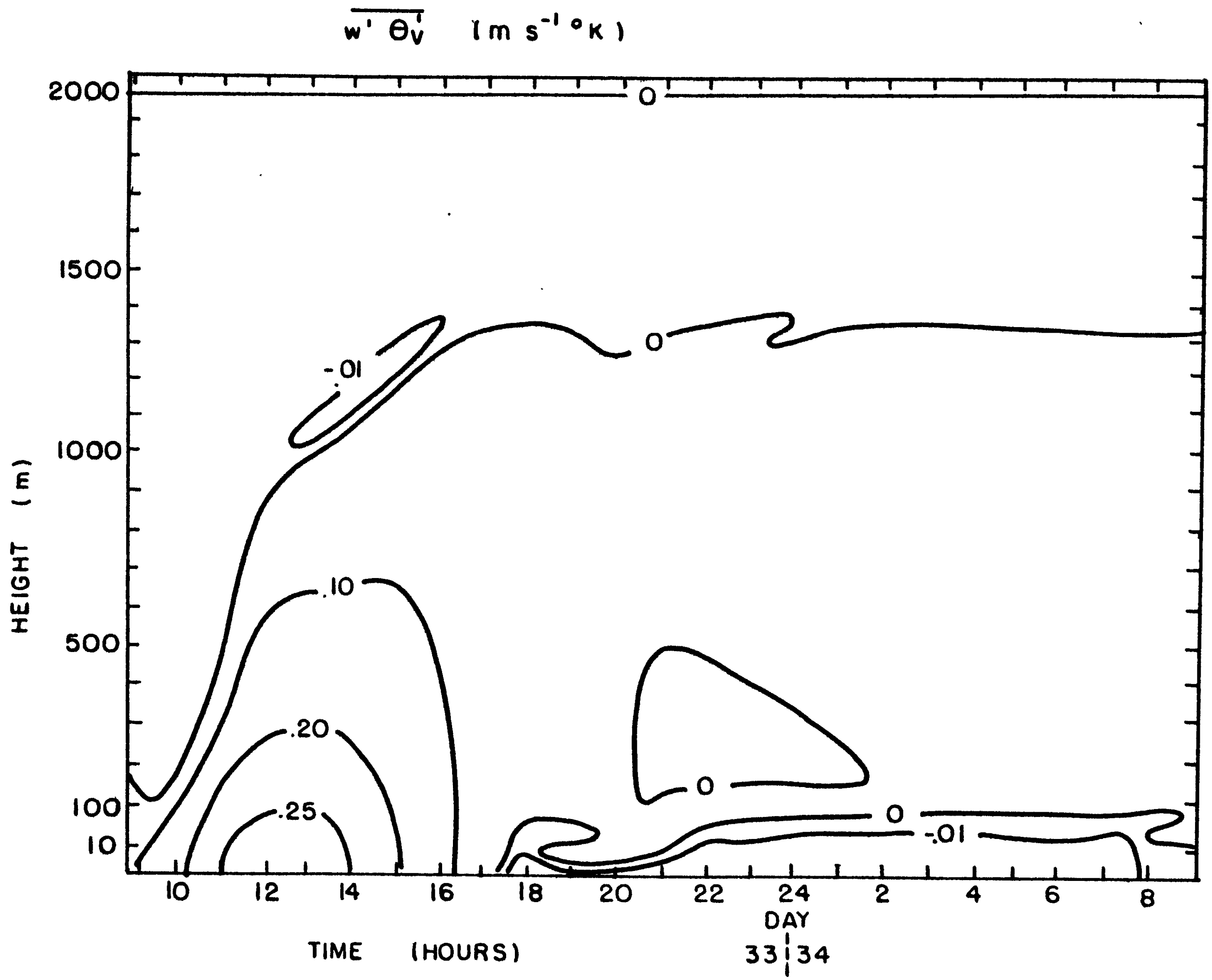


Fig. 26. Variation of the heat flux component, $\overline{w'\theta_v'}$, as a function of time and height.

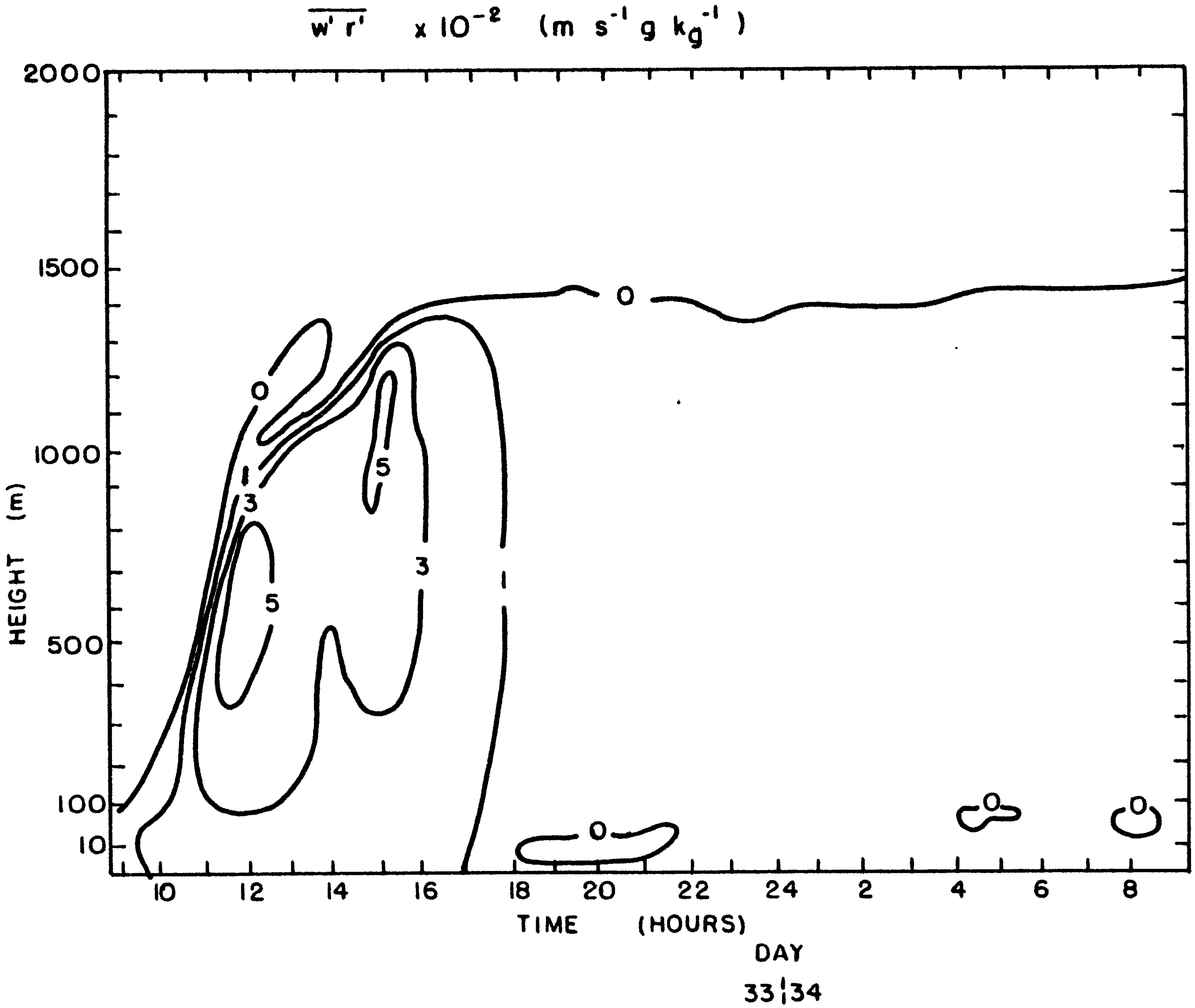


Fig. 27. Variation of the moisture flux component, $\overline{w'r'}$, as a function of time and height.

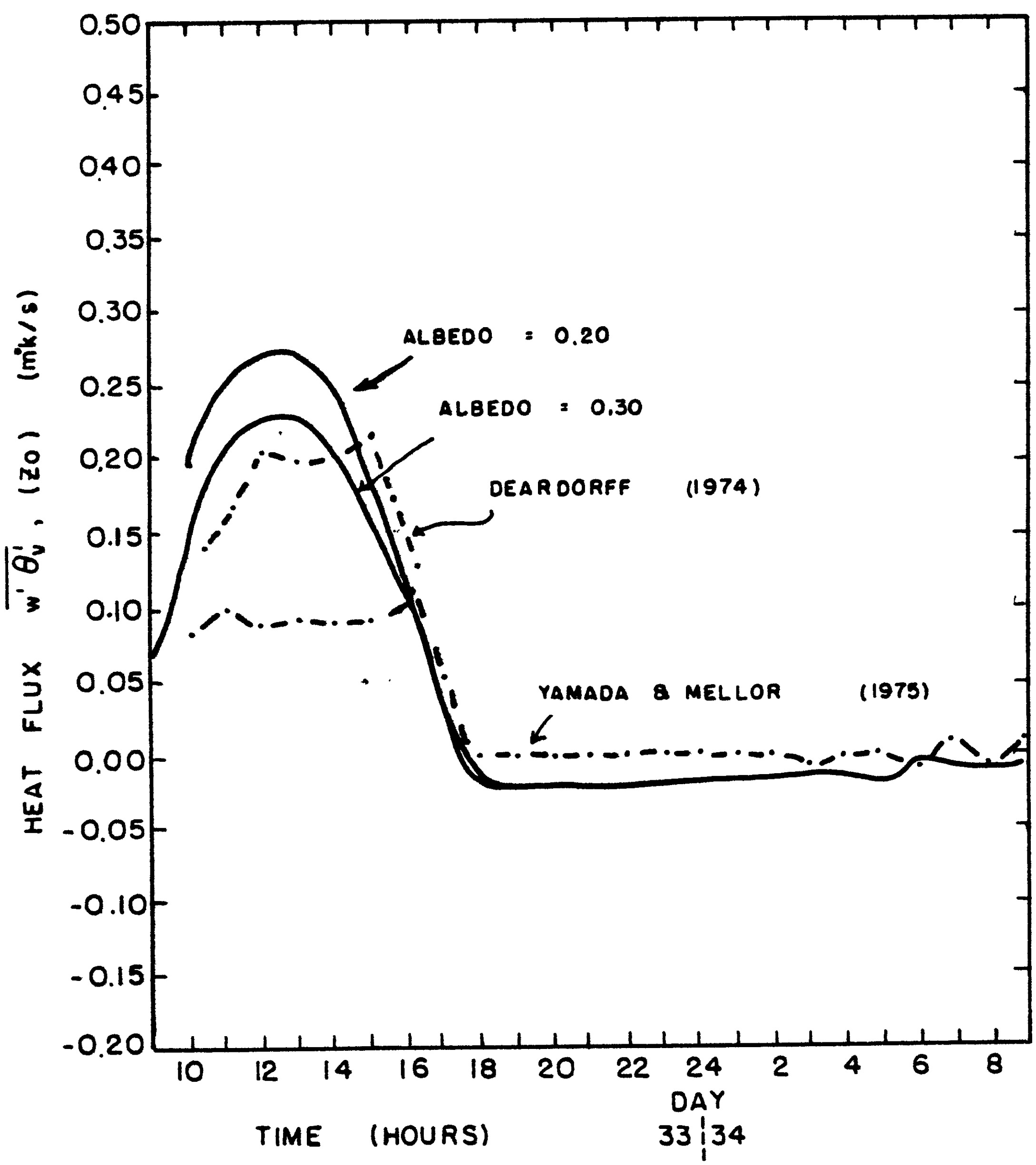


Fig. 28. Calculated surface heat flux for two values of the surface albedo, as a function of time. The values of Deardorff (1974), and Yamada and Mellor (1975) are also shown.

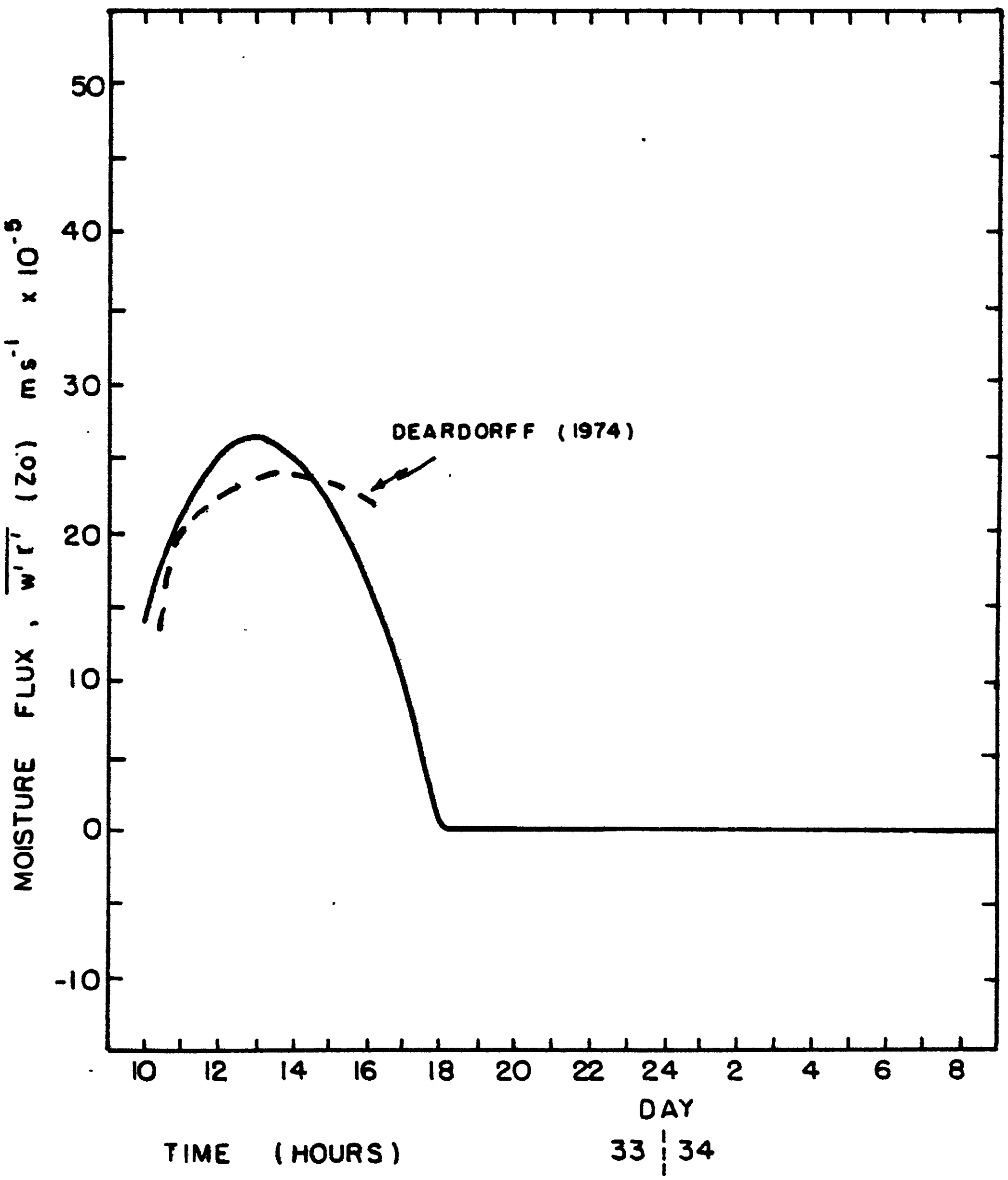


Fig. 29. Calculated surface moisture flux as a function of time. The results of Deardorff (1974) are also shown.

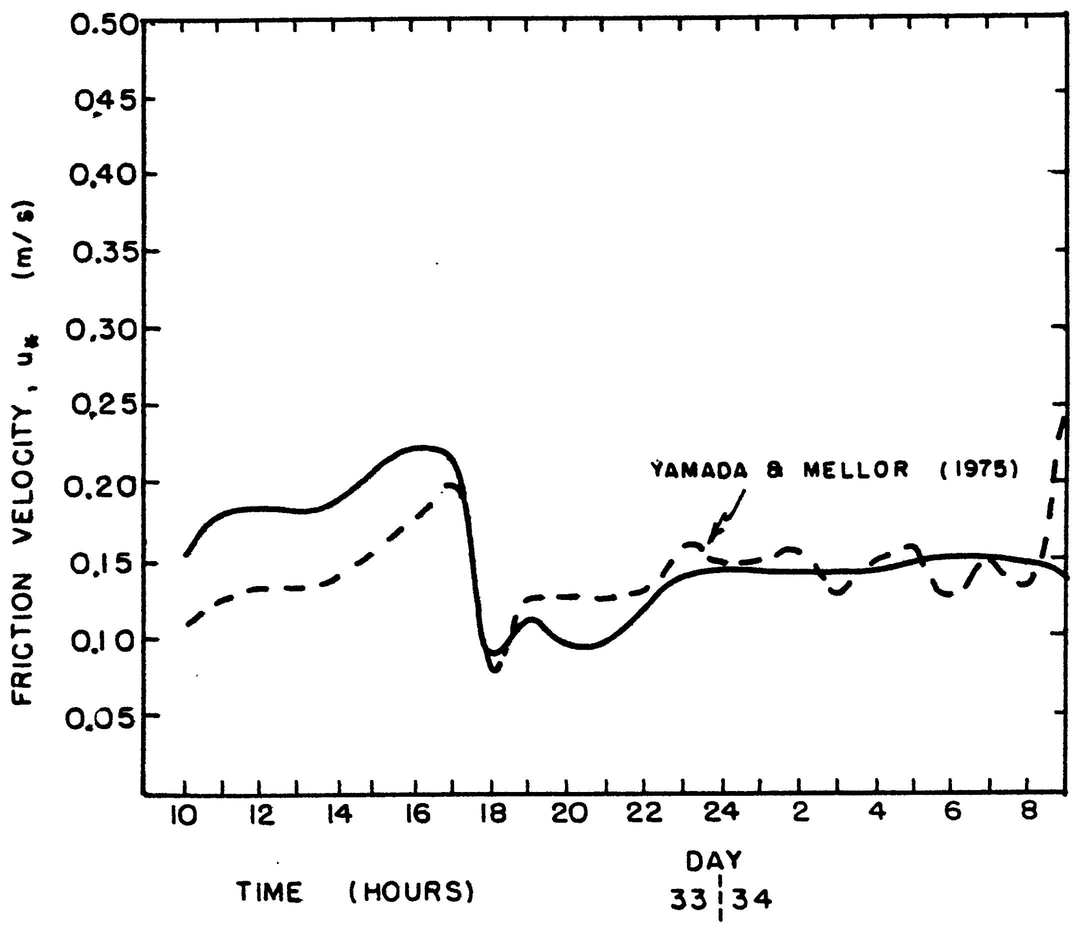


Fig. 30. Calculated friction velocity, $u_*$, as a function of time. The results of Yamada and Mellor (1975) are also shown.

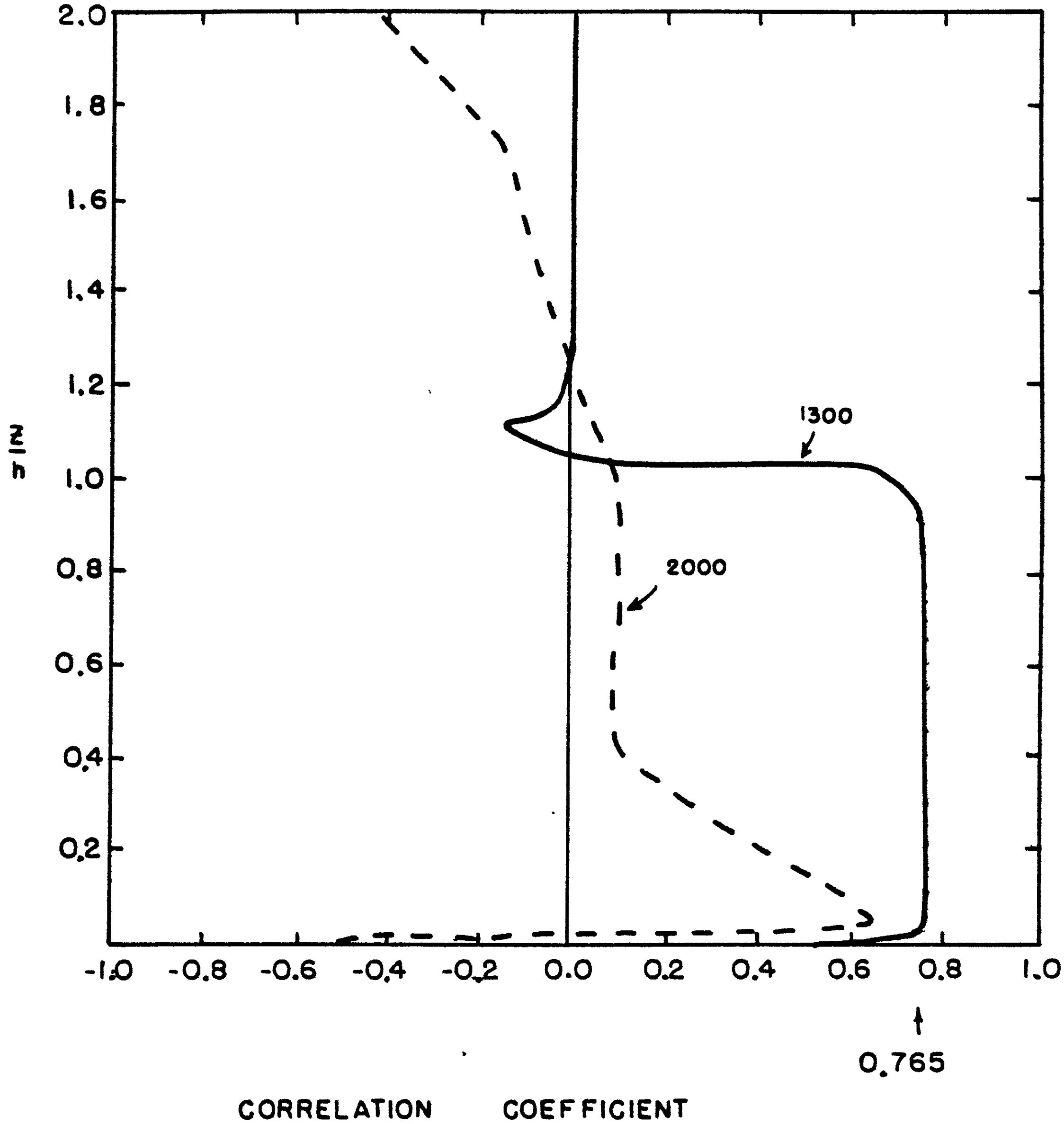


$$r_{w\theta} = \frac{\overline{w' \ \theta_v'}}{\sqrt{\overline{w'^2} \ \overline{\theta_v'^2}}}$$

Fig. 31. The correlation coefficient for $w'$-$\theta_v'$ as a function of z/h, for 1300 hours and 2000 hours, Day 33.

component (Deardorff, 1973). The return-to-isotropy (pressure correlation) term, proportional to $1/\ell$, tries to eliminate this anisotropy. The bouyant energy - $\overline{w'^2}$ energy transfer is exemplified in Figure 31. The $w'$-$\theta_v'$ correlation coefficient is a high constant value (.765) throughout the daytime PBL. The nocturnal (8:00 pm) boundary layer profile of the correlation coefficient clearly does not exhibit this behavior.

# 7. EFFECTS OF THE CORIOLIS TERMS ON TURBULENT FLUXES IN THE PBL

Most higher order closure models of the PBL contain assumptions to the effect that the Coriolis terms of the turbulence moment equations are negligible (e.g., Mellor and Yamada, 1974, 1975). Wyngaard et al. (1974), however, discuss the importance of the Coriolis terms in the Reynolds stress equations. In order to evaluate the importance of these terms in influencing the results in the simulated boundary layer, runs were made in which the rotation terms were included (turned on) and set equal to zero (turned off).

The inclusion of the Coriolis terms in the $\overline{u_i'u_j'}$ and $\overline{u_i'\theta_v'}$ equations presented no problems other than to increase the complexity of the equations. Computational problems, however, were encountered with the level 3 moisture equations with rotation. An examination of equations (A-16 - A-18) for $\overline{w'r'}$ indicates that the effect of the Coriolis terms will be to increase the moisture flux if the momentum flux is in the same direction (upward or downward) as the moisture flux. If the momentum is in the opposite direction of the moisture flux, the Coriolis terms tend to decrease $\overline{w'r'}$. Consider a situation in which $\partial\overline{R}/\partial z = 0$. Equation (A-21) reduces to:

$$\overline{w'r'} = A\overline{r'\theta_v'} \tag{87}$$

A is defined by equation (A-22). Equation (48) is approximately:

$$\frac{\partial}{\partial t}(\overline{r'\theta'_v}) \simeq - \overline{w'r'} \frac{\partial\overline{\Theta}_v}{\partial z} - \frac{2q}{\Lambda_2}\overline{r'\theta'_v}$$

$$= -(A\frac{\partial\overline{\Theta}_v}{\partial z} + \frac{2q}{\Lambda_2})\ \overline{r'\theta'_v} \quad (88)$$

Usually the second term in parentheses dominates in the unstable boundary layer. In the stable region above the boundary layer, the first term is usually larger. An analysis of the terms of equation (A-22) reveals:

$$A \simeq \frac{3\ell_2\beta g q^2}{q^3 + 9\ell_2^2 q f_Y \frac{\partial\overline{u}}{\partial z}} \quad (89)$$

The turbulence in the region above the boundary layer is weak, indicating $q^3$ is a small positive number. Since $f_Y$ is positive, a region of $\partial\overline{u}/\partial z < 0$ can make A negative. This occurred in the stable region above h. Equation (88) reduces to:

$$\frac{\partial}{\partial t}(\overline{r'\theta'_v}) \simeq C_1\overline{r'\theta'_v} \quad (90)$$

where $C_1 \sim -A\,\frac{\partial\overline{\Theta}_v}{\partial z} > 0$. The resulting solution is a growing exponential.

In order to evaluate the effects of the Coriolis terms in the $\overline{u_i'u_j'}$ and $\overline{u_i'\theta_v'}$ equations it was necessary to set $f_y = f_z = 0$ in the moisture equations above the PBL top. The moisture equations are decoupled from the other equations. No moisture variable is used in the calculation of $\overline{u_i'u_j'}$, or $\overline{u_i'\theta_v'}$ and, therefore, the Reynolds stresses and heat fluxes are unaffected by this change in the $\overline{u_i'r'}$ equations. In addition, the area of interest is the boundary layer, and in this region, no restriction on $f_y$ or $f_z$ was necessary.

Figures 32-35 contain $\overline{u'w'}$, $\overline{v'w'}$, $\overline{w'\theta_v'}$, and $\overline{w'r'}$ profiles for runs with and without this Coriolis terms. There is no difference in the linear $\overline{w'\theta_v'}$ profile throughout the boundary layer (Figure 34). The $\overline{w'r'}$ profile also shows little sensitivity to the inclusion of rotation. The Reynolds stress components $\overline{u'w'}$ and $\overline{v'w'}$, however, are influenced somewhat (Figures 32-33). The $\overline{u'w'}$ profile retains the same shape as without rotation, but the $\overline{v'w'}$ profile is flattened.

None of the prognostic turbulence equations contains Coriolis terms. Their inclusion affects $q^2$, $\overline{\theta_v'^2}$, $\overline{r'^2}$ and $\overline{r'\theta_v'}$ only through the diagnostically determined $\overline{u_i'u_j'}$, $\overline{u_i'\theta_v'}$, and $\overline{u_i'r'}$ equations. Time-height variation plots for the mean variables and the prognostic turbulence variables are almost identical for runs with and without the Coriolis terms. The effects of the Coriolis terms, therefore, are

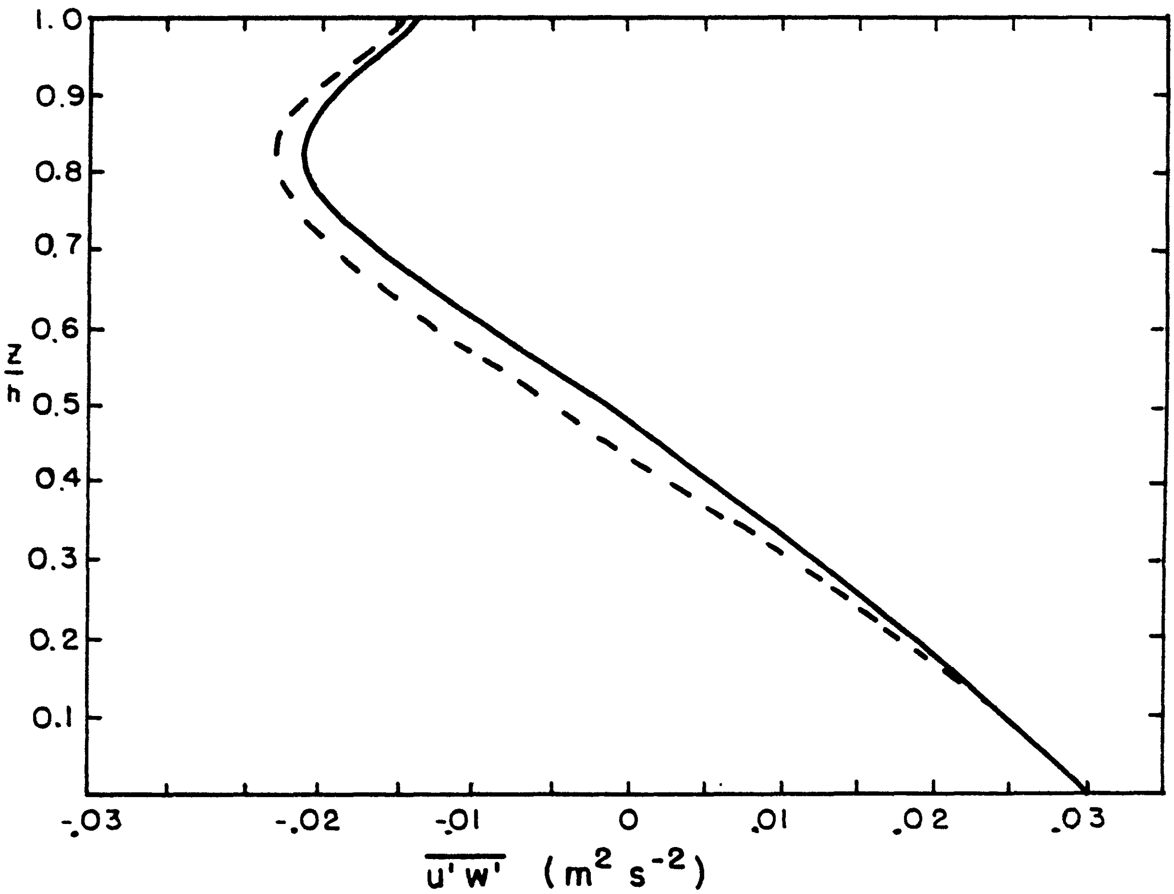


Fig. 32. Profiles of the Reynolds stress component $\overline{u'w'}$ at 1200 hours, Day 33, for two cases [Coriolis terms on (---) and Coriolis terms off (——)] as a function of z/h.

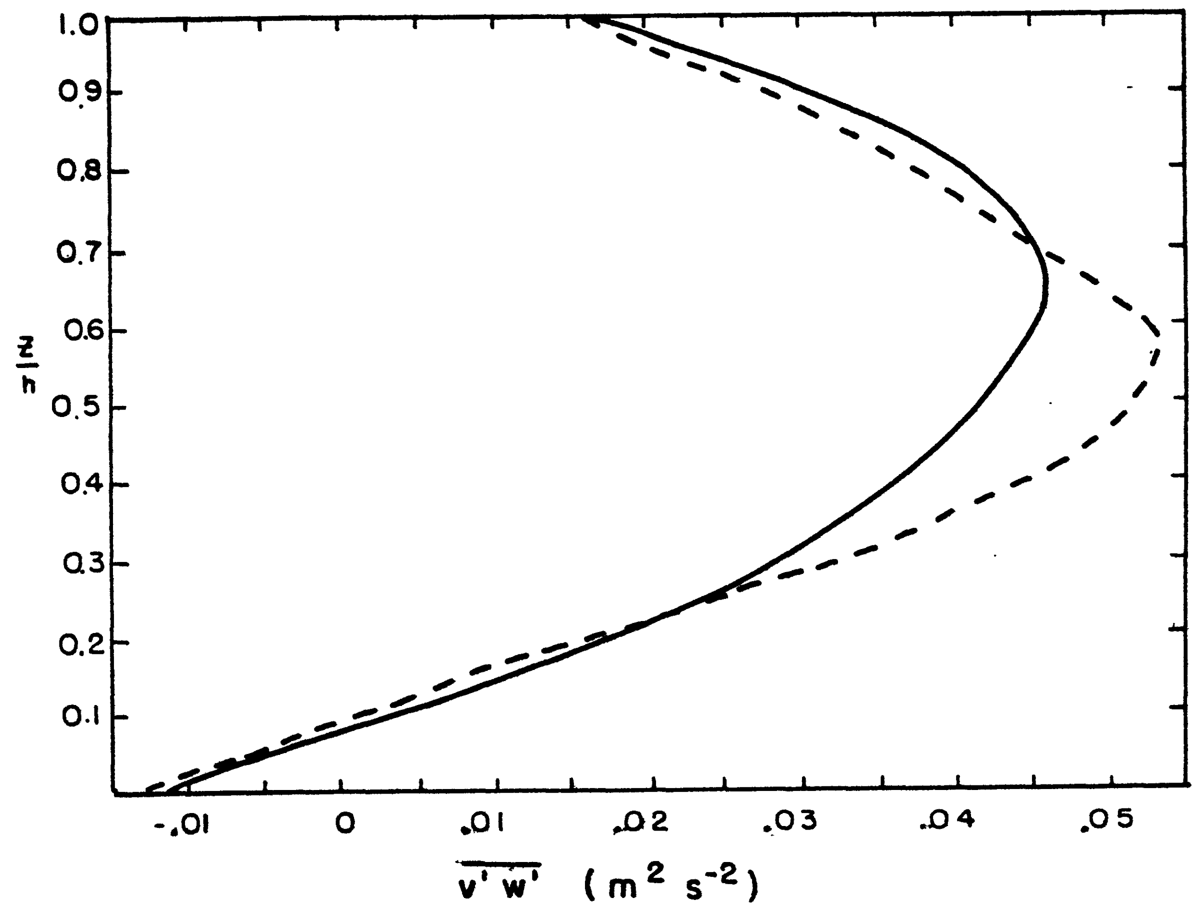


Fig. 33. Profiles of the Reynolds stress component $\overline{v'w'}$ at 1200 hours, Day 33, for two cases [Coriolis terms on (---) and Coriolis terms off (——)] as a function of z/h.

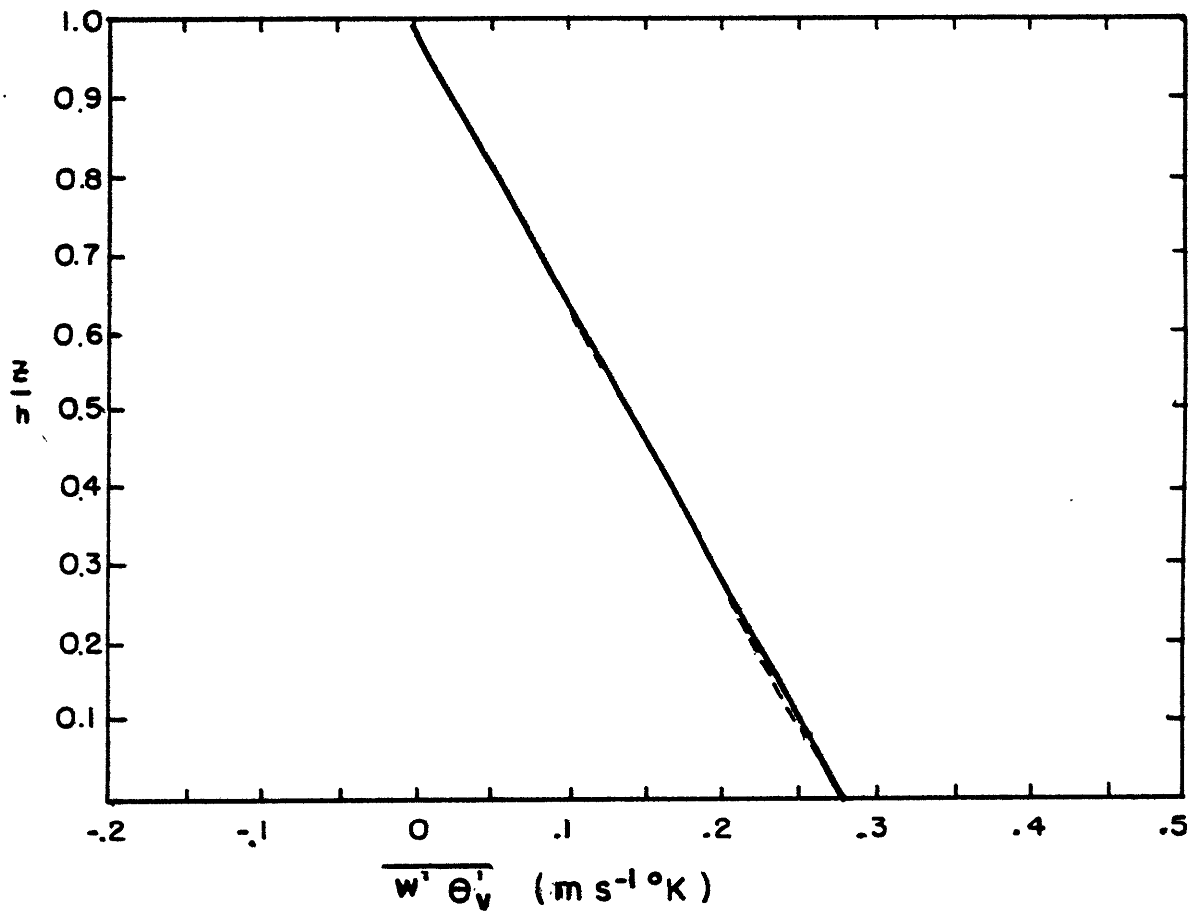


Fig. 34. Profiles of the heat flux component $\overline{w'\theta_v'}$ at 1200 hours, Day 33, for two cases [Coriolis terms on (---) and Coriolis terms off (——)] as a function of z/h.

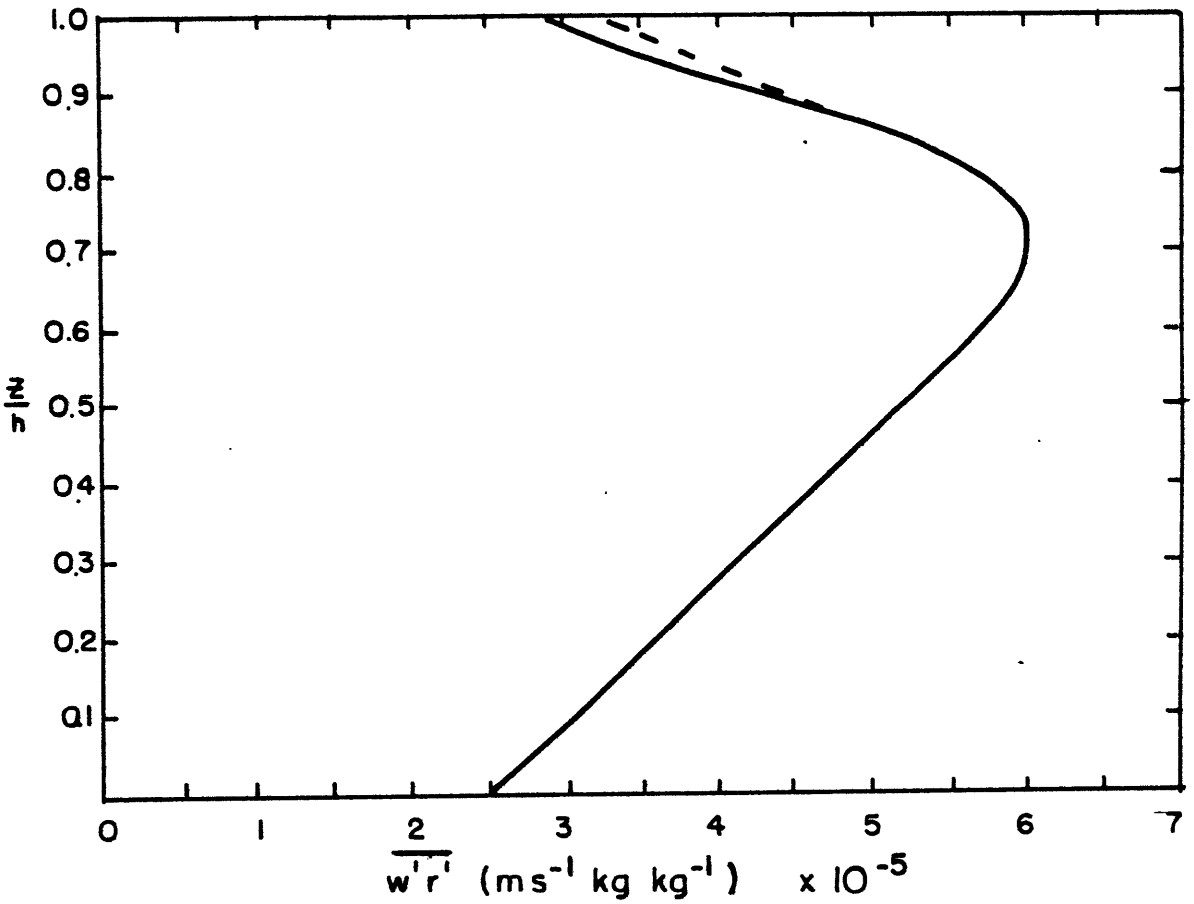


Fig. 35. Profiles of the moisture flux component, $\overline{w'r'}$, at 1200 hours, Day 33, for two cases [Coriolis terms on (---) and Coriolis terms off (——)] as a function of z/h.

felt mainly in the details of the $\overline{u'w'}$ and $\overline{v'w'}$ profiles. These terms can therefore usually be safely neglected.

# 8. EVALUATION OF THE SIMILARITY FUNCTIONS A, B, C AND D

## 8.1 Definition of the Scales and Derivation of A, B, C, and D

The similarity theory proposed by Monin and Obukhov (1954) assumes, for a stationary, horizontally homogeneous flow, that the surface layer profiles of all mean and turbulent variables, when appropriately non-dimensionalized, are universal functions of a small number of dimensionless parameters. The theory is applied in the surface layer where the Reynolds stress, and the heat and moisture fluxes may be considered constant with height. It is assumed that the surface layer structure is determined by the dimensional variables:

$$z,\ z_o,\ g/\overline{\Theta}_{v_o},\ u_*,\ \overline{w'\theta_v'}\Big|_o,\ \overline{w'r'}\Big|_o \quad . \tag{91}$$

The flow is assumed to be of sufficiently high Reynolds number so that the kinematic viscosity, thermal diffusivity, and water vapor diffusivity need not be included in (91). It is possible to form two dimensionless combinations of these dimensional variables:

$$z/z_o,\ z/L \tag{92}$$

where, $L \equiv \dfrac{-u_*^3}{\kappa(g/\overline{\Theta}_{v_o})\overline{w'\theta'_v}\big|_o}$ is the Monin-Obukhov length, and $\kappa$ is the von Karman constant, which is traditionally included in the definition of L.

The assumption that (91) contains all the relevant information needed to specify the structure of the surface layer implies that the non-dimensional forms of the mean velocity components, virtual potential temperature, and mixing ratio must be functions of only $z/z_o$ and $z/L$. The appropriate scaling factor to nondimensionalize the velocity components is the friction velocity $u_*$. Scaling factors for virtual potential temperature and mixing ratio are obtained from (91) and are given by:

$$\overline{\Theta}_* = \frac{-\overline{w'\theta'_v}\big|_o}{\kappa u_*} \tag{93}$$

$$\overline{R}_* = \frac{-\overline{w'r'}\big|_o}{\kappa u_*} \, . \tag{94}$$

Therefore, in the surface layer,

$$\frac{\overline{u}}{u_*} = F_1(z/z_o,\ z/L) \tag{95}$$

$$\frac{\overline{v}}{u_*} = F_2(z/z_o,\ z/L) \tag{96}$$

$$\frac{\overline{\Theta}_v - \overline{\Theta}_{v_o}}{\overline{\Theta}_*} = F_3(z/z_o, z/L) \tag{97}$$

$$\frac{\overline{R} - \overline{R}_o}{\overline{R}_*} = F_4(z/z_o, z/L) \quad . \tag{98}$$

In this section, the velocity components $\overline{u}$ and $\overline{v}$ are in surface coordinates, i.e., $\overline{u}$ is defined to be in the direction of the surface wind and $\overline{v}$ is perpendicular to it.

If the non-dimensional vertical gradients of $\overline{u}$, $\overline{v}$, $\overline{\Theta}_v$, and $\overline{R}$ are assumed to be independent of $z/z_o$ (Monin and Obukhov, 1954), it is possible to identify the $z/z_o$ dependence of the mean variables as logarithmic. Equations (96-98) can be written in the form:

$$\frac{\overline{u}}{u_*} = \frac{1}{\kappa} \; [\ln \; (z/z_o) \; - \; \phi_m(z/L)] \tag{99}$$

$$\frac{\overline{v}}{u_*} = 0 \tag{100}$$

$$\frac{\overline{\Theta}_v - \overline{\Theta}_{v_o}}{\overline{\Theta}_*} = \frac{Pr}{\kappa} \; [\ln \; (z/z_o) \; - \; \phi_h(z/L)] \tag{101}$$

$$\frac{\overline{R} - \overline{R}_o}{R_*} = \frac{Pr}{\kappa} \; [\ln \; (z/z_o) \; - \; \phi_R(z/L)] \tag{102}$$

For the remainder of the PBL, above the surface layer, Monin-Obukhov similarity theory does not apply, and the parameters in (91) do not suffice to determine the structure. The roughness parameter, $z_o$, is not important for $z >> z_o$, and can be eliminated from the list. Other effects, such as rotation and baroclinicity, should be included. The height of the PBL, h, representing externally determined influences, such as diurnal heating, subsidence, etc., must also be included. The similarity theory applied to the region of the PBL above the surface layer is called Ekman layer similarity theory.

Ekman layer similarity theory has evolved through the years and is based on the work of many people. Kazanski and Monin (1960, 1961), Csanady (1967), Gill (1968), Blackadar and Tennekes (1968), Clarke and Hess (1973), Deardorff (1972a,b), Hess (1973), Arya and Wyngaard (1975), and others have contributed to its development. In an analogous fashion with the surface layer, the non-dimensional forms of the mean variables can be represented as universal functions of non-dimensional combinations. The Ekman layer relations are:

$$\frac{\overline{u} - \overline{u}_m}{u_*} = G_1(z/h,\ h/L,\ |f|h/u_*) \tag{103}$$

$$\frac{\overline{v} - \overline{v}_m}{u_*} = G_2(z/h,\ h/L,\ |f|h/u_*) \tag{104}$$

$$\frac{\overline{\Theta}_v - \overline{\Theta}_{v_m}}{\overline{\Theta}_*} = G_3(z/h,\ h/L,\ |f|h/u_*) \tag{105}$$

$$\frac{\overline{R} - \overline{R}_m}{R_*} = G_4(z/h,\ h/L,\ |f|h/u_*) \tag{106}$$

The variables $\overline{u}_m$, $\overline{v}_m$, $\overline{\Theta}_{v_m}$, and $\overline{R}_m$ used in the deficit relations (103-106) are PBL mean values of velocity, virtual potential temperature, and mixing ratio.

$$\chi_m = \frac{1}{h} \int_{z_o}^{h} \chi dz, \qquad \chi = \overline{u},\ \overline{v},\ \overline{\Theta}_v,\ \overline{R} \tag{107}$$

The use of the PBL averaged quantities allows the effects of baroclinicity to be included implicitly, and thus simplifies the analysis (Arya, 1978).

The relations (99-102) apply in the surface layer, while (103-106) are their counterparts in the rest of the boundary layer. Assuming there is a transition region, or matching layer, in which both sets of relations apply, it is possible to obtain the following relations:

$$\frac{\overline{u}}{u_*} = \frac{1}{\kappa}\ [\ln(z/z_o) - \phi_m(z/L)] = \frac{\overline{u}_m}{u_*} + G_1(z/h,\ h/L,\ |f|h/u_*) \tag{108}$$

Writing $\ln(z/z_o)$ as $\ln(z/h) + \ln(h/z_o)$, and absorbing the $z/h$ dependence into the unknown function $G_1$ yields:

$$\ln(h/z_o) - \frac{\kappa \overline{u}_m}{u_*} = \kappa G_1'(z/h,\ h/L,\ |f|h/u_*) \tag{109}$$

The function $G_1'$, however, must be independent of z because the left hand side of (94) is independent of z. Eliminating the z dependence of $G_1'$, and calling the unknown function A, we obtain:

$$A(h/L,\ |f|h/u_*) = \ln(h/z_o) - \kappa \frac{\overline{u}_m}{u_*} \tag{110}$$

A similar matching argument for the relations (100-102, 104-106) yields the other universal similarity functions B, C, and D.

$$B(h/L,\ |f|n/u_*) = -\frac{\kappa \overline{v}_m}{u_*} \text{ sign } f \tag{111}$$

$$C(h/L,\ |f|h/u_*) = \ln(h/z_o) + \kappa\left[\frac{\overline{\Theta}_{vo} - \overline{\Theta}_{vm}}{\overline{\Theta}_*}\right] \tag{112}$$

$$D(h/L,\ |f|h/u_*) = \ln(h/z_o) + \kappa\left[\frac{\overline{R}_o - \overline{R}_m}{R_*}\right] \tag{113}$$

Attempts have been made to determine the similarity functions from an empirical data base. Clarke and Hess (1974) evaluated A and B using the geostrophic wind in their definition instead of $\bar{u}_m$ and $\bar{v}_m$, and assumed $h = u_*/|f|$. Melgarejo and Deardorff (1974) used the components of the wind $\bar{u}$ and $\bar{v}$ at the PBL top, h, in the deficit relations. The PBL top was determined by profiles of $\bar{\Theta}_v$ and $\bar{R}$ (unstable conditions) or $\bar{u}$ and $\bar{v}$ (stable conditions). Both studies, however, show a large amount of scatter in the data points, especially on the stable side. Arya (1975) reanalyzed the data of previous studies in an attempt to reduce the huge amounts of scatter. The results, although somewhat better, still retain considerable scatter.

The similarity theories discussed assume that a steady-state, horizontally homogeneous situation exists. In the real atmosphere neither condition is satisfied. Diurnal variations and large scale changes in the flow pattern violate the assumption of a steady-state. Changes in the surface characteristics and horizontal advection are usually present to violate the horizontal homogeneity assumption. In addition, it is very difficult to measure Reynolds stresses or heat and moisture fluxes in the field. It is not surprising, therefore, that empirical determinations of the similarity functions contain a considerable amount of scatter.

An alternative approach, the use of a model, has been used to determine the similarity functions (Arya, 1977; Yamada, 1976; Arya and Wyngaard, 1975). The assumptions of horizontal homogeneity and stationarity can be satisfied using this approach. There is no "measurement error" as with an empirical determination. The main limitation is the ability of the model, with its modeling assumptions and approximations, to faithfully reproduce nature.

## 8.2 Results

The similarity functions A, B, C, and D are evaluated for five cases and are tabulated with h, $u_*$, $T_*$, $R_*$, L, $Ri_B$, $h/z_o$, h/L, and $|f|h/u_*$ (see Tables VI-X). The bulk Richardson number, $Ri_B$, is defined as:

$$Ri_B \equiv \frac{Bgh(\overline{\Theta}_{vm} - \overline{\Theta}_{vo})}{\overline{u}_m^2 + \overline{v}_m^2} \qquad (114)$$

In each case, a 24-hour simulation is started at 0900 hours local time, using the initial conditions described in section 6.1. The results contained in section 6.2 are from case B.

| Case | Table | Surface Albedo | Geostrophic Winds |
|---|---|---|---|
| A | VI | 0.10 | Wangara |
| B | VII | 0.20 | Wangara |
| C | VIII | 0.25 | Wangara |
| D | IX | 0.30 | Wangara |
| E | X | 0.20 | constant |

As summarized above, cases A-D use the observed geostrophic winds from the Wangara experiment, as described by Yamada and Mellor (1975). Spatially and temporally constant geostrophic winds are used in case E ($u_g = v_g = -4$ m/s).

The similarity function A is plotted as a function of h/L in Figure 36. Hourly values of A (from Tables VI-X) are used in the construction of Figure 36. The data for the 9th and 10th simulated hours (6:00 - 7:00 p.m. local time) are not used because in this period the boundary layer height is very rapidly changing. Similarity theory cannot be expected to do well under these highly non-stationary conditions. Figures 37-39 are the same as Figure 36 except for the similarity functions B, C, and D.

On the unstable side, there is a small amount of scatter in the similarity functions which is probably attributable to the fact that all values of $h/z_o$ and $|f|h/u_*$ are allowed. In other words, the dependence of A, B, C, and D on $h/z_o$ and $|f|h/u_*$ is not considered in

## List of the Variables in Tables VI - X

| | |
|---|---|
| t (hours) | simulated time starting at 9:00 a.m. local time (i.e., time = 1 corresponds to 10:00 a.m., time = 2 corresponds to 11:00 a.m., etc.) |
| h (m) | Boundary layer height |
| $u_*$(m/s) | Friction velocity |
| $\overline{\Theta}_*$ (°K) | Scaling factor for virtual potential temperature (eqn. 93) |
| $\overline{R}_*$ (gm/gm) | Scaling factor for water vapor mixing ratio (eqn. 94) multiplied by 1000 |
| L (m) | Monin-Obukhov length |
| $Ri_B$ | Bulk Richardson number (eqn. 114) |
| A | Similarity function A |
| B | Similarity function B |
| C | Similarity function C |
| D | Similarity function D |
| $h/z_o$ | Ratio of boundary layer height to surface roughness parameter ($z_o$ = 0.01 m) |
| h/L | Ratio of boundary layer height to Monin-Obukhov length |
| $\|f\|h/u_*$ | Ratio of the magnitude of the Coriolis parameter ($f = -8.2 \times 10^{-5}\ s^{-1}$) to $u_*/h$ |

Table VI

## Similarity Functions - Case A

| t | h | $u_*$ | $\overline{\Theta}_*$ | $\overline{R}_*$ | L | $Ri_B$ | A | B | C | D | $h/z_o$ | h/L | $\frac{\lvert f\rvert h}{u_*}$ |
|---|---|---|---|---|---|---|---|---|---|---|---|---|---|
| 0.25 | 154.4 | 0.139 | -3.379 | -0.1857 | -1.39 | -10.08 | 3.810 | 0.889 | 8.540 | 8.264 | 15443.8 | -111.30 | 0.0915 |
| 0.50 | 154.4 | 0.151 | -3.522 | -0.2204 | -1.59 | -12.06 | 4.477 | 0.562 | 8.473 | 8.396 | 15443.8 | -97.36 | 0.0841 |
| 0.75 | 201.1 | 0.158 | -3.740 | -0.2557 | -1.65 | -15.98 | 4.870 | 0.544 | 8.731 | 8.691 | 20113.6 | -121.94 | 0.1046 |
| 1.00 | 248.5 | 0.163 | -3.976 | -0.2915 | -1.66 | -20.37 | 5.175 | 0.538 | 8.943 | 8.900 | 24849.3 | -149.74 | 0.1253 |
| 1.25 | 296.3 | .168 | -4.153 | -0.3228 | -1.69 | -24.45 | 5.403 | 0.465 | 9.113 | 9.068 | 29629.4 | -174.83 | 0.1449 |
| 1.50 | 392.8 | 0.175 | -4.284 | -0.3463 | -1.78 | -29.92 | 5.610 | 0.639 | 9.389 | 9.304 | 39277.0 | -220.90 | 0.1850 |
| 1.75 | 538.8 | 0.183 | -4.336 | -0.3603 | -1.93 | -41.33 | 6.094 | 0.520 | 9.689 | 9.555 | 53681.8 | -279.64 | 0.2426 |
| 2.00 | 685.8 | 0.187 | -4.419 | -0.3759 | -1.98 | -54.33 | 6.463 | 0.436 | 9.927 | 9.781 | 68580.3 | -346.43 | 0.3020 |
| 2.25 | 784.1 | .188 | -4.539 | -0.3943 | -1.96 | -67.15 | 6.764 | 0.411 | 10.069 | 9.915 | 78412.8 | -400.78 | 0.3431 |
| 2.50 | 833.4 | 0.187 | -4.669 | -0.4149 | -1.89 | -76.76 | 6.930 | 0.392 | 10.142 | 10.010 | 83336.7 | -441.28 | 0.3663 |
| 2.75 | 882.6 | 0.186 | -4.799 | -0.4365 | -1.81 | -87.98 | 7.082 | 0.386 | 10.211 | 10.101 | 88264.9 | -488.78 | 0.3916 |
| 3.00 | 932.0 | 0.184 | -4.915 | -0.45[illegible]4 | -1.73 | -100.39 | 7.227 | 0.387 | 10.276 | 10.185 | 93196.9 | -539.65 | 0.4182 |
| 3.25 | 981.3 | 0.182 | -5.001 | -0.4741 | -1.66 | -113.09 | 7.358 | 0.402 | 10.335 | 10.258 | 98132.4 | -589.79 | 0.4451 |
| 3.50 | 981.3 | 0.181 | -5.031 | -0.4859 | -1.64 | -114.23 | 7.350 | 0.361 | 10.340 | 10.289 | 98132.4 | -599.56 | 0.4476 |
| 3.75 | 981.3 | 0.180 | -5.011 | -0.4929 | -1.64 | -114.83 | 7.365 | 0.335 | 10.340 | 10.292 | 98132.4 | -597.64 | 0.4479 |
| 4.00 | 1030.7 | 0.181 | -4.936 | -0.4928 | -1.68 | -118.53 | 7.419 | 0.318 | 10.383 | 10.339 | 103071.1 | -611.75 | 0.4680 |
| 4.25 | 1030.7 | 0.183 | -4.815 | -0.4887 | -1.75 | -113.84 | 7.400 | 0.282 | 10.374 | 10.327 | 103071.1 | -587.40 | 0.4643 |
| 4.50 | 1030.7 | 0.185 | -4.645 | -0.4789 | -1.87 | -105.64 | 7.346 | 0.252 | 10.359 | 10.312 | 103071.1 | -552.02 | 0.4582 |
| 4.75 | 1080.1 | 0.188 | -4.439 | -0.4644 | -2.02 | -103.39 | 7.377 | 0.229 | 10.388 | 10.327 | 108012.5 | -535.80 | 0.4725 |
| 5.00 | 1129.6 | 0.192 | -4.264 | -0.4469 | -2.20 | -98.36 | 7.371 | 0.210 | 10.411 | 10.338 | 112956.6 | -512.63 | 0.4853 |
| 5.25 | 1129.6 | .196 | -3.941 | -0.4258 | -2.44 | -86.30 | 7.272 | 0.193 | 10.390 | 10.314 | 112956.6 | -462.94 | 0.4760 |
| 5.50 | 1179.0 | 0.200 | -3.658 | -0.4026 | -2.74 | -79.28 | 7.242 | 0.191 | 10.408 | 10.317 | 117903.0 | -430.89 | 0.4865 |
| 5.75 | 1179.0 | 0.204 | -3.358 | -0.3783 | -3.10 | -67.86 | 7.127 | 0.193 | 10.381 | 10.288 | 117903.0 | -380.00 | 0.4763 |
| 6.00 | 1179.0 | 0.208 | -3.045 | -0.3528 | -3.56 | -56.78 | 6.982 | 0.200 | 10.350 | 10.277 | 117903.0 | -330.78 | 0.4661 |
| 6.25 | 1179.0 | 0.213 | -2.723 | -0.3265 | -4.15 | -46.82 | 6.825 | 0.209 | 10.316 | 10.261 | 117903.0 | -283.91 | 0.4560 |
| 6.50 | 1228.5 | 0.218 | -2.395 | -0.2993 | -4.92 | -40.30 | 6.743 | 0.222 | 10.317 | 10.240 | 122851.6 | -249.56 | 0.4645 |
| 6.75 | 1228.5 | 0.222 | -2.066 | -0.2 22 | -5.91 | -32.32 | 6.572 | 0.229 | 10.273 | 10.196 | 122851.6 | -207.73 | 0.4556 |
| 7.00 | 1228.5 | 0.226 | -1.740 | -0.2458 | -7.22 | -25.40 | 6.370 | 0.243 | 10.221 | 10.163 | 122851.6 | -170.16 | 0.4486 |
| 7.25 | 1228.5 | .228 | -1.418 | -0.2197 | -9.02 | -19.49 | 6.139 | 0.262 | 10.156 | 10.111 | 122851.6 | -136.22 | 0.4438 |
| 7.50 | 1228.5 | 0.229 | -1.101 | -0.19[illegible]7 | -11.66 | -14.45 | 5.870 | 0.284 | 10.073 | 10.022 | 122851.6 | -105.35 | 0.4422 |
| 7.75 | 1278.0 | 0.228 | -0.788 | -0.1677 | -16.04 | -10.58 | 5.604 | 0.321 | 9.993 | 9.910 | 127802.2 | -79.67 | 0.4625 |
| 8.00 | 1278.0 | 0.223 | -0.479 | -0.1415 | -25.19 | -6.48 | 5.160 | 0.363 | 9.807 | 9.763 | 127802.2 | -50.73 | 0.4724 |
| 8.25 | 1278.0 | 0.213 | -0.172 | -0.1147 | -63.73 | -2.69 | 4.505 | 0.437 | 9.279 | 9.558 | 127802.2 | -20.05 | 0.4947 |
| 8.50 | 1327.5 | 0.191 | 0.134 | -0.0861 | 65.16 | 1.11 | 3.329 | 0.624 | 10.423 | 9.146 | 132754.7 | 20.37 | 0.5729 |
| 8.75 | 1377.1 | 0.141 | 0.426 | -0.0490 | 11.19 | 5.16 | -0.115 | 1.295 | 9.302 | 7.443 | 137708.9 | 123.11 | 0.8022 |
| 9.00 | 1377.1 | 0.085 | 0.582 | -0.0103 | 2.94 | 12.99 | -8.753 | 3.598 | 7.588 | -5.110 | 137708.9 | 467.75 | 1.3279 |
| 9.25 | 1377.1 | 0.108 | 0.608 | -0.0066 | 4.47 | 16.16 | -5.212 | 3.146 | 6.324 | -10.724 | 137708.9 | 308.39 | 1.0497 |
| 9.50 | 1327.5 | 0.113 | 0.592 | -0.0050 | 4.96 | 16.51 | -5.279 | 3.486 | 5.242 | -15.332 | 132754.7 | 267.82 | 0.9710 |
| 9.75 | 1327.5 | 0.114 | 0.580 | -0.0039 | 5.13 | 16.73 | -5.769 | 4.062 | 4.443 | -2[illegible].728 | 132754.7 | 258.89 | 0.9623 |
| 10.00 | 1278.0 | 0.113 | 0.569 | -0.0030 | 5.17 | 15.96 | -6.521 | 4.712 | 3.701 | -28.160 | 127802.2 | 247.01 | 0.9295 |
| 10.25 | 1179.0 | 0.112 | 0.559 | -0.0022 | 5.17 | 14.40 | -7.435 | 5.382 | 2.965 | -39.009 | 117903.0 | 228.01 | 0.8642 |
| 10.50 | 108.8 | 0.096 | 0.526 | -0.0007 | 4.19 | 1.38 | -12.013 | 4.206 | 0.497 | -95.206 | 10881.5 | 25.99 | 0.0912 |
| 10.75 | 65.2 | 0.093 | 0.519 | -0.0001 | 3.82 | 0.93 | -12.132 | 3.930 | 0.114 | -545.749 | 6521.4 | 17.08 | 0.0576 |
| 11.00 | 65.2 | 0.096 | 0.498 | -0.0004 | 4.21 | 0.91 | -12.168 | 4.209 | -0.556 | -129.986 | 6521.4 | 15.49 | 0.0559 |
| 11.25 | 65.2 | 0.097 | 0.477 | -0.0006 | 4.46 | 0.84 | -12.595 | 4.604 | -0.808 | -56.160 | 6521.4 | 14.61 | 0.0554 |
| 11.50 | 65.2 | 0.097 | 0.477 | -0.0006 | 4.47 | 0.78 | -13.159 | 5.063 | -0.669 | -53.173 | 6521.4 | 14.58 | 0.0554 |
| 11.75 | 65.2 | 0.099 | 0.464 | -0.0009 | 4.58 | 0.72 | -13.296 | 5.396 | -0.385 | -49.188 | 6521.4 | 14.24 | 0.0543 |
| 12.00 | 108.8 | 0.101 | 0.490 | -0.0010 | 4.69 | 1.00 | -15.539 | 7.544 | -0.818 | -58.087 | 10881.5 | 23.22 | 0.0891 |
| 12.25 | 108.8 | 0.098 | 0.475 | -0.0011 | 4.61 | 0.93 | -16.720 | 8.370 | -1.043 | -52.317 | 10881.5 | 23.62 | 0.0912 |
| 12.50 | 108.8 | 0.095 | 0.460 | -0.0012 | 4.47 | 0.88 | -18.115 | 9.292 | -1.284 | -46.579 | 10881.5 | 24.33 | 0.0941 |
| 12.75 | 108.8 | 0.103 | 0.492 | -0.0015 | 4.93 | 0.83 | -16.605 | 8.887 | -0.526 | -37.405 | 10881.5 | 22.08 | 0.0867 |
| 13.00 | 108.8 | 0.116 | 0.513 | -0.0017 | 5.92 | 0.78 | -14.377 | 8.114 | -0.018 | -31.043 | 10881.5 | 18.39 | 0.0775 |
| 13.25 | 108.8 | 0.124 | 0.505 | -0.0019 | 6.91 | 0.74 | -13.172 | 7.635 | -0.054 | -27.179 | 10881.5 | 15.74 | 0.0722 |
| 13.50 | 108.8 | 0.130 | 0.462 | -0.0020 | 7.96 | 0.71 | -12.439 | 7.760 | -0.381 | -24.507 | 10881.5 | 13.66 | 0.0689 |
| 13.75 | 108.8 | 0.135 | 0.451 | -0.0021 | 9.09 | 0.68 | -11.981 | 7.767 | -0.910 | -22.515 | 10881.5 | 11.97 | 0.0666 |
| 14.00 | 108.8 | 0.136 | 0.419 | -0.0022 | 10.27 | 0.66 | -11.707 | 7.809 | -1.579 | -20.954 | 10881.5 | 10.59 | 0.0651 |
| 14.25 | 108.8 | 0.141 | 0.390 | -0.0023 | 11.50 | 0.63 | -11.485 | 7.771 | -2.243 | -19.665 | 10881.5 | 9.47 | 0.0637 |
| 14.50 | 108.8 | 0.142 | 0.364 | -0.0024 | 12.64 | 0.62 | -11.415 | 7.771 | -2.941 | -18.346 | 10881.5 | 8.61 | 0.0629 |
| 14.75 | 108.8 | 0.144 | 0.342 | -0.0025 | 13.67 | 0.60 | -11.406 | 7.792 | -3.592 | -17.264 | 10881.5 | 7.96 | 0.0624 |
| 15.00 | 108.8 | 0.144 | 0.324 | -0.0026 | 14.55 | 0.59 | -11.440 | 7.845 | -4.164 | -16.333 | 10881.5 | 7.48 | 0.0621 |
| 15.25 | 108.8 | 0.145 | 0.310 | -0.0026 | 15.27 | 0.57 | -11.498 | 7.943 | -4.646 | -15.534 | 10881.5 | 7.13 | 0.0620 |
| 15.50 | 108.8 | 0.145 | 0.299 | -0.0026 | 15.82 | 0.56 | -11.563 | 8.091 | -5.040 | -14.845 | 10881.5 | 6.88 | 0.0620 |
| 15.75 | 108.8 | 0.144 | 0.290 | -0.0027 | 16.25 | 0.55 | -11.621 | 8.285 | -5.358 | -14.244 | 10881.5 | 6.70 | 0.0621 |
| 16.00 | 108.8 | 0.144 | 0.283 | -0.0027 | 16.57 | 0.55 | -11.660 | 8.520 | -5.613 | -13.712 | 10881.5 | 6.57 | 0.0623 |
| 16.25 | 108.8 | 0.143 | 0.277 | -0.0027 | 16.81 | 0.54 | -11.672 | 8.791 | -5.823 | -13.236 | 10881.5 | 6.47 | 0.0625 |
| 16.50 | 108.8 | 0.143 | 0.272 | -0.0027 | 17.01 | 0.54 | -11.654 | 9.091 | -6.002 | -12.806 | 10881.5 | 6.40 | 0.0628 |
| 16.75 | 108.8 | 0.142 | 0.267 | -0.0028 | 17.18 | 0.53 | -11.601 | 9.415 | -6.162 | -12.416 | 10881.5 | 6.33 | 0.0630 |
| 17.00 | 108.8 | 0.142 | 0.263 | -0.0028 | 17.34 | 0.53 | -11.511 | 9.756 | -6.313 | -12.058 | 10881.5 | 6.28 | 0.0632 |
| 17.25 | 108.8 | 0.141 | 0.258 | -0.0028 | 17.50 | 0.53 | -11.382 | 10.109 | -6.462 | -11.731 | 10881.5 | 6.22 | 0.0635 |
| 17.50 | 108.8 | 0.141 | 0.254 | -0.0028 | 17.67 | 0.53 | -11.213 | 10.466 | -6.614 | -11.429 | 10881.5 | 6.16 | 0.0637 |
| 17.75 | 108.8 | 0.140 | 0.250 | -0.0028 | 17.86 | 0.53 | -11.005 | 10.824 | -6.773 | -11.151 | 10881.5 | 6.09 | 0.0639 |
| 18.00 | 108.8 | 0.140 | 0.246 | -0.0028 | 18.08 | 0.53 | -10.759 | 11.176 | -6.941 | -10.893 | 10881.5 | 6.02 | 0.0640 |
| 18.25 | 108.8 | 0.140 | 0.242 | -0.0029 | 18.35 | 0.53 | -10.482 | 11.460 | -7.108 | -10.645 | 10881.5 | 5.93 | 0.0641 |
| 18.50 | 108.8 | 0.140 | 0.238 | -0.0029 | 18.66 | 0.53 | -10.194 | 11.722 | -7.263 | -10.404 | 10881.5 | 5.83 | 0.0640 |
| 18.75 | 108.8 | 0.140 | 0.235 | -0.0029 | 19.02 | 0.54 | -9.888 | 11.896 | -7.382 | -10.160 | 10881.5 | 5.72 | 0.0639 |
| 19.00 | 108.8 | 0.141 | 0.232 | -0.0029 | 19.37 | 0.54 | -9.594 | 12.020 | -7.477 | -9.927 | 10881.5 | 5.62 | 0.0637 |
| 19.25 | 108.8 | 0.141 | 0.229 | -0.0029 | 19.73 | 0.54 | -9.314 | 12.112 | -7.564 | -9.711 | 10881.5 | 5.52 | 0.0634 |
| 19.50 | 108.8 | 0.142 | 0.228 | -0.0029 | 20.10 | 0.54 | -9.017 | 12.142 | -7.589 | -9.633 | 10881.5 | 5.41 | 0.0631 |
| 19.75 | 154.4 | 0.137 | 0.401 | 0.0001 | 10.54 | 0.79 | -9.996 | 15.964 | -2.426 | 1176.338 | 15443.8 | 14.65 | 0.0930 |
| 20.00 | 154.4 | 0.132 | 0.357 | 0.0001 | 11.08 | 0.80 | -9.349 | 17.817 | -3.898 | 1018.288 | 15443.8 | 13.94 | 0.0961 |
| 20.25 | 154.4 | 0.132 | 0.175 | -0.0023 | 22.39 | 0.76 | -8.170 | 19.093 | -16.802 | -18.518 | 15443.8 | 6.90 | 0.0967 |
| 20.50 | 154.4 | 0.134 | -0.019 | -0.0051 | -207.62 | 0.74 | -6.635 | 19.774 | 239.516 | -3.874 | 15443.8 | -0.74 | 0.0952 |
| 20.75 | 154.4 | 0.131 | -0.024 | -0.0046 | -164.16 | 0.75 | -5.469 | 20.983 | 198.305 | -5.226 | 15443.8 | -0.94 | 0.0968 |
| 21.00 | 65.2 | 0.123 | 0.111 | -0.0018 | 30.97 | 0.35 | -6.667 | 12.519 | -13.942 | -11.567 | 6521.4 | 2.11 | 0.0436 |
| 21.25 | 65.2 | 0.124 | 0.072 | -0.0021 | 48.19 | 0.34 | -6.209 | 13.127 | -25.666 | -8.780 | 6521.4 | 1.35 | 0.0434 |
| 21.50 | 65.2 | 0.126 | 0.088 | -0.0016 | 41.08 | 0.33 | -5.584 | 13.458 | -19.752 | -13.836 | 6521.4 | 1.59 | 0.0426 |
| 21.75 | 65.2 | 0.128 | 0.131 | -0.0007 | 28.15 | 0.34 | -5.031 | 13.789 | -10.737 | -40.539 | 6521.4 | 2.32 | 0.0420 |
| 22.00 | 65.2 | 0.129 | 0.166 | -0.0000 | 22.70 | 0.34 | -4.536 | 14.127 | -7.048 | -2660.723 | 6521.4 | 2.87 | 0.0416 |
| 22.25 | 65.2 | 0.130 | 0.089 | -0.0010 | 42.94 | 0.33 | -4.036 | 14.418 | -19.516 | -27.687 | 6521.4 | 1.52 | 0.0413 |
| 22.50 | 65.2 | 0.132 | 0.008 | -0.0020 | 483.85 | 0.32 | -3.525 | 14.633 | -292.965 | -10.467 | 6521.4 | 0.13 | 0.0408 |
| 22.75 | 65.2 | 0.136 | -0.048 | -0.0032 | -88.67 | 0.30 | -2.690 | 14.422 | 57.262 | -4.485 | 6521.4 | -0.74 | 0.0394 |
| 23.00 | 65.2 | 0.134 | -0.037 | -0.0031 | -108.48 | 0.30 | -2.443 | 15.004 | 70.660 | -5.084 | 6521.4 | -0.60 | 0.0401 |
| 23.25 | 65.2 | 0.133 | -0.030 | -0.0030 | -132.63 | 0.31 | -2.114 | 15.447 | 86.443 | -5.668 | 6521.4 | -0.49 | 0.0405 |
| 23.50 | 65.2 | 0.132 | -0.024 | -0.0030 | -161.24 | 0.31 | -1.742 | 15.786 | 104.749 | -6.248 | 6521.4 | -0.40 | 0.0408 |
| 23.75 | 65.2 | 0.131 | -0.020 | -0.0029 | -194.22 | 0.31 | -1.344 | 16.034 | 125.438 | -6.820 | 6521.4 | -0.34 | 0.0409 |
| 24.00 | 65.2 | 0.131 | -0.017 | -0.0029 | -231.09 | 0.31 | -0.934 | 16.212 | 148.241 | -7.387 | 6521.4 | -0.28 | 0.0410 |

# Table VII

## Similarity Functions - Case B

| $t$ | $h$ | $u_*$ | $\overline{\Theta}_*$ | $\overline{R}_*$ | $L$ | $Ri_B$ | $\Lambda$ | $B$ | $C$ | $D$ | $h/z_o$ | $h/L$ | $\frac{\lvert f\rvert h}{u_*}$ |
|---|---|---|---|---|---|---|---|---|---|---|---|---|---|
| 0.25 | 154.4 | 0.135 | -2.969 | -.1617 | -1.48 | -8.93 | 3.636 | 0.962 | 8.534 | 8.191 | 15443.8 | -104.11 | 0.0942 |
| 0.50 | 154.4 | 0.148 | -3.080 | -0.1890 | -1.73 | -10.66 | 4.348 | 0.597 | 8.457 | 8.362 | 15443.8 | -89.28 | 0.0859 |
| 0.75 | 201.1 | 0.155 | -3.304 | -0.2197 | -1.76 | -14.14 | 4.725 | 0.670 | 8.722 | 8.659 | 20113.6 | -113.97 | 0.1072 |
| 1.00 | 248.5 | 0.159 | -3.528 | -0.2518 | -1.75 | -18.17 | 5.010 | 0.686 | 8.928 | 8.866 | 24849.3 | -141.74 | 0.1290 |
| 1.25 | 296.3 | 0.164 | -3.683 | -0.2778 | -1.80 | -21.83 | 5.248 | 0.633 | 9.096 | 9.028 | 29629.4 | -164.79 | 0.1490 |
| 1.50 | 344.4 | 0.169 | -3.821 | -0.3006 | -1.86 | -25.04 | 5.441 | 0.639 | 9.244 | 9.166 | 34441.2 | -185.53 | 0.1676 |
| 1.75 | 441.3 | 0.176 | -3.896 | -0.3161 | -1.98 | -30.65 | 5.718 | 0.706 | 9.482 | 9.363 | 44131.4 | -223.38 | 0.2064 |
| 2.00 | 587.7 | 0.183 | -3.929 | -0.3265 | -2.11 | -41.93 | 6.187 | 0.515 | 9.755 | 9.594 | 58773.2 | -278.18 | 0.2650 |
| 2.25 | 685.8 | 0.185 | -4.005 | -0.3398 | -2.14 | -50.78 | 6.455 | 0.433 | 9.913 | 9.770 | 68580.3 | -321.10 | 0.3048 |
| 2.50 | 784.1 | 0.186 | -4.096 | -0.3542 | -2.11 | -62.55 | 6.743 | 0.420 | 10.053 | 9.888 | 78412.8 | -372.01 | 0.3472 |
| 2.75 | 833.4 | 0.185 | -4.192 | -0.3699 | -2.04 | -71.01 | 6.896 | 0.397 | 10.124 | 9.983 | 83336.7 | -408.41 | 0.3709 |
| 3.00 | 882.- | 0.183 | -4.282 | -0.3856 | -1.97 | -80.74 | 7.043 | 0.387 | 10.191 | 10.069 | 88264.9 | -449.03 | 0.3964 |
| 3.25 | 932.0 | 0.182 | -4.347 | -0.3988 | -1.91 | -90.87 | 7.184 | 0.384 | 10.252 | 10.145 | 93196.9 | -488.49 | 0.4218 |
| 3.50 | 932.0 | 0.181 | -4.375 | -0.4090 | -1.87 | -91.93 | 7.176 | 0.347 | 10.257 | 10.187 | 93196.9 | -497.32 | 0.4245 |
| 3.75 | 981.3 | 0.181 | -4.356 | -0.4139 | -1.88 | -98.58 | 7.276 | 0.351 | 10.307 | 10.239 | 98132.4 | -520.82 | 0.4469 |
| 4.00 | 981.3 | 0.182 | -4.292 | -0.4151 | -1.93 | -94.69 | 7.225 | 0.315 | 10.302 | 10.255 | 98132.4 | -509.52 | 0.4453 |
| 4.25 | 1030.7 | 0.183 | -4.183 | -0.4110 | -2.02 | -97.45 | 7.308 | 0.306 | 10.340 | 10.279 | 103071.1 | -510.92 | 0.4629 |
| 4.50 | 1030.7 | 0.186 | -4.034 | -0.4027 | -2.14 | -89.28 | 7.226 | 0.270 | 10.328 | 10.281 | 103071.1 | -481.05 | 0.4572 |
| 4.75 | 1030.7 | 0.189 | -3.854 | -0.3915 | -2.31 | -82.07 | 7.177 | 0.239 | 10.311 | 10.255 | 103071.1 | -445.65 | 0.4501 |
| 5.00 | 1030.7 | 0.192 | -3.641 | -0.3769 | -2.54 | -73.04 | 7.069 | 0.217 | 10.290 | 10.235 | 103071.1 | -405.51 | 0.4415 |
| 5.25 | 1080.1 | 0.196 | -3.408 | -0.3598 | -2.83 | -68.84 | 7.095 | 0.197 | 10.312 | 10.238 | 108012.5 | -381.79 | 0.4530 |
| 5.50 | 1080.1 | 0.201 | -3.156 | -0.3410 | -3.18 | -59.26 | 6.975 | 0.185 | 10.287 | 10.218 | 108012.5 | -339.66 | 0.4435 |
| 5.75 | 1129.6 | 0.205 | -2.893 | -0.3210 | -3.62 | -53.97 | 6.947 | 0.174 | 10.303 | 10.210 | 112956.6 | -312.12 | 0.4537 |
| 6.00 | 1129.6 | 0.209 | -2.619 | -0.3001 | -4.16 | -45.54 | 6.819 | 0.172 | 10.273 | 10.175 | 112956.6 | -271.77 | 0.4444 |
| 6.25 | 1179.0 | 0.214 | -2.339 | -0.2785 | -4.84 | -40.12 | 6.757 | 0.178 | 10.280 | 10.164 | 117903.0 | -243.63 | 0.4543 |
| 6.50 | 1179.0 | 0.218 | -2.054 | -0.2569 | -5.70 | -32.97 | 6.609 | 0.188 | 10.241 | 10.120 | 117903.0 | -206.74 | 0.4460 |
| 6.75 | 1179.0 | 0.221 | -1.767 | -0.2352 | -6.83 | -26.53 | 6.431 | 0.203 | 10.195 | 10.083 | 117903.0 | -172.67 | 0.4388 |
| 7.00 | 1179.0 | 0.224 | -1.482 | -0.2134 | -8.33 | -20.83 | 6.216 | 0.225 | 10.139 | 10.055 | 117903.0 | -141.59 | 0.4332 |
| 7.25 | 1179.0 | 0.226 | -1.199 | -0.1915 | -10.42 | -15.91 | 5.967 | 0.250 | 10.070 | 10.009 | 117903.0 | -113.17 | 0.4299 |
| 7.50 | 1179.0 | 0.226 | -0.919 | -0.1695 | -13.57 | -11.68 | 5.674 | 0.279 | 9.979 | 9.930 | 117903.0 | -86.90 | 0.4296 |
| 7.75 | 1179.0 | 0.224 | -0.642 | -0.1472 | -19.01 | -7.99 | 5.321 | 0.312 | 9.851 | 9.800 | 117903.0 | -62.01 | 0.4334 |
| 8.00 | 1228.5 | 0.219 | -0.367 | -0.1244 | -31.66 | -4.91 | 4.922 | 0.366 | 9.666 | 9.636 | 122851.6 | -38.80 | 0.4620 |
| 8.25 | 1278.0 | 0.208 | -0.092 | -0.1010 | -113.60 | -1.72 | 4.283 | 0.460 | 8.754 | 9.413 | 127802.2 | -11.25 | 0.5051 |
| 8.50 | 1278.0 | 0.184 | 0.181 | -0.0758 | 44.59 | 1.75 | 2.860 | 0.670 | 10.057 | 8.880 | 127802.2 | 28.66 | 0.5734 |
| 8.75 | 1327.5 | 0.134 | 0.440 | -0.0415 | 9.71 | 6.43 | -0.924 | 1.443 | 9.097 | 6.812 | 132754.7 | 136.74 | 0.8153 |
| 9.00 | 1327.5 | 0.090 | 0.620 | -0.0091 | 3.05 | 12.67 | -7.972 | 3.498 | 7.694 | -6.760 | 132754.7 | 435.46 | 1.2169 |
| 9.25 | 1327.5 | 0.107 | 0.599 | -0.0054 | 4.45 | 15.41 | -5.555 | 3.262 | 6.162 | -14.795 | 132754.7 | 298.44 | 1.0202 |
| 9.50 | 1278.0 | 0.112 | 0.585 | -0.0041 | 4.93 | 15.68 | -5.612 | 3.605 | 5.090 | -20.506 | 127802.2 | 259.06 | 0.9418 |
| 9.75 | 1228.5 | 0.113 | 0.574 | -0.0031 | 5.11 | 15.19 | -6.164 | 4.130 | 4.269 | -27.310 | 122851.6 | 240.33 | 0.8957 |
| 10.00 | 1179.0 | 0.113 | 0.564 | -0.0024 | 5.17 | 14.40 | -6.908 | 4.766 | 3.547 | -37.396 | 117903.0 | 228.23 | 0.8610 |
| 10.25 | 108.8 | 0.101 | 0.519 | -0.0008 | 4.51 | 1.38 | -10.933 | 3.556 | 0.849 | -85.017 | 10881.5 | 24.11 | 0.0885 |
| 10.50 | 65.2 | 0.093 | 0.517 | -0.0001 | 3.81 | 0.93 | -11.800 | 3.535 | 0.449 | -559.393 | 6521.4 | 17.11 | 0.0577 |
| 10.75 | 65.2 | 0.096 | 0.516 | -0.0000 | 4.01 | 0.92 | -11.952 | 3.845 | 0.024 | -2238.906 | 6521.4 | 16.27 | 0.0562 |
| 11.00 | 65.2 | 0.097 | 0.475 | -0.0007 | 4.45 | 0.84 | -12.344 | 4.212 | -0.572 | -59.807 | 6521.4 | 14.64 | 0.0556 |
| 11.25 | 65.2 | 0.097 | 0.475 | -0.0008 | 4.46 | 0.78 | -12.941 | 4.660 | -0.436 | -54.302 | 6521.4 | 14.62 | 0.0556 |
| 11.50 | 65.2 | 0.096 | 0.473 | -0.0009 | 4.45 | 0.72 | -13.582 | 5.143 | -0.317 | -49.777 | 6521.4 | 14.65 | 0.0557 |
| 11.75 | 108.8 | 0.097 | 0.472 | -0.0010 | 4.55 | 0.99 | -16.066 | 7.312 | -0.848 | -60.476 | 10881.5 | 23.91 | 0.0921 |
| 12.00 | 108.8 | 0.097 | 0.473 | -0.0011 | 4.54 | 0.93 | -16.702 | 7.902 | -0.734 | -52.840 | 10881.5 | 23.96 | 0.0921 |
| 12.25 | 108.8 | 0.094 | 0.456 | -0.0012 | 4.43 | 0.87 | -18.104 | 8.833 | -1.001 | -47.686 | 10881.5 | 24.56 | 0.0949 |
| 12.50 | 108.8 | 0.103 | 0.487 | -0.0014 | 4.91 | 0.82 | -16.546 | 8.493 | -0.269 | -38.764 | 10881.5 | 22.16 | 0.0873 |
| 12.75 | 108.8 | 0.115 | 0.510 | -0.0016 | 5.91 | 0.77 | -14.265 | 7.739 | 0.263 | -32.564 | 10881.5 | 18.40 | 0.0777 |
| 13.00 | 108.8 | 0.124 | 0.502 | -0.0018 | 6.91 | 0.73 | -13.083 | 7.467 | 0.232 | -28.487 | 10881.5 | 15.75 | 0.0725 |
| 13.25 | 108.8 | 0.130 | 0.479 | -0.0019 | 7.96 | 0.70 | -12.373 | 7.425 | -0.085 | -25.614 | 10881.5 | 13.67 | 0.0691 |
| 13.50 | 108.8 | 0.134 | 0.448 | -0.0021 | 9.09 | 0.67 | -11.942 | 7.454 | -0.608 | -23.460 | 10881.5 | 11.97 | 0.0669 |
| 13.75 | 108.8 | 0.137 | 0.415 | -0.0022 | 10.29 | 0.64 | -11.689 | 7.518 | -1.271 | -21.909 | 10881.5 | 10.58 | 0.0653 |
| 14.00 | 108.8 | 0.140 | 0.386 | -0.0022 | 11.54 | 0.62 | -11.467 | 7.507 | -1.928 | -20.792 | 10881.5 | 9.43 | 0.0639 |
| 14.25 | 108.8 | 0.142 | 0.360 | -0.0023 | 12.71 | 0.60 | -11.397 | 7.514 | -2.615 | -19.325 | 10881.5 | 8.56 | 0.0631 |
| 14.50 | 108.8 | 0.143 | 0.338 | -0.0024 | 13.78 | 0.58 | -11.389 | 7.545 | -3.260 | -18.167 | 10881.5 | 7.89 | 0.0626 |
| 14.75 | 108.8 | 0.144 | 0.320 | -0.0024 | 14.70 | 0.57 | -11.424 | 7.601 | -3.821 | -17.156 | 10881.5 | 7.40 | 0.0622 |
| 15.00 | 108.8 | 0.145 | 0.306 | -0.0025 | 15.46 | 0.56 | -11.483 | 7.691 | -4.267 | -16.272 | 10881.5 | 7.04 | 0.0620 |
| 15.25 | 108.8 | 0.145 | 0.2[illegible]5 | -0.0025 | 16.05 | 0.55 | -11.552 | 7.826 | -4.661 | -15.4[illegible]8 | 10881.5 | 6.78 | 0.0620 |
| 15.50 | 108.8 | 0.144 | 0.287 | -0.0026 | 16.49 | 0.54 | -11.617 | 8.009 | -4.956 | -14.817 | 10881.5 | 6.60 | 0.0621 |
| 15.75 | 108.8 | 0.144 | 0.280 | -0.0026 | 16.82 | 0.53 | -11.668 | 8.233 | -5.186 | -14.211 | 10881.5 | 6.47 | 0.0622 |
| 16.00 | 108.8 | 0.144 | 0.274 | -0.0026 | 17.07 | 0.52 | -11.695 | 8.494 | -5.369 | -13.665 | 10881.5 | 6.38 | 0.0624 |
| 16.25 | 108.8 | 0.143 | 0.269 | -0.0027 | 17.26 | 0.52 | -11.694 | 8.786 | -5.519 | -13.170 | 10881.5 | 6.31 | 0.0626 |
| 16.50 | 108.8 | 0.143 | 0.265 | -0.0027 | 17.42 | 0.51 | -11.461 | 9.102 | -5.649 | -12.718 | 10881.5 | 6.25 | 0.0628 |
| 16.75 | 108.8 | 0.142 | 0.261 | -0.0027 | 17.56 | 0.51 | -11.592 | 9.439 | -5.770 | -12.303 | 10881.5 | 6.20 | 0.0630 |
| 17.00 | 108.8 | 0.142 | 0.257 | -0.0027 | 17.70 | 0.51 | -11.486 | 9.788 | -5.889 | -11.922 | 10881.5 | 6.15 | 0.0633 |
| 17.25 | 108.8 | 0.141 | 0.253 | -0.0027 | 17.86 | 0.50 | -11.342 | 10.146 | -6.011 | -11.570 | 10881.5 | 6.09 | 0.0635 |
| 17.50 | 108.8 | 0.141 | 0.249 | -0.0027 | 18.02 | 0.50 | -11.159 | 10.507 | -6.139 | -11.246 | 10881.5 | 6.04 | 0.0637 |
| 17.75 | 108.8 | 0.140 | 0.245 | -0.0028 | 18.22 | 0.50 | -10.937 | 10.865 | -6.278 | -10.945 | 10881.5 | 5.97 | 0.0638 |
| 18.00 | 108.8 | 0.140 | 0.242 | -0.0028 | 18.44 | 0.51 | -10.667 | 11.205 | -6.416 | -10.660 | 10881.5 | 5.90 | 0.0639 |
| 18.25 | 108.8 | 0.140 | 0.238 | -0.0028 | 18.71 | 0.51 | -10.372 | 11.486 | -[illegible].539 | -10.387 | 10881.5 | 5.81 | 0.0639 |
| 18.50 | 108.8 | 0.141 | 0.235 | -0.0028 | 19.02 | 0.51 | -10.064 | 11.691 | -6.633 | -10.115 | 10881.5 | 5.72 | 0.0638 |
| 18.75 | 108.8 | 0.141 | 0.233 | -0.0028 | 19.37 | 0.51 | -9.748 | 11.835 | -6.704 | -9.840 | 10881.5 | 5.62 | 0.0636 |
| 19.00 | 108.8 | 0.142 | 0.230 | -0.0028 | 19.71 | 0.51 | -9.456 | 11.941 | -6.769 | -9.598 | 10881.5 | 5.52 | 0.0633 |
| 19.25 | 108.8 | 0.143 | 0.230 | -0.0029 | 20.10 | 0.51 | -9.095 | 11.907 | -6.681 | -9.218 | 10881.5 | 5.41 | 0.0628 |
| 19.50 | 154.4 | 0.142 | 0.361 | -0.0007 | 12.62 | 0.74 | -9.958 | 14.636 | -2.943 | -75.612 | 15443.8 | 12.24 | 0.0896 |
| 19.75 | 154.4 | 0.145 | 0.234 | -0.0027 | 20.21 | 0.72 | -9.548 | 14.187 | -9.090 | -12.469 | 15443.8 | 7.64 | 0.0880 |
| 20.00 | 154.4 | 0.148 | 0.366 | -0.0006 | 13.47 | 0.75 | -8.959 | 13.889 | -2.760 | -89.741 | 15443.8 | 11.46 | 0.0861 |
| 20.25 | 154.4 | 0.147 | 0.199 | -0.0030 | 24.60 | 0.73 | -8.820 | 14.017 | -12.221 | -9.781 | 15443.8 | 6.28 | 0.0866 |
| 20.50 | 154.4 | 0.149 | 0.358 | -0.0004 | 14.03 | 0.77 | -8.132 | 13.865 | -3.031 | -130.702 | 15443.8 | 11.01 | 0.0854 |
| 20.75 | 154.4 | 0.148 | 0.260 | -0.0018 | 19.09 | 0.76 | -8.201 | 14.023 | -7.270 | -21.433 | 15443.8 | 8.09 | 0.0860 |
| 21.00 | 154.4 | 0.149 | 0.071 | -0.0048 | 71.05 | 0.74 | -7.808 | 13.947 | -49.799 | -2.635 | 15443.8 | 2.17 | 0.0852 |
| 21.25 | 154.4 | 0.149 | 0.341 | -0.0003 | 14.76 | 0.80 | -7.561 | 13.989 | -3.571 | -145.593 | 15443.8 | 10.46 | 0.0853 |
| 21.50 | 154.4 | 0.149 | 0.284 | -0.0012 | 17.59 | 0.80 | -7.336 | 14.069 | -5.860 | -35.741 | 15443.8 | 8.78 | 0.0856 |
| 21.75 | 154.4 | 0.147 | 0.198 | -0.0025 | 24.79 | 0.80 | -7.160 | 14.236 | -12.062 | -12.824 | 15443.8 | 6.23 | 0.0864 |
| 22.00 | 154.4 | 0.147 | 0.124 | -0.0036 | 39.32 | 0.80 | -6.838 | 14.279 | -24.320 | -5.910 | 15443.8 | 3.93 | 0.0866 |
| 22.25 | 154.4 | 0.148 | 0.262 | -0.0014 | 18.96 | 0.85 | -6.324 | 14.157 | -6.975 | -29.473 | 15443.8 | 8.14 | 0.0859 |
| 22.50 | 154.4 | 0.144 | 0.190 | -0.0020 | 24.84 | 0.87 | -6.305 | 14.566 | -13.209 | -16.739 | 15443.8 | 6.22 | 0.0881 |
| 22.75 | 154.4 | 0.153 | 0.145 | -0.0035 | 36.79 | 0.85 | -4.975 | 13.651 | -18.665 | -6.623 | 15443.8 | 4.20 | 0.0830 |
| 23.00 | 154.4 | 0.149 | 0.156 | -0.0034 | 32.08 | 0.88 | -4.974 | 14.039 | -16.571 | -7.176 | 15443.8 | 4.81 | 0.0856 |
| 23.25 | 154.4 | 0.146 | 0.165 | -0.0033 | 29.25 | 0.91 | -4.781 | 14.224 | -15.082 | -7.595 | 15443.8 | 5.28 | 0.0871 |
| 23.50 | 154.4 | 0.144 | 0.171 | -0.0033 | 27.58 | 0.94 | -4.476 | 14.304 | -14.168 | -7.897 | 15443.8 | 5.60 | 0.0882 |
| 23.75 | 154.4 | 0.143 | 0.175 | -0.0032 | 26.63 | 0.98 | -4.102 | 14.309 | -13.642 | -8.165 | 15443.8 | 5.80 | 0.0888 |
| 24.00 | 154.4 | 0.142 | 0.176 | -0.0032 | 26.13 | 1.02 | -3.698 | 14.272 | -13.423 | -8.371 | 15443.8 | 5.91 | 0.0894 |

# Table VIII

## Similarity Functions - Case C

| t | h | $u_*$ | $\overline{\theta}_*$ | $\overline{R}_*$ | L | $Ri_B$ | A | B | C | D | $h/z_o$ | h/L | $\frac{\lvert f\rvert h}{u_*}$ |
|---|---|---|---|---|---|---|---|---|---|---|---|---|---|
| 0.25 | 154.4 | 0.133 | -2.760 | -0.1502 | -1.54 | -8.33 | 3.541 | 1.001 | 8.531 | 8.148 | 15443.8 | -100.06 | 0.0956 |
| 0.50 | 154.4 | 0.146 | -2.858 | -0.1742 | -1.82 | -9.94 | 4.278 | 0.619 | 8.450 | 8.343 | 15443.8 | -84.97 | 0.0869 |
| 0.75 | 201.1 | 0.152 | -3.067 | -0.2029 | -1.82 | -13.20 | 4.635 | 0.763 | 8.719 | 8.636 | 20113.6 | -110.29 | 0.1090 |
| 1.00 | 201.1 | 0.156 | -3.270 | -0.2309 | -1.82 | -14.90 | 4.881 | 0.502 | 8.702 | 8.667 | 20113.6 | -110.29 | 0.1062 |
| 1.25 | 248.5 | .161 | -3.433 | -.2552 | -1.87 | -18.42 | 5.153 | .496 | 8.914 | 8.874 | 24849.3 | -133.22 | 0.1268 |
| 1.50 | 296.3 | 0.166 | -3.569 | -0.2776 | -1.91 | -21.72 | 5.352 | 0.501 | 9.086 | 9.037 | 29629.4 | -155.10 | 0.1468 |
| 1.75 | 392.8 | .172 | -3.656 | -0.2935 | -2.01 | -26.52 | 5.566 | 0.703 | 9.360 | 9.261 | 39277.0 | -195.11 | 0.1876 |
| 2.00 | 538.8 | 0.179 | -3.691 | -0.3036 | -2.16 | -36.41 | 6.019 | 0.619 | 9.659 | 9.491 | 53881.8 | -249.13 | 0.2473 |
| 2.25 | 63 .7 | .183 | -3.741 | -0.3142 | -2.23 | -43.99 | 6.303 | 0.470 | 9.826 | 9.674 | 63 73.1 | -285.01 | 0.2859 |
| 2.50 | 734.9 | 0.185 | -3.815 | -0.3264 | -2.23 | -53.84 | 6.582 | 0.430 | 9.975 | 9.814 | 73493.8 | -330.14 | 0.3275 |
| 2.75 | 833.4 | .185 | -3.892 | -0.3390 | -2.18 | -65.61 | 6.840 | 0.431 | 10.107 | 9.933 | 83336.7 | -381.85 | 0.3716 |
| 3.00 | 833.4 | 0.183 | -3.967 | -0.3526 | -2.11 | -68.90 | 6.889 | 0.377 | 10.118 | 9.993 | 83336.7 | -394.96 | 0.3746 |
| 3.25 | 882.6 | 0.182 | -4.022 | -0.3641 | -2.06 | -77.27 | 7.025 | 0.367 | 10.181 | 10.068 | 88264.9 | -429.46 | 0.3995 |
| 3.50 | 932.0 | 0.181 | -4.043 | -0.3723 | -2.03 | -84.81 | 7.142 | 0.359 | 10.238 | 10.139 | 93196.9 | -459.12 | 0.4245 |
| 3.75 | 932.0 | 0.1 1 | -4.02[illegible] | -0.3777 | -2.03 | -84.26 | 7.129 | 0.331 | 10.238 | 10.167 | 93196.9 | -458.30 | 0.4240 |
| 4.00 | 981.3 | 0.182 | -3.966 | -0.3779 | -2.09 | -87.71 | 7.200 | 0.326 | 10.284 | 10.216 | 98132.4 | -470.49 | 0.4443 |
| 4.25 | 981.3 | .183 | -3.867 | -.3751 | -2.17 | -82.32 | 7.132 | 0.295 | 10.275 | 10.226 | 98132.4 | -451.63 | 0.4408 |
| 4.50 | 1030.7 | 0.186 | -3.729 | -0.3677 | -2.32 | -82.75 | 7.198 | 0.282 | 10.308 | 10.242 | 103071.1 | -444.69 | 0.4564 |
| 4.75 | 1030.7 | 0.189 | -3.558 | -0.3571 | -2.50 | -73.74 | 7.085 | 0.256 | 10.293 | 10.244 | 103071.1 | -411.57 | 0.4493 |
| 5.00 | 1030.7 | 0.193 | -3.364 | -.3437 | -2.75 | -66.94 | 7.043 | 0.216 | 10.276 | 10.199 | 103071.1 | -375.40 | 0.4411 |
| 5.25 | 1030.7 | 0.196 | -3.146 | -0.3294 | -3.05 | -58.93 | 6.945 | 0.198 | 10.250 | 10.187 | 103071.1 | -337.93 | 0.4325 |
| 5.50 | 1030.7 | 0.201 | -2.911 | -0.3129 | -3.44 | -51.04 | 6.842 | 0.186 | 10.224 | 10.165 | 103071.1 | -299.68 | 0.4230 |
| 5.75 | 1080.1 | 0.205 | -2.684 | -0.2946 | -3.92 | -45.38 | 6.808 | 0.178 | 10.241 | 10.170 | 108012.5 | -275.53 | 0.4336 |
| 6.00 | 1080.1 | 0.209 | -2.404 | -0.2761 | -4.50 | -39.02 | 6.670 | 0.177 | 10.209 | 10.139 | 108012.5 | -239.76 | 0.4249 |
| 6.25 | 1129.6 | .214 | -2.144 | -.2565 | -5.26 | -34.50 | 6.615 | 0.174 | 10.217 | 10.116 | 112956.6 | -214.89 | 0.4351 |
| 6.50 | 1129.6 | 0.218 | -1.883 | -0.2366 | -6.20 | -28.27 | 6.458 | 0.179 | 10.177 | 10.069 | 112956.6 | -182.12 | 0.4272 |
| 6.75 | 1179.0 | 0.221 | -1.617 | -.2169 | -7.44 | -24.09 | 6.360 | 0.191 | 10.170 | 10.035 | 117903.0 | -158.40 | 0.4387 |
| 7.00 | 1179.0 | 0.224 | -1.351 | -.1971 | -9.09 | -18.96 | 6.152 | 0.209 | 10.114 | 9.980 | 117903.0 | -129.77 | 0.4337 |
| 7.25 | 1179. | 0.224 | -1.088 | -0.1772 | -11.38 | -14.57 | 5.919 | 0.230 | 10.042 | 9.901 | 117903.0 | -103.56 | 0.4312 |
| 7.50 | 1179.0 | 0.225 | -0.827 | -0.1572 | -14.90 | -10.65 | 5.620 | 0.260 | 9.947 | 9.826 | 117903.0 | -79.15 | 0.4317 |
| 7.75 | 1179.0 | 0.222 | -0.568 | -0.1369 | -21.13 | -7.17 | 5.240 | 0.301 | 9.809 | 9.739 | 117903.0 | -55.79 | 0.4366 |
| 8.00 | 1179.0 | 0.217 | -0.310 | -0.1160 | -36.63 | -4.03 | 4.738 | 0.358 | 9.561 | 9.602 | 117903.0 | -32.19 | 0.4482 |
| 8.25 | 1228.5 | 0.206 | -0.052 | -0.0943 | -196.94 | -1.15 | 4.053 | 0.467 | 7.921 | 9.392 | 122851.6 | -6.24 | 0.4923 |
| 8.50 | 1228.5 | 0.179 | 0.204 | -0.0706 | 37.42 | 2.01 | 2.479 | 0.710 | 9.883 | 8.804 | 122851.6 | 32.83 | 0.5659 |
| 8.75 | 1278.0 | 0.130 | 0.447 | -0.0377 | 8.97 | 5.37 | -1.514 | 1.554 | 8.962 | 6.576 | 127802.2 | 142.47 | 0.8092 |
| 9.00 | 1278.0 | 0.091 | 0.586 | -0.0076 | 3.30 | 12.10 | -7.099 | 3.513 | 7.350 | -9.199 | 127802.2 | 386.73 | 1.1567 |
| 9.25 | 1278.0 | 0.107 | 0.526 | -0.0043 | 5.05 | 14.58 | -5.826 | 3.323 | 5.302 | -20.389 | 127802.2 | 253.07 | 0.9835 |
| 9.50 | 1228.5 | 0.112 | 0.503 | -0.0032 | 5.70 | 14.77 | -5.888 | 3.647 | 3.960 | -27.082 | 122851.6 | 215.46 | 0.9070 |
| 9.75 | 1129.6 | .113 | 0.490 | -0.0025 | 5.96 | 13.61 | -6.523 | 4.137 | 2.919 | -35.126 | 112956.6 | 189.57 | 0.8247 |
| 10.00 | 981.3 | 0.113 | 0.481 | -0.0018 | 6.04 | 11.58 | -7.408 | 4.637 | 1.980 | -47.574 | 98132.4 | 162.39 | 0.7173 |
| 10.25 | 65.2 | 0.098 | 0.468 | -0.0003 | 4.68 | 0.93 | -10.311 | 2.843 | 0.095 | -158.526 | 6521.4 | 13.92 | 0.0548 |
| 10.50 | 65.2 | 0.094 | 0.460 | 0.0001 | 4.35 | .92 | -11.801 | 3.520 | -0.630 | 476.406 | 6521.4 | 14.98 | 0.0572 |
| 1 .75 | 65.2 | 0.096 | 0.415 | -0.0006 | 5.07 | 0.88 | -11.959 | 3.810 | -1.834 | -77.700 | 6521.4 | 12.86 | 0.0558 |
| 11.00 | 65.2 | 0.097 | 0.412 | -0.0007 | 5.13 | .81 | -12.533 | 4.229 | -1.743 | -62.080 | 6521.4 | 12.70 | 0.0556 |
| 11.25 | 65.2 | 0.096 | 0.413 | -0.0007 | 5.11 | 0.75 | -13.176 | 4.691 | -1.556 | -56.799 | 6521.4 | 12.77 | 0.0557 |
| 11.50 | 65.2 | 0.096 | 0.414 | -0.0008 | 5.03 | .69 | -13.866 | 5.200 | -1.357 | -51.238 | 6521.4 | 12.95 | 0.0560 |
| 11.75 | 108.8 | 0.097 | 0.427 | -0.0009 | 5.02 | 0.96 | -16.291 | 7.353 | -1.636 | -59.621 | 10881.5 | 21.69 | 0.0922 |
| 12.00 | 108.8 | 0.095 | 0.433 | -0.0011 | 4.77 | 0.89 | -17.408 | 8.125 | -1.387 | -50.995 | 10881.5 | 22.82 | 0.0939 |
| 12.25 | 108.8 | 0.095 | 0.456 | -0.0012 | 4.50 | 0.84 | -18.123 | 8.792 | -0.765 | -42.624 | 10881.5 | 24.17 | 0.0942 |
| 12.50 | 108.8 | 0.110 | 0.502 | -0.0015 | 5.44 | 0.79 | -15.125 | 7.806 | 0.236 | -34.035 | 10881.5 | 20.01 | 0.0817 |
| 12.75 | 108.8 | 0.120 | 0.507 | -0.0017 | 6.44 | 0.74 | -13.502 | 7.374 | 0.440 | -29.091 | 10881.5 | 16.90 | 0.0747 |
| 13.00 | 108.8 | 0.127 | 0.489 | -0.0016 | 7.46 | .71 | -12.636 | 7.271 | .238 | -26.433 | 10881.5 | 14.60 | 0.0707 |
| 13.25 | 108.8 | 0.132 | 0.461 | -0.0019 | 8.54 | .68 | -12.119 | 7.293 | -0.204 | -24.058 | 10881.5 | 12.73 | 0.0680 |
| 13.50 | 108.8 | 0.136 | 0.428 | -0.0020 | 9.72 | 0.65 | -11.783 | 7.346 | -0.794 | -22.118 | 10881.5 | 11.19 | 0.0661 |
| 13.75 | 108.8 | 0.138 | 0.396 | -0.0021 | 10.96 | .62 | -11.582 | 7.417 | -1.484 | -21.021 | 10881.5 | 9.93 | 0.0648 |
| 14.00 | 108.8 | 0.141 | 0.369 | -0.0022 | 12.20 | .60 | -11.412 | 7.387 | -2.129 | -19.487 | 10881.5 | 8.92 | 0.0636 |
| 14.25 | 108.8 | 0.143 | 0.345 | -0.0023 | 13.35 | 0.58 | -11.374 | 7.411 | -2.795 | -18.225 | 10881.5 | 8.15 | 0.0629 |
| 14.50 | 108.8 | 0.144 | 0.326 | -0.0023 | 14.36 | 0.57 | -11.395 | 7.455 | -3.391 | -17.162 | 10881.5 | 7.58 | 0.0624 |
| 14.75 | 108.8 | 0.144 | 0.310 | -0.0024 | 15.21 | 0.55 | -11.446 | 7.529 | -3.896 | -16.234 | 10881.5 | 7.16 | 0.0622 |
| 15.00 | 108.8 | 0.145 | 0.298 | -0.0024 | 15.89 | 0.54 | -11.512 | 7.639 | -4.304 | -15.419 | 10881.5 | 6.85 | 0.0620 |
| 15.25 | 108.8 | 0.145 | 0.289 | -0.0025 | 16.41 | .53 | -11.582 | 7.793 | -4.625 | -14.701 | 10881.5 | 6.63 | 0.0620 |
| 15.50 | 108.8 | 0.144 | 0.281 | -0.0025 | 16.80 | .52 | -11.645 | 7.992 | -4.873 | -14.066 | 10881.5 | 6.48 | 0.0621 |
| 15.75 | 108.8 | 0.144 | 0.275 | -0.0025 | 17.09 | 0.51 | -11.690 | 8.232 | -5.064 | -13.497 | 10881.5 | 6.37 | 0.0622 |
| 16.00 | 108.8 | 0.144 | 0.270 | -0.0025 | 17.30 | .51 | -11.710 | 8.505 | -5.215 | -12.982 | 10881.5 | 6.29 | 0.0624 |
| 16.25 | 108.8 | 0.143 | 0.266 | -0.0026 | 17.47 | .50 | -11.701 | 8.807 | -5.340 | -12.513 | 10881.5 | 6.23 | 0.0626 |
| 16.50 | 108.8 | 0.143 | 0.262 | -0.0026 | 17.62 | 0.50 | -11.656 | 9.132 | -5.451 | -12.084 | 10881.5 | 6.18 | 0.0629 |
| 16.75 | 108.8 | 0.142 | 0.258 | -0.0026 | 17.75 | 0.49 | -11.580 | 9.474 | -5.556 | -11.689 | 10881.5 | 6.13 | 0.0631 |
| 17.00 | 108.8 | 0.142 | 0.254 | -0.0026 | 17.89 | .49 | -11.465 | 9.828 | -5.662 | -11.325 | 10881.5 | 6.08 | 0.0633 |
| 17.25 | 108.8 | 0.141 | 0.251 | -0.0026 | 18.04 | 0.49 | -11.312 | 10.188 | -5.774 | -10.989 | 10881.5 | 6.03 | 0.0635 |
| 17.50 | 108.8 | 0.141 | 0.247 | -0.0026 | 18.21 | 0.49 | -11.120 | 10.550 | -5.893 | -10.678 | 10881.5 | 5.98 | 0.0637 |
| 17.75 | 108.8 | 0.141 | 0.243 | -0.0027 | 18.41 | 0.49 | -10.884 | 10.903 | -6.020 | -10.386 | 10881.5 | 5.91 | 0.0638 |
| 18.00 | 108.8 | 0.140 | 0.240 | -0.0027 | 18.63 | 0.49 | -10.606 | 11.234 | -6.139 | -10.111 | 10881.5 | 5.84 | 0.0639 |
| 18.25 | 108.8 | 0.141 | 0.237 | -0.0027 | 18.92 | .49 | -10.284 | 11.488 | -6.223 | -9.832 | 10881.5 | 5.75 | 0.0638 |
| 18.50 | 108.8 | 0.141 | 0.234 | -0.0027 | 19.21 | 0.50 | -9.974 | 11.677 | -6.292 | -9.565 | 10881.5 | 5.66 | 0.0636 |
| 18.75 | 108.8 | 0.141 | 0.232 | -0.0027 | 19.54 | 0.50 | -9.666 | 11.814 | -6.354 | -9.305 | 10881.5 | 5.57 | 0.0634 |
| 19.00 | 154.4 | 0.142 | 0.230 | -0.0028 | 19.91 | .67 | -10.101 | 14.796 | -8.774 | -12.185 | 15443.8 | 7.76 | 0.0895 |
| 19.25 | 154.4 | 0.151 | 0.256 | -0.0028 | 20.07 | 0.68 | -9.200 | 13.413 | -6.810 | -11.558 | 15443.8 | 7.69 | 0.0844 |
| 19.50 | 108.8 | 0.139 | 0.253 | -0.0024 | 17.35 | 0.52 | -9.822 | 11.460 | -5.162 | -10.617 | 10881.5 | 6.27 | 0.0644 |
| 19.75 | 108.8 | 0.139 | 0.223 | -0.0025 | 19.64 | .52 | -9.479 | 11.804 | -6.903 | -8.960 | 10881.5 | 5.54 | 0.0644 |
| 20.00 | 108.8 | 0.140 | 0.253 | -0.0018 | 17.51 | 0.53 | -9.055 | 12.001 | -5.049 | -15.244 | 10881.5 | 6.21 | 0.0640 |
| 20.25 | 108.8 | 0.142 | 0.307 | -0.0009 | 14.79 | 0.54 | -8.585 | 12.043 | -2.717 | -41.820 | 10881.5 | 7.36 | 0.0633 |
| 20.50 | 154.4 | 0.143 | 0.349 | -0.0000 | 13.21 | 0.76 | -8.531 | 15.245 | -3.133 | -2114.559 | 15443.8 | 11.69 | 0.0891 |
| 20.75 | 154.4 | 0.152 | 0.126 | -0.0038 | 41.20 | .72 | -7.491 | 14.123 | -23.361 | -4.961 | 15443.8 | 3.75 | 0.0839 |
| 21.00 | 154.4 | 0.151 | 0.364 | -0.0000 | 14.07 | 0.78 | -7.685 | 13.841 | -2.544 | -1253.191 | 15443.8 | 10.97 | 0.0844 |
| 21.25 | 154.4 | .151 | 0.326 | -0.0007 | 15.83 | 0.77 | -7.475 | 13.707 | -3.718 | -67.476 | 15443.8 | 9.76 | 0.0842 |
| 21.50 | 154.4 | 0.150 | 0.265 | -0.0012 | 17.84 | .78 | -7.330 | 13.804 | -5.398 | -32.542 | 15443.8 | 8.66 | 0.0848 |
| 21.75 | 154.4 | .149 | 0.258 | -0.0016 | 19.50 | 0.79 | -7.106 | 13.902 | -6.831 | -23.217 | 15443.8 | 7.92 | 0.0853 |
| 22.00 | 154.4 | 0.148 | 0.253 | -0.0016 | 19.62 | 0.80 | -6.841 | 14.007 | -7.088 | -23.102 | 15443.8 | 7.87 | 0.0859 |
| 22.25 | 154.4 | 0.146 | 0.319 | -0.0002 | 15.05 | 0.85 | -6.697 | 14.261 | -4.063 | -209.164 | 15443.8 | 10.26 | 0.0873 |
| 22.50 | 154.4 | 0.146 | 0.194 | -0.0020 | 24.77 | 0.84 | -6.254 | 14.263 | -11.933 | -15.073 | 15443.8 | 6.24 | 0.0872 |
| 22.75 | 154.4 | .153 | 0.156 | -0.0033 | 34.02 | 0.83 | -5.141 | 13.560 | -16.102 | -6.750 | 15443.8 | 4.54 | 0.0833 |
| 23.00 | 154.4 | 0.149 | 0.164 | -0.0032 | 30.59 | .86 | -5.068 | 13.917 | -14.758 | -7.261 | 15443.8 | 5.05 | 0.0856 |
| 23.25 | 154.4 | .146 | 0.170 | -0.0031 | 28.45 | 0.89 | -4.830 | 14.102 | -13.771 | -7.646 | 15443.8 | 5.43 | 0.0870 |
| 23.50 | 154.4 | 0.145 | 0.174 | -0.0031 | 27.16 | 0.92 | -4.496 | 14.188 | -13.163 | -7.942 | 15443.8 | 5.68 | 0.0880 |
| 23.75 | 154.4 | 0.144 | 0.177 | -0.0031 | 26.48 | .96 | -4.098 | 14.192 | -12.826 | -8.168 | 15443.8 | 5.83 | 0.0886 |
| 24.00 | 154.4 | 0.143 | 0.177 | -0.0030 | 26.13 | 1.00 | -3.674 | 14.150 | -12.713 | -8.350 | 15443.8 | 5.91 | 0.0891 |

## Table IX

### Similarity Functions - Case D

| t | h | $u_*$ | $\overline{\Theta}_*$ | $\overline{R}_*$ | L | $Ri_B$ | A | B | C | D | $h/z_o$ | h/L | $\frac{\lvert f\rvert h}{u_*}$ |
|---|---|---|---|---|---|---|---|---|---|---|---|---|---|
| 0.25 | 154.4 | 0.131 | -2.547 | -0.1389 | -1.62 | -7.71 | 3.439 | 1.040 | 8.527 | 8.100 | 15443.8 | -95.63 | 0.0972 |
| 0.50 | 154.4 | 0.145 | -2.635 | -0.159 | -1.92 | -9.20 | 4.200 | 0.645 | 8.443 | 8.320 | 15443.8 | -80.53 | 0.0879 |
| 0.75 | 201.1 | 0.149 | -2.867 | -0.1867 | -1.89 | -12.24 | 4.534 | 0.869 | 8.717 | 8.606 | 20113.6 | -106.61 | 0.1110 |
| 1.00 | 201.1 | 0.154 | -3.021 | -0.2104 | -1.92 | -13.80 | 4.804 | 0.542 | 8.693 | 8.651 | 20113.6 | -104.66 | 0.1074 |
| 1.25 | 248.5 | 0.159 | -3.193 | -0.2337 | -1.94 | -17.14 | 5.067 | 0.602 | 8.907 | 8.854 | 24849.3 | -128.01 | 0.1287 |
| 1.50 | 296.3 | 0.164 | -3.319 | -0.2543 | -1.99 | -20.27 | 5.265 | 0.601 | 9.076 | 9.010 | 29629.4 | -149.23 | 0.1491 |
| 1.75 | 344.4 | 0.169 | -3.411 | -0.2706 | -2.07 | -22.92 | 5.444 | 0.621 | 9.222 | 9.147 | 34441.2 | -166.52 | 0.1678 |
| 2.00 | 490.0 | 0.176 | -3.457 | -0.2814 | -2.21 | -30.99 | 5.819 | 0.780 | 9.558 | 9.384 | 49000.5 | -221.95 | 0.2297 |
| 2.25 | 587.7 | 0.181 | -3.482 | -0.2897 | -2.33 | -38.14 | 6.156 | 0.530 | 9.733 | 9.562 | 58773.2 | -251.99 | 0.2672 |
| 2.50 | 685.8 | 0.183 | -3.536 | -0.2997 | -2.35 | -45.93 | 6.408 | 0.465 | 9.891 | 9.732 | 68580.3 | -291.37 | 0.3082 |
| 2.75 | 784.1 | .184 | -3.596 | -0.3100 | -2.33 | -56.17 | 6.688 | 0.442 | 10.029 | 9.846 | 78412.8 | -335.83 | 0.3511 |
| 3.00 | 833.4 | 0.183 | -3.654 | -0.3207 | -2.28 | -63.31 | 6.843 | 0.413 | 10.099 | 9.932 | 83336.7 | -365.29 | 0.3747 |
| 3.25 | 882.6 | 0.182 | -3.700 | -0.3309 | -2.23 | -70.65 | 6.979 | 0.395 | 10.161 | 10.013 | 88264.9 | -396.03 | 0.3992 |
| 3.50 | 932.0 | 0.182 | -3.714 | -0.3382 | -2.21 | -77.64 | 7.095 | 0.381 | 10.216 | 10.082 | 93196.9 | -422.02 | 0.4228 |
| 3.75 | 932.0 | 0.182 | -3.695 | -0.3421 | -2.22 | -76.67 | 7.080 | 0.337 | 10.218 | 10.121 | 93196.9 | -419.68 | 0.4228 |
| 4.00 | 932.0 | 0.182 | -3.642 | -0.3433 | -2.27 | -74.50 | 7.054 | 0.311 | 10.214 | 10.139 | 93196.9 | -410.76 | 0.4214 |
| 4.25 | 981.3 | .184 | -3.548 | -0.3400 | -2.37 | -75.76 | 7.108 | 0.304 | 10.255 | 10.182 | 98132.4 | -413.76 | 0.4396 |
| 4.50 | 981.3 | 0.186 | -3.423 | -0.3343 | -2.51 | -69.47 | 7.020 | 0.277 | 10.242 | 10.191 | 98132.4 | -390.28 | 0.4346 |
| 4.75 | 1030.7 | 0.189 | -3.266 | -0.3252 | -2.72 | -68.52 | 7.071 | 0.263 | 10.272 | 10.199 | 103071.1 | -378.57 | 0.4489 |
| 5.00 | 1030.7 | 0.193 | -3.083 | -0.3132 | -2.99 | -60.55 | 6.972 | 0.237 | 10.254 | 10.194 | 103071.1 | -344.31 | 0.4404 |
| 5.25 | 1030.7 | 0.197 | -2.884 | -0.3002 | -3.32 | -52.88 | 6.857 | 0.220 | 10.231 | 10.179 | 103071.1 | -310.49 | 0.4321 |
| 5.50 | 1030.7 | 0.201 | -2.667 | -0.2853 | -3.74 | -46.28 | 6.777 | 0.196 | 10.205 | 10.135 | 103071.1 | -275.45 | 0.4229 |
| 5.75 | 1030.7 | 0.205 | -2.438 | -0.2693 | -4.27 | -39.39 | 6.652 | 0.189 | 10.175 | 10.110 | 103071.1 | -241.49 | 0.4138 |
| 6.00 | 1080.1 | 0.210 | -2.202 | -0.2526 | -4.92 | -35.46 | 6.611 | 0.181 | 10.187 | 10.098 | 108012.5 | -219.58 | 0.4246 |
| 6.25 | 1080.1 | 0.214 | -1.959 | -0.2351 | -5.74 | -29.48 | 6.470 | 0.175 | 10.151 | 10.058 | 108012.5 | -188.20 | 0.4162 |
| 6.50 | 1080.1 | 0.21 | -1.715 | -0.2176 | -6.77 | -24.06 | 6.297 | 0.164 | 10.109 | 10.023 | 108012.5 | -159.46 | 0.4091 |
| 6.75 | 1129.6 | .221 | -1.469 | -0.1997 | -8.14 | -20.57 | 6.200 | 0.188 | 10.101 | 9.978 | 112956.6 | -138.82 | 0.4212 |
| 7.00 | 1129.6 | 0.223 | -1.222 | -0.1814 | -9.97 | -16.14 | 5.985 | 0.201 | 10.042 | 9.919 | 112956.6 | -113.34 | 0.4166 |
| 7.25 | 1129.6 | 0.224 | -0.978 | -0.1634 | -12.53 | -12.33 | 5.738 | 0.220 | 9.967 | 9.835 | 112956.6 | -90.13 | 0.4147 |
| 7.50 | 1129.6 | 0.224 | -0.736 | -0.1450 | -16.53 | -8.98 | 5.440 | 0.245 | 9.866 | 9.725 | 112956.6 | -68.33 | 0.4156 |
| 7.75 | 1129.6 | 0.221 | -0.495 | -0.1263 | -23.91 | -5.96 | 5.051 | 0.286 | 9.718 | 9.611 | 112956.6 | -47.24 | 0.4208 |
| 8.00 | 1129.6 | 0.215 | -0.254 | -0.1072 | -43.98 | -3.20 | 4.536 | 0.346 | 9.434 | 9.455 | 112956.6 | -25.69 | 0.4323 |
| 8.25 | 1377.1 | 0.204 | -0.012 | -0.0874 | -799.71 | -0.77 | 4.225 | 0.450 | 2.752 | 8.828 | 137708.9 | -1.72 | 0.5569 |
| 8.50 | 1327.5 | 0.176 | 0.226 | -0.0653 | 32.49 | 2.58 | 2.420 | 0.725 | 9.840 | 8.321 | 132754.7 | 40.86 | 0.6230 |
| 8.75 | 1278.0 | 0.128 | 0.453 | -0.0342 | 8.49 | 6.68 | -1.806 | 1.563 | 8.864 | 5.694 | 127802.2 | 150.53 | 0.8255 |
| 9.00 | 1278.0 | 0.091 | 0.564 | -0.0067 | 3.32 | 12.25 | -7.983 | 3.461 | 7.279 | -13.776 | 127802.2 | 384.37 | 1.1540 |
| 9.25 | 1228.5 | 0.107 | 0.522 | -0.0037 | 5.07 | 13.99 | -5.948 | 3.253 | 5.197 | -27.823 | 122851.6 | 242.26 | 0.9460 |
| 9.50 | 1179.0 | 0.111 | 0.501 | -0.0028 | 5.70 | 14.09 | -6.044 | 3.610 | 3.875 | -37.120 | 117903.0 | 206.71 | 0.8720 |
| 9.75 | 1030.7 | 0.113 | 0.488 | -0.0021 | 5.95 | 12.24 | -6.810 | 4.039 | 2.800 | -48.358 | 103071.1 | 173.11 | 0.7541 |
| 10.00 | 108.8 | 0.100 | 0.460 | -0.0006 | 4.96 | 1.36 | -10.821 | 3.184 | 0.257 | -120.097 | 10881.5 | 21.92 | 0.0896 |
| 10.25 | 65.2 | 0.093 | 0.461 | 0.0000 | 4.29 | 0.93 | -11.49 | 3.144 | -0.184 | 1198.467 | 6521.4 | 15.21 | 0.0576 |
| 10.50 | 65.2 | 0.096 | 0.461 | 0.0002 | 4.51 | 0.91 | -11.648 | 3.430 | -0.679 | 308.199 | 6521.4 | 14.44 | 0.0561 |
| 10.75 | 65.2 | 0.097 | 0.414 | -0.0006 | 5.13 | .84 | -12.072 | 3.765 | -1.598 | -78.074 | 6521.4 | 12.70 | 0.0555 |
| 11.00 | 65.2 | 0.097 | 0.414 | -0.0007 | 5.12 | 0.77 | -12.731 | 4.230 | -1.427 | -70.631 | 6521.4 | 12.75 | 0.0556 |
| 11.25 | 65.2 | 0.096 | 0.414 | -0.0007 | 5.07 | 0.72 | -13.436 | 4.712 | -1.264 | -64.557 | 6521.4 | 12.86 | 0.0558 |
| 11.50 | 65.2 | 0.094 | 0.415 | -0.0008 | 4.88 | 0.66 | -14.443 | 5.320 | -1.076 | -56.281 | 6521.4 | 13.37 | 0.0569 |
| 11.75 | 108.8 | 0.096 | 0.433 | -0.0009 | 4.82 | 0.92 | -16.889 | 7.487 | -1.237 | -65.411 | 10881.5 | 22.57 | 0.0934 |
| 12.00 | 108.8 | 0.094 | 0.441 | -0.0010 | 4.50 | 0.86 | -18.199 | 8.351 | -0.941 | -56.887 | 10881.5 | 24.18 | 0.0958 |
| 12.25 | 108.8 | 0.105 | 0.492 | -0.0013 | 5.04 | 0.80 | -15.962 | 7.773 | 0.196 | -45.044 | 10881.5 | 21.57 | 0.0857 |
| 12.50 | 108.8 | 0.116 | 0.507 | -0.0014 | 6.01 | 0.76 | -14.012 | 7.254 | 0.577 | -38.688 | 10881.5 | 18.10 | 0.0773 |
| 12.75 | 108.8 | 0.124 | 0.497 | -0.0016 | 7.01 | 0.72 | -12.932 | 7.075 | 0.505 | -34.249 | 10881.5 | 15.52 | 0.0723 |
| 13.00 | 108.8 | 0.130 | 0.472 | -0.0017 | 8.07 | 0.68 | -12.293 | 7.069 | 0.166 | -31.333 | 10881.5 | 13.49 | 0.0692 |
| 13.25 | 108.8 | 0.134 | 0.440 | -0.0018 | 9.21 | 0.65 | -11.907 | 7.134 | -0.364 | -28.993 | 10881.5 | 11.82 | 0.0670 |
| 13.50 | 108.8 | 0.137 | 0.407 | -0.0019 | 10.42 | 0.63 | -11.670 | 7.220 | -1.019 | -26.673 | 10881.5 | 10.44 | 0.0655 |
| 13.75 | 108.8 | 0.140 | 0.378 | -0.0020 | 11.70 | 0.60 | -11.462 | 7.237 | -1.675 | -25.118 | 10881.5 | 9.30 | 0.0641 |
| 14.00 | 108.8 | 0.142 | 0.353 | -0.0020 | 12.91 | 0.58 | -11.390 | 7.255 | -2.341 | -23.473 | 10881.5 | 8.43 | 0.0633 |
| 14.25 | 108.8 | 0.143 | 0.331 | -0.0021 | 14.00 | 0.57 | -11.386 | 7.298 | -2.968 | -21.990 | 10881.5 | 7.77 | 0.0627 |
| 14.50 | 108.8 | 0.144 | 0.314 | -0.0022 | 14.94 | 0.55 | -11.423 | 7.363 | -3.508 | -20.663 | 10881.5 | 7.28 | 0.0623 |
| 14.75 | 108.8 | 0.144 | 0.300 | -0.0022 | 15.70 | 0.54 | -11.485 | 7.460 | -3.951 | -19.487 | 10881.5 | 6.93 | 0.0621 |
| 15.00 | 108.8 | 0.144 | 0.290 | -0.0023 | 16.31 | 0.53 | -11.555 | 7.592 | -4.298 | -18.440 | 10881.5 | 6.67 | 0.0620 |
| 15.25 | 108.8 | 0.144 | 0.282 | -0.0023 | 16.77 | 0.52 | -11.623 | 7.767 | -4.564 | -17.507 | 10881.5 | 6.49 | 0.0621 |
| 15.50 | 108.8 | 0.144 | 0.276 | -0.0023 | 17.11 | 0.51 | -11.680 | 7.984 | -4.766 | -16.672 | 10881.5 | 6.36 | 0.0622 |
| 15.75 | 108.8 | 0.144 | 0.270 | -0.0024 | 17.35 | 0.50 | -11.718 | 8.239 | -4.920 | -15.919 | 10881.5 | 6.27 | 0.0623 |
| 16.00 | 108.8 | 0.143 | 0.266 | -0.0024 | 17.54 | 0.49 | -11.730 | 8.526 | -5.042 | -15.236 | 10881.5 | 6.20 | 0.0625 |
| 16.25 | 108.8 | 0.143 | 0.262 | -0.0024 | 17.69 | 0.49 | -11.711 | 8.839 | -5.144 | -14.612 | 10881.5 | 6.15 | 0.0627 |
| 16.50 | 108.8 | 0.143 | 0.258 | -0.0024 | 17.82 | 0.48 | -11.659 | 9.172 | -5.237 | -14.040 | 10881.5 | 6.11 | 0.0629 |
| 16.75 | 108.8 | 0.142 | 0.255 | -0.0025 | 17.94 | 0.48 | -11.570 | 9.520 | -5.328 | -13.515 | 10881.5 | 6.06 | 0.0631 |
| 17.00 | 108.8 | 0.142 | 0.251 | -0.0025 | 18.08 | 0.48 | -11.445 | 9.878 | -5.422 | -13.033 | 10881.5 | 6.02 | 0.0633 |
| 17.25 | 108.8 | 0.141 | 0.248 | -0.0025 | 18.23 | .48 | -11.282 | 10.241 | -5.524 | -12.589 | 10881.5 | 5.97 | 0.0635 |
| 17.50 | 108.8 | 0.141 | 0.244 | -0.0025 | 18.40 | 0.48 | -11.079 | 10.603 | -5.635 | -12.177 | 10881.5 | 5.91 | 0.0637 |
| 17.75 | 108.8 | 0.141 | 0.241 | -0.0025 | 18.60 | 0.48 | -10.828 | 10.948 | -5.743 | -11.791 | 10881.5 | 5.85 | 0.0638 |
| 18.00 | 108.8 | 0.141 | 0.238 | -0.0026 | 18.84 | 0.48 | -10.530 | 11.260 | -5.833 | -11.421 | 10881.5 | 5.78 | 0.0638 |
| 18.25 | 108.8 | 0.141 | 0.235 | -0.0026 | 19.11 | 0.48 | -10.203 | 11.499 | -5.894 | -11.062 | 10881.5 | 5.69 | 0.0637 |
| 18.50 | 108.8 | 0.141 | 0.233 | -0.0026 | 19.41 | 0.48 | -9.863 | 11.672 | -5.944 | -10.711 | 10881.5 | 5.61 | 0.0635 |
| 18.75 | 108.8 | 0.142 | 0.230 | -0.0026 | 19.73 | 0.49 | -9.579 | 11.801 | -5.996 | -10.392 | 10881.5 | 5.52 | 0.0633 |
| 19.00 | 154.4 | 0.149 | 0.244 | -0.0027 | 20.54 | 0.65 | -9.398 | 13.865 | -7.272 | -13.337 | 15443.8 | 7.52 | 0.0856 |
| 19.25 | 154.4 | 0.143 | 0.230 | -0.0027 | 20.08 | 0.67 | -10.144 | 14.257 | -8.590 | -12.316 | 15443.8 | 7.69 | 0.0892 |
| 19.50 | 154.4 | 0.146 | 0.206 | -0.0031 | 23.43 | 0.68 | -9.591 | 13.859 | -10.568 | -9.448 | 15443.8 | 6.59 | 0.0872 |
| 19.75 | 154.4 | 0.148 | 0.110 | -0.0046 | 45.30 | 0.67 | -9.045 | 13.639 | -27.340 | -3.289 | 15443.8 | 3.41 | 0.0857 |
| 20.00 | 154.4 | 0.148 | 0.376 | -0.0000 | 13.18 | 0.73 | -8.833 | 13.753 | -1.965 | -1226.105 | 15443.8 | 11.72 | 0.0859 |
| 20.25 | 154.4 | 0.149 | 0.366 | -0.0001 | 13.63 | 0.74 | -8.515 | 13.779 | -2.242 | -646.024 | 15443.8 | 11.33 | 0.0857 |
| 20.50 | 154.4 | 0.149 | 0.359 | -0.0000 | 13.89 | 0.75 | -8.237 | 13.821 | -2.414 | -1261.161 | 15443.8 | 11.12 | 0.0856 |
| 20.75 | 154.4 | 0.149 | 0.357 | 0.0000 | 13.99 | 0.76 | -7.971 | 13.855 | -2.472 | 1700.975 | 15443.8 | 11.04 | 0.0855 |
| 21.00 | 154.4 | 0.150 | 0.081 | -0.0044 | 63.04 | 0.71 | -7.614 | 13.799 | -40.106 | -3.042 | 15443.8 | 2.45 | 0.0850 |
| 21.25 | 154.4 | 0.148 | 0.159 | -0.0030 | 31.37 | 0.74 | -7.495 | 13.947 | -15.872 | -8.467 | 15443.8 | 4.92 | 0.0857 |
| 21.50 | 154.4 | 0.148 | 0.216 | -0.0020 | 22.92 | 0.76 | -7.244 | 14.013 | -9.327 | -16.394 | 15443.8 | 6.74 | 0.0860 |
| 21.75 | 154.4 | 0.149 | 0.282 | -0.0010 | 17.71 | 0.79 | -6.847 | 13.979 | -5.158 | -43.579 | 15443.8 | 8.72 | 0.0856 |
| 22.00 | 154.4 | 0.148 | 0.330 | -0.0001 | 14.90 | 0.82 | -6.580 | 14.089 | -3.221 | -499.031 | 15443.8 | 10.36 | 0.0862 |
| 22.25 | 154.4 | 0.148 | 0.286 | -0.0007 | 17.28 | 0.83 | -6.176 | 14.087 | -4.984 | -58.003 | 15443.8 | 8.94 | 0.0861 |
| 22.50 | 154.4 | 0.143 | 0.208 | -0.0016 | 22.42 | 0.85 | -6.195 | 14.536 | -10.228 | -22.284 | 15443.8 | 6.89 | 0.0887 |
| 22.75 | 154.4 | 0.153 | 0.148 | -0.0032 | 35.90 | 0.82 | -4.863 | 13.548 | -16.727 | -7.221 | 15443.8 | 4.30 | 0.0832 |
| 23.00 | 154.4 | 0.149 | 0.156 | -0.0031 | 31.98 | 0.85 | -4.816 | 13.916 | -15.198 | -7.761 | 15443.8 | 4.83 | 0.0857 |
| 23.25 | 154.4 | 0.146 | 0.163 | -0.0031 | 29.54 | 0.88 | -4.599 | 14.100 | -14.067 | -8.166 | 15443.8 | 5.23 | 0.0872 |
| 23.50 | 154.4 | 0.144 | 0.168 | -0.0030 | 28.10 | 0.91 | -4.277 | 14.172 | -13.346 | -8.476 | 15443.8 | 5.50 | 0.0881 |
| 23.75 | 154.4 | 0.143 | 0.171 | -0.0030 | 27.26 | 0.95 | -3.902 | 14.174 | -12.946 | -8.720 | 15443.8 | 5.66 | 0.0888 |
| 24.00 | 154.4 | 0.143 | 0.171 | -0.0030 | 26.86 | 0.99 | -3.491 | 14.119 | -12.777 | -8.912 | 15443.8 | 5.75 | 0.0893 |

# Table X

## Similarity Functions - Case E

| t | h | $u_*$ | $\overline{\Theta}_*$ | $\overline{R}_*$ | L | $Ri_B$ | A | B | C | D | $h/z_o$ | h/L | $\frac{\|f\|h}{u_*}$ |
|---|---|---|---|---|---|---|---|---|---|---|---|---|---|
| 0.25 | 154.4 | 0.146 | -2.799 | -0.1531 | -1.85 | -7.14 | 3.456 | 0.777 | 8.481 | 8.107 | 15443.8 | -83.58 | 0.0869 |
| 0.50 | 154.4 | 0.170 | -2.727 | -0.1694 | -2.57 | -6.88 | 4.007 | 0.425 | 8.364 | 8.257 | 15443.8 | -60.04 | 0.0748 |
| 0.75 | 201.1 | 0.186 | -2.791 | -0.1888 | -3.03 | -7.64 | 4.220 | 0.426 | 8.597 | 8.525 | 20113.6 | -66.38 | 0.0889 |
| 1.00 | 248.5 | 0.199 | -2.869 | -0.2088 | -3.40 | -4.39 | 4.343 | 0.386 | 8.775 | 8.700 | 24849.3 | -73.18 | 0.1026 |
| 1.25 | 296.3 | .214 | -2.883 | - .2225 | -3.91 | -4.76 | 4.461 | 0.302 | 8.917 | 8.833 | 29629.4 | -75.83 | 0.1140 |
| 1.50 | 344.4 | 0.229 | -2.865 | -0.2328 | -4.50 | -8.85 | 4.555 | 0.265 | 9.041 | 8.944 | 34441.2 | -76.62 | 0.1237 |
| 1.75 | 441.3 | 0.247 | -2.840 | -0.2371 | -5.32 | -9.51 | 4.710 | 0.245 | 9.255 | 9.102 | 44131.4 | -82.99 | 0.1469 |
| 2.00 | 587.7 | 0.266 | -2.766 | -0.2376 | -6.31 | -11.13 | 5.028 | 0.091 | 9.500 | 9.285 | 58773.2 | -93.21 | 0.1822 |
| 2.25 | 685.8 | 0.28 | -2.720 | -0.2393 | -7.12 | -11.65 | 5.177 | 0.032 | 9.633 | 9.422 | 68580.3 | -96.34 | 0.2018 |
| 2.50 | 784.1 | 0.291 | -2.684 | -0.2418 | -7.82 | -12.20 | 5.288 | 0.027 | 9.745 | 9.494 | 78412.8 | -100.21 | 0.2217 |
| 2.75 | 833.4 | 0.3 1 | -2.651 | - .2448 | -8.44 | -12.00 | 5.311 | 0.039 | 9.788 | 9.573 | 83336.7 | -98.73 | 0.2283 |
| 3.00 | 882.6 | 0.309 | -2.615 | -0.2473 | -9.03 | -11.83 | 5.320 | 0.0 9 | 9.828 | 9.638 | 88264.9 | -97.79 | 0.2355 |
| 3.25 | 882.6 | .316 | -2.572 | - .2491 | -9.60 | -11.06 | 5.272 | 0.055 | 9.814 | 9.663 | 88264.9 | -91.98 | 0.2304 |
| 3.50 | 882.6 | 0.321 | -2.526 | -0.2506 | -10.13 | -10.36 | 5.267 | 0.060 | 9.798 | 9.695 | 88264.9 | -87.10 | 0.2263 |
| 3.75 | 932. | 0.327 | -2.468 | -0.2500 | -10.76 | -10.19 | 5.194 | 0.070 | 9.834 | 9.733 | 93196.9 | -86.59 | 0.2346 |
| 4.00 | 32.0 | 0.332 | -2.412 | -0.2490 | -11.37 | -9.53 | 5.126 | 0.067 | 9.818 | 9.748 | 93196.9 | -81.94 | 0.2313 |
| 4.25 | 981.3 | .336 | -2.330 | -0.2470 | -12.02 | -9.38 | 5.096 | 0.075 | 9.847 | 9.755 | 98132.4 | -81.63 | 0.2406 |
| 4.50 | 981.3 | 0.340 | -2.244 | -0.2433 | -12.78 | -8.74 | 5.035 | 0.069 | 9.832 | 9.766 | 98132.4 | -76.79 | 0.2377 |
| 4.75 | 981.3 | .343 | -2.153 | - .2392 | -13.55 | -8.16 | 4.965 | 0.070 | 9.813 | 9.726 | 98132.4 | -72.44 | 0.2357 |
| 5.00 | 981.3 | 0.345 | -2.053 | -0.2341 | -14.39 | -7.60 | 4.887 | 0.067 | 9.792 | 9.715 | 98132.4 | -68.21 | 0.2341 |
| 5.25 | 1030.7 | 0.348 | -1.945 | -0.2279 | -15.37 | -7.37 | 4.844 | 0.070 | 9.816 | 9.707 | 103071.1 | -67.04 | 0.2443 |
| 5.50 | 1030.7 | 0.349 | -1.825 | -0.2204 | -16.50 | -6.78 | 4.758 | 0.065 | 9.795 | 9.696 | 103 71.1 | -62.47 | 0.2434 |
| 5.75 | 1030.7 | 0.349 | -1.699 | -0.2125 | -17.75 | -6.21 | 4.660 | 0.063 | 9.769 | 9.656 | 103071.1 | -58.06 | 0.2430 |
| 6.00 | 1080.1 | 0.350 | -1.566 | -0.2036 | -19.29 | -5.89 | 4.584 | 0.068 | 9.784 | 9.644 | 108 12.5 | -56.01 | 0.2543 |
| 6.25 | 1080.1 | 0.349 | -1.422 | -0.1937 | -21.15 | -5.29 | 4.471 | 0.071 | 9.753 | 9.615 | 108012.5 | -51.08 | 0.2547 |
| 6.50 | 1080.1 | 0.348 | -1.272 | -0.1834 | -23.42 | -4.70 | 4.343 | 0.077 | 9.718 | 9.574 | 108012.5 | -46.13 | 0.2556 |
| 6.75 | 1129.6 | .347 | -1.113 | -0.1721 | -26.47 | -4.27 | 4.235 | 0.087 | 9.718 | 9.574 | 112956.6 | -42.67 | 0.2685 |
| 7.00 | 1129.6 | 0.343 | -0.948 | -0.1605 | -30.45 | -3.66 | 4.085 | 0.092 | 9.668 | 9.569 | 112956.6 | -37.10 | 0.2710 |
| 7.25 | 1080.1 | 0.338 | -0.777 | -0.1485 | -35.97 | -2.92 | 3.878 | 0.094 | 9.566 | 9.506 | 108012.5 | -30.03 | 0.2630 |
| 7.50 | 1080.1 | 0.332 | -0.600 | -0.1361 | -44.61 | -2.32 | 3.653 | 0.105 | 9.479 | 9.434 | 108012.5 | 24.21 | 0.2683 |
| 7.75 | 1080.1 | 0.323 | -0.415 | -0.1231 | -61.02 | -1.68 | 3.370 | 0.121 | 9.345 | 9.322 | 108 12.5 | -17.70 | 0.2754 |
| 8.00 | 1129.6 | 0.312 | -0.221 | -0.1093 | -106.27 | -1.04 | 3.013 | 0.152 | 9.084 | 9.214 | 112956.6 | -10.63 | 0.2986 |
| 8.25 | 1179.0 | 0.293 | -0.017 | -0.0948 | -1183.40 | -0.28 | 2.415 | 0.200 | 3.316 | 9.048 | 117903.0 | -1.00 | 0.3312 |
| 8.50 | 1179.0 | 0.259 | 0.197 | -0.0783 | 81.65 | .68 | 1.116 | 0.310 | 9.846 | 8.631 | 117903.0 | 14.44 | 0.3750 |
| 8.75 | 1278.3 | 0.203 | 0.431 | -0.0549 | 22.78 | 2.18 | -1.871 | 0.693 | 9.229 | 7.487 | 127802.2 | 56.11 | 0.5181 |
| 9.00 | 1327.5 | 0.141 | 0.616 | -0.0262 | 7.74 | 4.43 | -7.958 | 1.8 4 | 8.242 | 3.681 | 132754.7 | 171.45 | 0.7742 |
| 9.25 | 1327.5 | 0.117 | 0.630 | -0.0115 | 4.26 | 5.20 | -14.249 | 3.721 | 6.976 | -4.609 | 132754.7 | 311.58 | 1.0189 |
| 9.50 | 1327.5 | .112 | 0.660 | -0.0071 | 4.36 | 7.46 | -13.343 | 4.241 | 6.219 | -12.115 | 132754.7 | 304.15 | 0.9804 |
| 9.75 | 1278.1 | 0.115 | 0.635 | -0.0048 | 4.78 | 7.93 | -12.490 | 4.662 | 5.330 | -21.397 | 127802.2 | 267.41 | 0.9178 |
| 10.00 | 1228.5 | 0.113 | 0.611 | -0.0032 | 4.77 | 8.27 | -13.111 | 5.469 | 4.459 | -35.610 | 122851.6 | 257.61 | 0.8989 |
| 10.25 | 1179.0 | 0.109 | 0.587 | -0.0019 | 4.66 | 8.53 | -13.739 | 6.439 | 3.553 | -61.557 | 117903.0 | 252.74 | 0.8882 |
| 10.50 | 1228.5 | 0.107 | 0.574 | -0.0006 | 4.51 | 4.45 | -14.250 | 7.448 | 2.859 | -214.176 | 122851.6 | 272.52 | 0.9500 |
| 10.75 | 108.8 | 0.090 | 0.513 | -0.0005 | 3.57 | 1.25 | -15.323 | 6.800 | -0.069 | 175.977 | 10881.5 | 30.50 | 0.0999 |
| 11.00 | 108.8 | 0.085 | 0.408 | -0.0003 | 3.99 | 1.30 | -16.272 | 8.480 | -2.823 | -285.921 | 10881.5 | 27.28 | 0.1057 |
| 11.25 | 108.8 | 0.081 | 0.375 | -0.0004 | 4.00 | 1.30 | -16.812 | 10.129 | -3.843 | -195.668 | 10881.5 | 27.23 | 0.1103 |
| 11.50 | 108.8 | 0.079 | 0.358 | -0.0004 | 3.98 | 1.31 | -16.836 | 11.563 | -4.371 | -203.207 | 10881.5 | 27.32 | 0.1130 |
| 11.75 | 108.8 | 0.078 | 0.348 | -0.0004 | 4.00 | 1.31 | -16.532 | 12.790 | -4.710 | -200.280 | 10881.5 | 27.22 | 0.1145 |
| 12.00 | 108.8 | 0.078 | 0.342 | -0.0004 | 4.03 | 1.32 | -15.091 | 13.793 | -4.866 | -197.617 | 10881.5 | 26.99 | 0.1150 |
| 12.25 | 108.8 | 0.078 | 0.338 | -0.0004 | 4.07 | 1.33 | -15.328 | 14.618 | -4.965 | -186.042 | 10881.5 | 26.71 | 0.1150 |
| 12.50 | 108.8 | 0.078 | 0.336 | -0.0004 | 4.12 | 1.34 | -14.602 | 15.309 | -4.984 | -175.748 | 10881.5 | 26.42 | 0.1147 |
| 12.75 | 108.8 | 0.078 | 0.335 | -0.0004 | 4.16 | 1.35 | -13.852 | 15.882 | -4.969 | -163.905 | 10881.5 | 26.14 | 0.1143 |
| 13.00 | 108.8 | 0.079 | 0.333 | -0.0004 | 4.20 | 1.37 | -13.113 | 16.400 | -4.959 | -156.944 | 10881.5 | 25.90 | 0.1140 |
| 13.25 | 108.8 | 0.079 | 0.332 | -0.0005 | 4.23 | 1.39 | -12.379 | 16.859 | -4.946 | -147.666 | 10881.5 | 25.70 | 0.1138 |
| 13.50 | 108.8 | 0.079 | 0.331 | -0.0005 | 4.26 | 1.41 | -11.656 | 17.249 | -4.928 | -138.477 | 10881.5 | 25.52 | 0.1136 |
| 13.75 | 108.8 | 0.079 | 0.329 | -0.0005 | 4.28 | 1.43 | -10.968 | 17.633 | -4.940 | -128.030 | 10881.5 | 25.40 | 0.1137 |
| 14.00 | 108.8 | 0.079 | 0.327 | -0.0006 | 4.30 | 1.46 | -10.289 | 17.963 | -4.944 | -118.560 | 10881.5 | 25.32 | 0.1138 |
| 14.25 | 108.8 | 0.079 | 0.325 | -0.0006 | 4.30 | 1.49 | -9.640 | 18.268 | -4.962 | -111.235 | 10881.5 | 25.29 | 0.1141 |
| 14.50 | 108.8 | 0.078 | 0.323 | -0.0006 | 4.30 | 1.52 | -9.023 | 18.559 | -4.996 | -105.214 | 10881.5 | 25.33 | 0.1146 |
| 14.75 | 108.8 | 0.077 | 0.316 | -0.0007 | 4.26 | 1.56 | -8.573 | 19.018 | -5.224 | -97.576 | 10881.5 | 25.55 | 0.1163 |
| 15.00 | 108.8 | 0.075 | 0.306 | -0.0007 | 4.16 | 1.60 | -8.301 | 19.738 | -5.622 | -89.959 | 10881.5 | 26.17 | 0.1196 |
| 15.25 | 65.2 | 0.072 | 0.292 | -0.0006 | 4.06 | 1.08 | -6.084 | 15.215 | -4.167 | -55.324 | 6521.4 | 16.08 | 0.0743 |
| 15.50 | 65.2 | 0.077 | 0.309 | -0.0009 | 4.37 | 1.09 | -7.793 | 14.112 | -3.344 | -47.903 | 6521.4 | 14.91 | 0.0696 |
| 15.75 | 65.2 | 0.084 | 0.324 | -0.0010 | 4.99 | 1.10 | -6.304 | 12.660 | -2.664 | -42.146 | 6521.4 | 13.08 | 0.0636 |
| 16.00 | 65.2 | 0.0 0 | 0.326 | -0.0011 | 5.61 | 1.12 | -5.186 | 11.719 | -2.447 | -38.315 | 6521.4 | 11.62 | 0.0598 |
| 16.25 | 65.2 | 0.0 4 | 0.320 | -0.0011 | 6.27 | 1.14 | -4.288 | 11.057 | -2.509 | -35.500 | 6521.4 | 10.39 | 0.0570 |
| 16.50 | 65.2 | 0.097 | 0.308 | -0.0012 | 6.97 | 1.17 | -3.554 | 10.585 | -2.805 | -33.358 | 6521.4 | 9.35 | 0.0552 |
| 16.75 | 65.2 | 0.100 | 0.292 | -0.0013 | 7.72 | 1.21 | -2.929 | 10.233 | -3.302 | -31.650 | 6521.4 | 8.45 | 0.0539 |
| 17.00 | 65.2 | 0.101 | 0.272 | -0.0013 | 8.55 | 1.24 | -2.382 | 9.962 | -3.990 | -30.261 | 6521.4 | 7.63 | 0.0530 |
| 17.25 | 65.2 | 0.102 | 0.252 | -0.0014 | 9.46 | 1.29 | -1.891 | 9.746 | -4.877 | -29.106 | 6521.4 | 6.89 | 0.0524 |
| 17.50 | 65.2 | 0.103 | 0.230 | -0.0014 | 10.50 | 1.34 | -1.442 | 9.565 | -5.976 | -28.131 | 6521.4 | 6.21 | 0.0520 |
| 17.75 | 65.2 | 0.104 | 0.2 4 | -0.0015 | 11.69 | 1.39 | -1.026 | 9.407 | -7.315 | -27.302 | 6521.4 | 5.58 | 0.0518 |
| 18.00 | 65.2 | 0.104 | 0.188 | -0.0015 | 13.06 | 1.45 | -0.638 | 9.262 | -8.928 | -26.598 | 6521.4 | 4.99 | 0.0517 |
| 18.25 | 65.2 | 0.1 4 | 0.168 | -0.0015 | 14.66 | 1.51 | -0.276 | 9.124 | -10.863 | -26.005 | 6521.4 | 4.45 | 0.0516 |
| 18.50 | 65.2 | 0.104 | 0.149 | -0.0016 | 16.53 | 1.58 | 0.059 | 8.988 | -13.179 | -25.514 | 6521.4 | 3.95 | 0.0516 |
| 18.75 | 65.2 | 0.104 | 0.131 | -0.0016 | 1 .73 | 1.65 | 0.368 | 8.852 | -15.949 | -25.120 | 6521.4 | 3.48 | 0.0516 |
| 19.00 | 65.2 | 0.103 | 0.1 5 | -0.0004 | 12.21 | 1.79 | 0.546 | 8.834 | -8.303 | -116.623 | 6521.4 | 5.34 | 0.0523 |
| 19.25 | 65.2 | 0.100 | 0.207 | 0.0001 | 10.90 | 1.90 | 0.573 | 8.944 | -7.560 | 379.597 | 6521.4 | 5.99 | 0.0538 |
| 19.50 | 65.2 | 0.102 | 0.051 | -0.0022 | 45.99 | 1.87 | 0.954 | 8.566 | -53.524 | -15.611 | 6521.4 | 1.42 | 0.0526 |
| 19.75 | 65.2 | 0.102 | 0.095 | -0.0013 | 24.99 | 1.98 | 1.139 | 8.375 | -25.383 | -32.728 | 6521.4 | 2.61 | 0.0525 |
| 20.00 | 65.2 | 0.103 | 0.132 | -0.0005 | 18.04 | 2.09 | 1.288 | 8.197 | -16.163 | -98.731 | 6521.4 | 3.61 | 0.0524 |
| 20.25 | 65.2 | 0.103 | 0.163 | 0.0002 | 14.58 | 2.19 | 1.404 | 8.026 | -11.622 | 278.719 | 6521.4 | 4.47 | 0.0524 |
| 20.50 | 65.2 | 0.104 | 0.001 | -0.0023 | 1782.84 | 2.14 | 1.594 | 7.749 | -2284.300 | -15.086 | 6521.4 | 0.04 | 0.0517 |
| 20.75 | 65.2 | 0.103 | 0.053 | -0.0013 | 45.46 | 2.25 | 1.617 | 7.626 | -51.247 | -32.967 | 6521.4 | 1.43 | 0.0519 |
| 21.00 | 65.2 | 0.103 | 0.097 | -0.0005 | 24.79 | 2.34 | 1.619 | 7.501 | -24.739 | -108.449 | 6521.4 | 2.63 | 0.0521 |
| 21.25 | 65.2 | 0.103 | 0.134 | 0.0003 | 17.82 | 2.43 | 1.599 | 7.376 | -15.821 | 214.870 | 6521.4 | 3.66 | 0.0523 |
| 21.50 | 65.2 | 0.104 | -0.030 | -0.0024 | -81.20 | 2.33 | 1.664 | 7.148 | 111.978 | -15.181 | 6521.4 | -0.80 | 0.0516 |
| 21.75 | 65.2 | 0.103 | 0.053 | -0.0004 | 29.08 | 2.44 | 1.560 | 7.072 | -30.143 | -128.845 | 6521.4 | 2.24 | 0.0520 |
| 22.00 | 65.2 | 0.103 | 0.060 | -0.0004 | 30.30 | 2.45 | 1.480 | 6.966 | -31.836 | -134.176 | 6521.4 | 2.15 | 0.0521 |
| 22.25 | 65.2 | 0.103 | 0.061 | 0.0003 | -30.03 | 2.33 | 1.401 | 6.851 | 46.877 | 209.668 | 6521.4 | -2.17 | 0.0520 |
| 22.50 | 65.2 | 0.104 | 0.00 | -0.0012 | 259.55 | 2.38 | 1.306 | 6.742 | -326.562 | -38.458 | 6521.4 | 0.25 | 0.0518 |
| 22.75 | 65.2 | 0.107 | -0.022 | -0.0018 | -119.02 | 2.30 | 1.437 | 6.427 | 148.934 | -23.442 | 6521.4 | -0.55 | 0.0500 |
| 23.00 | 65.2 | 0.106 | -0.018 | -0.0018 | -143.03 | 2.29 | 1.216 | 6.478 | 182.822 | -24.238 | 6521.4 | -0.46 | 0.0508 |
| 23.25 | 65.2 | 0.105 | -0.014 | -0.0017 | -172.86 | 2.25 | 1.002 | 6.514 | 223.972 | -25.011 | 6521.4 | -0.38 | 0.0514 |
| 23.50 | 65.2 | 0.104 | -0.012 | -0.0017 | -210.12 | 2.21 | 0.792 | 6.540 | 274.321 | -25.764 | 6521.4 | -0.31 | 0.0518 |
| 23.75 | 65.2 | 0.103 | -0.009 | -0.0017 | -256.70 | 2.16 | 0.585 | 6.563 | 336.236 | -26.500 | 6521.4 | -0.25 | 0.0520 |
| 24.00 | 65.2 | 0. 03 | -0.008 | -0.0017 | -315.08 | 2.10 | 0.380 | 6.588 | 412.846 | -27.221 | 6521.4 | -0.21 | 0.0521 |

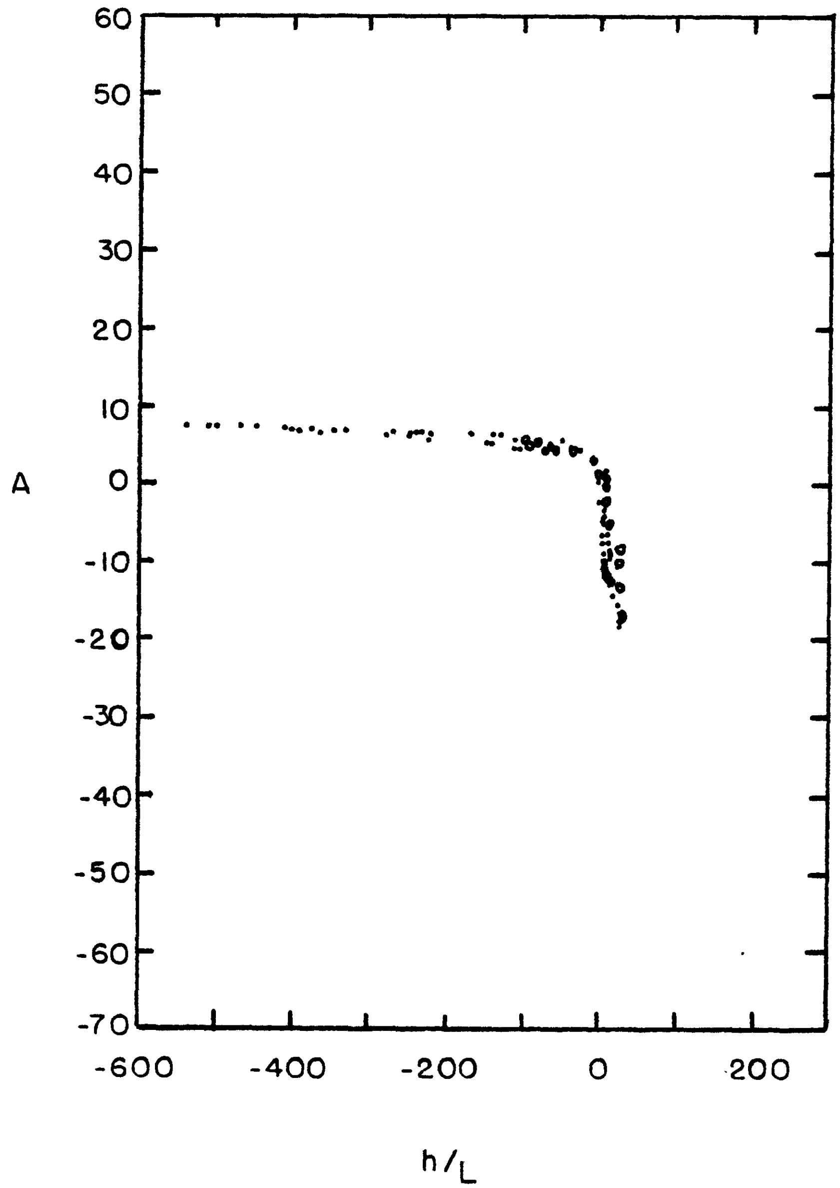


Fig. 36. Similarity function A as a function of h/L: open circles (o) - case E; closed circles (·) - cases A-D.

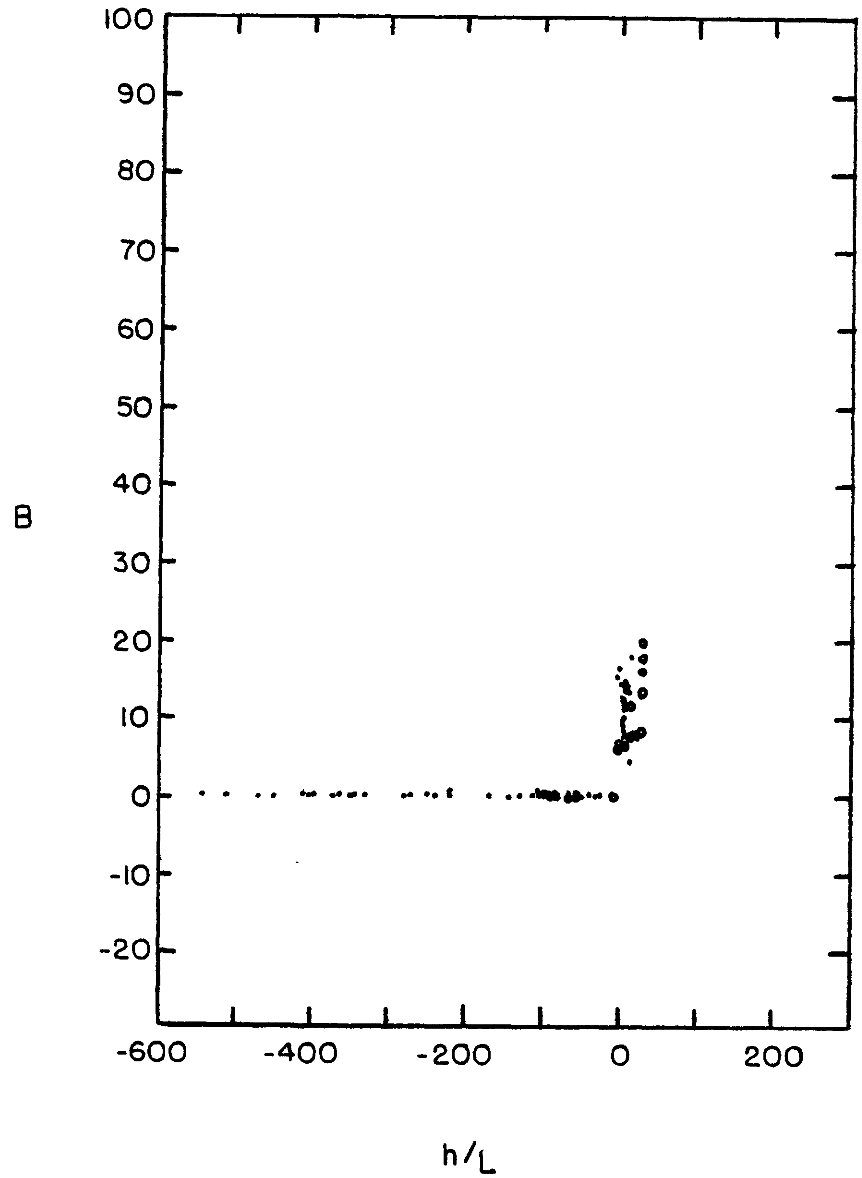


Fig. 37. Similarity function B as a function of h/L: open circles (o) - case E; closed circles (·) - cases A-D.

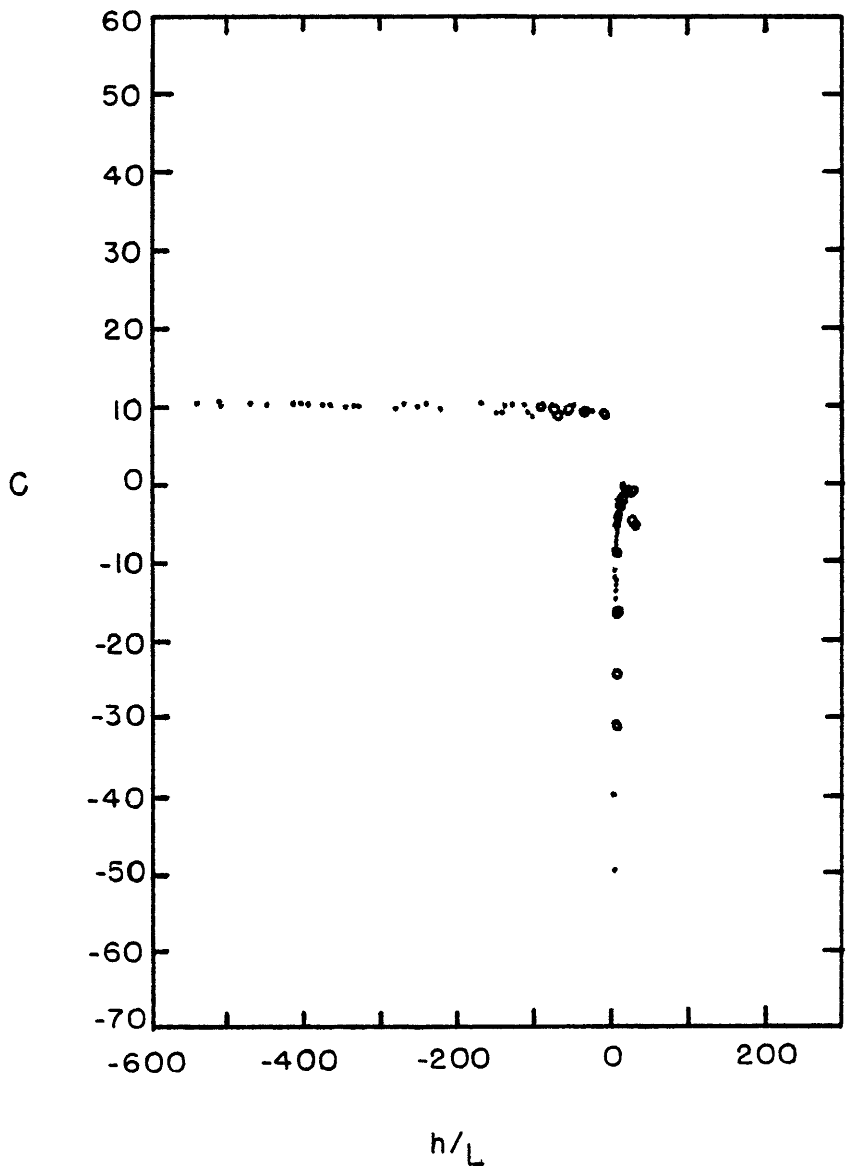


Fig. 38. Similarity function C as a function of h/L: open circles (o) - case E; closed circles (·) - cases A-D.

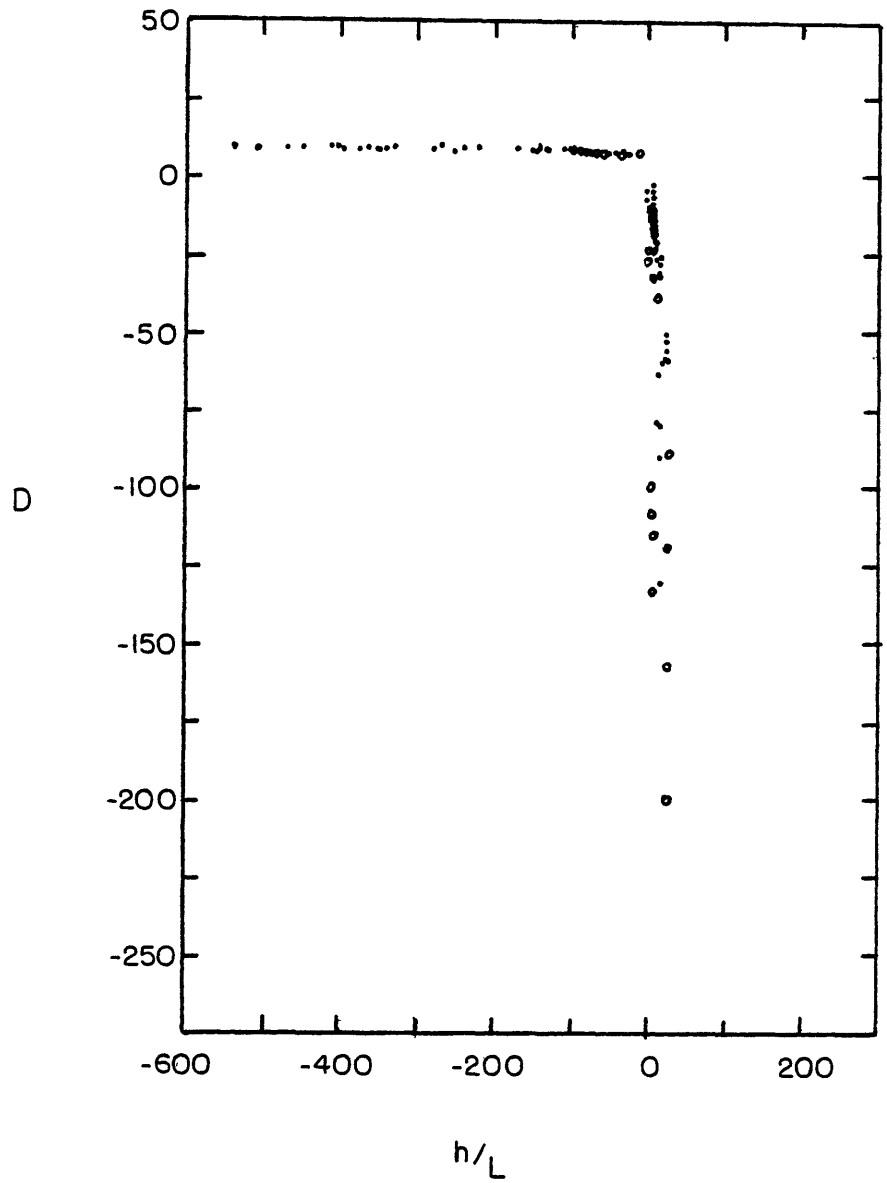


Fig. 39. Similarity function D as a function of h/L: open circles (o) - case E; closed circles (.) - cases A-D.

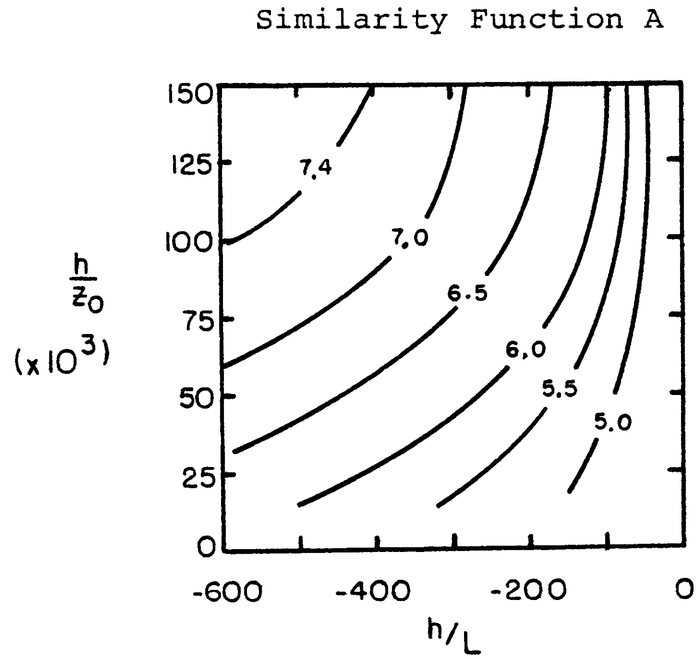


(a)

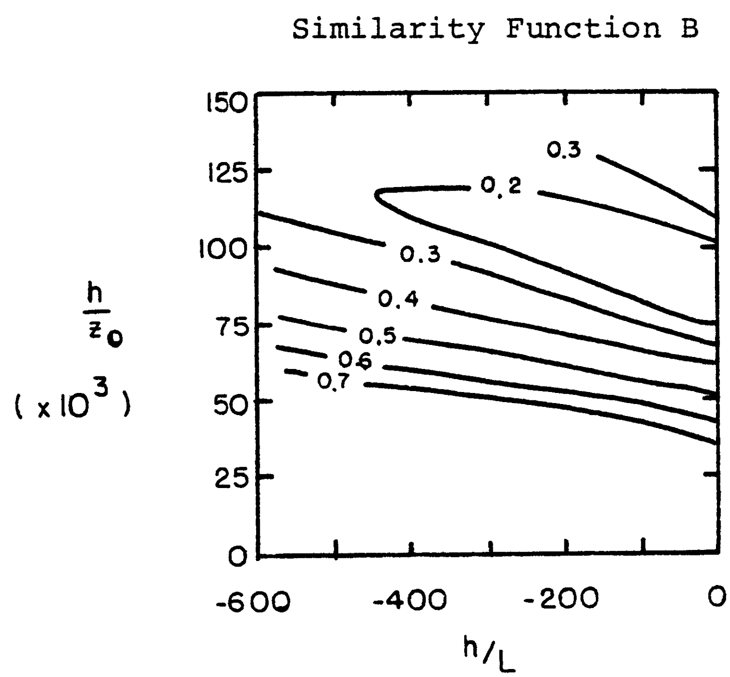


(b)

Fig. 40. (a) Similarity function A as a function of h/L and $h/z_o$ for values of $|f|h/u_* \geq 0.1$.
(b) Similarity function B as a function of h/L and $h/z_o$ for values of $|f|h/u_* \geq 0.1$.

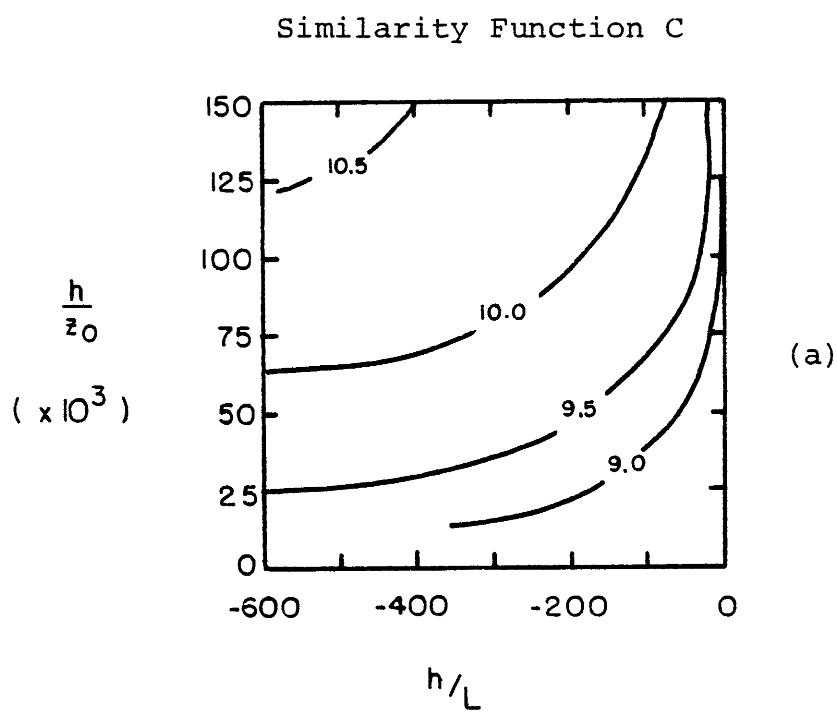


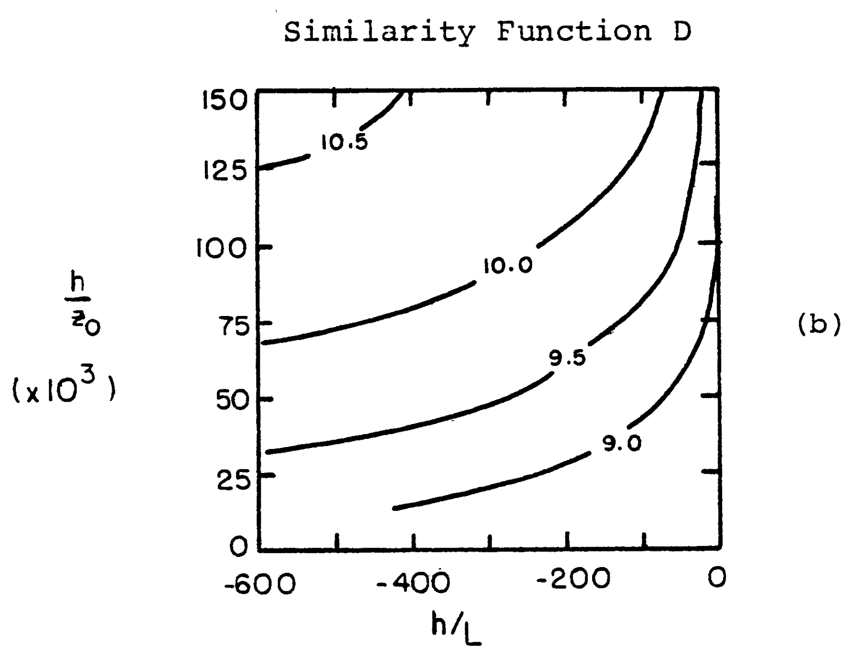


Fig. 41. (a) Similarity function C as a function of h/L and $h/z_o$ for values of $|f|h/u_* \geq 0.1$.
(b) Similarity function D as a function of h/L and $h/z_o$ for values of $|f|h/u_* \geq 0.1$.

Figures 36-39. Figures 40 (a,b) and 41 (a,b) show isolines of A, B, C, and D as functions of $h/z_o$ and $h/L$ for a restricted range of values of $|f|h/u_*$.

An examinations of Tables VI-X indicates that the similarity functions C and D are equal (within a few percent) in the unstable boundary layer. Under stable conditions, however, C and D do not appear to be equal.

Brutsaert and Chan (1978), analyzing experimental data, evaluated the similarity functions C and D. With the height of the inversion as the length scale, $\delta$, they found D to be about 0.65 C. Their results, however, are based on the use of $\overline{\Theta}$ ($\delta$) and $\overline{R}$ ($\delta$) in the deficit relations instead of the vertically averaged variables $\overline{\Theta}_m$ and $\overline{R}_m$. As pointed out by Arya (1977, 1978) the use of $\overline{\theta}$ ($\delta$) and $\overline{R}$ ($\delta$) in the formulation of C and D is less desirable than the use of the vertically averaged variables because the results are more sensitive to baroclinicity and sampling errors.

# 9. SUMMARY

A higher order closure turbulence model, using the full level 3 equations (Mellor and Yamada, 1974; Yamada and Mellor, 1975) is described in detail in section 2. A new formulation for the length scale $\ell$, defined by equations (65a - 65c) is used. This length scale, appearing in each of the modeling parameterizations described in section 3, has the same shape in the PBL as Deardorff's (1974, 1975) profile of the turbulence energy dissipation length scale.

Equilibrium boundary conditions for the second moments are applied at the lower boundary. The surface mixing ratio and potential temperature are predicted with a single layer ground thermodynamics model (Deardorff, 1978).

The results of a simulation of Day 33-34 of the Wangara boundary layer are examined in section 6. The boundary layer grows through the day, reaching a maximum (1320 m) around 1800 hours (6:00 p.m. local time). About an hour after sunset, the PBL top falls rapidly to a more or less constant value of 100-150 m throughout the night.

Twenty-four hour simulations are made both with and without the Coriolis terms. The results are nearly identical for all the mean and prognostic turbulence variables. The details of the Reynolds stress components

$\overline{u'w'}$ and $\overline{v'w'}$, however, did show some sensitivity to the inclusion of the Coriolis terms.

Finally, the similarity functions A, B, C, and D are evaluated in section 8. Layer-averaged variables are used in the deficit relations. The similarity functions C and D are found to be equal in the unstable boundary layer, although this appears not to be true in the stable boundary layer.

# APPENDIX A

## SOLUTION OF THE DIAGNOSTIC REYNOLDS STRESS, HEAT FLUX, AND WATER VAPOR FLUX EQUATIONS

The level 3 equations for the Reynolds stress and the heat flux (equations 50-58) represent a closed set of 9 diagnostic equations. Once the prognostic equations for the mean variables ($\bar{u}$, $\bar{v}$, $\bar{\Theta}_v$, $\bar{R}$) and the turbulence variables ($q^2$, $\overline{\theta_v'^2}$) are solved, the individual components of the Reynolds stress tensor and the heat flux vector are determined. The solution of the simultaneous equations (50-58), however, requires a great deal of algebraic work. It is convenient to represent equations (50-58) in the matrix form (equations A-1).

The matrix is solved by performing elementary row reduction operations until all the non-diagonal elements are zero and the diagonal elements are equal to one. If, at each step in the matrix manipulation, a new variable is defined in terms of combinations of previously defined variables, the answer will be of the form $\overline{u_i'u_j'} = N_k$, where $N_k$ is defined in terms of M's, and the M's are defined in terms of L's, etc. This procedure will lead to the following:

$$\begin{bmatrix} 1 & 0 & 0 & \mathring{A}_5 & \mathring{A}_2+\mathring{A}_6 & \mathring{A}_3 & 0 & 0 & \mathring{A}_4 \\ 0 & 1 & 0 & \mathring{B}_5 & \mathring{B}_3 & \mathring{B}_2 & 0 & 0 & \mathring{B}_4 \\ 0 & 0 & 1 & 0 & \mathring{C}_2+\mathring{C}_5 & \mathring{C}_3 & 0 & 0 & \mathring{C}_4 \\ \mathring{D}_3 & \mathring{D}_5 & 0 & 1 & \mathring{D}_1 & \mathring{D}_2+\mathring{D}_4 & 0 & 0 & 0 \\ \mathring{E}_4 & 0 & \mathring{E}_1+\mathring{E}_5 & 0 & 1 & \mathring{E}_6 & \mathring{E}_3 & 0 & 0 \\ 0 & 0 & \mathring{F}_1 & \mathring{F}_4 & \mathring{F}_5 & 1 & 0 & \mathring{F}_3 & 0 \\ 0 & 0 & 0 & 0 & G_1 & 0 & 1 & \mathring{G}_4 & \mathring{G}_2+\mathring{G}_3 \\ 0 & 0 & 0 & 0 & 0 & \mathring{H}_1 & \mathring{H}_3 & 1 & \mathring{H}_2 \\ 0 & 0 & \mathring{I}_2 & 0 & 0 & 0 & \mathring{I}_3 & 0 & 1 \end{bmatrix} \begin{bmatrix} \overline{u'^2} \\ \overline{v'^2} \\ \overline{w'^2} \\ \overline{u'v'} \\ \overline{u'w'} \\ \overline{v'w'} \\ \overline{u'\theta'_v} \\ \overline{v'\theta'_v} \\ \overline{w'\theta'_v} \end{bmatrix} = \begin{bmatrix} \mathring{A}_1 \\ \mathring{B}_1 \\ \mathring{C}_1 \\ 0 \\ \mathring{E}_2 \\ \mathring{F}_2 \\ 0 \\ 0 \\ \mathring{I}_1 \end{bmatrix}$$

Equations A-1

$$\begin{bmatrix} 1 & 0 & 0 & 0 & 0 & 0 & 0 & 0 & 0 \\ 0 & 1 & 0 & 0 & 0 & 0 & 0 & 0 & 0 \\ 0 & 0 & 1 & 0 & 0 & 0 & 0 & 0 & 0 \\ 0 & 0 & 0 & 1 & 0 & 0 & 0 & 0 & 0 \\ 0 & 0 & 0 & 0 & 1 & 0 & 0 & 0 & 0 \\ 0 & 0 & 0 & 0 & 0 & 1 & 0 & 0 & 0 \\ 0 & 0 & 0 & 0 & 0 & 0 & 1 & 0 & 0 \\ 0 & 0 & 0 & 0 & 0 & 0 & 0 & 1 & 0 \\ 0 & 0 & 0 & 0 & 0 & 0 & 0 & 0 & 1 \end{bmatrix} \begin{bmatrix} \overline{u'^2} \\ \overline{v'^2} \\ \overline{w'^2} \\ \overline{u'v'} \\ \overline{u'w'} \\ \overline{v'w'} \\ \overline{u'\theta'_v} \\ \overline{v'\theta'_v} \\ \overline{w'\theta'_v} \end{bmatrix} = \begin{bmatrix} N_1 \\ N_2 \\ N_3 \\ N_4 \\ N_5 \\ N_6 \\ N_7 \\ N_8 \\ N_9 \end{bmatrix}$$

Equations (A-2)

where,

$$\mathring{A}_1 = q^2/3$$

$$\mathring{A}_2 = \frac{4\ell_1}{q} \frac{\partial\bar{u}}{\partial z}$$

$$\mathring{A}_3 = \frac{-2\ell_1}{q} \frac{\partial\bar{v}}{\partial z}$$

$$\mathring{A}_4 = \frac{+2\ell_1}{q} \beta g$$

$$\mathring{A}_5 = \frac{-6\ell_1}{q} f_z$$

$$\mathring{A}_6 = \frac{6\ell_1}{q} f_y$$

$$\mathring{B}_1 = q^2/3$$

$$\mathring{B}_2 = \frac{4\ell_1}{q} \frac{\partial\bar{v}}{\partial z}$$

$$\mathring{B}_3 = \frac{-2\ell_1}{q} \frac{\partial\bar{u}}{\partial z}$$

$$\mathring{B}_4 = \frac{+2\ell_1}{q} \beta g$$

$$\mathring{B}_5 = \frac{6\ell_1}{q} f_z$$

$$\mathring{C}_1 = q^2/3$$

$$\mathring{C}_2 = \frac{-2\ell_1}{q} \frac{\partial\bar{u}}{\partial z}$$

$$\mathring{C}_3 = \frac{-2\ell_1}{q} \frac{\partial\bar{u}}{\partial z}$$

$$\mathring{C}_4 = \frac{-4\ell_1}{q} \beta g$$

$$\mathring{C}_5 = \frac{-6\ell_1}{q} f_y$$

$$\mathring{D}_1 = \frac{3\ell_1}{q} \frac{\partial\bar{v}}{\partial z}$$

$$\mathring{D}_2 = \frac{3\ell_1}{q} \frac{\partial\bar{u}}{\partial z}$$

$$\mathring{D}_3 = \frac{3\ell_1}{q} f_z$$

$$\mathring{D}_4 = \frac{3\ell_1}{q} f_y$$

$$\mathring{D}_5 = \frac{-3\ell_1}{q} f_z$$

$$\mathring{E}_1 = \frac{3\ell_1}{q} \frac{\partial\bar{u}}{\partial z}$$

$$\mathring{E}_2 = 3\ell_1 Cq \frac{\partial\bar{u}}{\partial z}$$

$$\mathring{E}_3 = \frac{-3\ell_1}{q} \beta g$$

$$\mathring{E}_4 = \frac{-3\ell_1}{q} f_y$$

$$\mathring{E}_5 = \frac{3\ell_1}{q} f_y$$

$$\mathring{E}_6 = \frac{-3\ell_1}{q} f_z$$

$$\mathring{F}_1 = \frac{3\ell_1}{q} \frac{\partial\bar{v}}{\partial z}$$

$$\mathring{F}_2 = 3\ell_1 Cq \frac{\partial\bar{v}}{\partial z}$$

$$\mathring{F}_3 = \frac{-3\ell_1}{q} \beta g$$

$$\mathring{F}_4 = \frac{-3\ell_1}{q} f_y$$

$$\mathring{F}_5 = \frac{3\ell_1}{q} f_z$$

$$\mathring{G}_1 = \frac{3\ell_2}{q} \frac{\partial\bar{\Theta}_v}{\partial z}$$

$$\mathring{G}_2 = \frac{3\ell_2}{q} \frac{\partial\bar{u}}{\partial z}$$

$$\mathring{G}_3 = \frac{3\ell_2}{q} f_y$$

$$\mathring{G}_4 = \frac{-3\ell_2}{q} f_z$$

$$\mathring{H}_1 = \frac{3\ell_2}{q} \frac{\partial\bar{\Theta}_v}{\partial z}$$

$$\mathring{H}_2 = \frac{3\ell_2}{q} \frac{\partial\bar{v}}{\partial z}$$

$$\mathring{H}_3 = \frac{3\ell_2}{q} f_z$$

$$\mathring{I}_1 = \frac{3\ell_2}{q} \beta g \overline{\theta_v'^2}$$

$$\mathring{I}_2 = \frac{3\ell_2}{q} \frac{\partial\bar{\Theta}_v}{\partial z}$$

$$\mathring{I}_3 = \frac{-3\ell_2}{q} f_y$$

$N_1 = M_2/M_1$

$N_2 = M_4 - M_3(M_2/M_1)$

$N_3 = L_8 - L_7(M_2/M_1)$

$N_4 = M_6 - M_5(M_2/M_1)$

$N_5 = M_8 - M_7(M_2/M_1)$

$N_6 = M_{10} - M_9(M_2/M_1)$

$N_7 = M_{12} - M_{11}(M_2/M_1)$

$N_8 = M_{14} - M_{13}(M_2/M_1)$

$N_9 = M_{16} - M_{15}(M_2/M_1)$

$M_1 = L_1 - L_2L_7$

$M_2 = L_3 - L_2L_8$

$M_3 = L_4 - L_5L_7$

$M_4 = L_6 - L_5L_8$

$M_5 = K_4 - K_5L_7$

$M_6 = K_6 - K_5L_8$

$M_7 = E_{16} - E_{17}L_7$

$M_8 = E_{18} - E_{17}L_8$

$M_9 = K_7 - K_8L_7$

$M_{10} = K_9 - K_8L_8$

$M_{11} = K_{10} - K_{11}L_7$

$M_{12} = K_{12} - K_{11}L_8$

$M_{13} = K_{13} - K_{14}L_7$

$M_{14} = K_{15} - K_{14}L_8$

$M_{15} = K_{16} - K_{17}L_7$

$M_{16} = K_{18} - K_{17}L_8$

$L_1 = 1 - F_2K_4$

$L_2 = F_1 - F_2K_5$

$L_3 = F_3 - F_2K_6$

$L_4 = -F_5K_4$

$L_5 = F_4 - F_5K_5$

$L_6 = F_6 - F_5K_6$

$L_7 = K_1/K_2$

$L_8 = K_3/K_2$

$K_1 = F_7 - F_8(J_1/J_3)$

$K_2 = 1 - F_8(J_2/J_3)$

$K_3 = F_9 - F_8(J_4/J_3)$

$K_4 = -G_2(J_1/J_3)$

$K_5 = G_1 - G_2(J_2/J_3)$

$K_6 = G_3 - G_2(J_4/J_3)$

$K_7 = J_1/J_3$

$K_8 = J_2/J_3$

$K_9 = J_4/J_3$

$K_{10} = B_{32} - B_{34}(J_1/J_3)$

$K_{11} = B_{33} - B_{34}(J_2/J_3)$

$K_{12} = B_{35} - B_{34}(J_4/J_3)$

$K_{13} = I_6 - I_8(J_1J_3)$

$K_{14} = I_7 - I_8(J_2/J_3)$

$K_{15} = I_9 - I_8(J_4/J_3)$

$K_{16} = I_{10} - I_{12}(J_1/J_3)$

$K_{17} = I_{11} - I_{12}(J_2/J_3)$

$K_{18} = I_{13} - I_{12}(J_4/J_3)$

$J_1 = I_1$

$J_2 = I_2 - I_3G_1$

$J_3 = I_4 - I_3G_2$

$J_4 = I_5 - I_3G_3$

$I_1 = -H_4B_{32}$

$I_2 = H_1 - H_4B_{33}$

$I_3 = H_2$

$I_4 = H_3 - H_4B_{34}$

$I_5 = H_5 - H_4B_{35}$

$I_6 = -F_{15}B_{32}$

$I_7 = F_{13} - F_{15}B_{33}$

$I_8 = F_{14} - F_{15}B_{34}$

$I_9 = F_{16} - F_{15}B_{35}$

$I_{10} = -A_{44}B_{32}$

$I_{11} - A_{43} - A_{44}B_{33}$

$I_{12} - -A_{44}B_{34}$

$I_{13} = A_{45} - A_{44}B_{35}$

$H_1 = E_{19} - E_{21}F_{13}$

$H_2 = E_{20}$

$H_3 = 1 - E_{21}F_{14}$

$H_4 = -E_{21}F_{15}$

$H_5 = E_{22} - E_{21}F_{16}$

$G_1 = F_{10}/F_{11}$

$G_2 = 1/F_{11}$

$G_3 = F_{12}/F_{11}$

$F_1 = E_2/E_1$

$F_2 = E_3/E_1$

$F_3 = E_4/E_1$

$F_4 = E_6/E_5$

$F_5 = E_7/E_5$

$F_6 = E_8/E_5$

$F_7 = E_9/E_{10}$

$F_8 = 1/E_{10}$

$F_9 = E_{11}/E_{10}$

$F_{10} = E_{13} - E_{12}(E_6/E_5)$

$F_{11} = E_{14} - E_{12}(E_7/E_5)$

$F_{12} = E_{15} - E_{12}(E_8/E_5)$

$F_{13} = -A_{42}A_{43}$

$F_{14} = A_{40}$

$F_{15} = A_{41} - A_{42}A_{44}$

$F_{16} = -A_{42}A_{45}$

$E_1 = 1 - D_3(D_9/D_{11})$

$E_2 = D_1 - D_3(D_{10}/D_{11})$

$E_3 = D_2$

$E_4 = D_4 - D_3(D_{12}/D_{11})$

$E_5 = 1 - D_7(D_{13}/D_{16})$

$E_6 = D_5 - D_7(D_{14}/D_{16})$

$E_7 = D_6 - D_7(D_{15}/D_{16})$

$E_8 = D_8 - D_7(D_{17}/D_{16})$

$E_9 = D_9/D_{11}$

$E_{10} = D_{10}/D_{11}$

$E_{11} = D_{12}/D_{11}$

$E_{12} = D_{13}/D_{16}$

$E_{13} = D_{14}/D_{16}$

$E_{14} = D_{15}/D_{16}$

$E_{15} = D_{17}/D_{16}$

$E_{16} = B_{22} - B_{24}(D_9/D_{11})$

$E_{17} = B_{23} - B_{24}(D_{10}/D_{11})$

$E_{18} = B_{25} - B_{24}(D_{12}/D_{11})$

$E_{19} = D_{18}/D_{20}$

$E_{20} = D_{19}/D_{20}$

$E_{21} = D_{21}/D_{20}$

$E_{22} = D_{22}/D_{20}$

$D_1 = C_2/C_1$

$D_2 = C_3/C_1$

$D_3 = C_4/C_1$

$D_4 = C_5/C_1$

$D_5 = C_7 - C_6(C_2/C_1)$

$D_6 = C_8 - C_6(C_3/C_1)$

$D_7 = C_9 - C_6(C_4/C_1)$

$D_8 = C_{10} - C_6(C_5/C_1)$

$D_9 = C_{11} - B_{32}$

$D_{10} = C_{12} - B_{33}$

$D_{11} = C_{13} - B_{34}$

$D_{12} = C_{14} - B_{35}$

$D_{13} = B_{18}$

$D_{14} = B_{19} - B_{17}(C_2/C_1)$

$D_{15} = 1 - B_{17}(C_3/C_1)$

$D_{16} = B_{20} - B_{17}(C_4/C_1)$

$D_{17} = B_{21} - B_{17}(C_5/C_1)$

$D_{18} = B_{27} - B_{26}(C_2/C_1)$

$D_{19} = B_{28} - B_{26}(C_3/C_1)$

$D_{20} = B_{29} - B_{26}(C_4/C_1)$

$D_{21} = B_{30}$

$D_{22} = B_{31} - B_{26}(C_5/C_1)$

$C_1 = 1 - B_4(B_{12}/B_{15})$

$C_2 = B_1 - B_4(B_{13}/B_{15})$

$C_3 = B_2$

$C_4 = B_3 - B_4(B_{14}/B_{15})$

$C_5 = B_5 - B_4(B_{16}/B_{15})$

$C_6 = B_6 - B_{10}(B_{12}/B_{15})$

$C_7 = B_7 - B_{10}(B_{13}/B_{15})$

$C_8 = B_8$

$C_9 = B_9 - B_{10}(B_{14}/B_{15})$

$C_{10} = B_{11} - B_{10}(B_{16}/B_{15})$

$C_{11} = B_{12}/B_{15}$

$C_{12} = B_{13}/B_{15}$

$C_{13} = B_{14}/B_{15}$

$C_{14} = B_{16}/B_{15})$

$B_1 = A_1 - A_{43}A_5$

$B_2 = A_2$

$B_3 = A_3$

$B_4 = A_4 - A_{44}A_5$

$B_5 = A_6 - A_{45}A_5$

$B_6 = A_7$

$B_7 = A_8 - A_{43}A_{12}$

$B_8 = A_9$

$B_9 = A_{10}$

$B_{10} = A_{11} - A_{44}A_{12}$

$B_{11} = A_{13} - A_{45}A_{12}$

$B_{12} = A_{14}$

$B_{13} = 1 - A_{43}A_{17}$

$B_{14} = A_{15}$

$B_{15} = A_{16} - A_{44}A_{17}$

$B_{16} = A_{18} - A_{45}A_{17}$

$B_{17} = A_{19} - A_{23}(A_{58}/A_{51})$

$B_{18} = A_{20}$

$B_{19} = A_{21} - A_{23}(A_{49}/A_{51})$

$B_{20} = A_{22} - A_{23}(A_{50}/A_{51})$

$B_{21} = A_{24} - A_{23}(A_{52}/A_{51})$

$B_{22} = A_{25} - A_{28}(A_{48}/A_{51})$

$B_{23} = A_{26} - A_{28}(A_{49}/A_{51})$

$B_{24} = A_{27} - A_{28}(A_{50}/A_{51})$

$B_{25} = A_{29} - A_{28}(A_{52}/A_{51})$

$B_{26} = A_{30} - A_{33}(A_{48}/A_{51})$

$B_{27} = A_{31} - A_{33}(A_{49}/A_{51})$

$B_{28} = A_{32}$

$B_{29} = 1 - A_{33}(A_{50}/A_{51})$

$B_{30} = A_{34}$

$B_{31} = A_{35} - A_{33}(A_{52}/A_{51})$

$B_{32} = A_{48}/A_{51}$

$B_{33} = A_{49}/A_{51}$

$B_{34} = A_{50}/A_{51}$

$B_{35} = A_{52}/A_{51}$

$A_1 = (-\alpha_{17}\alpha_2)/(1-\alpha_{16}\alpha_2)$

$A_2 = \alpha_1/(1-\alpha_{16}\alpha_2)$

$A_3 = (\alpha_3-\alpha_{18}\alpha_2)/(1-\alpha_{16}\alpha_2)$

$A_4 = -\alpha_{19}\alpha_2/(1-\alpha_{16}\alpha_2)$

$A_5 = \alpha_4/(1-\alpha_{16}\alpha_2)$

$A_6 = (\mathring{A}_1-\alpha_2\mathring{E}_2)/(1-\alpha_{16}\alpha_2)$

$A_7 = -\alpha_{16}\alpha_6$

$A_8 = -\alpha_{17}\alpha_6$

$A_9 = \alpha_5$

$A_{10} = \alpha_7-\alpha_{18}\alpha_6$

$A_{11} = -\alpha_{19}\alpha_6$

$A_{12} = \alpha_8$

$A_{13} = \mathring{B}_1-\alpha_6\mathring{E}_2$

$A_{14} = -\alpha_{16}\alpha_9/(1-\alpha_{17}\alpha_9)$

$A_{15} = (\alpha_{10}-\alpha_{18}\alpha_9)/(1-\alpha_{17}\alpha_9)$

$A_{16} = -\alpha_{19}\alpha_9/(1-\alpha_{17}\alpha_9)$

$A_{17} = \alpha_{11}/(1-\alpha_{17}\alpha_9)$

$A_{18} = (\mathring{C}_1-\alpha_9\mathring{E}_2)/(1-\alpha_{17}\alpha_9)$

$A_{19} = \alpha_{12}-\alpha_{16}\alpha_{14}$

$A_{20} = \alpha_{13}$

$A_{21} = -\alpha_{17}\alpha_{14}$

$A_{22} = \alpha_{15}-\alpha_{18}\alpha_{14}$

$A_{23} = -\alpha_{19}\alpha_{14}$

$A_{24} = -\alpha_{14}\mathring{E}_2$

$A_{25} = \alpha_{16}$

$A_{26} = \alpha_{17}$

$A_{27} = \alpha_{18}$

$A_{28} = \alpha_{19}$

$A_{29} = \mathring{E}_2$

$A_{30} = -\alpha_{16}\alpha_{22}/(1-\alpha_{18}\alpha_{22})$

$A_{31} = (\alpha_{20}-\alpha_{17}\alpha_{22})/(1-\alpha_{18}\alpha_{22})$

$A_{32} = \alpha_{21}/(1-\alpha_{18}\alpha_{22})$

$A_{33} = -\alpha_{19}\alpha_{22}/(1-\alpha_{18}\alpha_{22})$

$A_{34} = \alpha_{23}/(1-\alpha_{18}\alpha_{22})$

$A_{35} = (\mathring{F}_2-\alpha_{22}\mathring{E}_2)/(1-\alpha_{18}\alpha_{22})$

$A_{36} = -\alpha_{16}\alpha_{24}/(1-\alpha_{19}\alpha_{24})$

$A_{37} = -\alpha_{17}\alpha_{24}/(1-\alpha_{19}\alpha_{24})$

$A_{38} = -\alpha_{18}\alpha_{24}/(1-\alpha_{19}\alpha_{24})$

$A_{39} = -\alpha_{24}\mathring{E}_2/(1-\alpha_{19}\alpha_{24})$

$A_{40} = \alpha_{27}$

$A_{41} = \alpha_{28}$

$A_{42} = \alpha_{29}$

$A_{43} = \alpha_{30}$

$A_{44} = \alpha_{31}$

$A_{45} = \mathring{I}_1$

$A_{46} = \alpha_{25}/(1-\alpha_{19}\alpha_{24})$

$A_{47} = \alpha_{26}/(1-\alpha_{19}\alpha_{24})$

$A_{48} = A_{36}$

$A_{49} = A_{37} - A_{43}(A_{47}-A_{42}A_{46})$

$A_{50} = A_{38} - A_{40}A_{46}$

$A_{51} = 1 - A_{41}A_{46} - A_{44}(A_{47}-A_{42}A_{46})$

$A_{52} = A_{39} - A_{45}(A_{47}-A_{42}A_{46})$

$\alpha_1 = \overset{\circ}{A}_5$
$\alpha_2 = \overset{\circ}{A}_2 + \overset{\circ}{A}_6$
$\alpha_3 = \overset{\circ}{A}_3$
$\alpha_4 = \overset{\circ}{A}_4$
$\alpha_5 = \overset{\circ}{B}_5$
$\alpha_6 = \overset{\circ}{B}_3$
$\alpha_7 = \overset{\circ}{B}_2$
$\alpha_8 = \overset{\circ}{B}_4$
$\alpha_9 = \overset{\circ}{C}_2 + \overset{\circ}{C}_5$
$\alpha_{10} = \overset{\circ}{C}_3$

$\alpha_{11} = \overset{\circ}{C}_4$
$\alpha_{12} = \overset{\circ}{D}_3$
$\alpha_{13} = \overset{\circ}{D}_5$
$\alpha_{14} = \overset{\circ}{D}_1$
$\alpha_{15} = \overset{\circ}{D}_2 + \overset{\circ}{D}_4$
$\alpha_{16} = \overset{\circ}{E}_4$
$\alpha_{17} = \overset{\circ}{E}_1 + \overset{\circ}{E}_5$
$\alpha_{18} = \overset{\circ}{E}_6$
$\alpha_{19} = \overset{\circ}{E}_3$
$\alpha_{20} = \overset{\circ}{F}_1$

$\alpha_{21} = \overset{\circ}{F}_4$
$\alpha_{22} = \overset{\circ}{F}_5$
$\alpha_{23} = \overset{\circ}{F}_3$
$\alpha_{24} = \overset{\circ}{G}_1$
$\alpha_{25} = \overset{\circ}{G}_4$
$\alpha_{26} = \overset{\circ}{G}_2 + \overset{\circ}{G}_3$
$\alpha_{27} = \overset{\circ}{H}_1$
$\alpha_{28} = \overset{\circ}{H}_3$
$\alpha_{29} = \overset{\circ}{H}_2$
$\alpha_{30} = \overset{\circ}{I}_2$
$\alpha_{31} = \overset{\circ}{I}_3$

The finite difference scheme described in section 5 requires that the turbulent moments $\overline{u'w'}$, $\overline{v'w'}$, and $\overline{w'\theta_v'}$ be known at time step k in order to solve equations (40-47) at time step k + 1. From equations (A-2), we see $\overline{u'w'}$, $\overline{v'w'}$, and $\overline{w'\theta_v'}$ are $N_5$, $N_6$, and $N_9$, respectively. Substitution of the $\overset{\circ}{A}$ through M into the N's results in a very long and complicated expression for each N. The model calculates the N's by evaluating the intermediate variables ($\overset{\circ}{A}$-M) first.

Matters are simplified considerably when the Coriolis terms are omitted. The model has an option to allow the Coriolis terms to be included or to be set equal to zero. Mellor and Yamada (1974) evaluated expressions for $\overline{u'w'}$, $\overline{v'w'}$, and $\overline{w'\theta_v'}$ in the case $f_y=f_z=0$. It is possible to to show that $N_5$, $N_6$, and $N_9$ reduce to their expressions in that special case.

With $f_y = f_z = 0$,

$$\overline{u'w'} = N_5 = E_{18} - E_{17}\left[\frac{E_{11}(1 - E_{21}A_{40}) - (E_{22} + E_{21}A_{42}A_{45})}{E_{10}(1 - E_{21}A_{40}) - (E_{19} + E_{21}A_{42}A_{43})}\right] \tag{A-3}$$

$$E_{18} = \left[\frac{3l_1 C q^4 - 27 l_1 l_2^2 (\beta g)^2 \overline{\theta_v'^2}}{q^3 + 9 l_1 l_2 q \beta g\, \partial\bar{\Theta}_v/\partial z}\right]\frac{\partial \bar{u}}{\partial z} \tag{A-4}$$

$$E_{17} = \left[\frac{3l_1 q^2 - 27 l_1 l_2 \beta g\, \partial\bar{\Theta}_v/\partial z}{q^3 + 9 l_1 l_2 q \beta g\, \partial\bar{\Theta}_v/\partial z}\right]\frac{\partial \bar{u}}{\partial z} \tag{A-5}$$

$$E_{11} = \left\{\left[q^4/3 + 6l_1^2 C q^2\left(\frac{\partial \bar{u}}{\partial z}\right)^2 + 12 l_1 l_2 (\beta g)^2 \overline{\theta_v'^2}\right]\left[q^3 + 9 l_1 l_2 q \beta g \frac{\partial\bar{\Theta}_v}{\partial z}\right]\right.$$
$$\left. - \left[54 l_1^3 l_2 C q^3 \beta g \frac{\partial\bar{\Theta}_v}{\partial z}\left(\frac{\partial \bar{u}}{\partial z}\right)^2 + 54 l_1^2 l_2^2 q (\beta g)^2 \overline{\theta_v'^2}\left(\frac{\partial \bar{u}}{\partial z}\right)^2\right]\right\} \div$$
$$\left\{-2l_1 q \frac{\partial \bar{v}}{\partial z}\left[q^3 + 9 l_1 l_2 q \beta g \frac{\partial\bar{\Theta}_v}{\partial z}\right]\right\} \tag{A-6}$$

$$[1 - E_{21}A_{40}] = \frac{1}{q^3}\left[q^3 + 9 l_1 l_2 q \beta g \frac{\partial\bar{\Theta}_v}{\partial z}\right] \tag{A-7}$$

$$\left[E_{22}+E_{21}A_{42}A_{45}\right]=\frac{1}{q^{3}}\left[3\ell_{1}c\,q^{4}\frac{\partial\bar{v}}{\partial z}-27\ell_{1}\ell_{2}^{2}(\beta g)^{2}\overline{\theta_{v}'^{2}}\frac{\partial\bar{v}}{\partial z}\right] \tag{A-8}$$

$$E_{10}=\left\{\left[q^{2}+6\ell_{1}^{2}\left(\frac{\partial\bar{u}}{\partial z}\right)^{2}+12\ell_{1}\ell_{2}\beta g\frac{\partial\bar{\Theta}_{v}}{\partial z}\right]\left[q^{3}+9\ell_{1}\ell_{2}q\beta g\frac{\partial\bar{\Theta}_{v}}{\partial z}\right]\right.$$
$$\left.-\left[54\ell_{1}^{3}\ell_{2}q\beta g\left(\frac{\partial\bar{u}}{\partial z}\right)^{2}\frac{\partial\bar{\Theta}_{v}}{\partial z}+54\ell_{1}^{2}\ell_{2}^{2}q\beta g\left(\frac{\partial\bar{u}}{\partial z}\right)^{2}\frac{\partial\bar{\Theta}_{v}}{\partial z}\right]\right\}\div$$
$$\left[-2\ell_{1}q\frac{\partial\bar{v}}{\partial z}\left(q^{3}+9\ell_{1}\ell_{2}q\beta g\frac{\partial\bar{\Theta}_{v}}{\partial z}\right)\right] \tag{A-9}$$

$$\left[E_{19}+E_{21}A_{42}A_{43}\right]=\frac{1}{q^{2}}\left[3\ell_{1}q^{2}\frac{\partial\bar{v}}{\partial z}-27\ell_{1}\ell_{2}^{2}\beta g\frac{\partial\bar{v}}{\partial z}\frac{\partial\bar{\Theta}_{v}}{\partial z}\right] \tag{A-10}$$

Substitution of equations (A-4 to A-10) into (A-3) will yield, after considerable manipulation, equation (A-11).

$$\overline{u'w'}=\frac{\partial\bar{u}}{\partial z}\frac{\left\{\ell_{1}\left[(3c-1)q^{5}+36\ell_{1}\ell_{2}c\,q^{3}\beta g\frac{\partial\bar{\Theta}_{v}}{\partial z}+9\ell_{2}^{2}q^{3}\beta g\frac{\partial\bar{\Theta}_{v}}{\partial z}-9(\beta g)^{2}q\ell_{2}(3\ell_{2}+4\ell_{1})\overline{\theta_{v}'^{2}}\right]\right\}}{\left\{q^{4}+6\ell_{1}^{2}q^{2}\left[\left(\frac{\partial\bar{u}}{\partial z}\right)^{2}+\left(\frac{\partial\bar{v}}{\partial z}\right)^{2}\right]+3\ell_{1}\ell_{2}\left[7q^{2}-18\ell_{1}\ell_{2}\left[\left(\frac{\partial\bar{u}}{\partial z}\right)^{2}+\left(\frac{\partial\bar{v}}{\partial z}\right)^{2}\right]+36\ell_{1}\ell_{2}\beta g\frac{\partial\bar{\Theta}_{v}}{\partial z}\right]\beta g\frac{\partial\bar{\Theta}_{v}}{\partial z}\right.} \tag{A-11}$$

Mellor and Yamada (1974) represent equation (A-11) in the form

$$-\overline{u'w'}=K_{m}\frac{\partial\bar{u}}{\partial z} \tag{A-12}$$

and

$$-\overline{v'w'} = K_m \frac{\partial \overline{v}}{\partial z} \tag{A-13}$$

From equations (A-2)

$$\overline{v'w'} = N_6 = K_9 - K_8 \left[\frac{E_{11}(1-E_{21}A_{40}) - (E_{22}+E_{21}A_{42}A_{45})}{E_{10}(1-E_{21}A_{40}) - (E_{19}+E_{21}A_{42}A_{43})}\right] \tag{A-14}$$

It can be easily shown that:

$$K_9/(\partial\overline{v}/\partial z) = E_{18}/(\partial\overline{u}/\partial z)$$

and

$$K_8/(\partial\overline{v}/\partial z) = E_{17}/(\partial\overline{u}/\partial z)$$

so comparing equation (A-14) with (A-3) and (A-11) yields

$$\overline{v'w'} = -K_m \frac{\partial \overline{v}}{\partial z}$$

The expressions for $N_5$ and $N_6$, therefore, reduce as expected to Mellor's and Yamada's expressions in the simplified case $f_y = f_z = 0$.

Prognostic equations (45, 48) require that $\overline{w'r'}$ be known at time step k to calculate $\overline{R}$ and $\overline{\theta_v' r'}$ at time step k+1. Once the Reynolds stresses and heat fluxes ($N_1$-$N_9$) have been calculated, the only unknowns at time step k will be $\overline{u'r'}$, $\overline{v'r'}$, and $\overline{w'r'}$. Equations (59-61) are three equations for these three unknowns. The solution for $\overline{w'r'}$ is:

$$\overline{w'r'} = \Big\{ (q^2 + 9\ell_z^2 f_z^2)\Big(3\ell_z \beta g \overline{r'\theta_v'} - 3\ell_z \overline{w'^2} \frac{\partial \bar{R}}{\partial z}\Big) - 9 q \ell_z^2 f_y \overline{u'w'} \frac{\partial \bar{R}}{\partial z} - 27 \ell_z^3 f_y f_z \overline{v'w'} \frac{\partial \bar{R}}{\partial z} \Big\} \div \Big\{ q^3 + 9 q \ell_z^2 \Big(f_z^2 + f_y^2 + f_y \frac{\partial \bar{u}}{\partial z}\Big) + 27 \ell_z^3 f_y f_z \frac{\partial \bar{v}}{\partial z} \Big\} \tag{A-15}$$

Expressing $\overline{w'r'}$ in the form:

$$-\overline{w'r'} = K_w \frac{\partial \bar{R}}{\partial z} - \gamma_R \tag{A-16}$$

and comparing equations (A-15) and (A-16) yields the following expressions for $K_w$ and $\gamma_R$.

$$K_w = \frac{(q^2 + 9\ell_z^2 f_z^2)(3\ell_z \overline{w'^2}) + 9 q \ell_z^2 f_y \overline{u'w'} + 27 \ell_z^3 f_y f_z \overline{v'w'}}{q^3 + 9 q \ell_z^2 \Big(f_z^2 + f_y^2 + f_y \frac{\partial \bar{u}}{\partial z}\Big) + 27 \ell_z^3 f_y f_z \frac{\partial \bar{v}}{\partial z}} \tag{A-17}$$

$$\gamma_R = \frac{(q^2 + 9\ell_2^2 f_z^2)\,(3\ell_2 \beta g\, \overline{r'\theta_v'})}{q^3 + 9\ell_2^2 q\left(f_z^2 + f_y^2 + f_y \frac{\partial \bar{u}}{\partial z}\right) + 27\ell_2^3 f_y f_z \frac{\partial \bar{v}}{\partial z}} \tag{A-18}$$

Once equation (A-16) is solved, $\overline{u'r'}$ can be evaluated by:

$$\overline{u'r'} = \frac{3\ell_2 q\left[-\overline{u'w'}\frac{\partial \bar{R}}{\partial z} - \overline{w'r'}\left(\frac{\partial \bar{u}}{\partial z} + f_y\right)\right] - 9\ell_2^2 f_z\left(\overline{v'w'}\frac{\partial \bar{R}}{\partial z} + \overline{w'r'}\frac{\partial \bar{v}}{\partial z}\right)}{q^2 + 9\ell_2^2 f_z^2} \tag{A-19}$$

Finally, $\overline{v'r'}$ is the only unknown and is determined by:

$$\overline{v'r'} = \frac{3\ell_2}{q}\left[-\overline{v'w'}\frac{\partial \bar{R}}{\partial z} - \overline{w'r'}\frac{\partial \bar{v}}{\partial z} - f_z\,\overline{u'r'}\right] \tag{A-20}$$

Numerical stability considerations for the $\overline{r'\theta_v'}$ equation require $\overline{w'r'}$ to be expressed as:

$$\overline{w'r'} = A\overline{r'\theta_v'} - B. \tag{A-21}$$

A comparison of equation (A-21) with equations (A-16 - A-18) yields expressions for A and B:

$$A = \frac{3\ell_2 \beta g \left(q^2 + 9\ell_2^2 f_z^2\right)}{q^3 + 9\ell_2^2 q\left[f_z^2 + f_y^2 + f_y \frac{\partial \bar{u}}{\partial z}\right] + 27\ell_2^3 f_y f_z \frac{\partial \bar{v}}{\partial z}} \tag{A-22}$$

$$B = \frac{3\ell_2 \left(q^2 + 9\ell_2^2 f_z^2\right)\overline{w'^2}\frac{\partial \bar{R}}{\partial z} + 9\ell_2^2 q f_y \overline{u'w'}\frac{\partial \bar{R}}{\partial z} + 27\ell_2^3 f_y f_z \overline{v'w'}\frac{\partial \bar{R}}{\partial z}}{q^3 + 9\ell_2^2 q\left[f_z^2 + f_y^2 + f_y \frac{\partial \bar{u}}{\partial z}\right] + 27\ell_2^3 f_y f_z \frac{\partial \bar{v}}{\partial z}}$$

(A-23)

# APPENDIX B

## THE STAGGERED GRID SYSTEM

A 44 point one dimensional staggered grid is used in the model. The mean variables are defined at integer grid points and turbulence energies and fluxes are defined at half integer grid points (see Figure B-1). A transformed coordinate system is used (Yamada and Mellor, 1975) which provides greater resolution near the ground where gradients are the largest. The lowest 26 meters contain 3 grid points. Above this level, the distance between grid points quickly approaches 50 meters and remains nearly constant with height thereafter. The new vertical coordinate, $\zeta$, is defined as:

$$\zeta = a_1 z + a_2 \ln(z/a_3) \tag{B-1}$$

$$(a_1, a_2, a_3) = (0.02,\ 0.25,\ 0.01) \tag{B-2}$$

The z-$\zeta$ values are tabulated in Table (B-1). Yamada and Mellor evaluate vertical derivatives in the $\zeta$ coordinate system and that approach is followed here. The derivative of any quantity, $\phi$, is:

$$\frac{\partial \phi}{\partial z} = a \frac{\partial \phi}{\partial \zeta} \tag{B-3}$$

$$a = a_1 + \frac{a_2}{z} \tag{B-4}$$

The lower boundary conditions for the mean variables are applied at $\zeta = 0$; those for the turbulence variables are applied at $\zeta = 1/2$. The upper boundary conditions (turbulence moments vanish, mean gradients constant) are evaluated at grid point 43-1/2 (2022 m).

Table (B-1)

z-$\zeta$ Values (Equation B-1)

| zeta | z(m) | zeta | z(m) | zeta | z(m) |
|---|---|---|---|---|---|
| 0 | 0.01 | 15 | 612.22 | 30 | 1352.32 |
| 1/2 | 0.07 | 15-1/2 | 636.73 | 30-1/2 | 1377.09 |
| 1 | 0.52 | 16 | 661.26 | 31 | 1401.87 |
| 1-1/2 | 3.14 | 16-1/2 | 685.80 | 31-1/2 | 1426.65 |
| 2 | 11.70 | 17 | 710.36 | 32 | 1451.43 |
| 2-1/2 | 26.48 | 17-1/2 | 734.94 | 32-1/2 | 1476.22 |
| 3 | 44.88 | 18 | 759.53 | 33 | 1501.01 |
| 3-1/2 | 65.21 | 18-1/2 | 784.13 | 33-1/2 | 1525.81 |
| 4 | 86.66 | 19 | 808.74 | 34 | 1550.61 |
| 4-1/2 | 108.81 | 19-1/2 | 833.37 | 34-1/2 | 1575.41 |
| 5 | 131.45 | 20 | 858.00 | 35 | 1600.21 |
| 5-1/2 | 154.44 | 20-1/2 | 882.65 | 35-1/2 | 1625.02 |
| 6 | 177.69 | 21 | 907.30 | 36 | 1649.83 |
| 6-1/2 | 201.14 | 21-1/2 | 931.97 | 36-1/2 | 1674.64 |
| 7 | 224.75 | 22 | 956.64 | 37 | 1699.46 |
| 7-1/2 | 248.49 | 22-1/2 | 981.32 | 37-1/2 | 1724.28 |
| 8 | 272.35 | 23 | 1006.01 | 38 | 1749.10 |
| 8-1/2 | 296.29 | 23-1/2 | 1030.71 | 38-1/2 | 1773.92 |
| 9 | 320.32 | 24 | 1055.41 | 39 | 1798.75 |
| 9-1/2 | 344.41 | 24-1/2 | 1080.12 | 39-1/2 | 1823.58 |
| 10 | 368.57 | 25 | 1104.84 | 40 | 1848.41 |
| 10-1/2 | 392.77 | 25-1/2 | 1129.57 | 40-1/2 | 1873.24 |
| 11 | 417.02 | 26 | 1154.29 | 41 | 1898.08 |
| 11-1/2 | 441.31 | 26-1/2 | 1179.03 | 41-1/2 | 1922.92 |
| 12 | 465.64 | 27 | 1203.77 | 42 | 1947.76 |
| 12-1/2 | 490.01 | 27-1/2 | 1228.52 | 42-1/2 | 1972.60 |
| 13 | 514.40 | 28 | 1253.27 | 43 | 1997.44 |
| 13-1/2 | 538.82 | 28-1/2 | 1278.02 | 43-1/2 | 2022.29 |
| 14 | 563.26 | 29 | 1302.78 | | |
| 14-1/2 | 587.73 | 29-1/2 | 1327.55 | | |

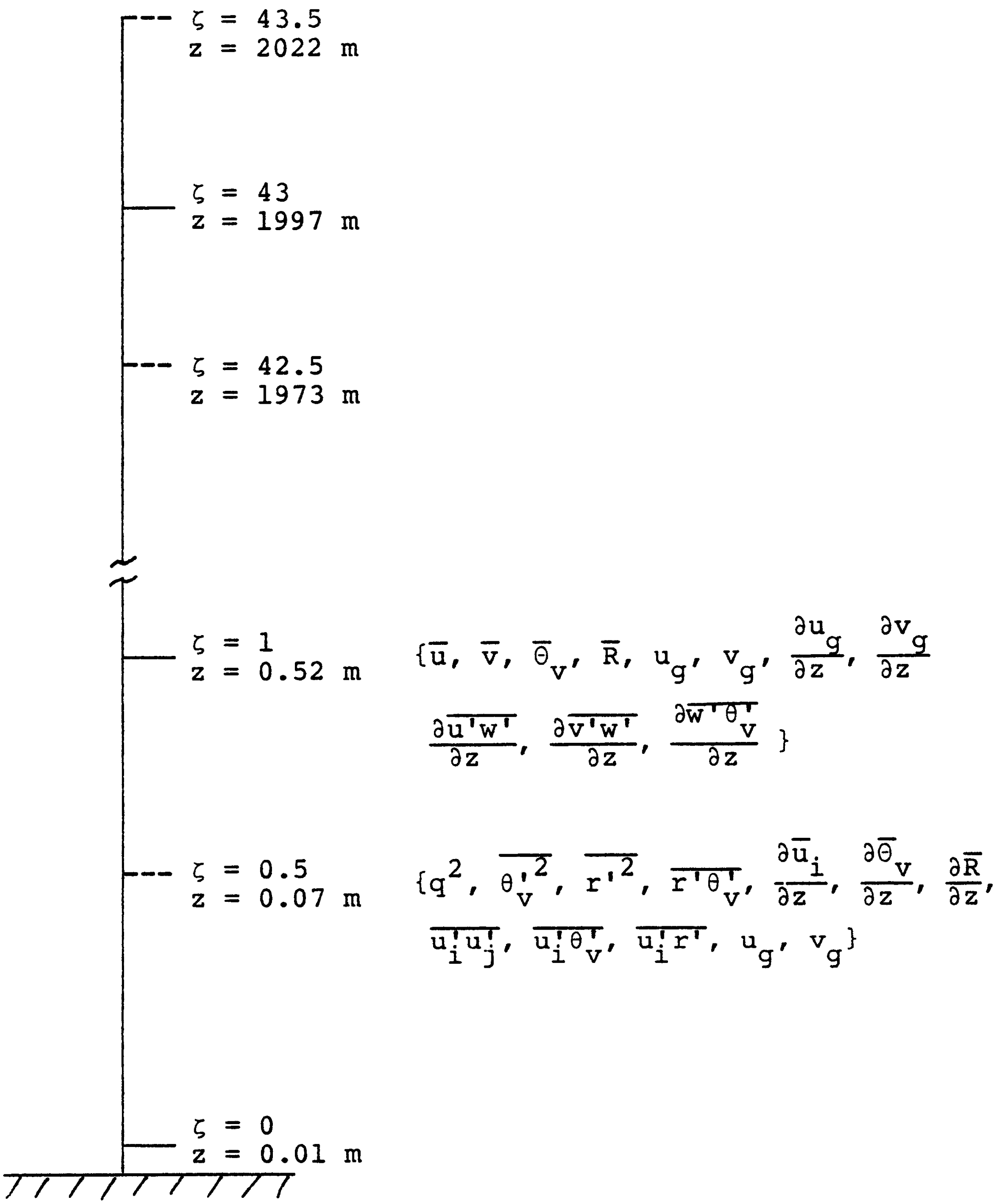


Fig. B-1. Staggered grid system used in the model.

APPENDIX C

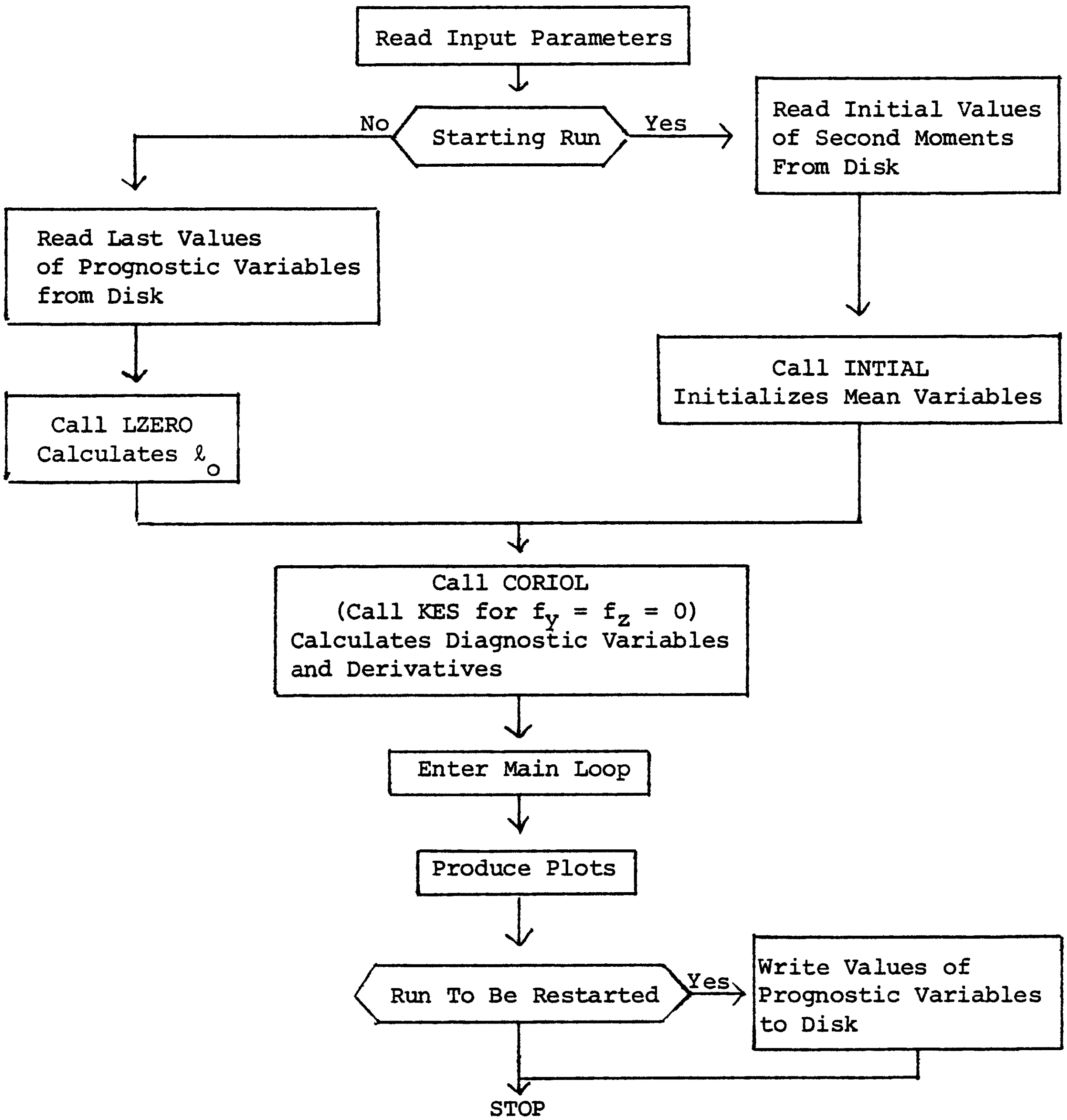


Fig. C-1. Flowchart of the level 3 model.

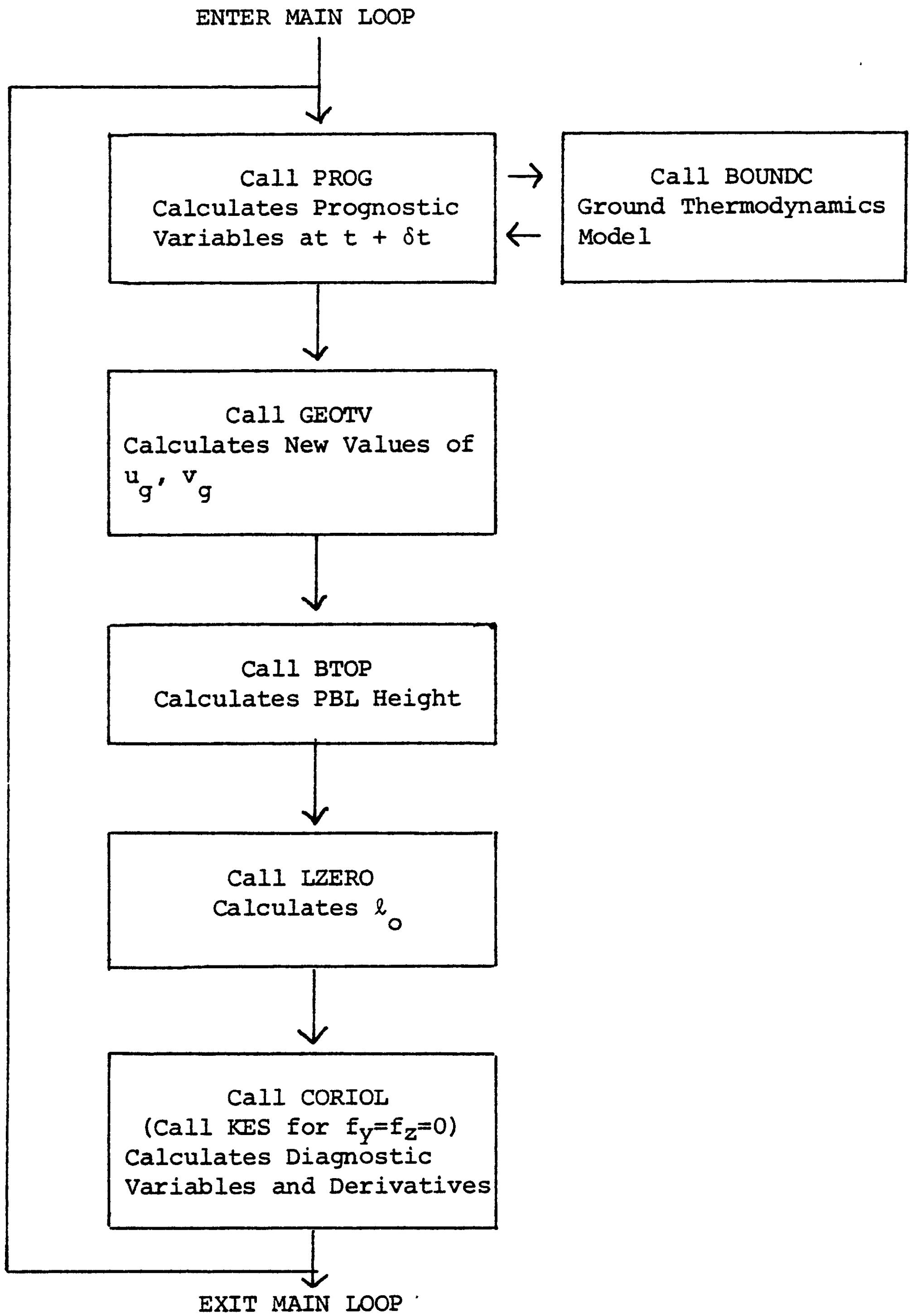


Fig. C-1 (continued)

REFERENCES

Arya, S. P. S., and E. J. Plate, 1969: Modeling of the stably stratified atmospheric boundary layer. J. Atmos. Sci., 26, 656-665.

Arya, S. P. S., 1975: Geostrophic drag and heat transfer relations for the atmospheric boundary layer. Quar. J. Roy. Met. Soc., 101, 147-161.

Arya, S. P. S., 1975: Comment on "Similarity theory for the planetary boundary layer of time-dependent height." J. Atmos. Sci., 32, 839-840.

Arya, S. P. S., and J. C. Wyngaard, 1975: Effect on baroclinicity on the wind profiles and the geostrophic drag laws for the convective planetary boundary layer. J. Atmos. Sci., 32, 767-778.

Arya, S. P. S., 1977: Suggested revisions to certain boundary layer parameterization schemes used in atmospheric circulation models. Mon. Wea. Rev., 105, 215-227.

Arya, S. P. S., 1978: Comparative effects of stability, baroclinicity and the scale-height ratio on drag laws for the atmospheric boundary layer. J. Atmos. Sci., 35, 40-46.

Blackadar, A. K., 1962: The vertical distribution of wind and turbulent exchange in a neutral atmosphere. J. Geophys. Res., 67, 3095-3102.

Blackadar, A. K., and H. Tennekes, 1968: Asymptotic similarity in neutral barotropic planetary boundary layers. J. Atmos. Sci., 25, 1015-1020.

Brutsaert, W., and F. K.-F. Chan, 1978: Similarity functions D for water vapor in the unstable atmospheric boundary layer. Bound.-Layer Meteor., 14, 441-456.

Busch, N. E., 1973: On the mechanics of atmospheric turbulence. Workshop on Micrometeorology, Amer. Meteor. Society, 1-65.

Clarke, R. H., A. J. Dyer, R. R. Brook, D. G. Reid and A. J. Troup: The Wangara Experiment: Boundary Layer Data. Tech. Paper 19, Div. Meteor. Phys. CSIRO, Australia.

Clarke, R. H., and G. D. Hess, 1973: On the appropriate scaling for velocity and temperature in the planetary boundary layer. J. Atmos. Sci., 30, 1346-1353.

Clarke, R. H. and G. D. Hess, 1974: Geostrophic departure and the functions A and B of Rossby number similarity theory. Bound. Layer Meteor., 7, 267-287.

Csanady, G. T., 1967: On the resistance law of a turbulent Ekman layer. J. Atmos. Sci., 24, 467-471.

Deardorff, J. W., 1972: Parameterization of the planetary boundary layer for use in general circulation models. Mon. Wea. Rev., 100, 93-106.

Deardorff, J. W., 1972: Numerical investigation of neutral and unstable planetary boundary layers. J. Atmos. Sci., 29, 91-115.

Deardorff, J. W., 1973: Three-dimensional numerical modeling of the plantary boundary layer. Workshop on Micrometeorology, Amer. Meteor. Society, 271-311.

Deardorff, J. W., 1973: The use of subgrid transport equations in a three-dimensional model of atmospheric turbulence. J. Fluids Eng., Sept. 429-438.

Deardorff, J. W., 1974: Three-dimensional numerical study of the height and mean structure of a heated planetary boundary layer. Bound.-Layer Meteor., 7, 81-106.

Deardorff, J. W., 1974: Three-dimensional numerical study of turbulence in an entraining mixed layer. Bound.-Layer Meteor., 7, 199-226.

Deardorff, J. W., 1978: Efficient prediction of ground surface temperature and moisture, with inclusion of a layer of vegetation. J. Geophy. Res., 83, 1889-1903.

Donaldson, C., duP, 1973: Construction of a dynamic model of the production of atmospheric turbulence and the dispersal of atmospheric pollutants. Workshop on Micrometeorology, Amer. Meteor. Society, 313-390.

Dyer, A. J., 1974: A review of flux-profile relationships. Bound.-Layer Meteor., 7, 363-374.

Hasse, L., 1977: Parameterization of the dissipation term in second order closure modelling of the planetary boundary layer under conditions of forced convection. Beitrage Zur Physik Der Atmosphare, 51, 166-173.

Hess, S. L., 1959: Introduction to Theoretical Meteorology. Holt, Rinehart, and Winston. 362 pp.

Hess, G. D., 1973: On Rossby-number similarity theory for a baroclinic planetary boundary layer. J. Atmos. Sci., 30, 1722-1723.

Kazansky, A. B., and A. S. Monin, 1960: A turbulent regime above the ground atmospheric layer. Izv. Acad. Sci., USSR, Geophys. Serv., No. 1, 110-112.

Kazansky, A. B., and A. S. Monin, 1961: On the dynamical interaction between the atmosphere and the Earth's surface. Izv. Acad. Sci., USSR, Geophys. Serv., No. 5, 514-515.

Kolmogoroff, A. N., 1941: The local structure of turbulence in incompressible viscous fluid for very large Reynolds number. C. R. Akad. Nauk. USSR, 30, 301-305. Translation, Friedlander, S. K. and L. Topper, Eds., 1961: Turbulence, Classic Papers on Statistical Theory, interscience.

Lewellen, W. S. and M. Teske, 1973: Prediction of the Monin-Obukhov similarity functions from an invariant model of turbulence. J. Atmos. Sci., 30, 1340-1345.

Lumley, S. L., and H. A. Panofsky, 1964: The Structure of Atmospheric Turbulence. John Wiley, 239 pp.

Lumley, J. L., and B. Khajeh-Nouri, 1974: Computational modeling of turbulent transport. Advances in Geophysics, Vol. 18A, Academic Press, 169-192.

Melgarejo, J. W. and J. W. Deardorff, 1974: Stability functions for the boundary layer resistance laws based upon observed boundary layer heights. J. Atmos. Sci., 31, 1324-1333.

Mellor, G. L., and H. J. Herring, 1973: A survey of mean turbulent field closure models. AIAA J., 11, 590-599.

Mellor, G. L., 1973: Analytic prediction of properties of stratified planetary surface layers. J. Atmos. Sci., 30, 1061-1069.

Mellor, G. L., and T. Yamada, 1974: A hierarchy of turbulence closure models for the planetary boundary layer. J. Atmos. Sci., 31, 1791-1806; 34, 1482-1483.

Monin, A. S., and A. M. Obukhov, 1954: Basic regularity in turbulent mixing in the surface layer of the atmosphere. Izv. Acad. Sci., USSR, Geophys. Serv., No. 24.

Richtmyer, R. D., and K. W. Morton, 1967: Difference Methods for Initial Value Problems, Interscience.

Rotta, J. C., 1951: Statistische Theorie Nichthomogener Turbulenz. Z. Phys., 129, 547-572; 131, 51-77.

Tennekes, H., and J. L. Lumley, 1972: A First Course in Turbulence, MIT Press, Cambridge, MA, 300 pp.

Wyngaard, J. C., 1973: On surface-layer turbulence. Workshop on Micrometeorology, Amer. Meteor. Soc., 101-149.

Wyngaard, J. C., O. R. Cote, and K. S. Rao, 1974: Modeling the atmospheric boundary layer. Advances in Geophysics, Vol. 18A, Academic Press, 193-211.

Wyngaard, J. C., S. P. S. Arya, and O. R. Cote, 1974: Some aspects of the structure of convective planetary boundary layers. J. Atmos. Sci., 31, 747-754.

Wyngaard, J. C., W. T. Pennell, D. H. Lenschow, and M. A. LeMonde, 1978: The temperature-humidity covariance budget in the convective boundary layer. J. Atmos. Sci., 35, 47-58.

Yamada, T., and G. L. Mellor, 1975: A simulation of the Wangara atmospheric boundary layer data. J. Atmos. Sci., 32, 2309-2329; 34, 1482-1483.

Yamada, T., 1976: On the similarity functions A, B, and C of the planetary boundary layer. J. Atmos. Sci., 33, 781-793.

Zilitinkevich, S. S., and J. W. Deardorff, 1974: Similarity theory for the planetary boundary layer of time-dependent height. J. Atmos. Sci., 31, 1449-1452.